UNIVERSITA' DEGLI STUDI DI TRIESTE

XXII CICLO DELLA SCUOLA DI DOTTORATO IN SCIENZE E TECNOLOGIE CHIMICHE E FARMACEUTICHE

DEVELOPMENT OF CHIRAL NITROGEN LIGANDS FOR APPLICATION IN HOMOGENEOUS CATALYSIS

Settore scientifico disciplinare : CHIM-06

DOTTORANDO

LIDIA FANFONI

RESPONSABILE DEL DOTTORATO DI RICERCA

PROF. *ENZO ALESSIO*

RELATORE

PROF.SSA *FULVIA FELLUGA*

UNIVERSITA' DEGLI STUDI DI TRIESTE

CORRELATORE

DOTT.SSA *BARBARA MILANI*

UNIVERSITA' DEGLI STUDI DI TRIESTE

ANNO ACCADEMICO 2008/2009

CONTENTS

ABBREVIATIONS

ATH = asymmetric transfer hydrogenation

B.Y. = baker's yeast

Bn = benzyl

Boc_2O = di-*tert*-butyl-dicarbonate

BQ =1,4-benzoquinone

Bu_4NF = tetrabutylammonium fluoride

CD = circular dichroism

COD = 1,5-cyclooctadiene

DBU = 1,8-diazabicyclo[5.4.0]undec-7-ene

DCC = N,N-dicyclohexylcarbodiimide

DCM = dichloromethane

DIEA = N,N-diisopropylethylamine

DKR = dynamic kinetic resolution

DMA = dimethylamine

DMAP = 4-(dimethylamino)pyridine

DMF = N,N-dimethylformamide

DMSO = dimethyl sulfoxyde

DPPA = diphenylphosphoroazidate

E = enantiomeric ratio

EDC = N-(3-dimethylaminopropyl)-N-carbodiimide

e.e. = enantiomeric excess

Et_2O = diethyl ether

Et_3N = triethyl amine

EtOAc = ethyl acetate

4-CH_3Py = 4-methylpiridine/ 4-picoline

4-CF_3Py = 4-trifluoromethylpyridine

GOC = growing oligomer chain

HOBt = 1-hydroxybenzotriazole

i-Pr = *iso*-propyl

KOt-Bu = potassium *tert*-butaloate

KR = kinetic resolution

MCPBA = 4-chloro perbenzoic acid

MeOH = methanol

MW = microwave

NaOi-Pr = sodium *iso*-propanolate

n-BuLi = *normal* butyl lithium

OAc = acetate

PE = petroleum ether

Phen = phenanthroline

PN = (1*R*,3a*S*)-(–)-1-phenyl-2-(pyridin-2-yl)hexahydro-1H-pyrrolo[1,2-c][1,3,2]-diazaphosphole

PNCO = (1*R*,3a*S*)-(–)-1-phenyl-2-(pyridin-2-yl)tetrahydro-1H-pyrrolo[1,2-c][1,3,2]-diazaphosphol-3(2H)-one

PP = generic phosphine

PPh3 = triphenyl phosphine

sec-Bu = secondary butyl

Tf = triflate

TFA = trifluoro acetic acid

TFE = 2,2,2-trifluoro ethanol

THF = tetrahydrofuran

TOF = tourn over frequesncy

TON = tourn over number

Ts = tosyl

RIASSUNTO

L'attività biologica di molti farmaci, composti agroalimentari ed aromi e le caratteristiche chimico-fisiche di molti polimeri sono direttamente legati alla configurazione assoluta dei centri chirali che li caratterizzano. La domanda di prodotti otticamente attivi è in continua crescita, e la catalisi asimmetrica è lo strumento maggiormente studiato per il loro ottenimento sia in campo accademico che industriale.

Lo scopo di questa tesi è la sintesi di leganti enantiomericamente puri per la sintesi di complessi metallici da utilizzare in catalisi asimmetrica. Il lavoro ha previsto la sintesi di tre differenti tipologie di leganti, in particolare i capitoli 2 e 3, riportano la sintesi di leganti di tipo CNN-pincer e N-N', ottenuti in entrambe le forme enantiomere grazie all'applicazione di metodi chemoenzimatici stereo complementari, mentre il capitolo 4 riporta la sintesi di leganti di tipo P-N a partire dalla L-prolina e l'attività catalitica dei relativi complessi di Pd(II).

LEGANTI CNN-PINCER

Recentemente, sono stati ottenuti degli ottimi risultati in reazioni di riduzione di chetoni prochirali, sia in idrogenazione che in trasferimento di idrogeno, catalizzate da complessi di Ru(II) e Os(II) coordinati da leganti CNN-pincer achirali (Figure 1) e da fosfine chirali. Negli esempi studiati si sono osservate infatti elevate produttività (TOF fino a 10^5 h^{-1}) e stereoselettività nella formazione degli alcoli chirali prodotti (e.e. fino al 99%).

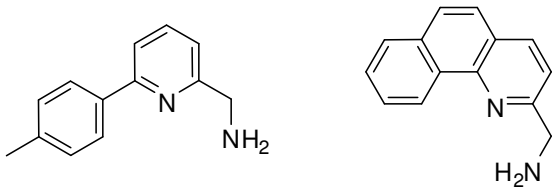

FIGURA 1.

Sulla base di tali risultati si è deciso di estendere questo studio a catalizzatori analoghi, in cui il legante pincer fosse chirale otticamente puro. E' stata messa a punto una strategia sintetica che ha permesso di ottenere i leganti amminici in Figura 2 con ottimo eccesso enantiomerico ed in entrambe le forme otticamente attive, direttamente dai rispettivi alcoli, sintetizzati a loro volta per via chemoenzimatica con e.e. ≥ 99%, attraverso due metodi enzimatici: uno basato sulla risoluzione cinetica dinamica

mediata da lipasi della miscela racema degli alcoli precursori, l'altro sulla riduzione asimmetrica mediata da lievito di birra del precursore chetonico.

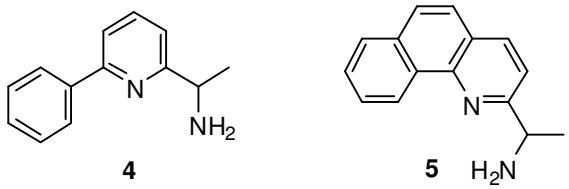

FIGURA 2.

Con lo scopo di verificare l'effetto di sostituenti arilici diversi in posizione 6 dell' anello piridinico centrale, sono stati sintetizzati dei leganti CNN-pincer caratterizzati da gruppi arilici di diverso ingombro sterico (**4a** e **4b**) o recanti in posizione 3,5 e 4 gruppi con affetti elettronici opposti (**4c-h**, Figure 3).

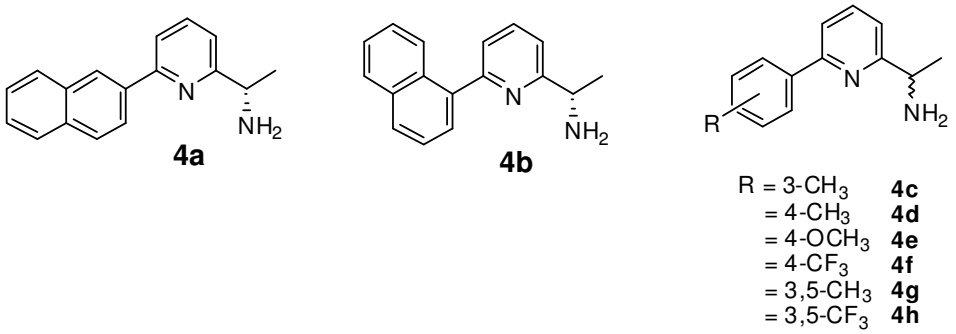

FIGURA 3.

Grazie alla messa a punto di una strategia comune per tutti i nuovi derivati che prevede, anche in questo caso, il passaggio attraverso un precursore alcolico ottenuto per via chemoenzimatica, i leganti **4a-h** sono stati ottenuti con ottimo eccesso enantiomerico (e.e. > 90%)

La coordinazione dei leganti e l'attività catalitica dei complessi di Ru(II) e Os(II) ottenuti sono stati studiati dal gruppo del Prof. Baratta e del Prof. Rigo dell'Università degli studi di Udine. I complessi dei nuovi leganti CNN-pincer (**4**, **5** e **4a-h**), in combinazione con fosfine chirali (Josiphos) hanno dimostrato buona attività ed enantioselettività nel catalizzare la reazione di riduzione di chetoni, sia in idrogenazione che in trasferimento di idrogeno.

La strategia sintetica per ottenere i leganti e i risultati relativi alle reazioni di riduzione svolte utilizzando i complessi contenenti questi nuovi derivati sono riportati nel Capitolo 2.

LEGANTI N-N'

Leganti di tipo 2,2'-bipiridina, piridina-imidazolina e 1,10-fenantrolina sono notoriamente leganti di elezione per la copolimerizzazione CO/stirene, permettendo di ottenere polichetoni stereoregolari e ad alto peso molecolare. Un ulteriore obbiettivo di questo lavoro di tesi è stato verificare l'effetto su complessi di Pd(II) dell'introduzione di un sostituente in posizione *orto* all'azoto di uno dei due anelli di un legante bi piridina. A questo scopo è stato sintetizzato il nuovo legante **29** (Figura 4), sia in forma racema che nelle sue forme otticamente attive a partire dagli alcoli precursori ottenuti per via chimica e chemoenzimatica rispettivamente. Anche in tal caso la bioriduzione con lievito di birra del precursore chetonico e la risoluzione cinetica dinamica mediata da lipasi si sono dimostrati metodi ottimali per l'ottenimento di alcoli secondari con alto eccesso enantiomerico (e.e. 99%). È stato inoltre sintetizzato un nuovo legante achirale del tipo piridina-triazolo (**30**) (Figura 4).

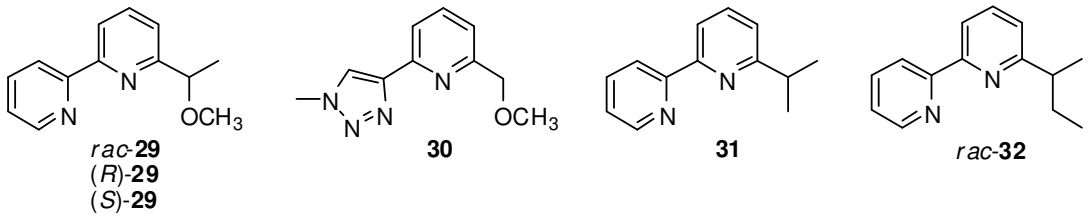

FIGURA 4.

L'attività dei complessi di Pd(II) contenenti i nuovi derivati nella reazione di copolimerizzazione CO/stirene è stata verificata e confrontata con quella di complessi caratterizzati dai già noti leganti **31** e **32**. Sorprendentemente, in ogni caso i complessi cationici, di formula generale $[Pd(N\text{-}N')(CH_3)(NCCH_3)][PF_6]$, hanno dimostrato completa selettività per la reazione di oligomerizzazione CO/stirene, dando prodotti a basso peso molecolare caratterizzati da 1-5 unità ripetitive. La formazione di prodotti regio- e diasteroisomerici in diversi rapporti denota una dipendenza dalla natura e dalla chiralità del legante usato.

Sono stati inoltre preparati complessi di palladio caratterizzati da un secondo legante coordinato di formula generale $[Pd(N\text{-}N')_2(CH_3)][PF_6]$. Pur non causando variazioni nella distribuzione dei prodotti, il loro studio ha permesso di verificare una forte dipendenza dalla presenza della seconda molecola di legante nel determinare la discriminazione fra le enantiofacce dello stirene durante l'inserzione delle prime unità della catena oligomerica.

LEGANTI P-N

La chimica dei leganti caratterizzati da differenti gruppi donatori, come fosforo e azoto, è in forte espansione grazie alla versatilità di tali sistemi. In particolare leganti P-N chirali hanno ottenuto particolare attenzione e sono stati utilizzati in vari complessi in catalisi asimmetrica.

Da un'idea originale del Prof. Castillòn (Università Rovira i Virgili, Tarragona, Spagna) sono stati sintetizzati a partire dalla L-prolina i due leganti P-N otticamente attivi in Figura 5, che differiscono per la presenza del carbonile sul ponte tra l'atomo di azoto legato all'anello piridinico e l'atomo di carbonio dell'anello pirrolidinico.

44 (PNCO) **45** (PN)

FIGURA 5.

I leganti **44** e **45** sono caratterizzati da due centri chirali: il carbonio in posizione 2 dell'anello pentatomico e l'atomo di fosforo, ma in entrambi i casi solo uno dei due possibili diasteroisomeri è stato riconosciuto come prodotto. Sono state studiate sia la capacità di complessazione di tali leganti al Pd(II) che l'attività dei sistemi ottenuti nella reazione di copolimerizzazione CO/stirene.

I due leganti, dipendentemente dalla loro natura, hanno dimostrato diversa attitudine alla formazione di complessi mono- e di-nucleari di palladio. La reazione di copolimerizzazione non viene catalizzata da complessi di questo tipo, ma, in particolare, il complesso con il legante **44** ha mostrato attività catalitica per la reazione di dimerizzazione dello stirene.

La sintesi dei leganti e dei rispettivi complessi e gli studi catalitici sono stati riportati nel Capitolo 4.

SUMMARY

The biological activity of drugs, agrochemicals and flavors as well as the chemical and physical characteristics of many polymers are strictly related to the their absolute configuration. The demand for optically active products is growing, and asymmetric catalysis is one of instruments for their achievement, in both the academic and industrial world.

Aim of this thesis is the synthesis of enantiomerically pure ligands for their application in asymmetric catalysis. In particular, the work is focused on the synthesis of three different classes of ligands. Chapters 2 and 3 deal with the synthesis of CNN-pincer and N-N' ligands respectively, obtained in both enantiomeric forms by stereocomplementary chemoenzymatic methods, while Chapter 4 presents the synthesis of P-N type ligands obtained from L-proline and the activity of their Pd(II) complexes.

CNN-PINCER LIGANDS

Recently, excellent results were obtained in the reduction of prochiral ketones catalyzed by Ru (II) and Os (II) complexes with achiral CNN-pincer (Figure 1) and chiral diphosphines, both in asymmetric hydrogenation and transfer hydrogenation reactions, with excellent productivity (TOF up to 10^5 h^{-1}) and enantioselectivities (e.e. up to 99% of the chiral alcohol products).

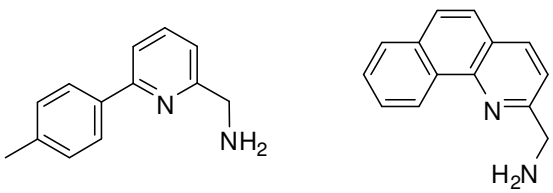

FIGURE 1.

Based on these results, we decided to extend this research on analogous complexes with the chiral optically active CNN pincer ligands represented in figure 2, which were obtained by a clean S_N2 reaction from their optically active alcohol precursors.

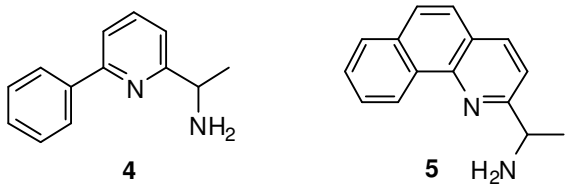

FIGURE 2.

The alcohols were synthesized by two enantiocomplementary chemoenzymatic methods, based on baker's yeast bioreduction of the parent prochiral ketone and the lipase mediated dynamic resolution of the racemic alcohol substrates. In order to verify the effect of substituent at the C-6 of the pyridine ring, CNN-pincer ligands with aryl groups differing in the steric (**4a** and **4b**) or and electronic properties (**4c-h**, Figure 3) have been synthesized by analogous strategy, with excellent enantiomeric excess (e.e. > 90%).

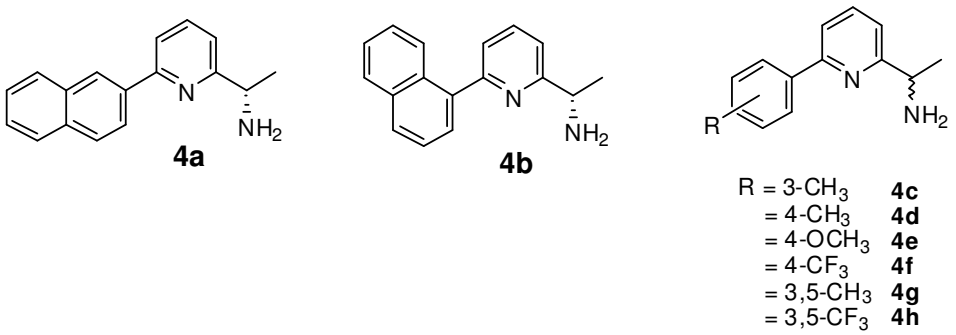

FIGURE 3.

The ligands coordination and the catalytic activity of the Ru (II) and Os (II) complexes obtained, were studied by Prof. Baratta and Prof. Rigo's group (University of Udine). Complexes stabilized by CNN-pincer ligands (**4**, **5** and **4a-h**), in combination with chiral phosphine (Josiphos) showed good activity and enantioselectivity in catalyzing the reaction of reduction of ketones, both in transfer hydrogen reaction and asymmetric hydrogenation. The synthesis and application of CNN pincer ligands are described in Chapter 2.

N-N'LIGANDS

2,2'-Bipyridine, pyridine-imidazoline and 1,10-phenanthroline derivatives are known as ligands of choice for the copolymerization CO/styrene, allowing stereoregular and high molecular weight polyketones. A further purpose of this thesis was to investigate the effect of an *ortho* chiral substituent on bipyridine, on the activity of their Pd(II) complexes. For this purpose, we have synthesized compounds **29** (Figure 4), in both

enantiomeric forms, by applying the chemoenzymatic methodologies seen before for the 6-arylpyridine pincer ligands for the synthesis of the corresponding optically active alcohol precursors, which were obtained in high enantiomeric excesses (e.e. 99%). It was also synthesized a new achiral ligand pyridine-triazole (**30**) (Figure 4).

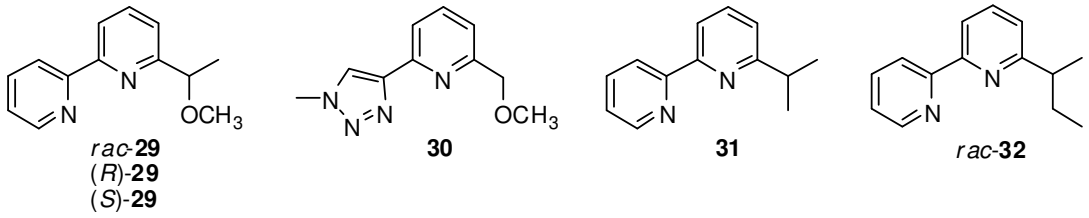

FIGURE 4.

The activity of the Pd(II) complexes containing the new derivatives was tested in the CO/styrene copolymerization reaction, the results obtained were compared with that of complexes characterized by already known ligands **31**and **32**.

Surprisingly, in each case the cationic complexes, of general formula [Pd(N-N')(CH_3)($NCCH_3$)][PF_6], showed complete selectivity for the CO/styrene oligomerization, giving oligomeric products of 1-5 units. The formation of different regio- and diasteroisomeric products was shown to depend on the ligand chirality and nature.

Palladium complexes with a second bipyridine of general formula [Pd(N-N')$_2$(CH_3)][PF_6], have been also prepared. The presence of the second ligand did not affect products distribution, but it played a crucial role in determining the enantioface discrimination at least for the first units inserted in the oligomeric chain.

The synthetic strategy for the N-N' ligands, the characterization of the complexes and application in catalysis are discussed in Chapter 3.

P-N LIGANDS

There is an increasing interest in the chemistry of the ligands characterized by different donor groups, such as phosphorus and nitrogen, due to the versatility of such systems. In particular chiral P-N ligands have received particular attention and were used in various complexes for asymmetric synthesis.

From an original idea of Prof. Castillòn (University of Rovira i Virgili, Tarragona, Spain) the synthesis of two optically active P-N ligands in Figure 5, starting from L-proline, has been developed.

44 (PNCO) **45** (PN)

FIGURE 5.

The ligands differ in the presence of the carbonyl group on the bridge connecting the nitrogen atom bound to the pyridine ring and the chiral carbon of the pyrrolidine ring: In spite of the presence of two chiral centers, the carbon in position 2 of pentatomic ring and the phosphorus atom, ligands **44** and **45** formed as a single diasteroisomer. Both the coordination to Pd(II) and the activity of the systems obtained in the copolymerization reaction of CO/styrene have been investigated.

Depending on their nature, the two ligands, have shown a different attitude to the formation of mono- and di-nuclear palladium complexes. They turned out not to catalyze any copolymerization reaction. Instead the complex with the ligand **44** proved active in styrene dimerization. The synthesis of ligands and their complexes and catalytic studies were reported in Chapter 4.

Introduction

Chapter 1

1.1. ASYMMETRIC CATALYSIS

Chirality is an intrinsic universal feature of a various level of matter, molecular chirality plays a key role in science and technology. Most physiological phenomena arise from hightly precise molecular interactions, in which chiral host molecules recognize two enantiomeric guests molecules in different ways. There are a lot of examples of enantiomer effects which are frequently dramatic: enantiomer often smell and taste different and the structural difference between enantiomers can be serious with respect to the actions of synthetic drugs. Thus, gaining access to optically pure compounds in the developments of pharmaceuticals, agrochemicals and flavors is a very significant endeavor.

Discovery of truly efficient methods to achieve this goal has been a substantial challenge for chemists in both academia and industry. Stereoselective conversion of a prochiral compound to a chiral product (Asymmetric Reaction), is a very attractive approach, practical access to pure enantiomer relied largely on biochemical or biological methods. However the scope of such methods using enzymes, cell cultures or whole organisms is limited because of the inherent single-hand specificity of biocatalyst. On the other hand, a chemical allows for a flexible synthesis of a wide array of enantiopure organic substances from achiral precursor. The requirements for practical asymmetric synthesis include high stereoselectivity, high rate and productivity, atom economy, cost efficiency, operational simplicity, environmental friendliness, and low-energy consumption.

Traditional asymmetric synthesis using a stoichiometric amount of a chiral compound, which is convenient for small to medium-scale reaction, is practical only if the expensive chiral auxiliary deliberately attached to a substrate or reagent is readily recyclable; otherwise it's a wasteful procedure!

A general principle of asymmetric catalysis using a chiral organometallic system is to provide an ideal way for multiplying molecular chirality (Figure 1).

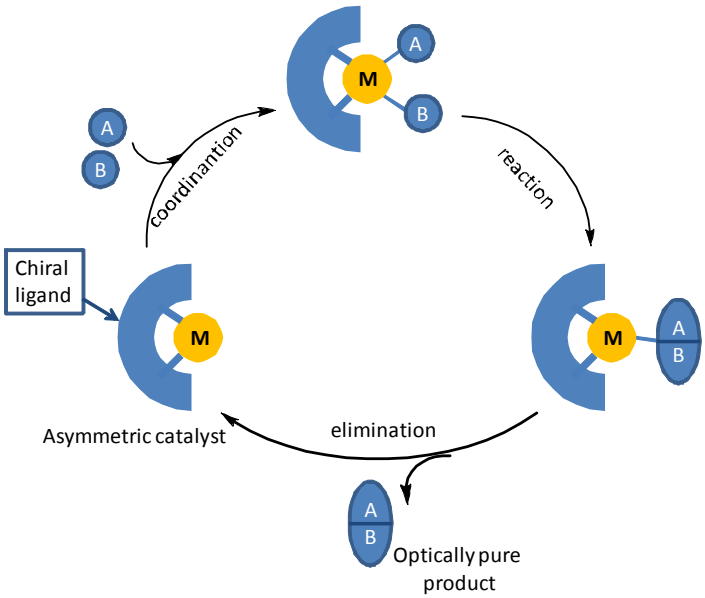

FIGURE 1. Schematic principle of asymmetric catalysis with chiral organometallic catalyst: M = metal; A, B = substrate and reactant.

A small amount of well-designed chiral catalyst can combine A and B, which produces the chiral AB compound stereoselectively in a large amount. Of various possibilities, the use of chiral organometallic molecular catalyst would be the most powerful strategy for this purpose. Asymmetric catalysis is an integrated chemical approach in which the maximum chiral efficiency can be obtained only by a combination of suitable molecular design with proper reaction conditions. The reaction must proceed with high turnover number (TON) and high turnover frequency (TOF), while the enantioselectivity range from 50:50 (nonselective) to 100:0 (perfectly selective).

The chiral ligands that modify intrinsically metal atoms must possess suitable three-dimensional structure and functionality, to generate sufficient reactivity and the desired stereoselectivity. The chiral catalyst can permit kinetically precise discrimination among the enantiotopic atoms, groups or faces in chiral molecules.[1] Well-defined chiral transition metal complexes not only decrease the activation energy of reactions but also differentiate between diasteromeric transition states. In asymmetric catalysis ligands induce asymmetry in a reaction, but not just though steric factors, also by generating electronic asymmetry on the metal centre through the presence of different donor atoms.[2] Playing with steric and electronic properties of the ligand is possible to perform a perfect selective environment which give desired

properties to the metal centre and thinking about the virtually unlimited variations of the organic ligand, the enormous opportunities for asymmetric catalysis is clear.

In conclusion to make an efficient transition metal catalyst, the following task are generally required: designing and synthesizing chiral ligand; preparing suitable substrates, catalyst precursor and metal-ligand complexes; and searching for appropriate reaction conditions. The significant challenges on asymmetric catalysis are two: discovering new catalytic reactions and inventing effective chiral catalysts. With regard to developing new metal-catalyzed reactions, it is important to focus on certain reactivity principles and experimental details: for example many inorganic and organometallic complexes can be converted to effective catalyst if proper conditions, proper ligands, suitable solvents and additives are used. Converting stoichiometric transformation into catalytic reactions and developing hightly active catalysts that feature broad under mild and simple conditions remain key problem. The combined use of organometallic and coordination chemistry has produced a number of new and powerful synthetic methods for important classes of compounds in general and for optically pure substances in particular. For this purpose complexes with optically active ligands have been used, the follow paragraphs report some example of ligands used in asymmetric catalysis focusing on the asymmetric reduction of ketones by hydrogen transfer or hydrogenation reaction and copolymerization reactions.

1.2. PINCER LIGANDS

Since 1970 pincer-type ligands have attracted increasing interest owing to the unusual properties of the metal centers imparted by this kind of ligand. The most common type of pincer skeleton is an anionic aryl ring *ortho,ortho*-disubstituted which bond the metal *via* M-C σ-bond; *ortho*-substituents could be heteroatom as CH_2NR_2, CH_2PR_2 or CH_2SR, which generally coordinate to the metal center too.[3]

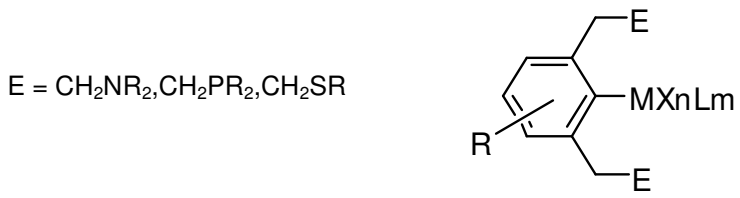

FIGURE 2. Generic structure of ECE pincer ligand.

The control of the properties of the metal center by a well-defined ligand system is an ultimate goal of inorganic and organometallic chemistry. Chelation, that is, the binding of a ligand to a metal through two or more bonds, is a versatile method to realize it. In organometallic complexes containing a direct transition metal-carbon bond, chelation leads to the formation of metallacycles, which provides an additional stabilization of M-C bond.[4] "Pincer" ligands have the general formula ECE and comprise a potentially E,C,E terdentate coordinating, monoanionic array, where E is a neutral two-electron donor such as N, P, O, S, while C represent the anionic aryl carbon atom. Metal complexation with pincer ligands usually occurs with formation of two five-member metallacycles to afford complexes $[MX_n(ECE)L_m]$, this bonding mode forces the central aryl group to a conformation which is approximately coplanar with the coordination plane of d^8 square-planar metal centers (Rh^I, Ir^I, Ni^{II}, Pd^{II}, Pt^{II}) or with the basal plane of d^6 square-pyramidal metal geometries (Ru^{II}, Rh^{III}, Ir^{III}). Modification of various ligand parameters allows for a refined adjustment of the steric and electronic properties of the complexed metal center without changing its bonding pattern significantly. In such pincer system the correlation of modification in the ligand with the properties of the metal center are exceptionally high: for instance steric influences may be varied by changing the size of the donor substituents or by introducing functional groups in the benzylic position. Clearly some of these modifications will also have electronic effects that are attributed to the type of donor atoms E and the electron-withdrawing or –releasing character of their substituents. Fine-tuning of electronic properties can also be achieved by further substitutions of the aromatic rings.[3]

So far, the majority of investigation have been carried out with pincer ligands containing nitrogen, phosphorus or sulfur donor group.

Complexes containing biscyclometalated pincer ligands offer particularly attractive possibilities for catalytic applications, since the tailoring of catalytic properties is readily achieved:

1. The terdentate binding mode and the covalent M-C σ bond stabilize the catalytically active metal site, preventing efficiently the metal leaching.
2. The electronic properties are highly sensitive towards modifications in the donor array.

3. The steric requirements around the catalytic site can be modified to discriminate against some substrates or to create a chiral pocket for asymmetric catalysis.

Unique characteristics of pincer ligands have attracted extensive research into them catalytic uses: Kharasch reactions, Heck reactions, Suzuki coupling, hydrogen transfer reactions, Michael reaction and aldol reactions are few examples of catalytic use of this system.[5]

1.2.1. PINCER LIGANDS IN ASYMMETRIC HYDROGENATION (AH) AND ASYMMETRIC TRANSFER HYDROGENATION (ATH)

Hydrogen (H_2) is the simplest molecule and its properties are fully understood. Because this clean resource is available in abundance at a very low cost, catalytic hydrogenation is a core technology in both research and industry. Nevertheless, the ways to manipulate H_2 chemically have remained limited. Among all asymmetric catalytic methods, asymmetric hydrogenation utilizing molecular hydrogen to reduce prochiral olefins, ketones and imines, have become one of the most efficient methods for constructing chiral compounds. In particular, there are many successful examples in which high enantioselectivities were achieved in asymmetric hydrogenation of prochiral ketones to yield optically active secondary alcohols by using chiral Ru, Rh, and Ir complexes.[6]

An attractive alternative to asymmetric hydrogenation for the production of chiral compound, due to its operational simplicity and easy availability of hydrogen sources, is the asymmetric transfer hydrogenation of prochiral substrates. 2-Propanol is the conventional hydrogen source having favorable properties: it is stable, easy to handle (bp 82 °C), nontoxic, environmentally friendly, and inexpensive and dissolves many organic compounds. The acetone product is readily removable.[7]

An interesting challenge, is the development of new catalytic system active in both symmetric hydrogenation and hydrogen transfer.

With this aim a new class of pincer ligands have been recently developed by the group of Prof. P. Rigo[8] The novel terdentate complexes of general structure in Figure 3, are bound to a diphosphane and an aminomethyl-based CNN pincer and show an extremely high efficiency in transfer hydrogenation of diaryl, dialkyl and aryl-alkyl ketones. The stability of the complex is assured by the rigid framework build up by the

association of the robust terdentate pincer and the chelating phosphane, consequently catalyst deactivation is significantly retarded.[8b]

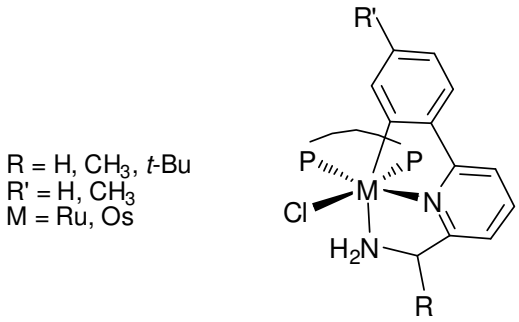

FIGURE 3. Example of new catalytic systems containing CNN pincer ligand for AH and ATH.

Mechanistic aspect of the catalyzed ATH of benzophenone in 2-propanol/NaOH with Ru(II) complexes has been studied (Scheme 1).[8a]

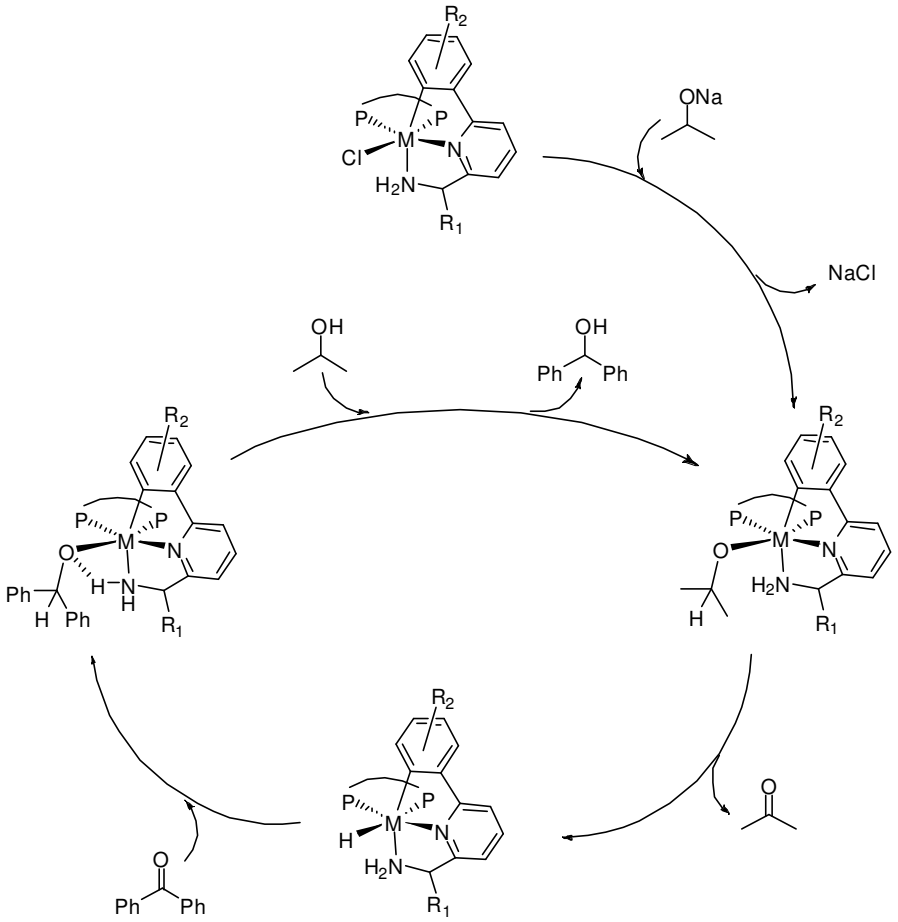

SCHEME 1. Catalyst activation in hydrogen transfer mechanism. M = Ru.

The catalytic species is the Rhutenium hydride formed by the reaction between the halide precursor complex and sodium isopropoxide, resulting in a covalent metal

alkoxide as a reactive intermediate that undergoes a facile β-hydrogen elimination reaction affording the active Ru-H species. Hydride complex reacts fast with an equimolar amount of benzophenone to give the alkoxide-amine complex through insertion of the ketone into Ru-H bond, this species beeing stabilized by an hydrogen N···H···O bond interaction. It is worth pointing out that for CNN ligands the presence of the primary $–NH_2$ group is crucial in enhancing the activity of the catalyst. Subsequent reaction with 2-propanol, which is present in large excess, leads the formation of Ru-isopropoxide closing the catalytic cycle.[8a] When an optically pure CNN pincer has been used, a fast enantioselective transfer hydrogenation has been observed. The structure of the terdentate pyridine ligand is therefore well suited for a modular synthetic approach, which allows for a fine tuning of stereochemical properties of CNN complexes. These pincer complexes are efficient catalysts for AH and ATH of alkyl aryl ketones. High enantioselectivities (up to 99%) have been achieved in ATH with a remarkably high rate (TOF = 10^5–10^6 h^{-1}) and low catalyst loading (0.005–0.002 mol%). By changing the reaction parameters, these pincer complexes also catalyze the AH of ketones (0.02–0.01 mol% of catalyst) with H_2 (5 atm) to give up to 99% e.e. of the alcohol products.

On account of the remarkably high activity and productivity of these complexes, this class of derivatives has a great potential for application in homogeneous asymmetric catalysis.[8]

1.3. N-N LIGANDS

The range of nitrogen donors is more extensive than that of any other atom. An appropriate classification of nitrogen donors can be based on the sp^3, sp^2 or sp hybridization of this atom. Complexes with nitrogen donors containing N-H bond, as sp^3 type ligands, are generally not suitable for most organometallic reactions because H atom on coordinated nitrogen are sufficiently acidic to react with a nucleophile, furthermore coordinated nitrogen atom containing nonbonding pairs of electrons are suitable to electrophile attacks. The only class of organic nitrogen donors with sp hybridization are nitriles, but their main function is as labile ligands that are replaced by appropriate reagents. Ligands containing sp^2-hybridized nitrogen atoms, particularly when N-atom is part of an aromatic system, instead have a very extensive coordination chemistry (Figure 4).[9]

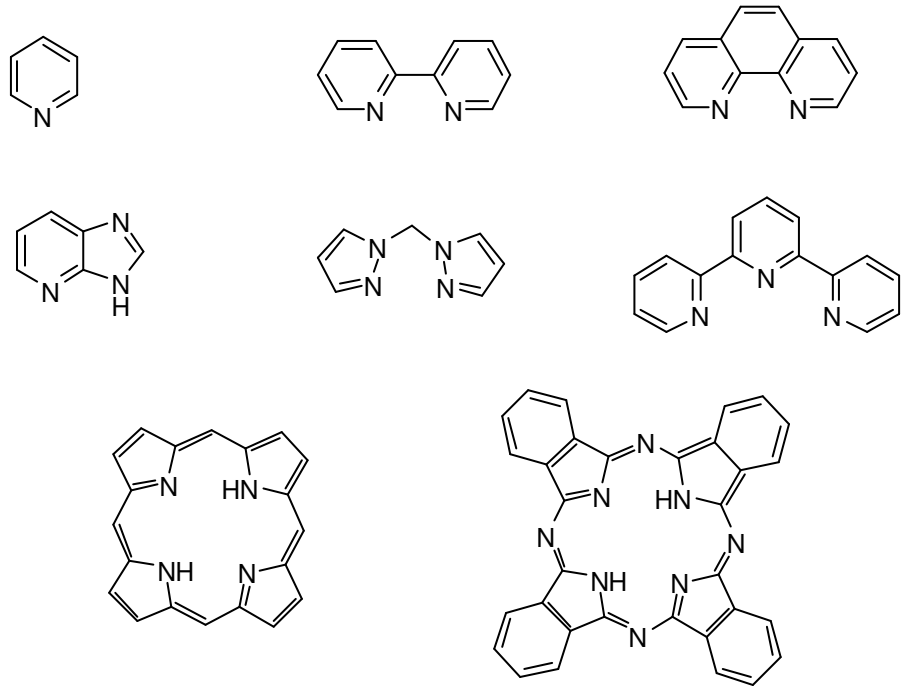

FIGURE 4. Some nitrogen-donors with sp^2-hybridized N atoms.

Also for this kind of donors, a much more extensive and useful coordination chemistry is possible if they are bi- or terdentate ligands, however the use of such ligands in asymmetric catalysis requires the presence of stereogenic substituents.

M-N bonds are most of σ-type but π interactions are possible with ligand containing sp^2-hybridized nitrogen donors, and π back-bonded effects, particularly between nitrogen heterocycles and metal centers, have been frequently invoked to explain a variety of observations.

Thus the following generalization can be made:

1. Donor-acceptor bonds formed by nitrogen donors with metal atoms of the transition series and the inner series are generally strong and their strength is unlikely to show drastic changes if the metal center, but not the ionic charge, is changed.
2. The strength of the M-N bonds will be much less affected by steric effects.
3. The nitrogen donors, generally, will not be as effective in producing low-spin complexes with the consequence that the species produced are less thermodynamically stable and more kinetically labile.

The consequence of this "boundary conditions" are that nitrogen-donor ligands forming robust complexes are di-, ter- or multidentate ligands, often macrocycles, with sp^2-hybridized N-atoms.

Nitrogen ligands in homogeneous catalysis have received increasing attention in recent years. In particular, the use of optically active, chelating, nitrogen-containing ligands made many significant contribution to the field of asymmetric catalysis. This important peculiarity increase the range of catalytic use which includes asymmetric hydrogenation and transfer hydrogenation, asymmetric cyclopropanation, asymmetric Dies-Alder reaction, asymmetric aldol condensation and much more.[9]

1.3.1. NITROGEN LIGANDS IN POLYKETONES SYNTHESIS[10]

The copolymerization reaction of carbon monoxide with terminal alkenes (Scheme 2) or strained cyclic olefins leads to the synthesis of alternated polyketones, most commonly this reaction is homogeneously catalyzed by Pd(II) complexes containing a wide array of bidentate ligands including bidentate phosphine donors, bidentate nitrogen donors, hybrid phosphorus-nitrogen systems and phosphino-phosphite ligands.[11]

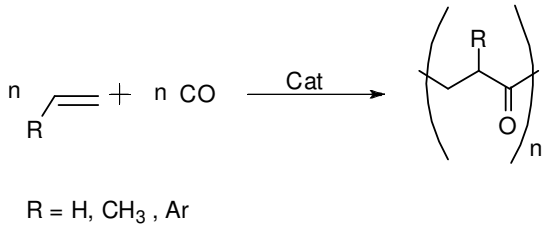

SCHEME 2. General catalyzed polyketones synthesis.

During the last two decades, considerable interest has been focused on the synthesis of polyketones originating from carbon monoxide with an aromatic alkene, like styrene or its substituted derivatives,[10,12] this copolymerization reaction requiring the use of Pd(II) complexes with N-N chelating ligands to be effectively accomplished.[10,11]

Copolymers of general formula $[CH(Ar)CH_2CO]_n$ show regio- and stereoisomerism due to the presence of truly stereogenic centers in the polymer backbone. Depending on the regioselectivity of the monomer insertion, primary (1,2 mode) or secondary (2,1 mode) into the polymer chain, three different arrangements might be possible during

the polymerization: tail-to-tail, head-to-tail and head-to-head (Figure 5). Styrene insertions in palladium complexes usually take place in the 2,1-fashion.

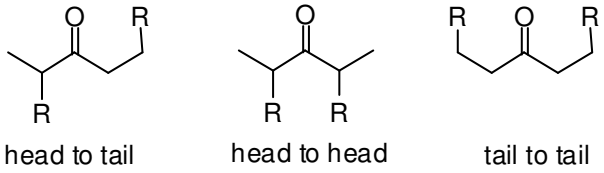

FIGURE 5. Regioselectivity of propagation chain during CO/styrene copolymerization.

The occurrence of the same insertion mode during the chain growth leads only to head-to-tail units. Moreover, the sequence of absolute configuration of the stereogenic centers in the backbone can control the formation of atactic (stereoirregular), syndiotactic (*RSRSRSRS* sequence) or isotactic (*RRRRRRRR* or *SSSSSSSS* sequence) copolymers (Figure 6). Syndiotactic and isotactic alternating copolymers are characterized by vanishing small and high optical activity respectively.[11]

FIGURE 6. Syndiotactic and isotactic copolymers in CO/styrene copolymerization.

The introduction of substituents of different nature and on different positions of the ligand skeleton and the use of chiral bidentate N-N ligands have a remarkable effect on the overall catalyst performance, including the catalyst activity, productivity and stability and on the features of the synthesized macromolecules like the molecular weight, the molecular weight distribution and the stereochemistry. In particular the control of the region- and enantioselectivities of styrene insertion, ultimately leading to a stereoregular polyketones, can be achieved through a suitable choice of bidentate ligands. Indeed the stereochemistry of copolymer could depends on both the efficient catalytic system enantioface discrimination strongly dependent on ligands nature and on the influence of the growing chain.

The first example of enantioselective copolymerizaton of styrene monomer and CO has been obtained with cationic palladium catalysts modified with enantiomerically pure C_2-symmetric bisoxazoline ligands (Figure 7). In a typical reaction the monomers react at room temperature yielding copolymers featured by both highly isotactic

microstructure and high optical activity.[9,13] The presence of substituents in the four position of oxazoline rings strongly controls the orientation of incoming styrene around the metal centre during the propagation process.[13] Surprisingly palladium catalysts modified with pyridine-oxazoline ligands give polymers that are largely syndiotactic, the same result is obtained using C_{2v}-symmetry ligands, such as 1,10-phenantroline and 2,2'-bipyridine.[10,11,12] (Figure 7).

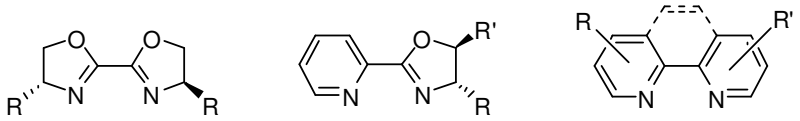

FIGURE 7. Few examples of N-N donor ligands used in CO/styrene copolimeryzation.

1.4. P-N LIGANDS

The most important and widely used of heterodentate ligands in asymmetric catalysis are those which bear phosphorous and nitrogen as their donor atoms. This kind of ligands have been definite *hemilable* because of the combination of soft and hard donor atoms.[14] The π-acceptor character of the phosphorous can stabilize a metal centre in a low oxidation state, while the nitrogen σ-donor ability makes the metal more susceptible to oxidative addition reaction. This combination can help to stabilize intermediate oxidation states or geometries which form during the catalytic cycle. The electronic asymmetry can also be used to optimize a ligand for use in particular reaction by appropriate choice of the nature of the donor atoms. For instance, bonding the phosphorous directly to a more electronegative atom such as oxygen or nitrogen will decrease its electron-donating ability while enhancing its π-acceptor capacity. Alternatively, the presence of an imino rather than an amino group will result in a nitrogen donor atom of greater σ-donating capabilities. Overall this will result in a greater electronic disparity between the donor atoms.

The P-N ligands are not classified by the reaction in which their metal complexes have been applied, but by the nature of their donor atoms. Based on this system it is possible to recognize: amino N donor-phosphine P donor (Figure 8-(a)), cyclic amino N donor-phosphine P donor (Figure 8-(b)), amino N donor-heteroatom bound P donor (Figure 8-(c)), imine N donor-phosphine P donor (Figure 8-(d)), cyclic imino N donor-phosphine P donor (Figure 8-(e)), imine N donor-heteroatom bound P donor (Figure 8-(f)), pyridine type N donor-phosphine P donor (Figure 8-(g)), pyridine type N donor-

heteroatom bound P donor (Figure 8-(h)) and ligands with chiral donor atoms; either chiral N donor (Figure 8-(i)) or phosphorous P donor (Figure 8-(l)).[2]

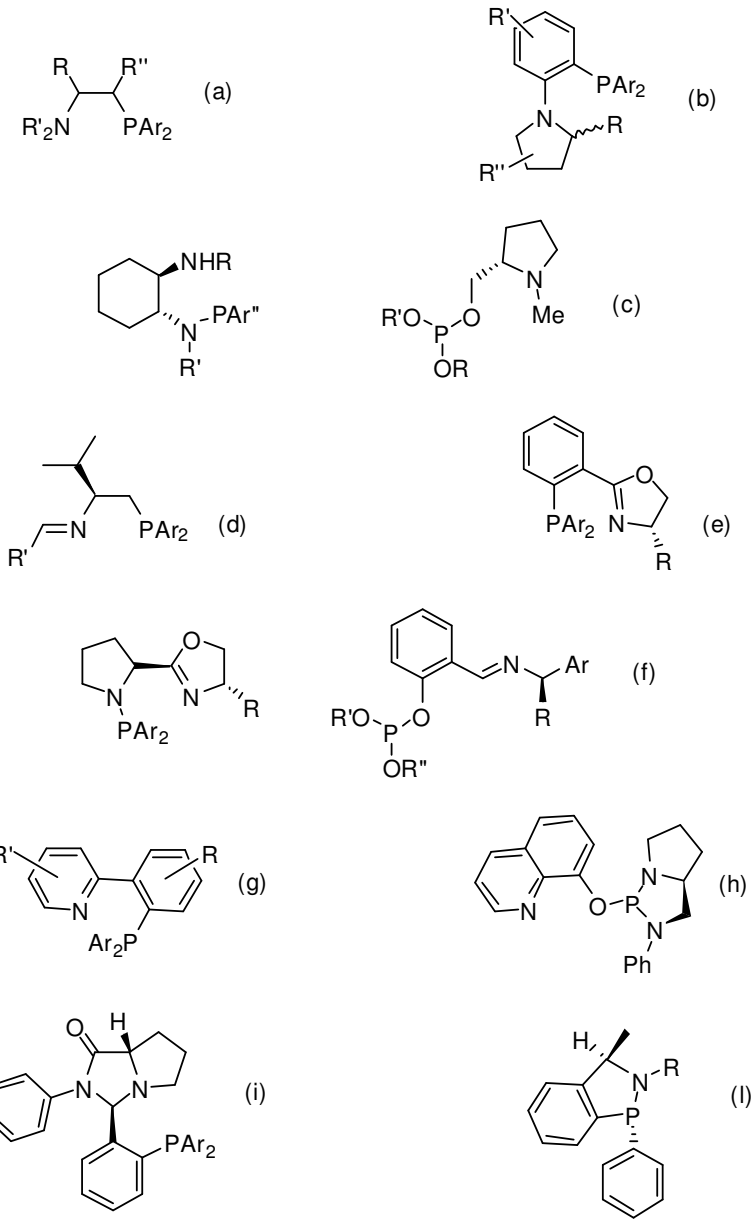

FIGURE 8. Few examples of P-N ligands.

Moreover, polydentate ligands having both hard and soft donors, are excellent candidates for the preparation of homo- or hetero-bimetallyc complexes. Compounds comprised of more than one metal center in close proximity might exhibit different properties, compared with the monometallic fragment that constitute them: cooperative reactivity patterns, stabilization of unusual ligand coordination modes, higher catalytic activity or different selectivity than the corresponding mononuclear moieties.[14,15]

Very recently attention has been focused on P-N chiral ligands: they have been used successfully in asymmetric catalysis reactions such as allylic substitution, hydrosilation, hydroboration of olefins and hydrogen transfer of ketones. The reason for their good performance is twofold: steric factors, but also the electronic asymmetry induced by the presence of very different donor atoms on the metal center.[14]

P,N-coordinated nickel or palladium complexes were also described as active compounds for the oligomerization[16] and polymerization of ethylene.[17]

The enantioselective copolymerization of CO and styrene has also been achieved with palladium catalysts with hybrid phosphine-nitrogen ligands.[18] The isolated material is isotactic and its optical activity is comparable to those obtained with the bioxazoline derived catalysts.

1.5. BIOCATALYSIS IN ORGANIC SYNTHESIS

Biocatalysis encompasses catalysis by bacteria, fungi, yeast, or their true catalytic components: enzymes. *Enzymes* are proteins that are able to accelerate organic transformations under mild reaction conditions. The available enzymes are traditionally divided into six classes according to the specific type of reaction catalyzed: oxidoreductases, transferases, hydrolases, lyases, isomerases and ligases.

The hallmark of enzymes is their remarkable ability to catalyze very specific chemical reactions, some enzymes are so well designed for this purpose that they can accelerate the rate of a chemical reaction by as much as 10^{12}-fold over the rate of spontaneous reaction. This incredible enhancement results from the juxtaposition of chemical reactive groups within the binding pocket of enzyme (the enzyme active site) and other groups from the target molecule (substrate), in a way that facilities the reaction steps required to convert the substrate into the product.[19]

Enzymes display three types of selectivities:

- Chemoselectivity: Since the purpose of an enzyme is to act on a single type of functional group, other sensitive functionalities, which would normally react to a certain extent under chemical catalysis, survive. As a result, biocatalytic reactions tend to be "cleaner" and laborious purification of product(s) from impurities emerging through side-reactions can largely be omitted.
- Regioselectivity and Diastereoselectivity: Due to their complex three-dimensional structure, enzymes may distinguish between functional groups which are chemically situated in different regions of the substrate molecule.

- Enantioselectivity: Since almost all enzymes are made from L-amino acids, enzymes are chiral catalysts. As a consequence, any type of chirality present in the substrate molecule is "recognized" upon the formation of the enzyme-substrate complex. Thus a prochiral substrate may be transformed into an optically active product and both enantiomers of a racemic substrate may react at different rates.

The interest in biocatalysts is mainly due to the need to synthesize enantiopure compounds as chiral building blocks for drugs and agrochemicals with a system which minimizes problems of undesired side-reactions such as decomposition, isomerization, racemization and rearrangement, which often plague traditional methodology. Biocatalysts could be use both in full cells and as isolated enzymes, the latter could be either native or immobilized on an inert support.

The enzymes action mechanism consist on a lock-and-key model: the active has the right shape and functional groups to bind, activate and draw up the reacting molecules forming of enzyme-substrate intermediate. After reaction the products are released and the enzyme is ready for a new cycle (Figure 9).

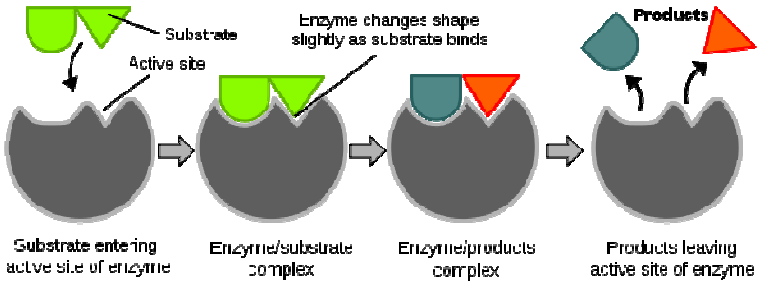

FIGURE 9. Schematic mechanism of enzymes catalysis.

Some enzymes require the association with additional chemicals to facilitate rapid reaction and regeneration. Thus enzymes incorporate non-protein molecules called cofactors through non-covalent interactions such as H-bonding and hydrophobic interactions. Cofactors can be either inorganic (*e.g.*, metal ions and iron-sulfur clusters) or organic compounds (*e.g.*, flavin and heme). Organic cofactors can be either prosthetic groups, which are tightly bound to an enzyme, or coenzymes, which are released from the enzyme's active site during the reaction. Coenzymes include NADH, NADPH and adenosine triphosphate, these molecules transfer chemical groups

between enzymes. Using enzymes as whole cells is possible to avoid the addition of cofactors to regenerate the enzyme during the reaction.

Enzymatic catalysis in organic solvents significantly broadens conventional aqueous-based biocatalysis. Water is a poor solvent for nearly all applications in industrial chemistry since most organic compounds of commercial interest are very sparingly soluble and are sometimes unstable in aqueous solutions. Furthermore, the removal of water is tedious and expensive due to its high boiling point and high heat of vaporization. In contrast, biocatalysis in organic solvents offer several advantages. Among these advantages are:

1. the use of low boiling point organic solvents, which facilitates the recovery of the product with better overall yield,
2. non-polar substrates are converted at a faster rate due to their increased solubility in the organic solvent,
3. deactivation and/or substrate or product inhibition is minimized,
4. immobilization of enzymes is not required,
5. denaturation of enzymes (loss of the native structure and thus catalytic activity) is minimized.

Stereoselectivity in an enzymatic reaction can be accomplished through kinetic control. This means that one enantiomer reacts faster than the other. The enantioselective performance of enzymes is expressed as the *enantiomeric ratio* E, which is a measure for the selectivity of a enzyme for one of the enantiomers of a substrate. From Michaelis-Menten kinetics equations have been developed for enzyme catalyzed reactions. These expressions relate the conversion of the (racemic) substrate, the enantiomeric excess, and the enantiomeric ratio (E-value). For instance, considering A and B two enantiomer, the faster and slower reacting respectively, that compete for the same active site and assuming the reaction virtually irreversible, and no product inhibition, the enantiomeric ratio is given in Equation 1.

$$E = \frac{\ln\,(A/A_0)}{\ln\,(B/B_0)} = \frac{(V_A/K_A)}{(V_B/K_B)}$$

EQUATION 1.

V_A, K_A and V_B, K_B denote maximal velocities and Michaelis constants of the fast- and

slow-reacting enantiomers, respectively. Equation 1 shows that the discrimination between two competing enantiomers (A and B) by enzymes is equal to the E-value. The relationship between the conversion (*c*) and the enantiomeric excess of the recovered substrate fraction (*ee*(S)) is expressed in the enantiomeric ratio (*E*). Likewise, a relation can be derived that involves the enantiomeric excess of the product (*ee*(*P*)) in an enzyme catalyzed reaction (Equation 2).

$$E = \frac{\ln[(1-c)(1-ee(S))]}{\ln[(1-c)(1+ee(S))]} = \frac{\ln[1-c(1-ee(P))]}{\ln[1-c(1+ee(P))]}$$

Where:

$$c = 1 - \frac{A+B}{A_0+B_0} \qquad ee(S) = \frac{B-A}{A+B}$$

EQUATION 2.

The use of biocatalysis to obtain enantiopure compounds can be divided in two main different methods:

1. Kinetic resolution of a racemic mixture (KR)
2. Biocatalyzed asymmetric synthesis

1.5.1. KINETIC RESOLUTION (KR) AND DYNAMIC KINETIC RESOLUTION (DKR)

In kinetic resolution (KR) of a racemic mixture, the presence of a chiral object (the enzyme) converts one of the enantiomers into product at a greater reaction rate than the other enantiomer (Scheme 3).

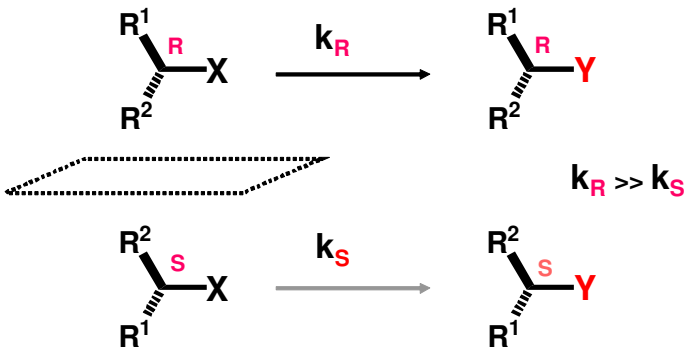

SCHEME 3. Schematic kinetic resolution mechanism.

In an almost ideal situation (E > 200) the difference in the reaction rates of both enantiomers is so high that the reactive enantiomer is transformed fast, and the other is not converted at all. As a consequence, the reaction ceases at 50% conversion, this allowing the isolation of the enantioresolved substrate and product in an optically pure form, which can be separated by conventional methods. In practice, however, most cases of enzymatic resolution do not show this ideal situation, but the ratio of the reaction rates of the enantiomers is not infinite. As a practical rule, Enantiomeric Ratios between 15 and 30 are regarded as moderate to good, and are excellent above this value.

The main limitation of kinetic resolutions is that they are intrinsically limited to a maximum yield of 50%. For this reason, deracemization strategies were developed to overcome this disadvantage.[20] Among them, chemoenzymatic Dynamic Kinetic Resolution (DKR) is one of the most elegant approach. It combines an enzymatic kinetic resolution (KR), with the *in situ* racemisation of the starting material, usually achieved by a chemocatalyst. In this process the *R* and *S* enantiomers, reacting at different rates ($k_R >> k_S$), are kept in rapid equilibrium, so that the racemic starting material can be converted into a single optically pure enantiomer of the product with a theoretical yield of 100%.

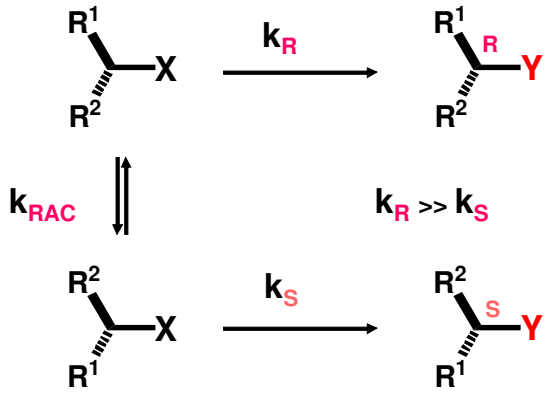

SCHEME 4. Schematic dynamic kinetic resolution mechanism.

In order to design a successful DKR, both the epimerization and resolution steps have to be carefully tuned. Here are a few established general guidelines for an efficient DKR:

1. The kinetic resolution should be irreversible in order to ensure high enantioselectivity.

2. The enantiomeric ratio should be at least greater than ~20.
3. To avoid depletion of the fast reacting enantiomer *R*, racemization (k_{rac}) should be at least equal or greater than the reaction rate of the fast enantiomer (k_R).
4. In case the selectivities are only moderate, k_{rac} should be greater than k_R by a factor of ~10.
5. Obviously, any spontaneous reaction involving the substrate enantiomers as well as racemization of the product should be absent.
6. The enzymatic process and the racemization must be compatible.

A number of common racemization techniques compatible with the biocatalyst used for the resolution has been developed. For instance the base-catalyzed racemization of α-substituted carboxylic acid derivatives and α-substituted carbonyls,[21] has been extensively applied in microbial reductions, as well as the nucleophilic halogen displacement of secondary α-haloesters,[22] combined with the enzymatic hydrolysis or ammonolysis of the ester group.

For the racemization of secondary alcohols transition metal complexes have been proved to be very useful,[23] in combination with the lipase mediated transesterification in organic solvents. Bäckwall and coworkers developed an efficient system for racemisation of sec-alcohols via hydrogen transfer based on the use of a redox Ruthenium catalyst (Shvo's catalyst), used in combination with the *Candida Antarctica* B (CALB) mediated transesterification with *p*-chlorophenyl acetate as acyl donor.[24]

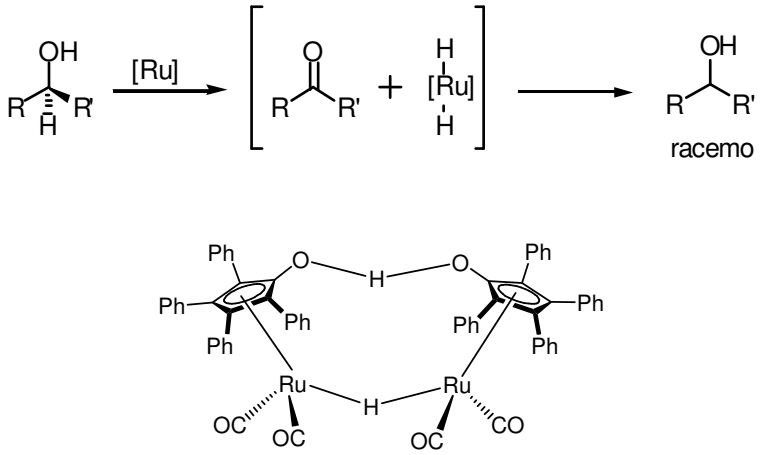

SCHEME 5. Shvo's catalyst

A wide range of substrates including substituted aromatic and aliphatic secondary alcohols and secondary diols[25] have been converted into the corresponding ester with a very high chemical and optical yield.

Biocatalytic methods, such as chemoenzymatic DKR of *sec*-alcohols and baker's yeast reduction of prochiral ketones have been employed for the synthesis of the nitrogen ligands, synthetic targets of the present work.

The next paragraphs briefly describes some features of Lipases and *Saccharomyces Cerevisiae.*

1.5.2. LIPASES

Lipases are ubiquitous enzymes and have been found in most organisms from the microbial, plant, and animal kingdom. Lipases not only hydrolyze fat in the digestion tract or interesterify triglycerides on a technical scale, but are surprisingly flexible biocatalysts for the acylation or deacylation of a wide range of unnatural substrates. Lipase-catalyzed transformations of racemic and prostereogenic compounds usually proceed with high enantioselectivity. If several functional groups amenable to lipase catalysis are present, the reaction is mostly regioselective. Lipases are quite stable and can be obtained from animals and plants as well as from natural and recombinant microorganisms in good yields. Therefore, they are used industrially as detergent enzymes, in paper and food technology, in the preparation of specialty fats, and as biocatalysts for the synthesis of organic intermediates. From an enzymological point of view, lipases exhibit a unique tertiary structure that exposes the catalytically active site only in the presence of a lipid phase or, presumably, in an organic solvent.

The activity of lipases is low on monomeric substrates but strongly enhanced once an aggregated "supersubstrate" (such as an emulsion or a micellar solution for instance) is formed above its saturation limit (Figure 10). This property is quite different from that of the usual esterases acting on water-soluble carboxylic ester molecules. X-ray crystallographic studies revealed a unique mechanism, unlike that of any other enzyme: their three-dimensional structures suggested that interfacial activation might be due to the presence of an amphiphilic peptidic loop covering the active site of the enzyme in solution, just like a lid or flap. From the X-ray structure of co-crystals between lipases and substrate analogues, there is strong indirect evidence that, when contact occurs with a lipid/water interface, this lid undergoes a conformational

rearrangement which renders the active site accessible to the substrate (Figure 11). However not all lipases subscribe to the phenomenon of interfacial activation.

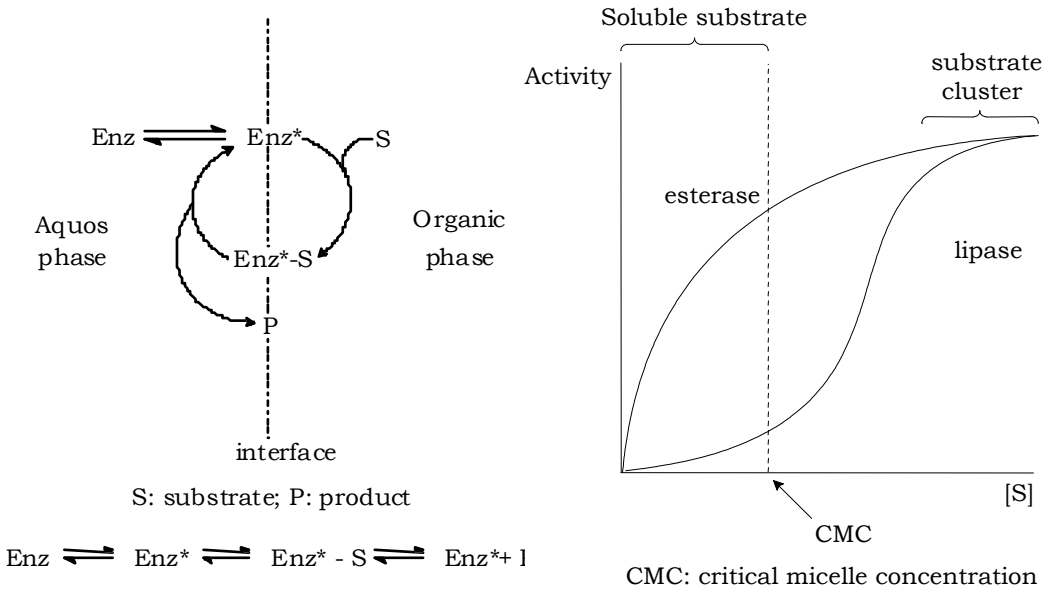

FIGURE 10. Interfacial activation.

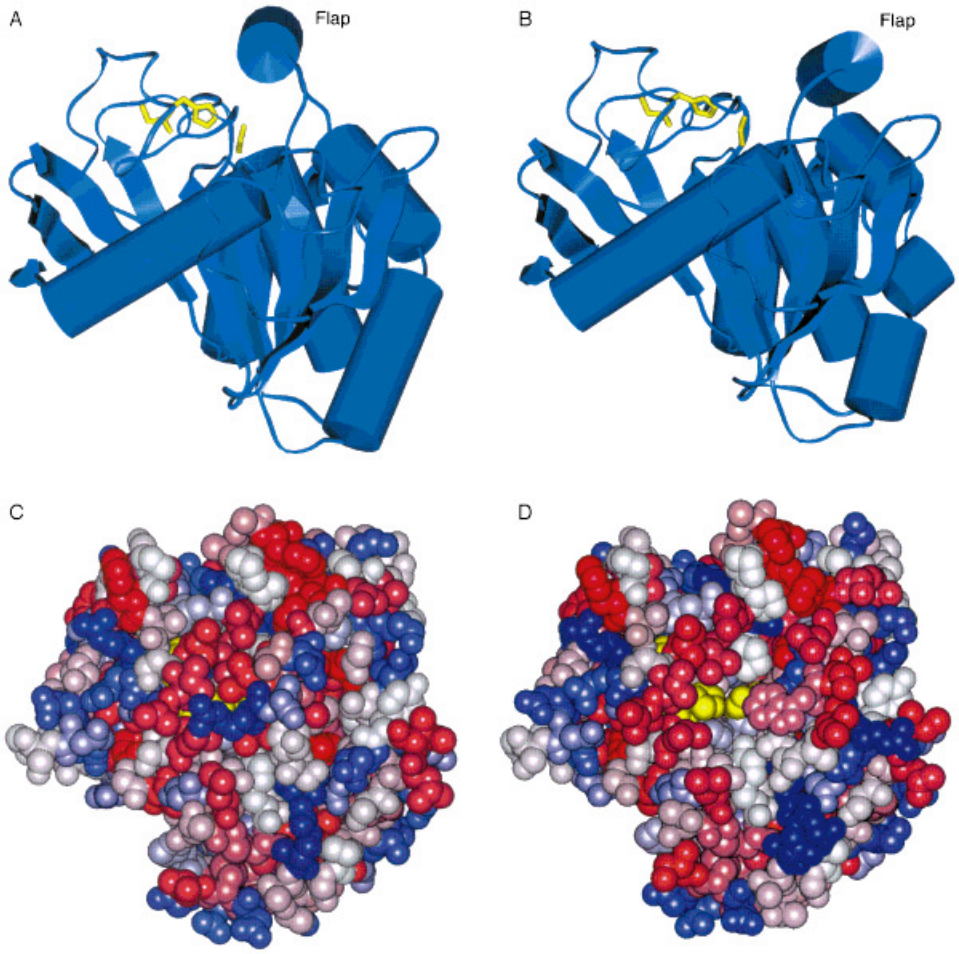

FIGURE 11. Structure of *Mucor miehei* lipase in closed (A, C) and open form (B, D). A and B (side view): the catalytic triad (yellow) and secondary structure elements showing the α/β-hydrolase fold common to all lipases. C and D (top view): space-filling model, colored by decreasing polarity (dark blue ± light blue ± white ± light red ± dark red). Upon opening of the lid, the catalytic triad (yellow) becomes accessible (D), and the region binding to the interphase becomes significantly more apolar.

Lipases hydrolyze ester bonds by means of a catalytic triad, composed of a nucleophilic serine residue activated by a hydrogen bond in relay with histidine and aspartate or glutamate (Scheme 6).[26]

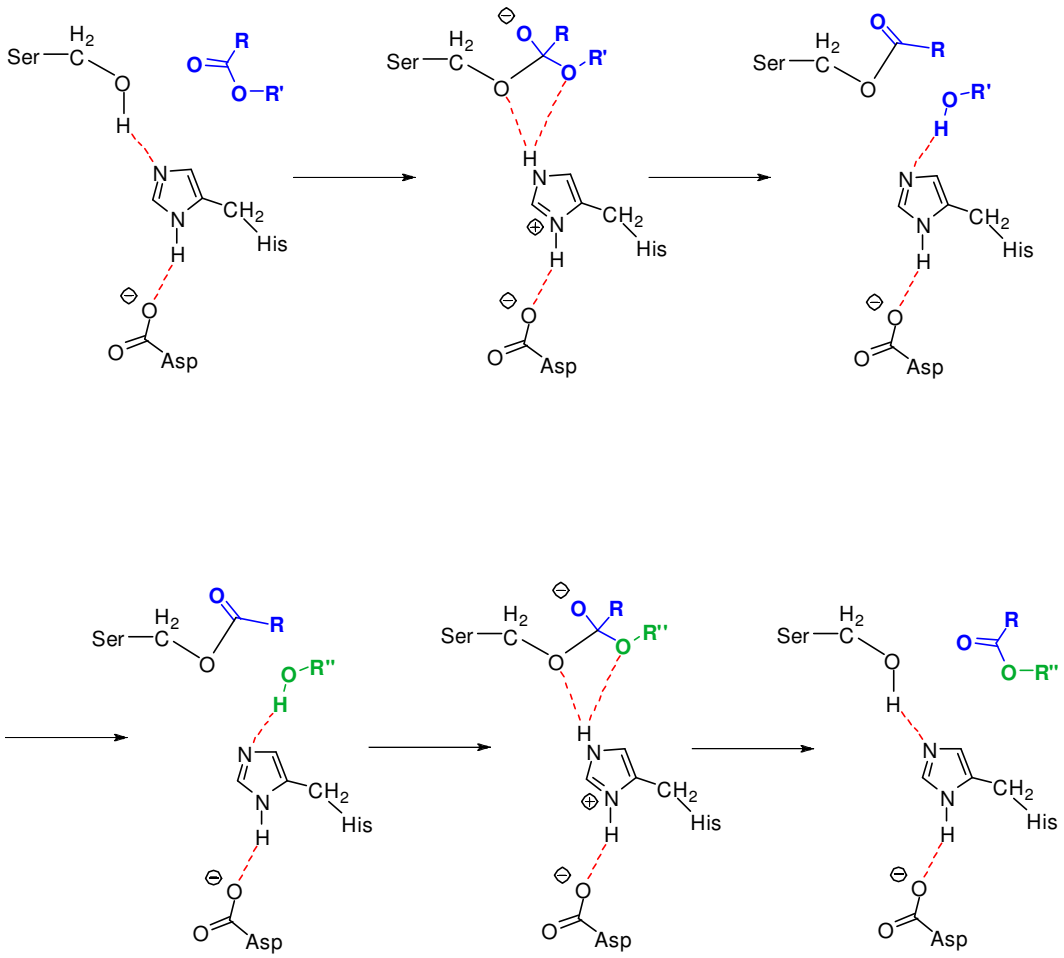

SCHEME 6. A serine protease calalyzed reaction.

The reaction rate and enantioselectivity of enzymatic reactions are affected by the reaction temperature. In general, enhanced temperatures cause an increase in catalytic activity, but at a certain temperature the enzyme can become completely deactivated. Protein denaturation and decrease in enantioselectivity could occur with increase temperature. A way to increase the (thermal) stability of lipases is based on immobilization. However, the use of immobilized lipases in organic solvents has many other advantages compared to their use in the native form:

1. Lipases are less sensitive to denaturation and therefore the observed reaction rate is increased.
2. Immobilization by adsorbing the enzymes onto solid matrices leads to a higher surface area to volume ratio and the enzyme-substrate interaction may be improved.
3. Their recovery is facilitated.
4. Both activity and selectivity can be increased.

Candida antarctica lipase B is one of the most frequently employed lipase in organic solvents for transesterification reactions. It is commercialized also in an immobilized form on polyacrylamide. (Novozyme® 435) (Figure 12).

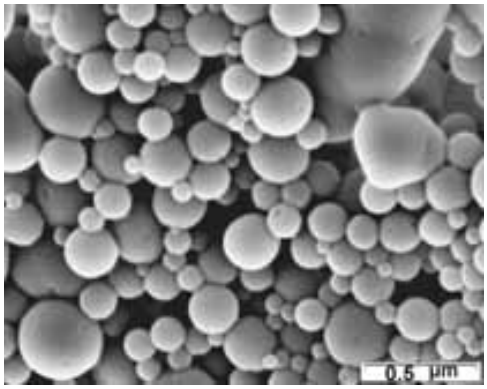

FIGURE 12. Novozyme® 435

Candida antarctica lipase B (CAL-B) shows a very high and general specificity for the (*R*)-enantiomer in the acylation of chiral secondary alcohols,[26,27] which has been fully explained at the molecular level.[28]

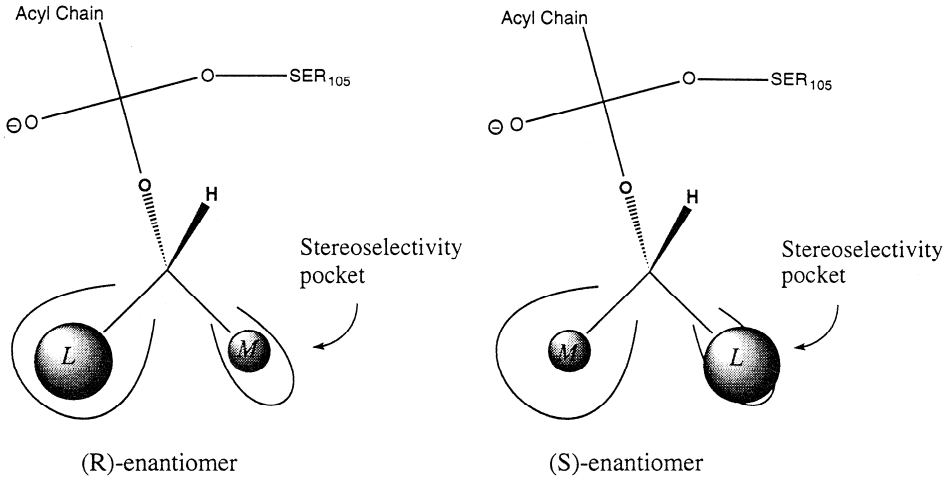

FIGURE 13. Schematic representation of CALB's productive binding modes for alcohol enantiomers.

1.5.3. BAKER'S YEAST

Saccharomyces cerevisiae is a species of budding yeast, it has been widely used in microbial transformations, and yeast-mediated transformations in particular, since the early days of mankind for the production of bread, dairy products, and alcoholic beverages. Baker's yeast (*Saccharomyces cerevisiae*) is commercially available as fresh or dry form and as immobilized yeast too (Figure 13)

(a)  (b) 

FIGURE 13. (a) dry baker's yeast. (b) fresh baker's yeast.

Baker's yeast is by far the most widely employed microorganism for the asymmetric reduction of ketones. It is ideal for non-microbiologists as it is readily available at a very low price, does not reqire sterile fermenters and can be therefore be handled using standard laboratory equpments. It is a very complex enzymatic system in which a number of different dehydrogenanses are present, possessing opposite stereochemical preferences. As a consequence, the stereochemical direction of the reduction may be controlled by careful design of the substrate. Bioreduction with B.Y. follows the empirical Prelog's rule (Scheme 7).

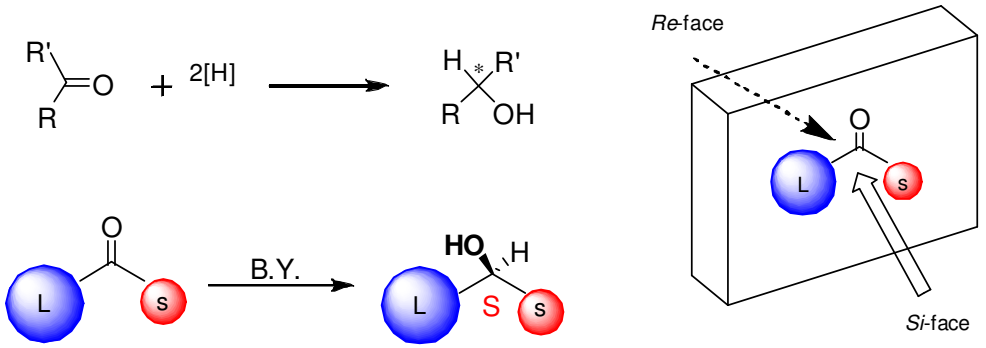

SCHEME 7. Prelog's rule.

For the yeast-catalyzed reduction of the prochiral ketone enzyme has to distinguish between the *Re* and the *Si* enantiotopic faces of the π-system to yield the optically pure chiral alcohol. Ketones with different alkyl side chains (CH_3, Et, *n*-Pr, *n*-Bu, Bz) were reduced by B.Y., and the secondary alcohols obtained were mainly of (*S*) configuration. Only few examples of product predominantly *R*-configured have been observed. Sterically hindered ketones were not reduced at all. These results suggest a hydrogen transfer to the *Re* face of the prochiral ketone (Scheme 7) with L representing a large substituent and S a small substituent adjacent to the carbonyl group to yield alcohol**.**

Thanks to its versatility and selectivity differen unnatural substrates were reduced by *Saccharomyces cerevisiae,* such as: cycloalkanones, aliphatic alkanones, sulphur containing molecules, nitrocarbonyl compounds, cyclic and acyclic dicarbonyl compounds (diketones, α,β-ketoesters), fluorine-containing compounds and organometallic compounds. Baker's yeast has been successful used also in some C-C bond formation reaction and cyclization which require high stereoselectivity.[29]

REFERENCES

1. Noyori, R. *Adv. Synth. Catal.* **2003**, *345*, 15-32.
2. Giury, P. J.; Saunders, C. P. *Adv. Synth. Catal***. 2004**, *346*, 497-537.
3. Albrecht, M.; van Kotem, G. *Angew. Chem. Int. Ed* **2001**, *40*, 3750-3781.
4. (a) Newkome, G.R. ; Puckett, W.E.; Gupta, V. K.; Kiefer, G. E. *Chem. Rev.* **1986**, *86*, 451-489. (b) Shilon, A. E.; Shul'pin, G. B. *Chem. Rev.* **1997**, *97*, 2879-2932.
5. Singleton, John T. *Tetrahedron* **2003**, *59*, 1837-1857.
6. (a) Pàmies, O.; Bäckvall, Jan-E. *Chem. Rev.* **2003**, *103*, 3247-3261. (b) Noyori, R. *Angew. Chem., Int. Ed.* **2002**, *41*, 2008-2022. (c) Noyori, R.; Ohkuma, T. *Angew. Chem., Int. Ed.* **2001**, *40*, 40-73. (d) Knowles, W. S. *Angew. Chem., Int. Ed.* **2002**, *41*, 1998-2007. (e) Rossen, K. *Angew. Chem., Int. Ed.* **2001**, *40*, 4611-4613. (f) Tang, W.; Zhang, X. *Chem. Re*v. **2003**, *103*, 3029-3070.
7. (a) Noyori, R.; Hashigughi, S. *Acc. Chem. Res.* **1997**, *30*, 97-102. (b) Mao, J.; Wan, B.; Wu, F.; Lu, S. *Tetrahedron Lett.* **2005**, *46*, 7341-7344.
8. (a) Baratta, W.; Chelucci, G.; Gladiali, S.; Siega, K.; Toniutti, M.; Zanette, M.; Zangrando, E.; Rigo, P. *Angew. Chem. Int. Ed*, **2005**, *44*, 6214-6219. (b) Baratta, W.; Bosco, M.; Chelucci, G.; Del Zotto, A.; Siega, K.; Toniutti, M.; Zangrando, E.; Rigo, P. *Organometallics*, **2006**, *25*, 2611-4620. (c) Baratta, W.; Chelucci, G.; Magnolia, S.; Siega.; Rigo,P. *Chem. Eur. J.* **2009**, *15*, 726-732.
9. Togni, A.; Venanzi, L. M. *Angew. Chem. Int. Ed. Engl.* **1994**, *33*, 497-526.
10. Durand, J.; Milani, B. *Coord. Chem. Rev.* **2006,** *250*, 542-560.
11. Bianchini, C.; Meli, A. *Coordination Chemistry Reviews* **2002,** *225*, 35-66.
12. (a) Milani, B.; Scarel, A.; Mestroni, G.; Gladiali, S.; Taras, R.; Carfagna, C.; Mosca, L. *Organometallics* **2002,** *21*, 1323-1325. (b) Scarel, A.; Milani, B.; Zangrando, E.; Stener, M.; Furlan, S.; Fronzoni, G.; Mestroni, G.; Gladiali, S.; Carfagna, C.; Mosca, L. *Organometallics* **2004,** *23*, 5593-5605. (c) Chelucci, G.; Thummel, R. P. *Chem. Rev*. **2002**, *102*, 3129-3170.
13. (a) Binotti, B.; Carfagna, C.; Gatti, G.; Martini, D.; Mosca L.; Pettinari, C. *Organometallics* **2003**, *22*, 1115. (b) Brookhart, M.; Wagner, M. I. *J. Am. Chem. Soc.* **1994**, *116*, 3641-3642.
14. Espinet, P.; Soulantica, K. *Coord. Chem. Rev.* **1999**, *193-195*, 499-556.
15. Maggini, S. *Coord. Chem. Rev*. **2009**, *253*, 1793-1832.
16. (a) Sun, W.-H.; Li, Z., Hu, H.; Wu, B.; Yang, H.; Zhu, N.; Leng, X.; Wang, H. *New J. Chem.* **2002**, *26*, 1474-1478. (b) Sun, W.-H.; Zhang, W.; Gao, T.; Tang, X.; Chen, L.; Li, Y.; Jin, X. *J. Organomet. Chem.* **2004**, *689*, 917-929.

17. (a) Chen, H.-P.; Liu, Y.-H.; Peng, S.-M.; Liu, S.-T. *Organometallics* **2003**, 22, 4893-4899. (b) O. Daugulis, M. Brookhart *Organometallics* **2002**, *21*, 5926-5934. (c) Jiang, Z.; Sen, A. *Organometallics* **1993**, *12*, 1406-1415.
18. (a) Aeby, A.; Bangerter, F.; Consiglio, G. *Helvetica Chimica Acta* **1998**, *81*, 764-769. (b) Gsponer, A.; Schmid, T. M:, Consiglio, G. *Helvetica Chimica Acta* **2001**, *84*, 2986-2995. (c) Sperrle, M.; Aeby, A.; Consiglio, G. *Helvetica Chimica Acta* **1996**, *79*, 1387-1392. (d) Aeby, A.; Gsponer, A.; Sperrle, M.; Consiglio, G. *J. Organomet. Chem.* **2000**, *603*, 122-127. (e) Aeby, A.; Consiglio, G. *Inorganica Chimica ACTA* **1999**, *296*, 45-51.
19. Robert A. Copeland, *Enzymes: A Practical Introduction to Structure, Mechanism, and Data Analysis*, **2000** by Wiley-VCH, Inc.
20. Strauss, U. T.; Felfer, U.; Faber, K. *Tetrahedron: Asymmetry* **1999**, *10*, 107-117.
21. (a) Fogal, E. *Tetrahedron: Asymmetry* **2001**, *11*, 2599-2614. (b) Dehli, J.; Gotor, V. *J. Org. Chem.* **2002**, *67*, 6816-6819.
22. (a) Badjic, J. D.; Kadnikova, E. N.; Kostic, N. M. *Org. Lett.* **2001**, *3*, 2025-2028. (b) Jones, M.M.; Williams, J. M. J. *Chem.Commun*. **1998**, *1,* 2519-2520.
23. (a) Riermeier, T. H.; Gross, P.; Monsees, A.; Hoff, M.; Harald Trauthwein, H. *Tetrahedron Letters* **2005,** *46*, 3403–3406. (b) Kim, M.-J.; Ahn, Y.; Park, J. *Curr. Opin. Biotechnol*. **2002**, *13*, 578–587. (c) Huerta, F. F.; Minidis, A. B. E.; Bäckvall *J.-E. Chem. Soc. Rev.* **2001**, *30*, 321–331.
24. B. Anders Persson, A.L.E. Larsson, M. Le Ray, Jan-E. Bäckvall *J. Am. Chem. Soc.* **1999**, *121*, 1645-1650.
25. van Nispen, Sjoerd F. G. M.; van Buijtenen, J.; Vekemans, Jef A. J. M.; Meuldijk, J.; Hulshof, L. A., *Tetrahedon: Asymmetry* **2006**, 17, 2299-2305.
26. Rotticci, D.; Hæffner, F.; Orrenius, C.; Norin, T.; Hult, K. *J. Mol. Catal. B: Enzym.* **1998**, *5*, 267–272. (b) Chen, C.-S.; Fujimoto, Y.; Girdaukas, G.; Sih, C. J. *J. Am. Chem. Soc.* **1982**, *104*, 7294–7299.
27. Schmid, R.D.; Verger, R. *Angew. Chem. Int. Ed*. **1998**, *37*, 1608-1633.
28. (a) Mccabe, R. W.; Rodger, A.; Taylor, A. *Enzyme Microb. Technol.* **2005**, *36*, 70–74. (b) Uppenberg, J.; Ohrner, N.; Norin, M.; Hult, K.; Kleywegt, G. J.; Patkar, S.; Waagen, V.; Anthonsen, T.; Jones, T. A. *Biochemistry* **1995**, *34*, 16838–16851. (c) Uppenberg, J.; Hansen, M. T.; Patkar, S.; Jones, T. A. *Structure* **1994**, *2*, 293–308.
29. Csuk, R., *Chem. Rev.* **1991**, 91, 49-97.

Chapter 2:
Synthesis and application of CNN pincer ligands

2.1. CHEMOENZYMATIC SYNTHESIS OF CHIRAL PINCER LIGANDS

Metal complexes of general structure **1** (Figure 1), in which ruthenium(II) and osmium(II) are bound to a diphosphine and a bi- or tricyclic, aminomethylpyridine-based, *C,N,N*-terdentate ligand (CNN pincer), have recently shown to be extremely efficient precatalysts for the catalytic reduction of aromatic ketones.[1] Ruthenium(II) complexes, in which the CNN pincer ligand **2** is present in combination with different diphosphines, are the most active catalysts in the transfer hydrogenation of alkyl aryl ketones in 2-propanol, displaying turnover frequencies of up to 10^6 h^{-1} at remarkably low catalyst loadings (0.005-0.001 mol %).[1a] Moreover, Ru(II)[1b] and Os(II)[1c] complexes containing the chiral CNN ligands (*R*)-**3** and (*R*)-**4** gave high enantioselectivities (up to 98% e.e. of the alcohol products) in the transfer hydrogenation of prochiral ketones. The Os(II) derivatives are also excellent catalysts for the asymmetric hydrogenation of ketones.[1c] More recently,[1d] comparably high enantioselectivities and productivities have been obtained with Ru and Os complexes prepared from the racemic tricyclic benzo[*h*]quinoline ligand **5** and chiral diphosphines. On account of their importance as scaffolds for chiral ligands and as bioactive compounds,[2] the synthesis of chiral aminoalkylpyridines is of special interest. Common approaches based on asymmetric synthesis include the addition of organometallics to chiral imines,[3] the enantioselective catalytic reduction of imines[4] and hydrazones,[5] and the catalytic hydroamination of alkenes.[6] The synthesis of chiral ligands (*R*)-**3** and (*R*)-**4** *via* the diastereoselective reduction of chiral N-*p*-toluenesulfinyl ketimines was also reported.[7] An alternative approach to (*R*)-**4** was also described,[7c] via mesylation of the corresponding (*S*)-alcohol **13**, obtained from a chiral precursor, and displacement with azide; this method, however, suffered from a significant loss of enantiopurity in the substitution step. Biocatalysis with whole cell systems and isolated enzymes provides a clean alternative for the synthesis of a variety of chiral building blocks with high degree of selectivity under mild reaction conditions.[8] Enantiomerically pure secondary alcohols, in particular, can be efficiently obtained by lipase-catalyzed resolution of the corresponding racemic mixtures[9] and by the asymmetric reduction of prochiral ketones with baker's yeast (*Saccharomyces Cerevisiae).*[10] The enantiospecific acylation of chiral amines is also described in the literature[11] but while the dynamic kinetic resolution (DKR)[12] of racemic *sec*-alcohols is well established, few protocols have been reported for the DKR of amines.[11] When we applied these conditions to the resolution of 6-substituted 2-(1-

aminoethyl)pyridines, the resulting enantiospecificity was unsatisfactory, and harsh conditions were required for the recovery of amines from the resolved acetamides.

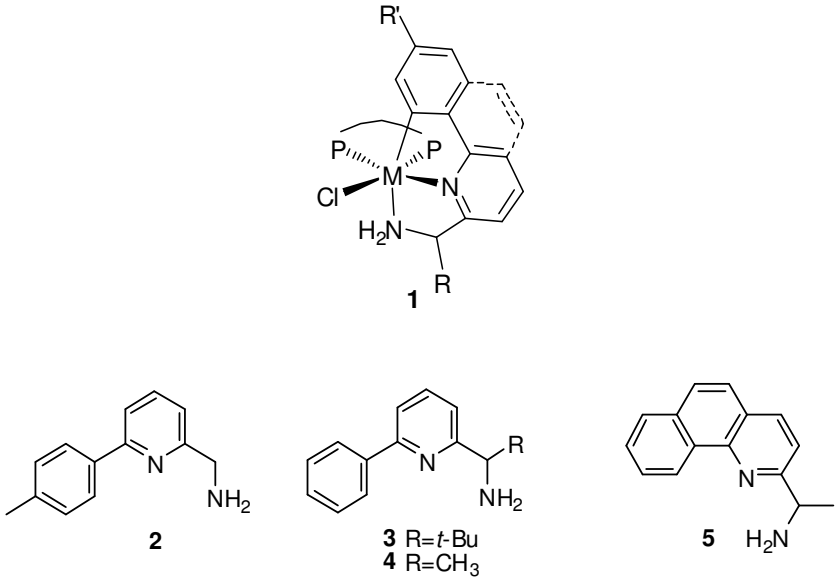

FIGURE 1. CNN pincer ligands and metal complexes.

This chapter describes the synthesis of both enantiomers of 1-(6-phenylpyridin-2-yl)ethanamine **4** and 1-(benzo[*h*]quinolin-2-yl)ethanamine **5** (Scheme 1),[13] starting from the prochiral ketones 6,7 by the application of biotransformation procedures. leading in enantiocomplementary fashion to both enantiomers of the *sec*-alcohols *S*- and (*R*)-**8,9**, intermediates to the final amine products (*R*)- and (*S*)-**4,5**

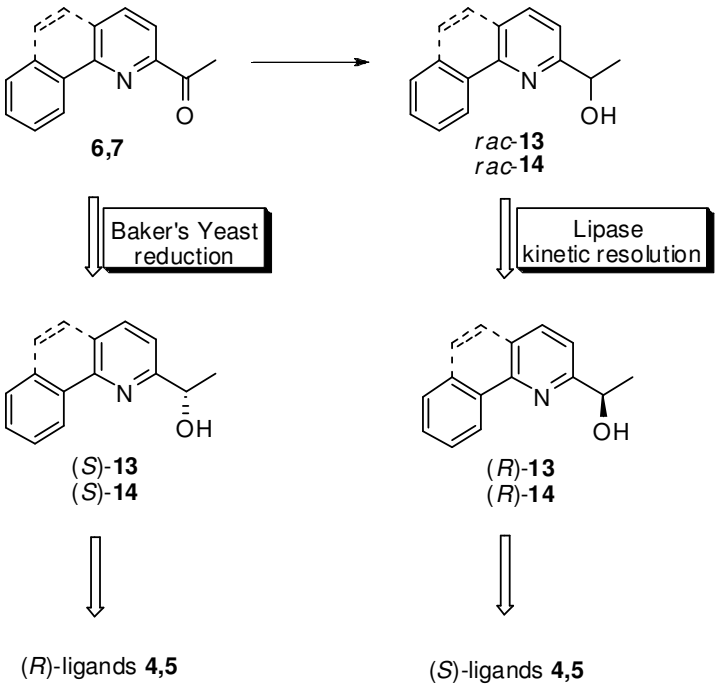

SCHEME 1. General strategy for the synthesis of chiral not racemic pincer ligands **4** and **5**.

2.2. SYNTHESIS OF PROCHIRAL KETONES AND RACEMIC ALCOHOLS

Prochiral ketones **6** and **7** were used as starting material for the synthesis of amine pincer ligands **4** and **5**.

2-Acetyl-6-phenylpyridine (**6**) was prepared by Suzuki coupling between commercial phenylboronic acid (**9**) and 2-acetyl-6-bromopyridine (**8**) (Scheme 2).[14]

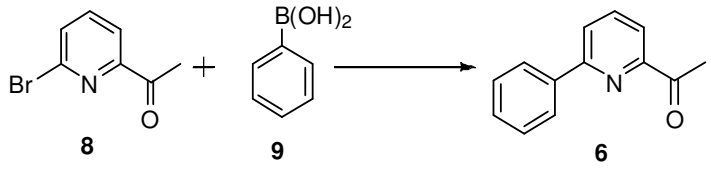

SCHEME 2. Reaction conditions: *n*-propanol, K_2CO_3 2M, H_2O, PPh_3, $Pd(OAc)_2$.

The coupling was carried out in *n*-propanol under mild basic condition, the catalysts beeing a Pd(0) system obtained *in situ* by reduction of $Pd(OAc)_2$ with PPh_3. The reaction mixture was refluxed overnight and after purification by column chromatography ketone **6** was obtained in 70-90% yield.

Ketone **7** was prepared from benzo[*h*]quinoline, by a five-steps procedure, (Scheme 3) involving the intermediacey of the more active N-oxide intermediate (**10**), obtained in

good yield (83%) by oxidation with *m*-chloroperbenzoic acid. Under the common oxidative conditions (H_2O_2/CH_3COOH[16]) the product was obtained in a much lower yield (50%). Chlorination with $POCl_3$[15] gave a 85:15 mixture of 2-chlorobenzo[*h*]quinoline (**11a**) and 4-chlorobenzo[*h*]quinoline (**11b**), from which the desired isomer (**11a**) was separated by flash chromatography. Compound **11a** was then converted into the more active 2-bromo derivative (**12**) by reaction with bromotrimethylsilane in refluxing propionitrile, or alternatively in a refluxing 33% solution of hydrobromic acid in acetic acid.[17] Lithiation of 2-bromobenzo[*h*]quinoline (**12**) (*n*-BuLi, -78°C, THF) followed by acetylation with N,N-dimethyl-acetamide afforded the tricyclic ketone **7** in 5 steps and 40% overall yield from benzo[*h*]quinoline.

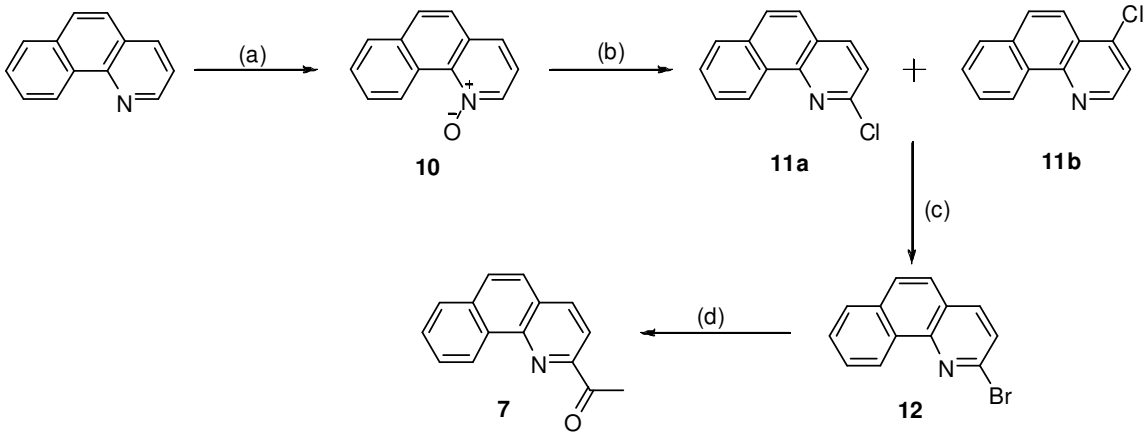

SCHEME 3. Synthesis of tricyclic ketone **7**. Reaction conditions: (a) MCPBA, $CHCl_3$, 4 days. (b) $POCl_3$, reflux, 30'. (c) $(CH_3)_3SiBr$, CH_3CH_2CN or HBr 33%, CH_3COOH, reflux. (d) THF, Ar, *n*-BuLi, -78°C, N,N-dimethyl-acetamide.

$NaBH_4$ reduction of **6**,**7** gave quantitatively the racemic alcohols *rac*-**13** and *rac*-**14**, which were treated for kinetic resolution as described in paragraph 1.3. (Scheme 4).

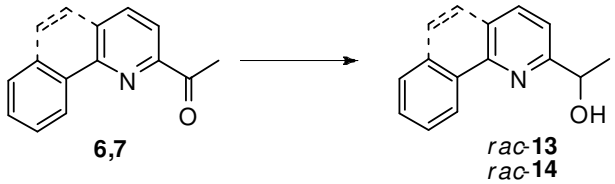

SCHEME 4. Chemical reduction of ketones. Reaction conditions: $NaBH_4$, EtOH.

2.3. BIOREDUCTION WITH BAKER'S YEAST (*Saccharomyces Cerevisiae*)

Asymmetric reduction of prochiral ketones with baker's yeast provides an efficient access to the synthesis of optically pure secondary alcohol.

Prelog's rule[18] anticipated that the baker's yeast reduction of prochiral ketones **6** and **7** would proceed with delivery of the hydride to the *Re* face of the carbonyl, affording the (*S*) alcohols (Figure 2, Scheme 5).

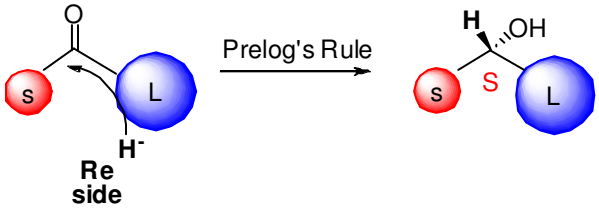

FIGURE 2. Hydride attack on the Re face: S= small group; L= large group.

Bioreduction of **6**,**7** was accomplished under fermenting conditions, by preincubating baker's yeast in the reaction medium for 30 minutes at 37°C before substrate addition. The reaction were monitored at regular intervals with HRGC, following the conversion of the starting ketone **6** and **7** into the corresponding alcohols **13** and **14**.

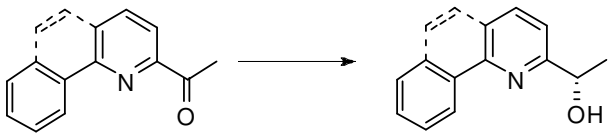

6,7 (*S*)-**13** (*S*)-**14**

SCHEME 5. Baker's yeast reduction of ketones **6**,**7**. Reaction conditions: baker's yeast, phosphate buffer Na_2HPO_4/KH_2PO_4 0.1 M pH 7.4, glucose.

Optimization of the reaction conditions needed a screening of solvents, as indicated in Table 1, which summarizes the most significant results**.**

TABLE 1. Bioreduction of ketone **6**.

Conc. (mM)	g B.Y./mmol subst.	B.Y. type	Solvent	Glucose (g/L)	Time (days)	Conv. (%)	e.e.% (*S*)[b]
50	10	wet	Water	_	10	35	> 99.9
26	5.6	wet	Water	163	6	44	> 99.9
3.6	31	wet	Buffer[a]	112	4-7	86	> 99.9
3.6	15.5	dry	Buffer[a]	112	6	98	> 99.9

[a]Buffer = phosphate buffer Na_2HPO_4/KH_2PO_4 0.1 M pH 7.4. [b] The conversion and e.e.% were determined by HRGC analysis.

The optically pure alcohol (*S*)-**13** was shown to be formed as a single product in each case. As far as the conversion and the reproducibility are concerned, the best results were obtained by using dry B.Y. in phosphate buffer.

All the intermediates and products were fully characterized by spectroscopic (IR, NMR, MS) and chirooptical (α, CD) tecniques, while enantiomeric excesses were determined by chiral HRGC.

Surprisingly, under the same conditions, the bioreduction of the tricyclic ketone **7** did not proceed beyond 12% conversion, probably as a consequence of both the steric hindrance of the rigid tricyclic aromatic structure, preventing the substrate from accessing the active site of the alcohol dehydrogenase, and the low solubility of the benzo[*h*]quinoline system in aqueous medium. An attempt to improve the conversion was made, by adding DMSO as an organic water miscible co-solvent[20] to the reaction mixture, in order to increase the solubility of the substrate (Table 2), but with unsatisfactory results.

TABLE 2. Bioreduction of ketone **7**.

Conc. (mM)	g B.Y./mmol subst.	DMSO (mL)	Solvent	Glucose (g/L)	Time (days)	Conv. (%)	e.e.% (*S*)[b]
3.6	15.5	10	Buffer[a]	112	9	4	–
4.1	22	10	Water	25	9	12	77

[a] Buffer = phosphate buffer Na_2HPO_4/KH_2PO_4 0.1 M pH 7.4. [b] The conversion and was determined by HRGC analysis; e.e.% was determined from the ^{1}H NMR analysis of the corresponding Mosher's ester.

The desired alcohol (*S*)-**14** was therefore provided by the classical kinetic resolution procedure, as described in paragraph 2.4..

2.4. KINETIC RESOLUTION

Candida antarctica lipase B (CAL-B) is known to show a very high and general specificity for the (*R*) enantiomer in the acylation of chiral secondary alcohols.[21] Therefore, we decided to use Novozyme® 435 (CAL-B immobilized on polyacrylamide) for the kinetic resolution of racemic alcohols **13** and **14** (Scheme 6). The resolution progress was monitored by HRGC, stopping the reaction at 50% conversion (1 h). The KR could be quenched just filtering-off the enzyme.

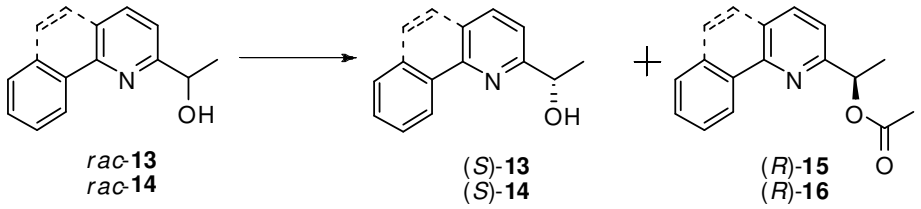

rac-**13**
rac-**14**
(*S*)-**13**
(*S*)-**14**
(*R*)-**15**
(*R*)-**16**

SCHEME 6. Kinetic resolution of racemic alcohol *rac*-**13** and *rac*-**14**. Reaction conditions: *t*-butylmethylether, Ar, vinyl aceate, CAL-B, 28 °C.

The lipase-catalyzed asymmetric acetylation of *rac*-**13**, with Novozyme® 435 and vinyl acetate in *t*-butylmethylether at room temperature gave the corresponding (*R*)-acetate **15** with excellent enantioselectivity (enantiomeric ratio $E > 500$) and with recovery of the unreacted alcohol (*S*)-**13** in a 79% e.e.. Similarly, the tricyclic alcohol **14** gave the corresponding (*R*)-acetate **16** in 40% yield (44% conversion) and e.e. > 99% ($E > 500$), while the recovered alcohol (*S*)-**14** had 86% e.e. (Table 3).

TABLE 3. Summary of KR data.

Substrate	E (enantiomeric ratio)	Conversion (%)	(*R*)-acetate e.e. % (yield %)	(*S*)-alcohol e.e.% (yield %)
(±)-**13**	> 500	46	**15**[a] > 99.9(45)	**13**[a] 79 (50)
(±)-**14**	> 500	44	**16**[b] > 99 (40)	**14**[b] 86 (47)

Reaction conditions: see Scheme 6. [a] The conversion and e.e.% (after hydrolysis of (*R*)-**15**) were determined by HRGC analysis. [b] The conversion was determined by HRGC analysis, e.e.% (after hydrolysis of (*R*)-**16**) was determined from the ^{1}H NMR analysis of the corresponding Mosher's ester.

After hydrolysis of the acetates **15** and **16** the corresponding (*R*)-alcohols **13** and **14** were isolated with the same e.e.. However, the yields in the enantioresolved compounds (*R*)-**13** and (*R*)-**14** were low, as intrinsically limited by the 50% maximum attainable in a kinetic resolution, and because of the need for a chromatographic separation of alcohol and ester.

Both limitations were overcome by applying to the lipase-catalyzed transesterification of *rac*-**13** and *rac*-**14** the conditions developed by Bäckvall et al. for the dinamic kinetic resolution of *sec*-alcohols.[22]

2.5. DYNAMIC KINETIC RESOLUTION

Based on the wide literature reported on this topic,[11,22] the dynamic kinetic resolution of *rac*-**13** and *rac*-**14** was run combining the CAL-B mediated enzymatic acetylation with the *in situ* racemization of the slow reacting enantiomer, catalysed by the Ru redox catalyst [$Ru_2(CO)_4(\mu$-H)(C_4Ph_4-$COHOCC_4Ph_4$)] (Shvo's catalyst) (Scheme 7).

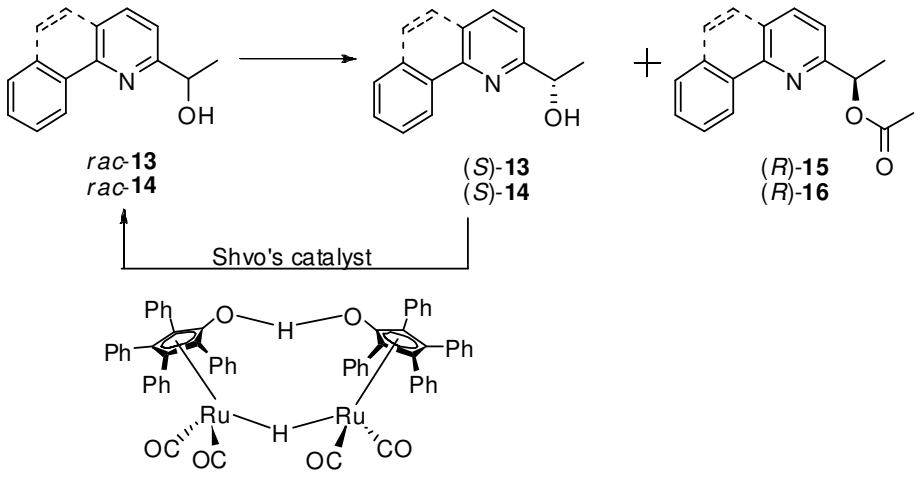

SCHEME 7. Dynamic kinetic resolution of alcohols **13** and **14**. Reaction conditions: toluene, Ar, 4-chlorophenylacetate, CAL-B, $[Ru_2(CO)_4(\mu\text{-}H)(C_4Ph_4COHOCC_4Ph_4)]$, 70°C.

Unlike KR, the DKR strategy needs *p*-chlorophenylacetate as the acyl donor, because this reagent is very mild and does not affect the ruthenium complex. The use of vinyl acetate or *iso*-propenylacetate in fact, causes oxidation of the alcohol substrate due to the reactivity of acetaldehyde and acetone as hydrogen acceptors, this limiting the yield of the acetylation. On the other hand, activated esters bearing protons in the α-position such as trichloroethyl- or trifluoroethylacetates, which are frequently used in the transesterification of alcohols, are not suitable in combination with Ru(II) since the alcohol released interfere with the ruthenium catalyst.

Aryl esters such as *p*-chlorophenylacetate avoid the problem encountered with vinylacetates and with activated trihaloethylacetates and have been used successfully.[22a]

The DKR reached a complete conversion, enantioconverging to the acetates (*R*)-**15** and (*R*)-**16** as unique products. These were isolated in 70% yield (not optimized) after column chromatography

Hydrolysis under mild basic conditions of the optically active esters gave the corresponding enantiopure secondary alcohols (*R*)-**13** and (*R*)-**14**, in 70% overall yield from the racemic alcohols (Table 4). The (*R*) configuration of the compounds thus obtained results from the well-known preferential recognition of (*R*) enantiomers by CAL-B,[21] and was confirmed by chirooptical techniques (α, CD).[23]

TABLE 4. summary of DKR data.

Substrate	Conversion (%)	(*R*)-alcohol[a] e.e.% (yield %)
(±)-**13**	93	**13**[b] >99.9(70)
(±)-**14**	92	**14**[c] > 99 (70)

Reaction conditions: see Scheme 7. [a] From ester hydrolysis under basic conditions. [b] The conversion and e.e.% were determined by HRGC analysis. [c] The conversion was determined by HRGC analysis, e.e.% (after hydrolysis of (*R*)-**16**) was determined from the ^{1}H NMR analysis of the corresponding Mosher's ester.

2.6. CONVERSION OF THE ALCOHOLS TO THE AMINES

To obtain the target amines (*S*)-**4** and (*S*)-**5** in an optically pure form from the homochiral alcohols **13** and **14**, different attempts were made involving an S_N2 strategy (Scheme 9) with inversion of configuration. Classical Mitsunobu conditions, lead to a complex mixture of unidentified products. Therefore the homochiral alcohols (*R*)-**13** and (*R*)-**14** were first converted into the corresponding azides (*S*)-**17** and (*S*)-**18**. This transformation was best carried out with diphenylphosphoroazidate (DPPA) in the presence of 1,8-diazabicyclo[5.4.0]undec-7-ene (DBU) (Scheme 9, entry 4).[26] These conditions lead to a clean S_N2 inversion, avoiding racemization and olefin formation, which are commonly observed in the classical Mitsunobu reaction. The reaction mechanism takes place in two discrete steps (Scheme 8), the first being the formation of a phosphate intermediate (**19**) followed by releasing of the N_3^- from the hindered DBU salt (**20**).

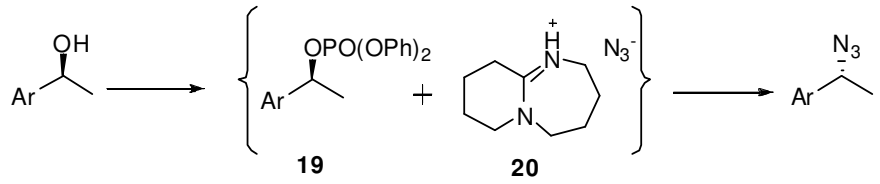

SCHEME 8. Nucleophilic displacement. Reaction conditions: toluene, DPPA, DBU, 0-50°C.

By this procedure, alcohols (*R*)-**13** and (*R*)-**14**, having >99.9% e.e. and >99% e.e. respectively, were converted into the corresponding azides (*S*)-**17** and (*S*)-**18**, with only a slight erosion of the enantiomeric purity, which dropped to 97% and 95% respectively.

On the other hand, conversion of the alcohols to the azides through the corresponding methansulphonate (entry 2) or with PPh_3, DIEA, DPPA (entry 3)[25] dramatically decreased the enantiomeric purity to an approximately 50% e.e. value (Scheme 9).

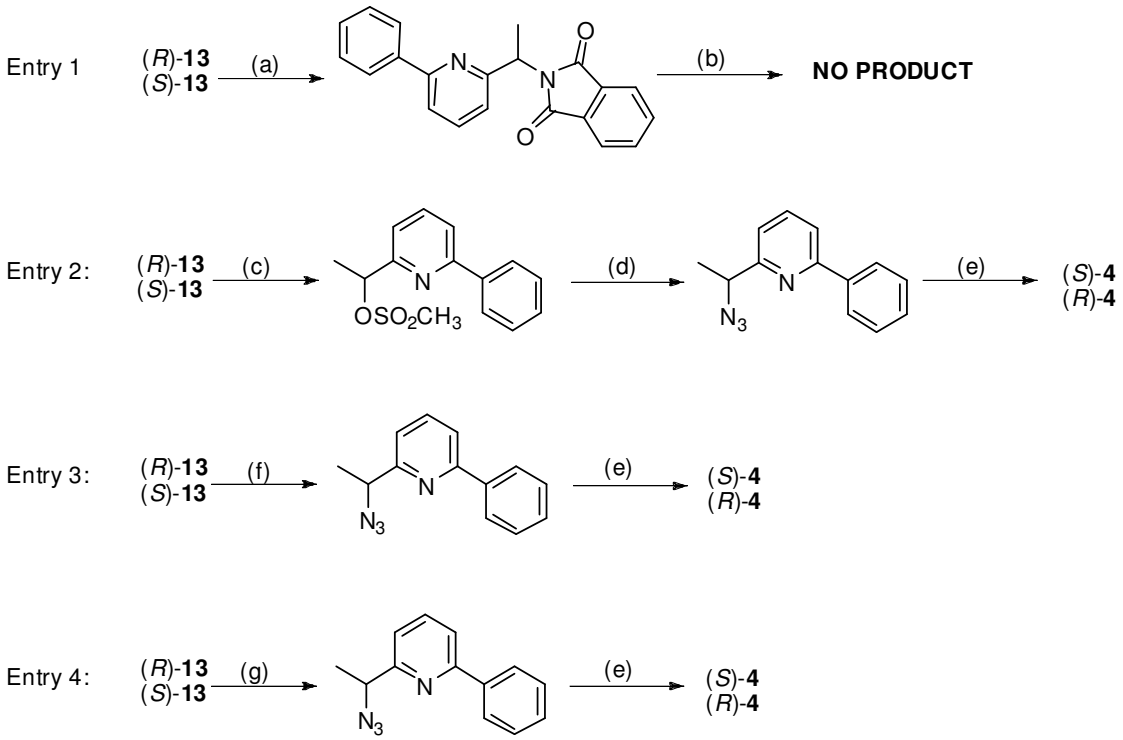

SCHEME 9. Attempted Mitsunobu reactions. Reactions conditions: Entry 1[24]: (a) phtalimide, PPh_3, THF, DIEA; (b) $NH_2NH_2*H_2O$, EtOH, reflux. Entry 2: (c) CH_3SO_2Cl, Et_3N; (d) NaN_3, 18_crown 6; (e) PPh_3, THF/H_2O. Entry 3: (f). PPh_3, DIEA, DPPA; (e) PPh_3, THF/H_2O. Entry 4: (g) DPPA, DBU, 0°C-50°C, (e) PPh_3, THF/H_2O.

Finally, conversion of the azides (*S*)-**17** and (*S*)-**18** into the corresponding amines (*S*)-**4** (97% e.e.) and (*S*)-**5** (95% e.e.) was carried out by treatment with Ph_3P in refluxing THF/H_2O.[27]

The best results observed in the conversion of the optically pure *sec*-alcohols (*R*) and (*S*)-**13**,**14** into both enantiomers of the corresponding amines (*R*) and (*S*)-**4**,**5** are summarized in the following table (Table 5).

TABLE 5. Enantiomeric excesses of azides **17** and **18** and amines **4** and **5**.

Alcohol e.e.%	Azide e.e.% (yield %)	Amine e.e.% (yield %)
(*R*)-**13** > 99.9	(*S*)-**17**[a] 97(75)	(*S*)-**4** 97 (95)
(*S*)-**13** > 99.9	(*R*)-**17**[a] > 99.9 (75)	(*R*)-**4** > 99.9 (95)
(*R*)-**14** > 99	(*S*)-**18** 95 (75)	(*S*)-**5**[b] 95 (95)
(*S*)-**14** 86	(*R*)-**18** 80 (75)	(*R*)-**5**[b] 80 (95)

Reaction conditions: see Scheme 9, entry 4. [a] e.e.% was determined by chiral HRGC analysis. [b] e.e.% was determined from the ^{1}H NMR analysis of the corresponding mandelic amide.

The e.e. % values reported for (*R*)- and (S)-**4** were determined directly by HRGC (β-cyclodextrin) analysis of the azides intermediates (*R*)-**17** and (*S*)**-17**, while in the case of (*R*)-**5** and (*S*)-**5**, derivatization into the corresponding mandelic acid amide derivative, followed by ^{1}H-NMR analysis of the diastereoisomeric mixture obtained was necessary.

The CD spectra of chiral ligands (*S*)-**4** and (*S*)-**5** thus obtained support the configurational assignments (Figure 3). In particular, the Cotton effect for at 280 nm is the same for both ligands, suggesting that they have the same configuration. The same, of course, must be true for all of their precursors. As the (*R*) configuration had already been attributed to the acetate **15** derived from the CAL-B catalyzed transesterification of racemic alcohol **13**, the same configuration can also be assigned to the acetate **16** derived from the kinetic resolution of **14**.

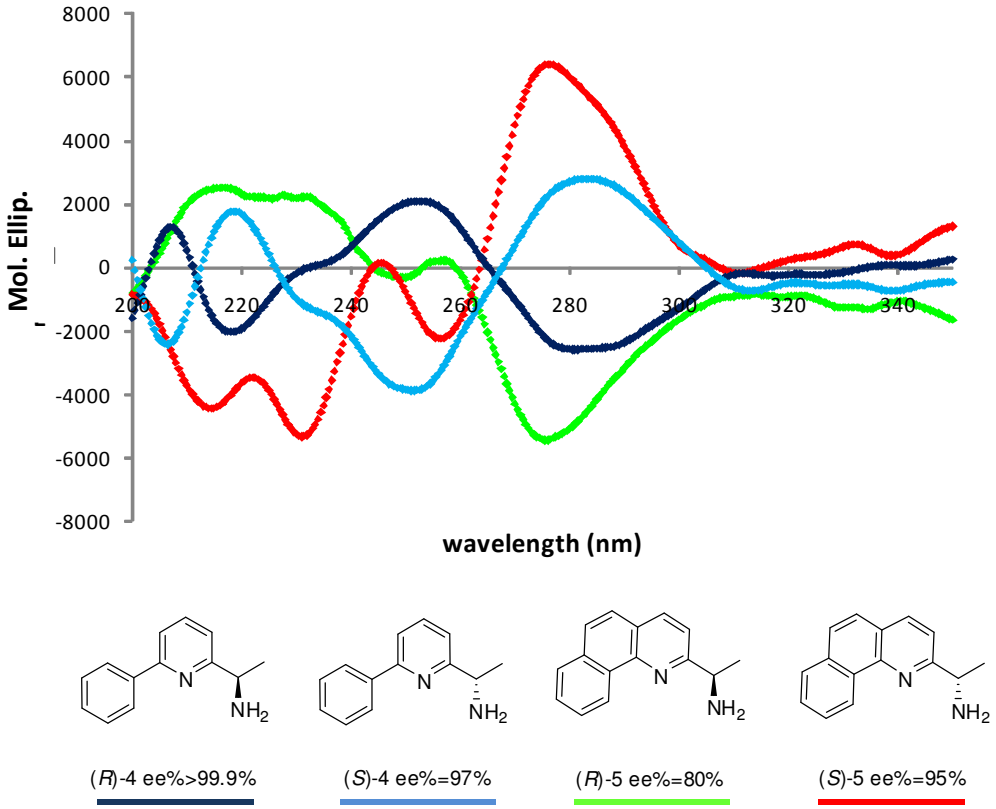

FIGURE 3. CD spectra of the four optically pure CNN pincer ligands (2.5×10^{-4} M in CH_3OH).

2.7. SYNTHESIS OF NEW CNN PINCER LIGANDS

As an extension of this work, we have synthesized new chiral CNN pincer ligands, analogous to 1-[6-phenylpyridin-2-yl]methanamine (sp^2 and sp^3 N donor atoms), having different steric and electronic properties, in order to investigate their effect on the formation of the [MCl(CNN)(PP)] complexes (M = Ru/Os) and on the catalytic activity of the relative complexes. These new pincer CNN ligands differed in the nature of the aryl group at position 6, which ranged from 1- and 2-naphtyl (derivatives **4a**,**b**) to differently substituted phenyl groups (derivatives **4d-h**)

The aim of this part of the work was to generate a library of new Ru(II) and Os(II) catalysts using commercially available chiral diphosphines, in search of the correct combination of the electronic and steric effects of the disphosphines and of the pincer ligand to achieve the best catalytic system in transfer hydrogenation reactions.

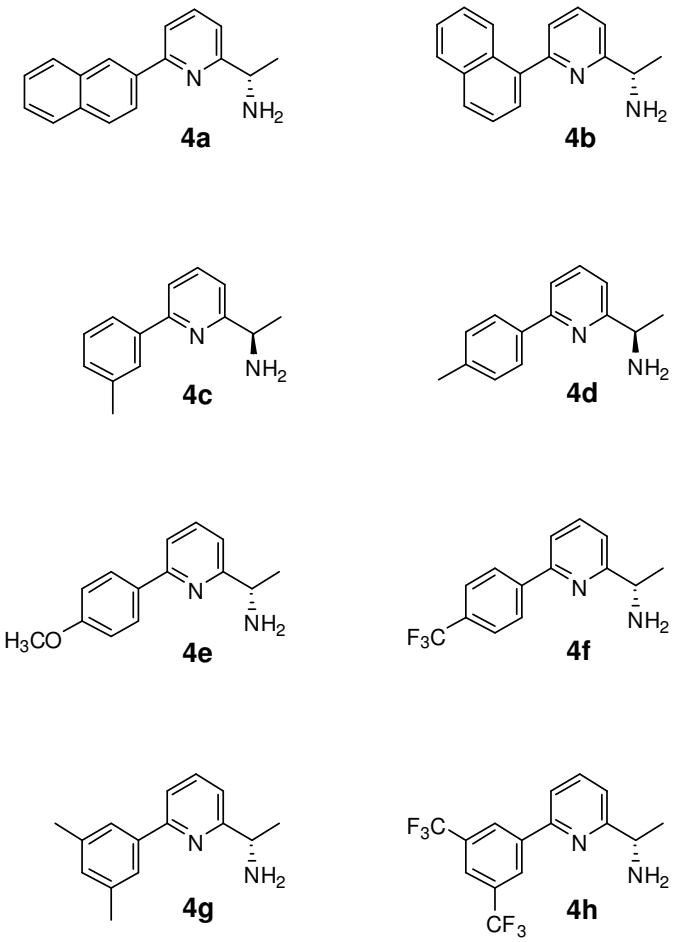

FIGURE 4.

The strategy for the synthesis of ligands **4a-h,** starting from the commercially available ketone 2-acetyl-6-bromo pyridine (Scheme 10) involved the application of the stereocomplementary biocatalytic approaches described above, to the obtainment of the alcohol (*R*)- and (*S*)-**14**, which were key intermediates to the final amines **4a-h**. These have been obtained with a very high optically purity in both the enantiomeric forms, by Suzuki coupling between the appropriate commercial boronic acid and (*S*)-**21** and (*R*)-**21**, enantiomers of 1-(6-bromopyridin-2-yl)ethanamine, derived from the alcohol intermediates (*R*)-**22** and (*S*)-**22** respectively.

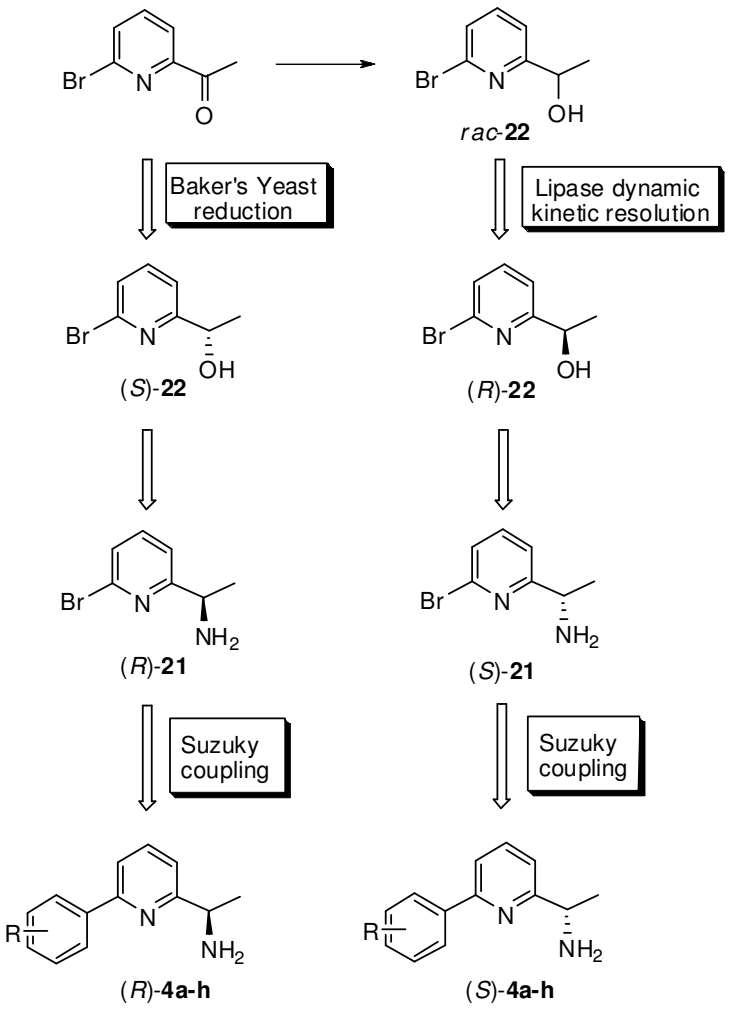

SCHEME 10. General strategy for the synthesis of chiral not racemic pincer ligands **4a-h**.

B.Y. asymmetric bioreduction of 2-acetyl-6-bromopyridine under the conditions discussed above, occurred in accordance with the Prelog's rule to give (*S*)-(+)-1-(6-bromopyridin-2-yl)ethanol ((*S*)-**22**). The reaction reached a complete conversion (99 %) in a very short time (24 h), this allowing the alcohol (*S*)-**22** to be isolated in a 96% enantiomeric excess (Scheme 11) and 80% yield after purification.

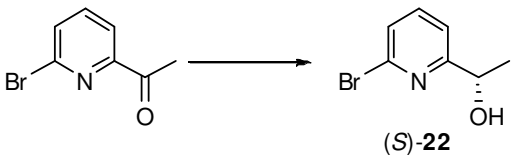

SCHEME 11. Reaction conditions: dry baker's yeast, saccharose, phosphate buffer Na_2HPO_4/KH_2PO_4 pH 7.4, substrate concentration 3.6 mM.

On the other hand, CAL-B mediated DKR of the racemic alcohol *rac*-**22**, in the presence of Shvo's catalyst, lead to optically pure (*R*)-(–)-1-(6-bromopyridin-2-yl)ethanol ((*R*)-**22**) obtained in 98% enantiomeric excess after hydrolysis of the acetate intermediate (*R*)-**23**.

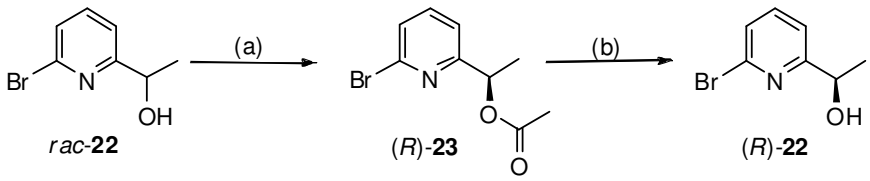

SCHEME 12. Reaction conditions: (a) DKR: toluene, Ar, *p*-chlorophenylacetate, CAL-B, $[Ru_2(CO)_4(\mu\text{-}H)(C_4Ph_4COHOCC_4Ph_4)]$, 70 °C.[22] (b) Basic hydrolysis: K_2CO_3, H_2O/CH_3OH.

The next step in the ligands synthesis was the nucleophilic displacement of the hydroxy for the amine group through the azide intermediate (**24**). Unfortunately epimerization occurred under the conditions described previously for amines **4** and **5**. In fact, starting from the alcohol (*R*)-**22** having 98% e.e., the corresponding (*S*)-**24**, isolated after the reaction, was shown to have a 85 % e.e. (Table 6, entry 1). An accurate screening of all the reaction conditions, including temperature, base, reaction time and reactants addition order, (Tables 6,7) allowed to establish the best conditions for the nucleophilic substitution, leading to the azide (*S*)-**24** with the maximum e.e.%.

TABLE 6. Variation on reactant addition order.

Entry	I addition	II addition	T (°C)	e.e.% [a] Alcohol-22	e.e.% [a] Azide-24 (yield %)
1	DPPA (1.2eq)	DBU (1.2 eq)	0°C 2h then 50°C o.n.	94	90 (74)
2	DBU (1.2 eq)	DPPA (1.2eq)		94	93 (74)

[a] e.e.% was determined by chiral HRGC analysis.

TABLE 7. Conditions variations.

Entry	Base	Conditions	e.e.% [a] Alcohol-22	e.e.% [a] Azide-24 (yield %)
1	DBU (1.2 eq)	0 °C x 2h + 50 °C o.n.	98	85 (79)
2	DBU (1.2 eq)	0 °C x 2h + t.a.o.n.	98	97 (70)
3	DBU (2 eq)	0 °C x 2h + t.a.o.n.	98	78 (76)
4	NaH (1.5 eq)	0 °C x 2h + t.a.o.n.	98	NO N_3
5	DBU (1.2 eq)	0 °C x 2h + 4 °C o.n.	98	98 (12)

[a] e.e.% was determined by chiral HRGC analysis.

These involved the addition of DBU first, followed by DPPA, at 0 °C. After two hours the reaction mixture was allowed to reach room temperature, until complete conversion into the azide (*S*)-**24**, which was obtained in a slightly lower e.e. with respect to the parent alcohol (*R*)-**22** (Table 7, entry 2). Application of this protocol to the enantiomeric alcohol (*S*)-**22** (e.e. 96%), allowed the amine (*R*)-**21** to be obtained in a 70% yield and 95% e.e..

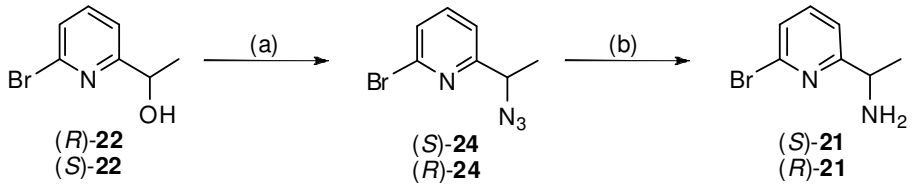

SCHEME 13. Reaction conditions: (a) DPPA, DBU, 0 °C, r. t.; (b) PPh_3, THF/H_2O.

After reduction of the azide with PPh_3/H_2O, the optically active amines (*S*)-and (*R*)-**21** so obtained were coupled to different aryl groups via Suzuki coupling with arylboronic acids (Scheme 14).

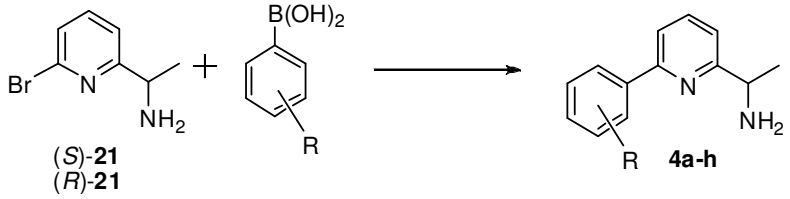

SCHEME 14. Reaction conditions: : *n*-propanol, K_2CO_3 2 M, H_2O, PPh_3, $Pd(OAc)_2$.

2.8. ACTIVITY OF RUTHENIUM AND OSMIUM COMPLEXES WITH CHIRAL CNN PINCER LIGANDS IN ASYMMETRIC REDUCTION OF PROCHIRAL KETONES

The use of the Ru(II) and Os(II) complexes of the optically pure CNN ligands described, in combination with chiral phosphanes, in transfer hydrogenation reaction (ATH) and asymmetric hydrogenation (AH) of aromatic and aliphatic prochiral ketones was explored by the group of Prof. Rigo and Prof. Baratta (University of Udine).

The results obtained with these new complexes were compared with those previously reported using the complexes of the ligands shown in Figure 1. In fact, ruthenium and osmium complexes derived from the *ortho*-metalation of achiral 1-(6-arylpyridin-2-yl)methanamines,[1] had already been found to be highly active catalysts in both AH and ATH[4a,28] of carbonyl compounds. For instance ruthenium complexes with ligand **2** and Josiphos as the chiral diphosphanes, converted quickly (TOF = 1×10^5 h^{-1}) and enantioselectively acetophenone into 1-phenylethanol in both ATH and AH processes with e.e. up to 90% and 70% respectively.[1f]

A method to obtain a Ru(II) complex as a predominantly diasteroisomer (> 92% major isomer) from *rac*-**4** has been performed[1f], by carrying out the reaction with an excess of racemic ligands (4 equiv) in the presence of NEt_3 and 0.5 equiv of acetic acid.

The weak acid proved to facilitate the formation of the thermodynamically most stable diastereoisomer, possibly through protonation and decoordination of the *ortho* metalated CNN ligand of the kinetic product.[1f]

Control experiments showed that the complexation reaction performed with (*R*)-**4** (60% e.e.) lead to the same diasteroisomer as the predominant product (Scheme 15).

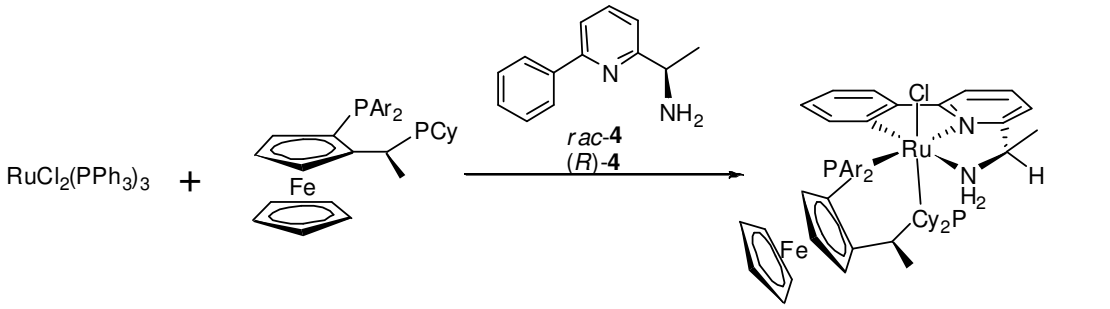

	diphosphane	Ar
25a	(*S*,*R*) Josiphos	Ph
25b	(*S*,*R*) Josiphos*	4-OCH_3-3,5-$(CH_3)_2C_6H_2$

SCHEME 15. Synthesis of complexes **25a** and **25b** with different phosphanes. Reaction conditions: toluene, precursor $[RuCl_2(PPh_3)_3]$, Josiphos, 105°C then CH_3COOH, Et_3N, **4**, refluxed 2-propanol.

In agreement with reported studies on Ru and Os complexes[1], the phosphane of (*S*,*R*)-configuration (either (*S*,*R*)-Josiphos or (*S*,*R*)-Josiphos*) was correctly matched with the ligand of *R* configuration in affording derivatives **25a** and **25b**. Indeed, in order to investigate the matched/mismatched ligand effect, the *in situ* prepared catalytic system $[RuCl_2(PPh_3)_3]$/(*R,S*)-Josiphos*/(*R*)-**4** afforded a slow reduction of acetophenone to (*R*)-1-phenylethanol (TOF = 3.6×10^4 h^{-1}, 74% e.e.), whereas the use of (*S,R*)-Josiphos* led to the *S* alcohol with a higher rate and enantioselectivity (TOF = 1.6×10^5 h^{-1}, 94% e.e.). These results and the NMR control experiments indicate that (*S,R*)-Josiphos*/(*R*)-**4** is the most correctly matched combination for the catalysis.

Complexes **25a**-**b** were found to be highly efficient catalysts for the ATH and AH of different alkyl-aryl ketones in alcohol medium (Figure 5).

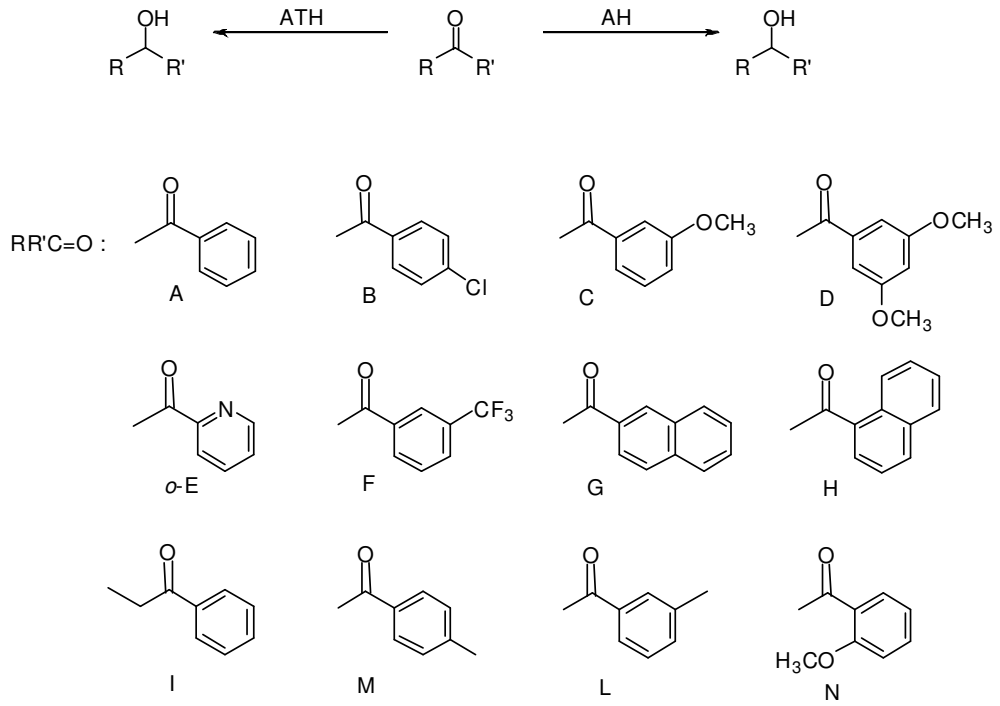

FIGURE 5. Asymmetric AH and ATH catalyzed by chiral pincer complexes **25a** and **25b** and ketones used as substrates. Reaction conditions: ATH: [Ru] complexes **25a-b**, 2-propanol/NaO*i*-Pr, 60°C. AH: [Ru] complex **25a-b**, H_2, EtOH or EtOH/CH_3OH, 40°C.

Comparing these results with those observed with complexes containing achiral CNN pincer[1f] ligand, the use of chiral CNN complexes in hydrogen transfer reaction leads to a slight accelleration of the reaction (TOF up to 10^6 h^{-1}) and a significant increase in e.e.% value of the alcohol products (Table 8).

TABLE 8. Catalytic ATH of alkyl aryl ketones with **25a-b**.

Entry	Complex	Ketone	Time (min)	Conv. (%)[a]	TOF (h^{-1})[b]	e.e. (%)[a]
1	**25a**	**A**	30	98	1.6×10^5	81 *S*
2	**25b**	**A**	10	98	1.8×10^5	95 *S*
3	**25b**[c]	**A**	30	94	2.1×10^5	95 *S*
4	**25b**	**B**	10	97	1.5×10^5	96 *S*
5	**25b**	**C**	30	97	1.4×10^5	97 *S*
6	**25b**	**D**	10	97	1.8×10^5	98 *S*
7	**25b**[d]	**D**	2	98	1.3×10^6	95 *S*
8	**25b**	***o*-E**	30	99	1.2×10^5	93 *S*
9	**25b**	**F**	30	98	1.6×10^5	95 *S*
10	**25b**[c]	**F**	30	96	2.1×10^5	95 *S*
11	**25b**[e]	**G**	5	97	2.0×10^5	97 *S*
12	**25b**[e]	**H**	60	98	5.5×10^4	98 *S*
13	**25b**	**I**	60	98	1.1×10^4	99 *S*

Reaction conditions: 0.1 M alkyl aryl ketones, 0.005 mol% **25a-b**, 2 mol% NaO*i*-Pr in 2-propanol as solvent, 60°C. [a] The conversion and e.e.% were determined by HRGC analysis. [b] Turnover frequency (moles of ketone converted into alcohol per mole of catalyst per hour) at 50% conversion. [c] [Ru] = 0.002 mol%. [d] T = 82°C. [e] [Ru] = 0.01 mol%.

Transfer hydrogenation of acetophenone (**A**), taken as a model substrate under the condition indicated the Table 8, afforded optically pure 1-phenyletanol with high TOF, (up to 2.1 10^5 h^{-1}) and good enantioselectivities (up to 95 %.) It is noteworthy that a lower loading of the bulky complex **25b** (0.002 mol %, 30 min) did not affect the reaction rate and the enantioselectivity (entry 3). **25b** also catalyzed the enantioselective reduction of different alky aryl ketones always in good rate (up to 1.3 $\times$ 10^6 h^{-1}, entry 7) and excellent enatiomeric excess (up to 99%, entry 13). The configuration of the alcohol products was *S* in all cases.

Interestingly, the chiral pincer complex **25b** dispalyed high catalytic activity also in the asymmetric hydrogenation of ketones in ethanol or methanol/ethanol mixtures, under 5 atm of H_2 (Table 9).

TABLE 9. Catalytic AH of alkyl aryl ketones with **25a-b**.

Entry	Complex	Ketone	Solvent	Time (min)	Conv. (%)[a]	TOF (h^{-1})[b]	e.e. (%)[a]
1	**25a**[d]	**A**	EtOH	60	> 99	1.7×10^4	77 *S*
2	**25b**[d]	**A**	MeOH/EtOH 3:7	30	> 99	2.8×10^4	87 *S*
3	**25b**[d]	**A**	MeOH/EtOH 1:1	30	> 99	3.3×10^4	90 *S*
4	**25b**	**L**	MeOH/EtOH 1:1	20	99	3.8×10^4	93 S
5	**25b**	**M**	MeOH/EtOH 1:1	30	99	3.0×10^4	90 S
6	**25b**	**N**	MeOH/EtOH 1:1	30	> 99	2.9×10^4	91 *S*
7	**25b**	**G**	MeOH/EtOH 1:1	30	> 99	3.6×10^4	93 *S*
8	**25b**	**I**	MeOH/EtOH 1:1	30	> 99	2.5×10^4	99 *S*

Reaction conditions: 0.5 M alkyl aryl ketones, 0.02 mol% **25b**, 6 mol% KO*t*-Bu, and 5 atm of H_2, 40 °C. [a] Ratio by volume. [b] The conversion and e.e.% were determined by HRGC analysis. [c] Turnover frequency (moles of ketone converted to alcohol per mole of catalyst per hour) at 50% conversion. [d] [Ru] = 0.01 mol%.

The results achieved clearly suggest that the alcoholic solvent plays an important role in AH of ketones mediated by pincer complex **25b**, improving both the catalytic activity and selectivity displayed in the model reaction with acetophenone. In the 1:1 CH_3OH/EtOH mixture, also ketones (**A**, **L**, **M**, **N**, **G**, **I**) have been converted completely to the corresponding *S* alcohol in 20-30 min and with e.e.% reaching 99% in the case of **I**.

Also Osmium complexes derived from orthometalation of 1-(6-arylpyridin-2-yl)methanamine ligands have been prepared. These systems were found to be highly active catalysts in hydrogenation (AH) as well as in asymmetric transfer hydrogenation (ATH) of prochiral carbonyl compounds, with reaction rates comparable to those of the analogous ruthenium complexes [RuCl(CNN)(diphosphane)].[1] It is worth noting

that on account of the stronger bonding ability, osmium is thought to give more stable and less active catalysts[29] compared to ruthenium for hydrogenation and transfer hydrogenation of ketones.[30]

Based on the excellent catalytic performances of the Ru and Os diphosphane derivatives containing an achiral CNN benzo[*h*]quinoline type ligand,[1d] a particular attention has been given to the 2-aminoethylbenzo[*h*]quinoline framework, characterized by a higher conformational rigidity, compared to CNN ligands containing the 2-arylpyridine moiety.

In order to isolate a catalysts displaying the highest enantioselectivity, the optically pure ligand **5** was employed in combination with a Josiphos ligand. Also in this case the best matching ligand effect was obtained by (*S*,*R*)-phosphane and the ligands with *R* configuration. The derivative **26** was prepared by reaction of $[OsCl_2(PPh_3)_3]$ with the bulkier diphosphane (*S*,*R*)-Josiphos* (Scheme 16).

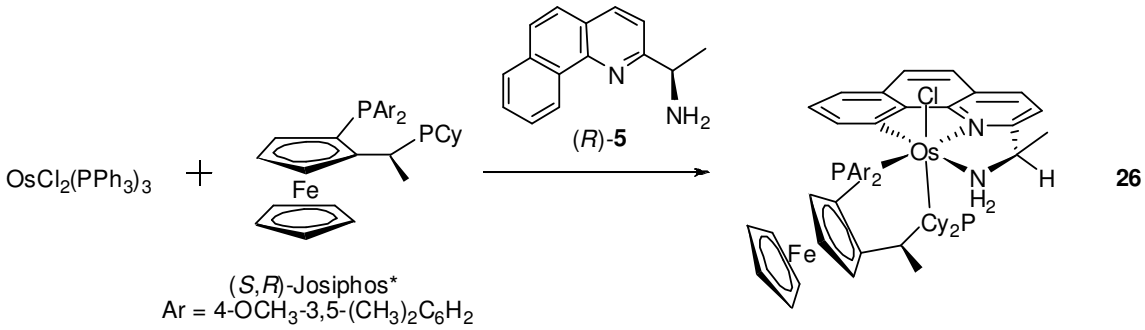

SCHEME 16. Synthesis of Os(II) complexes **26**. Reaction conditions: mesitylene, precursor $[OsCl_2(PPh_3)_3]$, Josiphos*, 110°C, then **5**, Et_3N and 140°C.

The complex **26** was isolated as a single stereoisomer in 64 % yield. The coordination chemistry and the catalytic potential of the new chiral pincer complexes have been tested. The selective hydrogenation (AH) of aryl-alkyl ketones (**A**, **C**, **G**, **I** in Figure 6) to secondary alcohols in methanol or methanol/ethanol mixtures was catalyzed by **26**. The results are reported in Table 10, compared with those obtained for the previous Os(II) and Ru(II) complexes (**Os1** and **Ru1** in Figure 6).

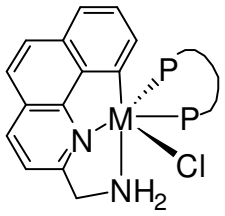

	M	diphosphane
Ru1	Ru	(*S*,*R*)-Josiphos*
Os1	Os	(*S*,*R*)-Josiphos

FIGURE 6. Ru and Os complexes of achiral benzo[*h*]quinoline type CNN pincer ligands.

TABLE 10. Catalytic AH of alkyl aryl ketones with **26**.

Entry	Complex	Ketone	T (°C)	Time (min)	Conv. (%)[a]	TOF (h^{-1})[b]	e.e.(%)[a]
1	**Ru1**	**A**	40	30	> 99	4.3×10^4	92 *S*
2	**Ru1**	**C**	40	60	> 99	1.6×10^4	94 *S*
3	**Ru1**	**G**	40	30	95	5.6×10^4	93 *S*
4	**Ru1**	**I**	40	60	97	2.0×10^4	> 99 *S*
5	**Os1**	**A**	70	30	> 99	2.0×10^4	86 S
6	**26**	**A**	70	60	97	1.4×10^4	92 S
7	**26** *in situ*[c]	**A**	70	30	> 99	2.4×10^4	90 *S*
8	**26** *in situ*[c]	**C**	70	30	> 99	2.2×10^4	91 *S*
9	**26** *in situ*[c]	**G**	70	30	> 99	1.6×10^4	94 *S*
10	**26** *in situ*[c]	**I**	70	60	> 99	1.3×10^4	> 99 *S*

Reaction conditions: Ketone/complex/KO*t*Bu = 10000/1/200, H_2 5 atm, solvent = CH_3OH/EtOH mixture (7:3 by volume). [a] The conversion and e.e. were determined by HRGC analysis. [b] Turnover frequency (moles of ketone converted to alcohol per mole of catalyst per hour) at 50 % conversion. [c] $[OsCl_2(PPh_3)_3]$/(*S*,*R*)-Josiphos*/benzo[*h*]quinoline = 1/1.5/2.

For the best performances, methanol/ethanol mixtures were used in analogy with the case of the chiral CNN Ru complexes catalysed reactions[1e,f]

The system **26** was an efficient catalyst for the reduction of acetophenone **A**, which was rapidly and selectively converted to (*S*)-1-phenylethanol in 92% e.e. (TOF = 1.4×10^4 h^{-1}) as in the case of the reaction catalyzed by **Ru1**. A good catalytic performance

was also observed with a Os/Josiphos*/(*R*)-benzo[*h*]quinoline system prepared *in situ*, in CH_3OH/EtOH mixture and using KO*t*-Bu/Os = 200. As a matter of fact, treatment of $[OsCl_2(PPh_3)_3]$ with the bulky (*S*,*R*)-Josiphos* in refluxing CH_3OH/EtOH for 3 h, followed by the addition of **5** (1 h), lead to a chiral Os system which catalyzed the asymmetric hydrogenation of **A** affording in 30 min the corresponding (*S*)-alcohol with 90 % e.e. and TOF = 2.4×10^4 h^{-1} (Table 10, entry 7). These results improve the ones obtained with the isolated complex **Os1** containing the less bulky (*S*,*R*)-Josiphos and the achiral pincer ligand 2-aminomethylbenzo[*h*]quinoline (see Figure 6). By employment of the *in situ* generated osmium catalyst **26** the ketones **C**, **G** and **I** have been fast reduced to the corresponding (*S*)-alcohols with 91-99 % e.e.

The Os benzo[*h*]quinoline based complexes **26** showed the same enantioselectivity for both AH in methanol/ethanol and ATH in 2-propanol. Thus, the **Ru1** complex catalyzed the reduction of **A** to *S*-alcohol with 92 vs. 96 [31] % e.e. in AH and ATH respectively, whereas the Os derivative **Os1** and the corresponding **26-**"*in situ"* system[31] led to 86 and 80 % e.e., respectively

Compared with **Ru1** and **Os1**, complex **26** shows a better enantioselectivity in the AH of **A** with (in particular with respect to **Os1**). Furthermore, the stronger bonding of osmium allowed to operate at higher temperature (70 °C), compared to ruthenium (40 °C).

The optically pure ligands (*S*)-**4a-b** and (*S*)-**4e-h** have been employed in the transfer hydrogenation reaction of acetophenone in both Ru(II) and Os(II) systems formed *in situ*. In these cases the best combination was with (*R,S*)-Josiphos*. The reactions were performed at 60°C in 2-propanol with 2% mol NaO*i*-Pr. The pre-catalysts systems consist on $[MCl_2(PPh_3)_3]$/(*R,S*)-Josiphos*/CNN (where M = Ru or Os). The results are listed in Table 11.

TABLE 11. Catalytic ATH of acetophenone (0.1M) with the systems $[MCl_2(PPh_3)_3]$/(*R,S*)-Josiphos*/ligand.

		Precursor $RuCl_2(PPh_3)_3$				Precursor $OsCl_2(PPh_3)_3$			
Entry	**Ligand**	**Conv. (%)[a]**	**Time (min)**	**TOF (h^{-1}) [b]**	**e.e. (%)[a]**	**Conv. (%)[a]**	**Time (min)**	**TOF (h^{-1}) [b]**	**e.e. (%)[a]**
1	**4a**	98	30	1.5×10^5	90 *R*	97	60	1.5×10^5	87 *R*
2	**4b**	95	60	6.5×10^4	85 *R*	70	120	6.6×10^4	81 *R*
3	**4e**	97	30	1.3×10^5	86 *R*	96	60	1.2×10^5	85 *R*
4	**4f**	95	30	6.5×10^4	85 *R*	76	120	6.0×10^4	83 *R*
5	**4g**	27	120	–	84 *R*	39	120	–	75 *R*
6	**4h**	4	60	–	–	8	60	–	–

Reaction conditions: Os: 0.005 mol %, Ru: 0.005 mol % and NaO*i*-Pr (2 mol %) in 2-propanol at 60°C.[a] The conversion and ee were determined by GC analysis. [b] turnover frequency (moles of ketone converted into alcohol per mole of catalyst per hour) at 50% conversion.

The reduction product was in each case (*R*)-1-phenylethanol with e.e. % up to 87 %.

The data collected in the table clearly suggest that the Ru complexes of ligands **4g** and **4h** (entries 5 and 6) are not efficient catalysts for the reduction of acetophenone. The double 3,5-disubstitution of the phenyl group results infact in a dramatic decrease of the productivity, which is undependent on the different electronic properties of the -CH_3 and -CF_3 groups, but is a consequence of the steric effect of the substituents at the *meta* position of the aromatic ring. On the contrary, different substituents at the *para* position of the phenyl group, played a relevant role on the catalysis. In fact, both Ru(II) and Os(II) complexes with ligand **4e** (entry 3), bearing the strong electron-releasing methoxy group, reduced acetophenone with a double rate (TOF = 1.3×10^5 h^{-1}) with respect to the case of the analogue complexes of ligand **4f** (entry 4, TOF = 6.5×10^4 h^{-1}) in which the strong electron-withdrawing effect of the CF_3 group affects the stability of the M-C σ-bond.

Of the ligands **4a** and **4b** (entries 1 and 2), having similar electronic properties but a different geometry of the naphtylic residue, **4a** gave the most productive and selective Ru and Os complexes, which displayed the highest TOF (1.5×10^5 h^{-1} in each cases) and gave the products with the highest enantiomeric excesses (up to 90%). Moreover

the variation of the geometric requirements in going from **4a** to **4b** had a stronger effect on the Os complexes.

On the basis of the good results obtained using ruthenium and osmium-**4a** "*in situ*" catalytic systems, the Ru(II) and Os(II) complexes with pincer ligands **4a** and chiral phosphane were isolated and tested in the transfer hydrogenation reaction of different prochiral ketones (Figure 7).

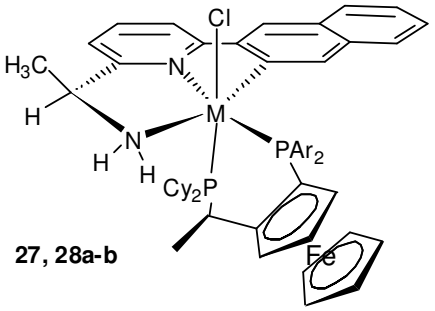

27: M = Ru; Ar = 4-OCH_3-3,5$(CH_3)_2C_6H_2$

28a: M = Os; Ar = Ph

28b: M = Os; Ar = 4-OCH_3-3,5$(CH_3)_2C_6H_2$

FIGURE 7.

The best results have been obtained in the catalytic ATH on aryl-alkyl ketones, while complexes **27** and **28a-b** showed a low activity in the reduction of diaryl and dialkyl ketones. The substrates chosen are shown in Figure 8, in addition to those already reported in Figure 5.

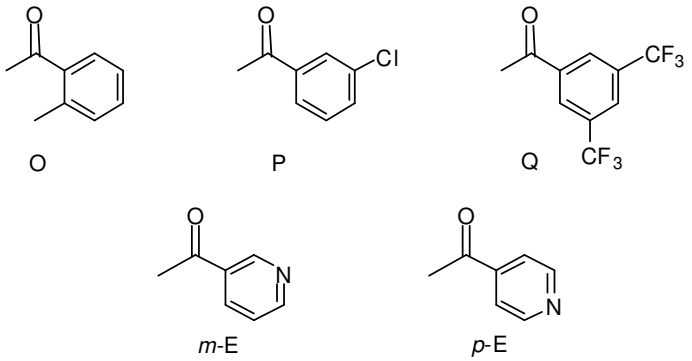

FIGURE 8.

Complexes **27** and **28a-b** showed good activity and selectivity giving the optically pure (*R*)-products with high enantiomeric excess (up to 99 %, Table 12).

TABLE 12. Catalytic ATH of alkyl aryl ketones with **27**, **28a-b**.

Entry	Complex	Ketone	Conv. (%)[a]	Time (min)	TOF(h^{-1}) [b]	e.e. (%)[a]
1	**27**	**A**	95	30	1.15×10^5	92 *R*
	28a		96	30	2.5×10^5	89 *R*
	28b		97	30	3.2×10^5	91 *R*
2	**27**	**C**	96	60	9.0×10^4	94 *R*
	28b		97	30	2.0×10^5	99 *R*
3	**27**[f]	**D**	97[i]	1	1.8×10^6	91 *R*
	27		97	30	2.5×10^5	95 *R*
	28b[g]		97[i]	10	9.0×10^5	97 *R*
4	**27**	***o*-E**	93	60	3.9×10^4	86 *R*
	28b		99	30	1.2×10^5	91 *R*
5	**27**[h]	***m*-E**	99	30	6.6×10^4	92 *R*
	28b[h]		99	30	7.6×10^4	90 *R*
6	**27**[c][h]	***p*-E**	99	10	1.2×10^5	97 *R*
	28b[c][h]		99	10	8.3×10^4	97 *R*
7	**27**	**F**	99	30	2.6×10^5	96 *R*
	28b		99	10	1.8×10^5	94 *R*
8	**27**[c]	**G**	96	30	1.6×10^5	93 *R*
	28b[c]		96	10	3.4×10^5	99 *R*
9	**27**	**H**	98	30	4.7×10^4	96 *R*
	28b		98	30	5.9×10^4	96 *R*

TABLE 12. Continuation.

Entry	Complex	Ketone	Conv. (%)[a]	Time (min)	TOF(h^{-1}) [b]	e.e. (%)[a]
10	**27**	**I**	90	120	7.7×10^4	99 *R*
	28b		93	30	1.4×10^5	99 *R*
11	**27**[c]	**O**	80	60	2.5×10^4	96 *R*
	28b[c]		93	60	5.9×10^4	94 *R*
12	**27**	**P**	99	30	1.25×10^5	99 *R*
	27[f]		99[i]	2	8.4×10^5	99 *R*
	28b[g]		99[i]	180	–	–
	28b[f]		99[i]	3	4.8×10^5	99 *R*
13	**27**[c][h]	**Q**	99	60	1.9×10^4	98 *R*
	28b[c][h]		99	30	5.1×10^4	98 *R*

[a] The conversion and e.e. % were determined by HRGC analysis. Reaction condition: NaO*i*-Pr (2 mol %) in 2-propanol at 60 °C. [b] Turnover frequency (moles of ketone converted to alcohol per mole of catalyst per hour) at 50% conversion. [c] substrate/M/base = 10000/1/200. [d] substrate/M/base = 5000/1/100. [e] substrate/M/base = 2000/1/40. [f] Reaction at reflux. [g] Reaction at reflux substrate/M/base = 50000/1/1000. [h] *In situ* reaction. [i] T = 100 °C.

Both ruthenium and osmium complexes were efficient systems for ATH process, in particular complex **28b** with a bulkier diphosphane showed a better activity and selectivity with respect to the corresponding complex **28a**, in analogy with the data previously reported for complexes **25a-b**. Catalyst **28b** reduced acetophenone (entry 1) with high TOF value (TOF = 3.2×10^5 h^{-1}) and selectivity (e.e. 91 %), comparable to the Ru(II) derivatives **27**.

Reactions reached conversion up to 99% in all cases but one (entry 11), and displayed very high enantioselectivity (e.e.% up to 99%). It is worth noting that pincer catalysts with ligand **4a** displayed TOF (10^5-10^6 h^{-1}) and enantiomeric excesses comparable with those of **25a-b** Ru complexes. Interestingly, Os complex **28b** gave the alcohols product with the best enantiomeric excess (see Table 12 entries 2, 8, and Table 8 entries 5, 11).

2.9. CONCLUSIONS

A new series of chiral CNN-pincer ligands have been synthesized in good yield and optical purity (e.e. from 80% to > 99%) through the *sec*-alcohol intermediates obtained in turn by two enantiocomplementary biotransformation procedures, such as the baker's yeast bioreduction of the parent prochiral ketones and the lipase catalyzed dynamic kinetic resolution of *rac*-alcohol mixtures.

The best conditions for a S_N2 conversion of the homochiral *sec*-alcohol to the corresponding amine ligands, with a clean inversion of configuration were found.

Chiral complexes **25a-b**, **26**, **27** and **28a-b**, of general formula [MCl(CNN)(PP)] (where M = Ru or Os), were formed by coordination of the synthesized pincer ligands and chiral Josiphos-type diphosphane. They were isolated and tested in the enantioselective reduction of different alky-aryl prochiral ketones. High e.e. % values (up to 99%) have been achieved in ATH with a remarkably high rate (TOF = 10^5-10^6 h^{-1}) and low catalyst loading (0.005–0.002 mol%) using complexes **25a-b**. By changing the reaction conditions (0.02–0.01 mol% of Ru) pincer complex **25a-b** were also used in the AH of ketones with H_2 (5 atm), where they displayed a very high degree of stereoselctivity. Under the same conditions the Os(II) complex **26**, of the rigid tricyclic ligand **5**, was active (TOF = 10^4 h^{-1}).in AH reactions producing the alcohol products with excellent e.e. % (> 99%). The group of optically pure aryl-pyridine-type pincers were tested in the reduction of acetophenone with ATH mechanism, forming *in situ* Ru and Os catalysts. The results obtained suggest a strict dependence of the complexes activity on the steric and electronic characteristics of the different aryl rings. In particular Ru and Os complexes with ligand **4a** displayed the best activity, thus complex **27** and **28a-b** were isolated and used in ATH reactions. The data observed showed that the activity of complexes **27** and **28a-b** is comparable to the one of complexes **25a-b** in transfer hydrogenation process.

On account of the remarkably high activity and productivity of these complexes, that could be applied both in ATH and AH reduction processes, this class of ruthenium and osmium derivatives have good potential for application in homogeneous asymmetric catalyst.

REFERENCES

1. (a) Baratta, W.; Chelucci, G.; Gladiali, S.; Siega, K.; Toniutti, M.; Zanette,M.; Zangrando, E.; Rigo, P. *Angew. Chem., Int. Ed.* **2005**, *44*, 6214–6219. (b) Baratta, W.; Bosco, M.; Chelucci, G.; Del Zotto, A.; Siega, K.; Toniutti, M.; Zangrando, E.; Rigo, P. *Organometallics* **2006**, *25*, 4611–4620. (c) Baratta, W.; Ballico, M.; Chelucci, G.; Siega, K.; Rigo, P. *Angew. Chem., Int. Ed.* **2008**, *47*, 4362–4365. (d) Baratta, W.; Ballico, M.; Baldino, S.; Chelucci, G.; Herdtweck, E.; Siega, K.; Magnolia, S.; Rigo, P. *Chem. Eur. J.* **2008**, *14*, 9148–9160. (e) Baratta, W.; Ballico, M.; Del Zotto, A.; Herdtweck, E.; Magnolia, S.; Peloso, R.; Siega, K.; Toniutti, M.; Zangrando, E.; Rigo, P. *Organometallics* **2009**, *28*, 4421-4430. (f) Baratta, W.; Chelucci, G.; Magnolia, S.; Siega, K.; Rigo, P. *Chem. Eur. J.* **2009**, *15*, 726-732.
2. (a) Lawson, E. C.; Hoekstra, W. J.; Addo, M. F.; Andrade-Gordon, P.; Damiano, B. P.; Kauffman, J. A.; Mitchell, J. A.; Maryanoff, B. E. *Bioorg. Med. Chem. Lett.* **2001**, *11*, 2619–2622. (b) Lloyd, G. K.; Williams, M. *J. Pharmacol. Exp. Ther.* **2000**, *292*, 461–467. (c) Wu, J. H.; Zamir, L. O. *Anti-Cancer Drug Des.* **2000**, *15*, 73–78.
3. Alvaro, G.; Pacioni, P.; Savoia, D. *Chem. Eur. J.* **1997**, *3*, 726–731.
4. (a) Gladiali, S.; Alberico, E. *Chem. Soc. Rev.* **2006**, *35*, 226–236. (b) Tang, W.; Zhang, X. *Chem. Rev.* **2003**, *103*, 3029–3069. (c) Hansen, M. C.; Buchwald, S. L. *Org. Lett.* **2000**, *2*, 713–715.
5. Burk, M. J.; Martinez, J. P.; Feaster, J. E.; Cosford, N. *Tetrahedron* **1994**, *50*, 4399–4428.
6. (a) Hultzsch, K. C. *Adv. Synth. Catal.* **2005**, *347*, 367–391. (b) Roesky, P. W.; Mueller, T. E. *Angew. Chem., Int. Ed.* **2003**, *42*, 2708–2710.
7. (a) Chelucci, G.; Baldino, S.; Chessa, S. *Tetrahedron* **2006**, *62*, 619– 636. (b) Chelucci, G. *Tetrahedron: Asymmetry* **2005**, *16*, 2353–2383. (c) Chelucci, G.; Cabras, M. A.; Saba, A. *Tetrahedron: Asymmetry* **1994**, *5*, 1973–1978.
8. Faber, K. *Biotransformations in Organic Chemistry*, 5th ed.; Springer: Berlin, **2004**.
9. (a) Bornscheuer, U. T.; Kazlauskas, R. J. *Hydrolases in Organic Synthesis: Regio- and Stereoselective Biotransformations*, 2nd ed.; Wiley-VCH: Weinheim, Germany, **2005**. (b) Schmid, R. D.; Verger, R. *Angew. Chem., Int. Ed.* **1998**, *37*, 1608–1633.
10. (a) Santaniello, E.; Ferraboschi, P.; Grisenti, P.; Manzocchi, A. *Chem. Rev.* **1992**, *92*, 1071–1140. (b) Czuck, S.; Blanzer, B. I. *Chem. Rev.* **1991**, *91*, 49–97. (c) Servi, S., *Synthesis* **1990**, 1–25.
11. (a) Paetzold, J; Bäckvall, J.-E. *J. Am. Chem. Soc.* **2005**, *127*, 17620–17621. (b) Parvulescu, A.; De Vos, D.; Jacobs, P. *Chem. Commun.* **2005**, 5307–5309.
12. (a) Martı´n-Matute, B.; Bäckvall, J.-E. *Curr. Opin. Chem. Biol.* **2007**, *11*, 226–232. (b) Pamies, O.; Bäckvall, J.-E. *Trends Biotechnol.* **2004**, *22*, 130–135. (c) Pamies, O.; Bäckvall, J.-E. *Chem. Rev.* **2003**, *103*, 3247–3262. (d) Faber,K. *Chem. Eur. J.* **2001**, *7*, 5005–5010.
13. Felluga, F.; Baratta, W.; Fanfoni, L.; Pitacco, G.; Rigo, P.; Benedetti, F. *J. Org. Chem.* **2009**, *74*, 3547-3550.
14. Kourist, R.; Gonzáles-Sabín, J.; Liz, R.; Rebolledo, F. *Adv. Synth. Catal.* **2005**, *347*, 695- 702.

15. Cappelli, A.; Anzini, M.; Vomero, S.; Mennuni, L.; Makovec, F.; Doucet, E.; Hamon, M.; Bruni, G.; Romeo, M.R.; De Benedetti, Pier G.; Langer, T. *J. Med. Chem.* **1998**, *41*, 728-741.
16. Sun, W.-H.; Jie, S.; Zhang, S.; Zhang, W.; Song, Y.; Wedeking, H.M.C.; Frohlich, R. *Organometallics*, **2006**, *25*, 666-677.
17. Mutterer, F.; Weis, C.D. *Helv. Chim. Acta* **1976**, *59*, 229-235.
18. Prelog, V. *Pure Appl. Chem.* **1964**, *9*, 119–122.
19. Benedetti, F.; Forzato, C.; Nitti, P.; Pitacco, G.; Valentin. E.; Vicario, M. *Tetrahedron : Asymmetry* **2001**, *12*, 505-511.
20. Li, F.; Cui, J.; Quian, X.; Ren, W.; Wang, X., *Chem. Comm.* **2006**, 865-867.
21. (a) Rotticci, D.; Hæffner, F.; Orrenius, C.; Norin, T.; Hult, K. *J. Mol. Catal. B: Enzym.* **1998**, *5*, 267–272. (b) Chen, C.-S.; Fujimoto, Y.; Girdaukas, G.; Sih, C. J. *J. Am. Chem. Soc.* **1982**, *104*, 7294–7299.
22. (a) Persson, B. A.; Larsson, A. L.; Le Ray, M.; Bäckvall, J.-E. *J. Am. Chem. Soc.* **1999**, *121*, 1645–1650. (b) Larsson, A. L. E.; Persson, B. A.; Bäckvall, J.-E. *Angew. Chem., Int. Ed.* **1997**, *36*, 1211–1212.
23. (a) Uenishi, J.; Hiraoka, T.; Hata, S.; Nishiwaki, K.; Yonemitsu, O. *J. Org. Chem.* **1998**, *63*, 2481–2487. (b) Bolm, C.; Ewan, M.; Feldre, M.; Schlingloff, G. *Chem. Ber*. **1992**, *125*, 1169-1190.
24. (a) Chen, C. K.; Prasad, O. Repic *Tetrahedron Letters* **1991**, *32*, 7175-7178. (b) Roush, W. R.; Straub, J. A.; Brown R. J. *J. Org. Chem.* **1987**, *52*, 5127-5136.
25. (a) Lebsack, A. D.; Guzner, J.; Wang, B.; Pracitto, R.; Schaffhauser, H.; Santini, A.; Aiyar, J.; Bezverkov, R.; Munoz, B.; Liu, W.; Venkatraman S. *Bioorg. Med. Chem. Lett.* **2004**, *14*, 2463-2467; (b) Lal, B.; Pramanik, B.N.; Manhas, M.S.; Bose, A.K., *Tetrahedron Letters* **1977**, *23*, 1977-1980; (c) Jia, Y.; Bois-Choussy, M.; Zhu, J. *Org. Lett.* **2007**, *9*, 2401-2404.
26. Thomson, A. S.; Humphrey, G. R.; De Marco, A. M.; Mathre, D. J.; Grabowski, E. J. J. *J. Org. Chem.* **1993**, *58*, 5886–5888.
27. Horner, L.; Gross, A. *Liebigs Ann. Chem.* **1955**, *591*, 117–134.
28. Baratta, W.; Rigo, P. *Eur. J. Inorg. Chem.* **2008**, *26*, 4041-4053.
29. (a) Morris, R. H. *The Handbook of Homogeneous Hydrogenation*, Vol. 1 (Eds.: J. G. de Vries, C. J. Elsevier), Wiley-VCH, Weinheim, **2007**, p. 45. (b) Esteruelas, M. A.; López, A. M.; Oliván, M. *Coord. Chem. Rev.* **2007**, *251*, 795-840. (c) Sánchez-Delgado, R. A.; Rosales, M.; Esteruelas, M. A.; Oro, L. O. *J. Mol. Catal. A: Chem.* **1995**, *96*, 231-243 and references herein.
30. (a) Schlünken, C.; Esteruelas, M. A.; Lahoz, F. J.; Oro, L. A.; Werner, H. *Eur. J. Inorg. Chem.* **2004**, 2477-2487. (b) Carmona, D.; Lamata, M. P.; Viguri, F.; Dobrinovich, I.; Lahoz, F. J.; Oro, L. A. *Adv. Synth. Catal.* **2002**, *344*, 499-502. (c) Faller, J. W.; Lavoie, A. R. *Org. Lett.* **2001**, *3*, 3703-3706.
31. (a) Abdur-Rashid, K.; Clapham, S. E.; Hadzovic, A.; A.; Harvey, A.; Lough, A. J.; Morris, R. H. *J. Am. Chem. Soc.* **2002**, *124*, 15104-15118. (b) Sandoval, C. A.; Ohkuma, T.; Muñiz, K.; Noyori, R. *J. Am. Chem. Soc.* **2003**, *125*, 13490-13503. (c) Hamilton, R. J.; Bergens, S. H. *J. Am. Chem. Soc.* **2006**, *128*, 13700-13701.
32. Baratta, W.; Ballico, M.; Chelucci, G.; Magnolia, S.; Siega, K.; Rigo, P. Patent PD2007A000237, **2007**.

Chapter 3:
Synthesis and application of pyridine ligands

3.1. SYNTHESIS OF PYRIDINE LIGANDS FOR CO-OLIGOMERIZATION REACTION

During the last two decades, the co- and terpolymerization reaction of carbon monoxide with terminal aliphatic and aromatic alkenes has attracted much interest from both academic and industrial point of view.[1] The products of this reaction are perfectly alternating polyketones (Scheme 1).

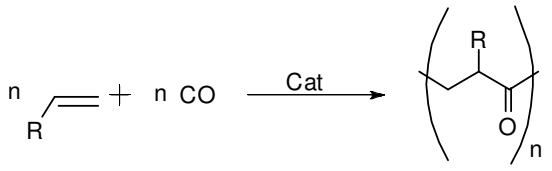

R = H, CH_3 , Ar

SCHEME 1. The CO/alkene copolymerization.

It is well known that when carbon monoxide is copolymerized with an aromatic alkene, like styrene or its substituted derivatives, the best performing catalytic systems are based on palladium complexes with bidentate nitrogen donors ligands.[1c] For the synthesis of syndiotactic CO/styrene copolymers, the best performing catalysts are based on Pd-complexes either with pyridine-imidazoline ligands[2,3] or with 1,10-phenanthrolines.[4,5] In the latter case, the introduction of fluorine atoms in positions 5 and 6, obtaining the 5,5,6,6-tetrafluoro-5,6-dihydro-1,10-phenanthroline, led to a long-lived catalysts with a lifetime longer than 96 h, yielding a polyketone with a high degree of stereoregularity (96% content of *uu* triad) and molecular weight up to 1000000.[6] When the substituents are on *ortho* positions with respect to the nitrogen donor atoms, like in the 2,9-dimethyl-1,10-phenanthroline or in the 6-R-2,2'-bipyridine (R = CH_3, Et, *i*-Pr), the related palladium complexes did not show any catalytic activity in the CO/vinyl arene copolymerization.[7]

Whereas there is an extensive literature on the synthesis of polyketones from carbon monoxide and aromatic alkenes, to the best of our knowledge, few data have been reported on the synthesis of the corresponding oligomers. The synthesis of low molecular weight compounds starting from CO and styrene, obtained as esters like the dimethyl-2-phenylbutanedioate, dimethyl-2,5-diphenyl-4-oxo-pimelate and 2-oxoglutarates, was achieved by using Pd-phenanthroline or Pd-diphosphine complexes in the presence of a large excess of 1,4-benzoquinone (BQ)[8,9] or under high pressure of carbon monoxide (350 bar).[10] On the other hand, the corresponding co- and ter-oligomers with terminal aliphatic alkenes, like ethylene and propylene, have been

exploited at industrial level under the trademark of Carilite®.[11] They show a range of potential applications, and among them the most promising, after proper curing, being an adhesive for wood.[12]

With the aim to investigate in more detail the effect of the substituents on *ortho* position with respect to the N-donors, the new chiral 6-(1-methoxyethyl)-2,2'-bipyridine (**29**) ligand, both as a racemate and in the enantiopure *R* and *S* forms, has been synthesized. The coordination chemistry of **29** to Pd(II) has been studied and compared with that of the known 6-*iso*-propyl-2,2'-bipyridine (**31**), *rac*-6-*sec*-butyl-2,2'-bipyridine (*rac*-**32**), and the new achiral 2-(methoxymethyl)-6-(1*H*-1,2,3-triazol-1-yl)pyridine (**30**) (Figure 1).

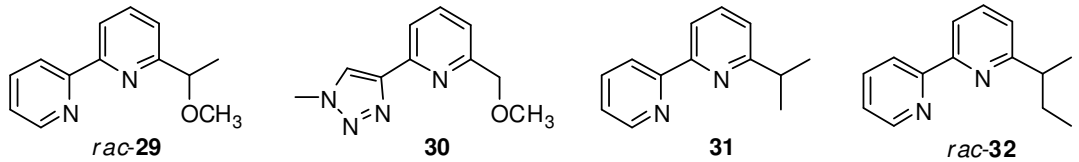

rac-**29** (*R*)-**29** (*S*)-**29** **30** **31** *rac*-**32**

FIGURE 1. The studied bipyridine and pyridine-triazole ligands.

The catalytic behavior of the corresponding monocationic organometallic Pd(II) complexes $[Pd(CH_3)(CH_3CN)(N\text{-}N')][PF_6]$ and $[Pd(CH_3)(N\text{-}N')_2][PF_6]$ (N-N' = **29-32**) in styrene carbonylation was analyzed in detail, together with some mechanistic investigations on their reactivity with carbon monoxide.

3.2. SYNTHESIS OF THE PYRIDINE TYPE LIGANDS

Racemic ligand *rac*-**29** was synthesized from ketone **33** obtained following a literature procedure (Scheme 2).[13] Ketone **33** was the parental compound also for optically pure (*R*) and (*S*)-**29** that have been afforded by chemoenzymatic methods.

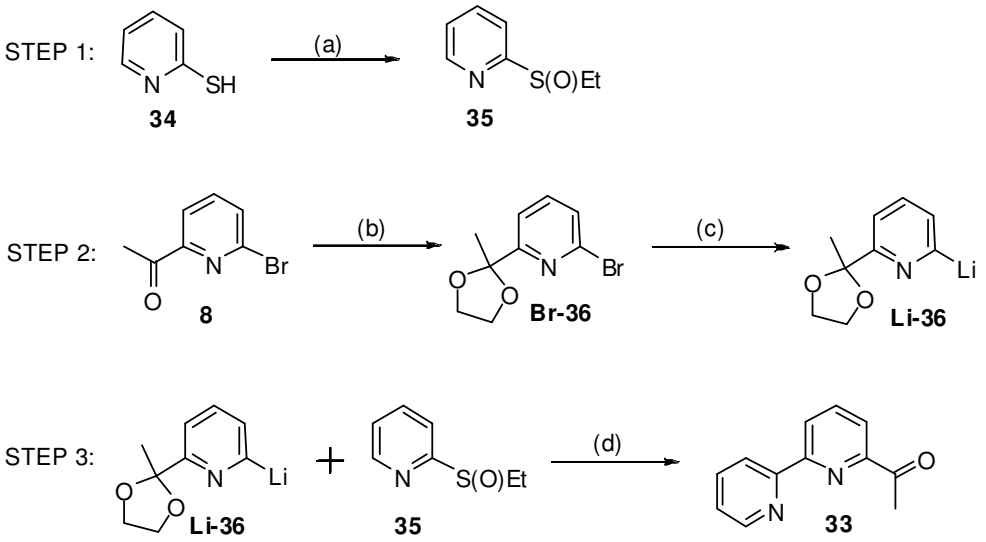

SCHEME 2. Synthesis of the ketonic precursor **33**. Reaction conditions: Step 1: (a) i. 1 M NaOH, EtI, room temperature; ii. magnesium monoperoxyphthalate, CH_3OH, 0 °C. Step 2: (b) ethane-1,2-diol, 4-toluensulfonic acid, benzene, reflux; (c) *n*-butyl-lithium, THF, -70 °C. Step 3: (d) i. THF, 25 °C; ii. 2M HCl, 60 °C.

Steps 1 and 2 involved two commercially available compounds: 2-mercaptopyridine (**34**) and 2-acetyl-6-bromopyridine (**8**). The first step was the oxidation of 2-mercaptopyridine into 2-(ethylsulfinyl)pyridine (**35**) by reaction with 1-iodoethane in basic medium and then with magnesium monoperoxyphthalate in methanol. Step 2 consisted on the protection of the carbonyl group as acetal with 1,2-ethandiol and *p*-toluensulfonic acid obtaining **Br-36** that has been lithiated at -70°C achieving the active species **Li-36**. Products **Li-36** and **35** were coupled at room temperature and, after deprotection of acetal under acid conditions, ketone **33** was isolated.

The desired methyl ether *rac*-**29** was synthesized in high yield by reduction of the carbonyl group of **33**, under standard conditions ($NaBH_4$ in EtOH at r. t.), followed by methylation of the corresponding alcohol **37** with CH_3I and NaH (Scheme 3).

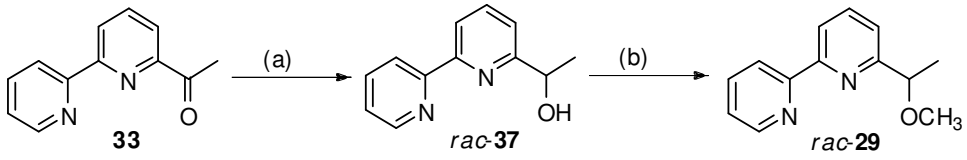

SCHEME 3. Synthesis of the racemic bipyridine ligand *rac*-**29**. Reaction conditions: (a) $NaBH_4$, EtOH; (b) NaH, CH_3I, THF.

The homochiral (*R*)-**29** and (*S*)-**29** were synthesized starting from **33** by chemoenzymatic methods, leading first to the alcohol intermediates (*R*)-**37** and (*S*)-**37**.

As shown in the case of pincer ligands, enantiomerically pure secondary alcohols are efficiently prepared from prochiral ketones by asymmetric microbial reduction with baker's yeast (*Saccharomyces cerevisiae*),[14] or, in a widely used alternative, by the lipase-catalyzed resolution of racemic *sec*-alcohols, by enantioselective acylation of the hydroxylic function.[15]

Based on the results obtained by us in the synthesis of chiral 1-heteroarylethanols in both enantiomeric forms by application of these biotransformation procedures,[16](see Chapter 2) and on the high selectivity already observed in the lipase-catalyzed transesterification of **37**,[17] we carried out the dynamic version of the reported classical kinetic resolution of *rac*-**37** by using Novozyme® 435 (*Candida antarctica* lipase B (CAL-B), immobilized on polyacrylamide) and the bioreduction with full cells of *Saccharomyces cerevisiae* (Scheme 4).

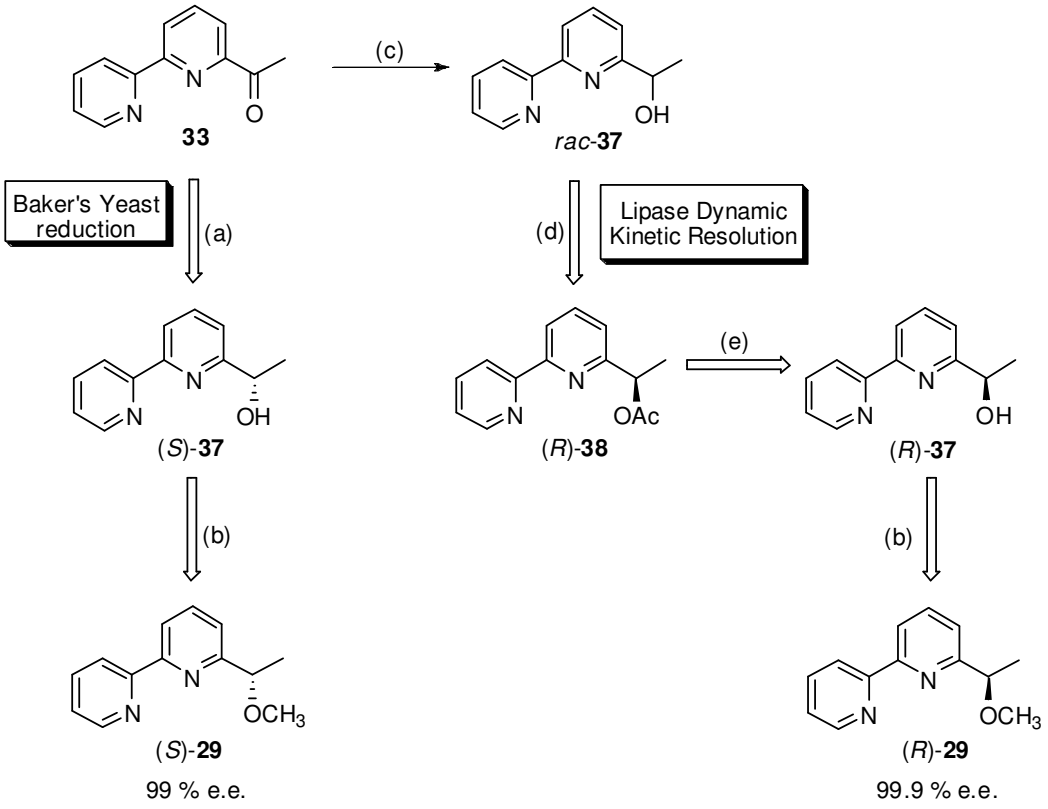

SCHEME 4. Synthesis of optically pure bipyridine ligands with chemoenzymatic methods. Reaction conditions: (a) baker's yeast, saccharose, phosphate buffer pH 7.4, 37 °C; (b) NaH, CH_3I, THF; (c) $NaBH_4$, EtOH; (d) *p*-chlorophenylacetate, toluene, 70 °C, $[Ru_2(CO)_4(\mu\text{-H})(C_4Ph_4COHOCC_4Ph_4)]$, Novozyme® 435; (e) H_2O/EtOH K_2CO_3.

DKR with *p*-chlorophenylacetate as the acyl donor, in the presence of the Ru-based redox catalyst $[Ru_2(CO)_4(\mu\text{-H})(C_4Ph_4\text{-}COHOCC_4Ph_4]$ (Shvo's catalyst) reached the

complete conversion in 48 h, giving the corresponding (*R*)-acetate **38** with excellent optical purity (e.e. > 99.9%) and in 70% yield (not optimized) after column chromatography. Its hydrolysis under mild basic conditions (aq. K_2CO_3) gave the corresponding enantiopure secondary alcohol (*R*)-**37** in 70% overall yield from the racemic alcohol **37**. The (*R*) configuration of this compound was verified by comparison with the reported optical rotation data.[17] This result confirms the well known enantiopreference of CAL-B for the (*R*) enantiomers of benzylic *sec*-alcohols.[18] As already observed by us,[16] baker's yeast (*Saccharomyces cerevisiae*) reduction of the prochiral ketone **33** proceeded in an enantiocomplementary fashion, allowing the obtainment of the opposite enantiomer (*S*)-**37** with comparable high stereoselectivity and yield. The reduction was run under fermenting conditions, (37 °C, saccharose, phosphate buffer, pH 7.4), reaching 93% conversion in 48 h. As predicted from the Prelog's rule, it afforded the alcohol in the *S* configuration,[19] isolated in 99% e.e., and 75% yield after purification. The methylation of the homochiral (*R*)**-37** and (*S*)-**37**, as described above, gave the target ligands (*R*)**-29** and (*S*)-**29** in both cases in 68% and 74% overall yield, respectively, from ketone **33**.

An alternative procedure for the synthesis of both racemic and optically pure **29** have been developed. Following the procedure already reported in Chapter 2 (Chapter 2: Figures 11 and 12), *rac*-, (*S*)- and (*R*)-**22** were synthesized. After alcohol methylation, the derivative **39** was lithiated and coupled with **35** affording product *rac*-, (*S*)- and (*R*)-**29** (Scheme 5) in the same yield obtained using the strategy previously reported (see Schemes 2 and 3).

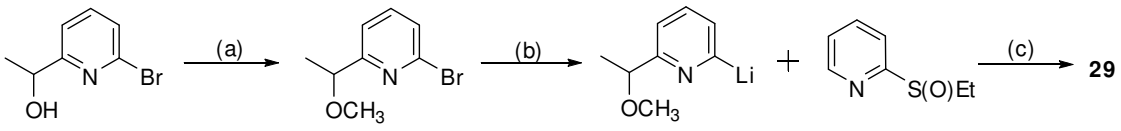

SCHEME 5. Alterantive synthesis of ligand **29**. Reaction conditions: (a) NaH, CH_3I, THF. (b) *n*-butyl-lithium, THF, -70°C. (c) THF, 25°C.

The synthesis of the achiral ligand **30** started from the known alcohol **40**,[20] which was the product of $NaBH_4$ reduction of the commercial 6-bromopicolinaldehyde (Scheme 6). The alcohol **40** was transformed into the acetylene **41**, following a procedure described in the literature for an analogous transformation,[21] which concerned a $[Pd(PPh_3)_4]$/CuI promoted coupling with trimethylsilylacetylene, followed by desilylation to **42** with Bu_4NF in THF. The conversion into the 1-methyl-1*H*-1,2,3-

triazolederivative **43** was run through a microwave-assisted copper(I)-catalyzed three-component reaction, involving the acetylene **42**, sodium azide and CH_3I, which afforded with complete regioselectivity the triazolylpyridine **43**.[22] The OH methylation was reached under the conditions described previously for **37** (Scheme 3), accessing the target ligand **30** in a 50% overall yield from the aldehyde.

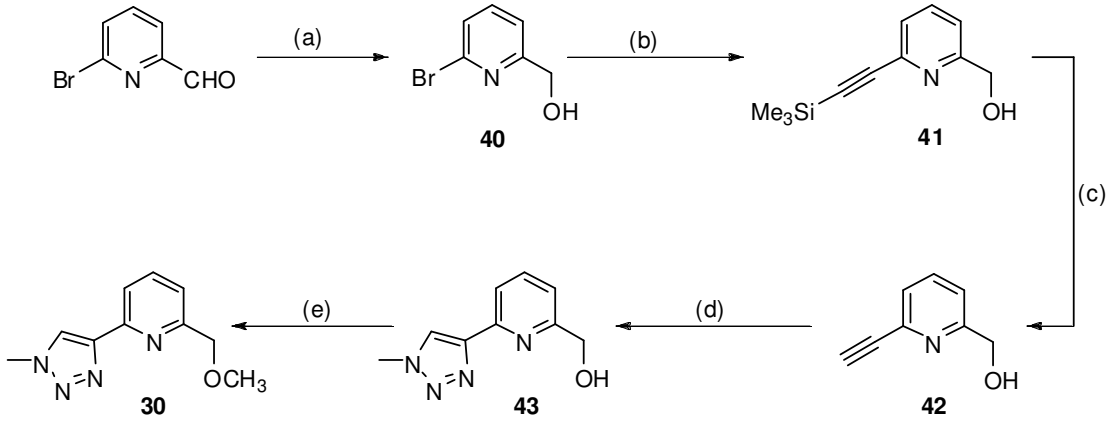

SCHEME 6. Synthesis of the achiral pyridine ligand **30**. Reaction conditions: (a) $NaBH_4$, EtOH; (b) trimethylsilylacetilene, $[Pd(PPh_3)_4]$ (cat), CuI/NEt_3; (c) Bu_4NF; (d) CH_3I, NaN_3, *t*-BuOH, H_2O, MW; (e) CH_3I, NaH, THF, 0°C.

Ligands **31** and *rac*-**32** were synthesized in the Prof. Gladiali's group (University of Sassari).[23]

3.3. SYNTHESIS OF THE Pd(II) COMPLEXES WITH LIGANDS 29-32

The synthesis of the monocationic Pd(II) complexes $[Pd(CH_3)(CH_3CN)(N\text{-}N')][PF_6]$ **29b-32b** was performed in the Dr. Milani's group (University of Trieste) starting from $[Pd(CH_3COO)_2]$ and following the five-steps procedure reported in the literature,[6] which involves a dehalogenation reaction of the neutral derivatives $[Pd(CH_3)(Cl)(N\text{-}N')]$ **29a-32a** (N-N' = **29-32**) as last step (Scheme 7).

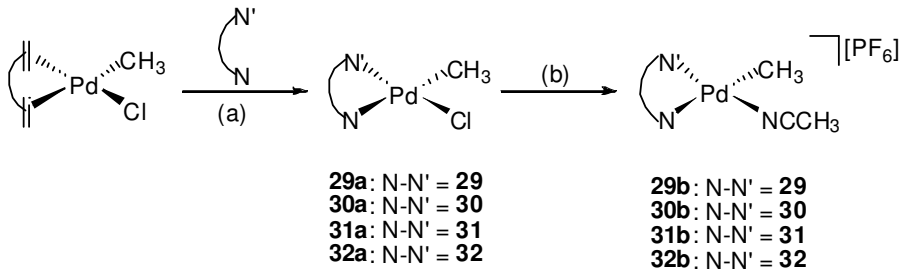

SCHEME 7. Synthesis of the Pd(II) complexes. Reaction conditions: (a) CH_2Cl_2, r. t.; (b) CH_3CN, $AgPF_6$, CH_2Cl_2.

Single crystals of the neutral derivative [Pd(CH_3)(*rac*-**29**)(Cl)] (*rac*-**29a**) were obtained at 4 °C, upon the addition of diethyl ether to a methylene chloride solution of the complex (Figure 2).

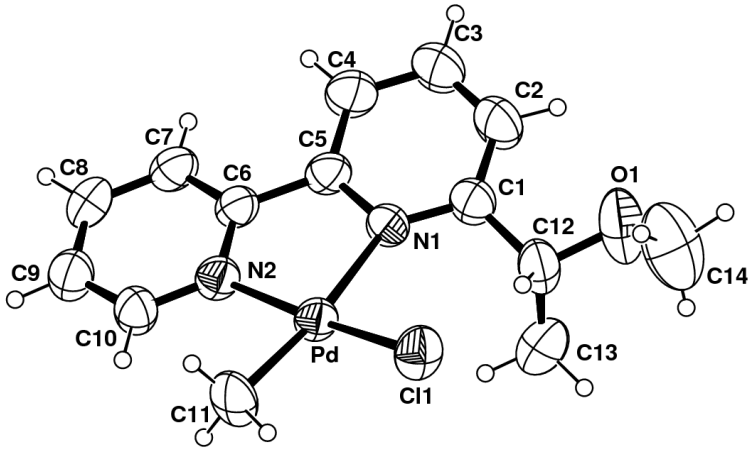

FIGURE 2. ORTEP drawing (ellipsoid 35% probability level) of the complex *rac*-**29a**. Coordination bond lengths [Å] and angles [°]: Pd-N(1) 2.229(4), Pd-N(2) 2.053(4), Pd-C(11) 2.033(5), Pd-Cl(1) 2.312(1), N(1)-Pd-N(2) 78.50(16)°, N(1)-Pd-Cl(1) 103.06(11)°, N(2)-Pd-Cl(1) 171.88(11)°, C(11)-Pd-N(2) 92.9(2)°, C(11)-Pd-N(1) 171.3(2)°, C(11)-Pd-Cl(1) 85.32(18)°.

The X-ray analysis revealed that the palladium atom attains the usual square planar geometry being bound to the chloride, to the methyl group and chelated by the nitrogen-atoms of **29**. The coordination bond lengths appear in the range usually found for Pd(II) complexes.[6]

The Pd–N(1) distance *trans* to the methyl bond is longer by about 0.17 Å with respect to the Pd-N(2) distance, due to the *trans* influence of the methyl group. The pyridine rings are twisted with a dihedral angle between the planes of 20°. In the unit cell only the isomer with Pd-CH_3 bond *trans* to the Pd-N bond of the substituted pyridine ring was found. Both complexes with the two enantiomeric forms of the racemic ligand were present.

Both neutral and monocationic complexes were characterized by elemental analysis, and NMR spectroscopy, recording the spectra in CD_2Cl_2 solution, at room temperature, for all complexes, but **30a-b** whose spectra were recorded in DMSO-d_6 solution at 60 °C. Coordination to palladium resulted in significant variation of protons chemical shifts in comparison with those of the free ligands (Figure 3).

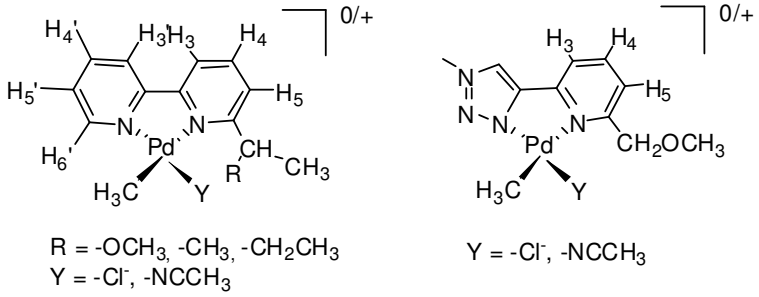

FIGURE 3. Protons numbering scheme for complexes **29-32a-b**.

The ^{1}H assignments were based on the number of signals, on their integration, on NOE and on 2D homonuclear COSY experiments. In particular, the number of signals and their integration indicate the presence of one species in solution. NOE experiments, performed upon irradiation of the $H^{6'}$ signal, indicated the *cis* relationship between the Pd-CH_3 moiety and $H^{6'}$, thus confirming the *trans* geometry between the Pd-CH_3 group and Pd-N bond where N belongs to the substituted pyridine ring. The *trans* isomer present in solution is in agreement with X-ray analysis of *rac*-**29**. This result differs from the literature data, which reported a preferential tendency of the methyl group to coordinate *trans* to less basic bipyridine N atom,[3,6,24] obviously in case of Pd complexes characterized by ligands with non-equivalent N-donor atoms. The different geometry shown by the complexes studied here might be due to the steric hindrance of the alkyl chain bound to bipyridine.

The discussion of NMR characterization starts from complexes **29a-b**, **31a-b** and **32a-b**. The most diagnostic bipyridine signals are H^3, H^4, $H^{3'}$ and $H^{4'}$, the -CH proton of the substituent in position 6 and the characteristic singlet of Pd-CH_3 moiety. Selected ^{1}H NMR data for **29a-b**, **31a-b** and **32a-b** and the corresponding free ligands are reported in Table 1.

TABLE 1. Selected ^{1}H NMR data for **29a-b**, **31a-b** and **32a-b**[a].

N-N′/complex	H^3	$H^{3'}$	H^4	$H^{4'}$	Pd-CH_3	-CH	CIS [b](δ_l-δ_c)
29	8.26(d)	8.45(d)	7.83(d)	7.81(pst)	–	4.51(m)	–
29a	7.97(m)	8.04(m)	7.97(m)	8.04(m)	1.34(s)	6.23(m)	-1.72
29b	8.17(m)	8.24(m)	8.17(m)	8.24(m)	1.35(s)	4.68(m)	-0.17
31	8.20(d)	8.50(d)	7.72(t)	7.80(pst)	–	3.13(m)	–
31a	7.88(m)	8.00(m)	7.88(m)	8.00(m)	1.32(s)	4.74(m)	-1.61
31b	8.01(m)	8.17(m)	8.01(m)	8.17(m)	1.30(s)	3.42(m)	-0.29
32	7.81(t)	8.50(d)	7.73(t)	8.22(d)	–	2.87(m)	–
32a	7.92(m)	8.00(m)	7.92(m)	8.00(m)	1.18(s)	4.57(m)	-1.7
32b	8.05(m)	8.00(m)	8.05(m)	8.00(m)	1.32(s)	3.22(m)	-0.36

[a] Spectra recorded in CD_2Cl_2 at room temperature, δ in ppm, s=singlet, t = triplet, pst = pseudo-triplet, m= multiplet. [b] CIS = Coordination Induced Shift for -CH in the complexes (δ_c) and in the free ligand (δ_l).

The singlet of the methyl bound to palladium appears in the range of frequency between 1.10 and 1.40 ppm in both neutral and cationic species.

The secondary carbon -CH proton was the most affected by the coordination to palladium. It was downfield shifted in comparison with the same signal in the free ligand spectra, in particular, for the neutral derivatives, the coordination induced shift (CIS) is about 1.70 ppm, and it is more pronounced than for the cationic complexes. This large chemical shift variation was due to the presence of Cl^- ion in *cis* position to it.[25] The aromatic protons H^3, H^4, $H^{3'}$ and $H^{4'}$ were also influenced by Pd coordination: in the free ligand their four well-separated signals were easily recognized, while in neutral and cationic derivatives the signals overlapped resulting in multiplets.

^{1}H NMR analysis of Pd-complexes bearing ligand **30** (**30a**-**b**) also showed that the most significant signals variations include the Pd-CH_3 moiety and H^4 and H^5 of the pyridine ring. Selected ^{1}H NMR data for free **30** and complexes **30a** and **30b** are reported in Table 2.

TABLE 2. Selected ^{1}H NMR data for **30** and **30a-b**[a].

N-N'/complex	Pd-CH_3	H^4	H^5
30	–	7.75(t)	8.00(d)
30a	1.01(s)	7.91(bs)	7.91(bs)
30b	0.98(s)	7.94(bs)	7.94(bs)

[a] Spectra recorded in DMSO-d_6 at 60 °C, δ in ppm, s = singlet, d = doublet, t = triplet, bs = broad singlet.

Complexes **30a-b** containing the triazolo-derived ligand were soluble in DMSO. The ^{1}H NMR spectra recorded in DMSO-d_6, at room temperature, showed broad signals that became sharp at 60 °C. Even for these complexes the NMR characterization indicated the presence in solution of one species only, that was not possible to recognize as the *cis* or the *trans* isomer via NOE experiments. In the spectrum of **30b** the signal of free acetonitrile (in 1:1 ratio with respect to the Pd-CH_3 moiety) was detected, due to the exchange process between the coordinated acetonitrile and dimethyl sulfoxide. The broadening of the signals observed at room temperature is indicative of a dynamic process in solution, that is reasonably attributed to an exchange process between dimethylsulfoxide and at least one of the Pd-N bond of the chelating ligand.

3.4. CATALYTIC ACTIVITY OF COMPLEXES 29b-32b

The monocationic complexes **29b**-**32b** were tested as pre-catalysts in the styrene carbonylation reaction under standard conditions: T = 30 °C, CO pressure = 1 atm, 1,4-benzoquinone (BQ) as oxidant with [BQ]/[Pd] = 40, solvent = 2,2,2-trifluoroethanol (TFE) and [styrene]/[Pd] = 6800.

At the end of the catalytic runs no solid was isolated, either upon addition of methanol. The reaction mixture was dried under vacuum, yielding a yellow/orange oil that was characterized by ESI-MS spectroscopy and ^{1}H and ^{13}C NMR experiments (in $CDCl_3$, at room temperature). The mass analysis revealed that the product was a mixture of low molecular weight molecules ($M_w \approx$ 368–896 Da). The repetitive unit corresponded to 132 Da and the molecular weight distribution was symmetrically centred at 655.3 Da,

that represented the oligomer with three repetitive units (Figure 4). On the basis of this analysis the product was characterized as CO/styrene oligoketones with a number of repetitive units ranging from 1 to 5.

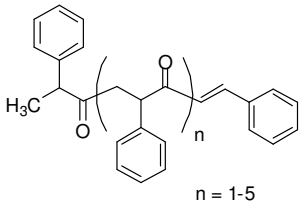

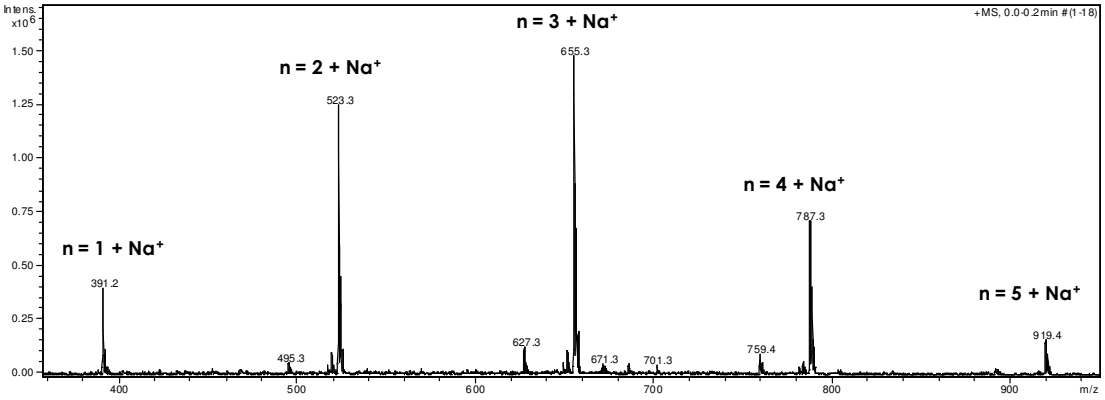

FIGURE 4. ESI-MS spectroscopy of CO/styrene oligoketones synthesized with **29b**.

The oligomeric nature of the reaction products was also confirmed by the comparison of the ^{1}H-NMR with that of a typical polyketone (Figure 5): in the spectrum of the copolymer three broad signals are observed for the methynic and the two diasterotopic methylenic protons, whereas in the spectrum of the oligomeric material several sharp signals are present, also allowing the recognition of the end groups.

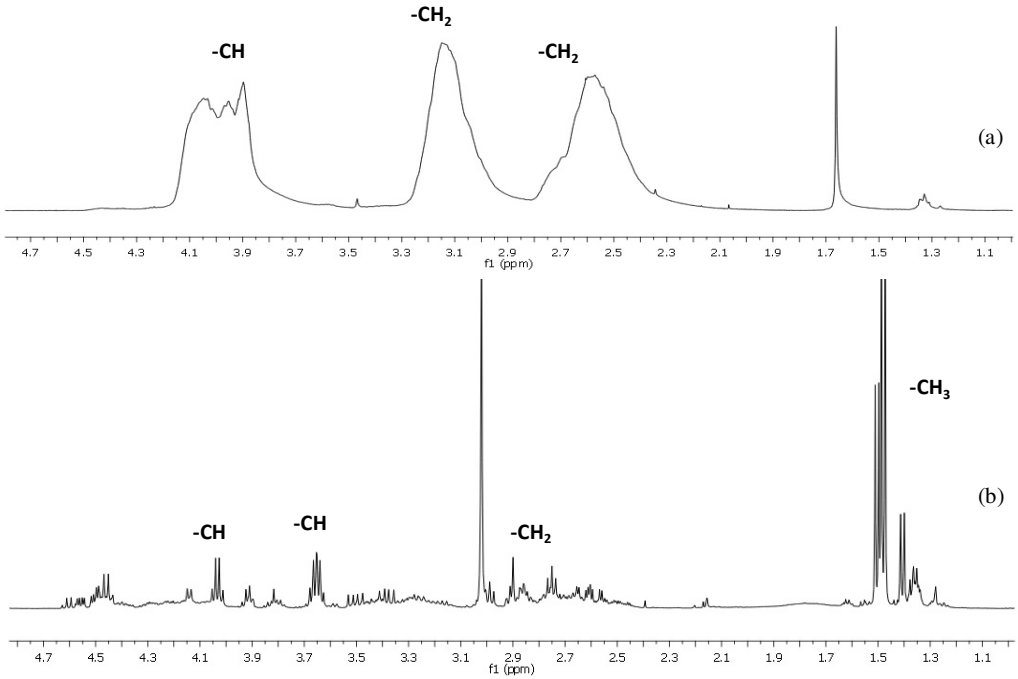

FIGURE 5. ^{1}H-NMR spectrum in $CDCl_3$, at r.t. of: (a) CO/styrene copolymer; (b) CO/styrene oligomer. Aliphatic region.

In agreement with literature data,[26] the set of doublets observed in the range 1.35-1.55 ppm was indicative of a diphenylpentyl-5-one end group (Figures 6 and 7). In particular, the two internal doublets (1.48 ppm and 1.50 ppm) were assigned to the *l* (like) and *u* (unlike) stereoisomeric forms of 2,5-diphenylpentyl-3-one group (A), which was the main termination present. The doublet at higher field (1.40 ppm) was analogously attributed to the regioisomeric termination 2,4-diphenylpentyl-3-one, of which only the signal of the *l* diastereoisomer (B) was observed (Figures 6 and 7).

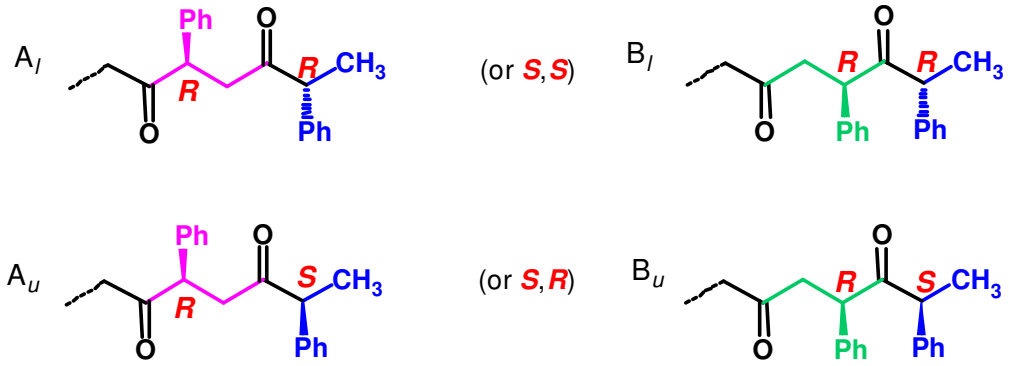

FIGURE 6. Possible CO/styrene oligomers chain ends.

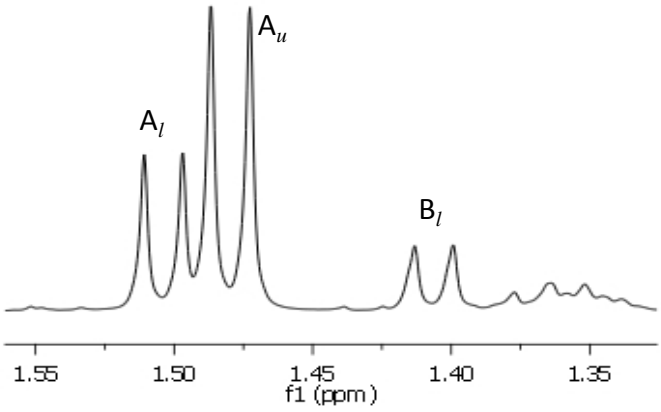

FIGURE 7. ^{1}H NMR spectra in $CDCl_3$: region of the methyl group signals of oligoketones obtained with *rac*-**29b**.

The CO/styrene oligomerizations were carried out with all the synthesized complexes (**29b-32b**) and all of them generated active species for this reaction. The ligand nature remarkably influenced the catalyst productivity. The cationic complex with the triazole ligand (**30b**) gave the least productive catalyst, while *rac*-**29b** afforded the most active one, among those tested, reaching a productivity of almost 200 g PK/g Pd (grams of oligoketones per gram of palladium) (Figure 8 and Table 3). In each case no decomposition to Pd metal was observed. The nature of the ligand did not affect the product distribution.

Thus, the introduction of a substituent on the *ortho* position, with respect to the N-donor, of one of the two pyridine rings of the bpy-derived ligand, remarkably affected the selectivity of the carbonylation reaction that was directed towards the synthesis of oligomers. When no substituents was present on this position, polymers of different molecular weight were the products.[27]

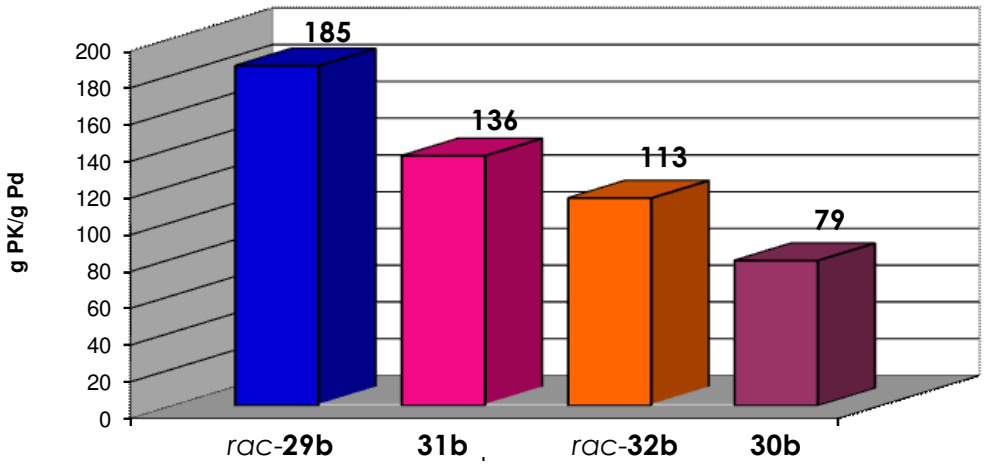

FIGURE 8. CO/styrene oligomerization: effect of nitrogen-donor ligand. Pre-cat.: $[Pd(CH_3)(N\text{-}N')(CH_3CN)][PF_6]$. Reaction conditions: $n_{Pd} = 1.27 \times 10^{-5}$, styrene V = 10 mL, TFE V = 20 mL, $p_{CO} = 1$ atm, [BQ]/[Pd] = 40, T = 30 °C, time = 24 h, [styrene]/[Pd] = 6800.

TABLE 3. CO/styrene oligomerization: effect of the ligand nature.

Entry	Pre-cat.	Yield (mg)	Productivity (g PK/g Pd)	A/B (%)	A (%)	
					l	*u*
1	*rac*-**29b**	254	185	63/37	40	60
2	**31b**	187	136	75/25	> 99	–
3	*rac*-**32b**	155	113	75/25	> 99	–
4	**30b**	103	79	88/12	80	20

Reaction conditions: see Figure 8.

The nature of the N-N' ligand affected the regioisomeric and the diasteroisomeric distribution of the end-groups. With all the tested pre-catalysts, the oligomer with the 2,5-diphenyl-pentan-3-one end group was the prevailing regioisomer: the A to B ratio depended on the substituent on the pyridine ring, being the least for *rac*-**29** and the highest for **30**. Even the ratio between the two diasteroisomers, A_l and A_u, appeared to be related to the nature of the substituent on the pyridine ring and it should be noted that the pre-catalyst containing ligands **31** and *rac*-**32** gave the A_l diasteroisomer, exclusively.

It is reasonable to assume that the high enantioface discrimination obtained with pre-catalysts **31b** and *rac*-**32b** might be due to the steric hindrance of the alkyl substituents of ligands **31** and *rac*-**32**, larger than that of the methoxy group of *rac*-**29** and **30**. Due to this steric hindrance, the growing chain is preferentially coordinated *trans* to the substituted pyridine ring, thus the incoming styrene has to coordinate *cis* to it by experiencing the presence of the bulky substituent that finally determines the styrene enantioface to be coordinated (Figure 9).

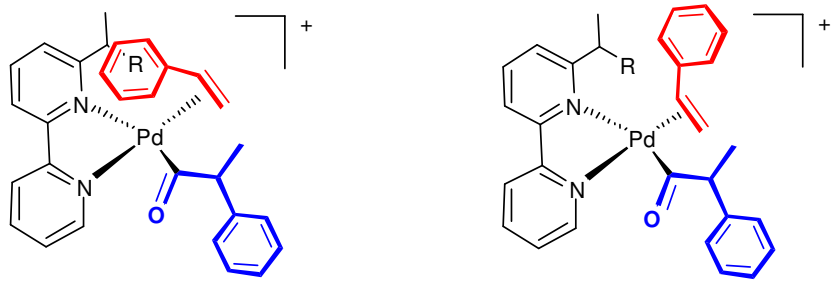

FIGURE 9. The two possible styrene coordinations on the Pd-aryl intermediate.

A similar mechanistic hypothesis, implying the site selective coordination of the alkene, was introduced by Consiglio for the CO/styrene copolymerization catalyzed by a Pd-complexes with P-N ligands,[28] later on was involced by Nozaki for the CO/propene copolymerization[29] and by us to explain the synthesis of the isotactic CO/styrene polyketone with Pd-amine-imine complexes.[30]

To optimize the reaction conditions, a series of experiments was carried out with pre-catalyst *rac*-**29b** varying some reaction parameters.

The variation of [BQ]/[Pd] ratio (Table 4) evidenced that the productivity increased on increasing the [BQ]/[Pd] ratio. Noteworthy, when the oxidant was not added to the reaction mixture the formation of inactive palladium black was observed after 2 h and no product was isolated after 24 h. The addition of a remarkable excess of 1,4-benzoquinone, with respect to palladium, resulted in a stabilization of the active species and in no formation of Pd(0) over the investigated range of time. The amount of benzoquinone did not show any effect on oligomers distribution.

TABLE 4. CO/styrene oligomerization: effect of [BQ]/[Pd] ratio.

[BQ]/[Pd]	Yield (mg)	Productivity (g PK/g Pd)
0	0	0
5	75	55
20	186	135
40	251	185

Pre-cat.: [Pd(*rac*-**29**)(CH_3)($NCCH_3$)][PF_6], reaction conditions: see Figure 8.

Prolonging the reaction time (Figure 10) from 8 to 48 h resulted in a remarkable increase in the productivity; the trend showed that the catalyst was still active after 48 h, without any evident decomposition to palladium metal. The reaction time did not affect the number of repetitive units inserted into the oligomer chain.

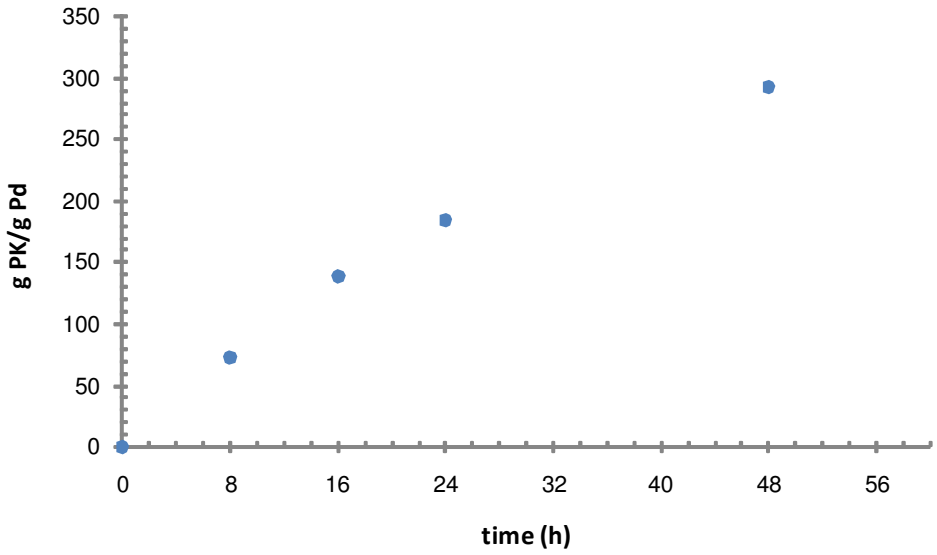

FIGURE 10. CO/styrene oligomerization: effect of reaction time. Pre-cat.: [Pd(CH_3)(*rac*-**29**)(CH_3CN)][PF_6], reaction conditions: see Figure 8.

With the aim to evaluate if chiral ligand effects were present, some CO/styrene oligomerizations were carried out using the complexes with ligand **29** in its enantiomerically pure forms: [Pd((*S*)-**29**)(CH_3)($NCCH_3$)][PF_6] ((*S*)-**29b**) and [Pd((*R*)-**29**)(CH_3)($NCCH_3$)][PF_6] ((*R*)-**29b**) (Table 5, entries 2, 3; Figure 11). The highest

productivity was achieved with (*S*)-**29b** as pre-catalyst, followed by *rac*-**29b** and (*R*)-**29b**. In all cases the A regioisomer was preferentially formed, even though the A/B ratio depended on the chirality of the ligand, being the highest with the (*S*) enantiomer and the lowest when the racemic ligand was used.

TABLE 5. CO/styrene oligomerization: effect of ligand chirality and of [Pd]/[ligand] ratio.

Entry	Pre-cat.	Yield (mg)	Productivity (g PK/g Pd)	A/B (%)	A (%)	
					l	*u*
1	*rac*-**29b**	254	185	63/37	40	60
2	(*S*)-**29b**	267	194	90/10	25	75
3	*(R)*-**29b**	211	153	75/25	75	25
4[a]	*rac*-**29b** + *rac*-**29**	203	158	75/25	> 99	–
5[a]	(*S*)-**29b** + (*S*)-**29**	145	105	79/21	> 99	–
6[a]	*(R)*-**29b** + (*R*)-**29**	129	94	69/31	> 99	–

Pre-cat.: $[Pd(CH_3)(N\text{-}N')(CH_3CN)][PF_6]$, reaction conditions: see Figure 8. [a] [Pd]/[free ligand] = 1/0.5.

As far as the diastereoisomeric relationship was concerned, the A_l/A_u ratio was low by using *rac*-**29b** (Table 5, entry 1), whereas with complexes (*S*)-**29b** and (*R*)-**29b** an increase in the ratio was obtained, but in the opposite diasteroisomer.

A series of oligomerization reaction was carried out with the addition of a free ligand excess ([Pd]/[free ligand] = 1/0.5) to the corresponding catalytic system (Table 5, entries 4, 5, 6). A decrease in the productivity was observed with respect to the catalytic system containing the pre-catalyst only, more pronounced for complex (*S*)-**29b**, thus suggesting that the excess of free ligand has an inhibiting effect: it should compete with the two monomers for the fourth coordination side on palladium.

Oligomers composition was not affected either by the ligand configuration or by the [Pd]/[ligand] ratio.

Free ligand addition slightly affected the regioisomer ratio: for the optically pure ligands, the A/B ratio decreased, while it increased when the racemic ligand was used. More interesting it was the effect of free ligand addition on oligomers stereochemistry:

regardless to the ligand configuration, complete stereoselectivity for the *l* diastereoisomers synthesis was observed (Table 5, Figure 11).

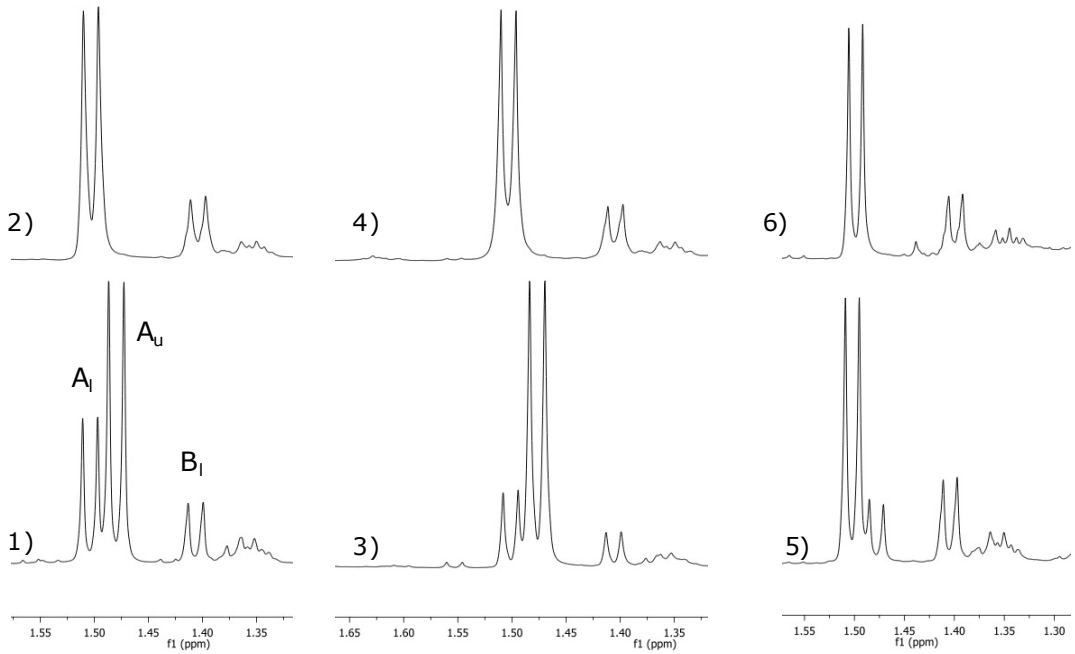

FIGURE 11. ^{1}H NMR spectra in $CDCl_3$: methyl group signals of oligoketones obyained with: 1) *rac*-**29b**; 2) *rac*-**29b** + *rac*-**29**; 3) (*S*)-**29b**; 4) (*S*)-**29b** + (*S*)-**29**; 5) (*R*)-**29b**; 6) (*R*)-**29b** + (*R*)-**29**. Reaction conditions: see Table 8.

The oligoketones obtained with the chiral complexes (*S*)-**29b** and (*R*)-**29b** and upon addition of the free enantiomerically pure ligand, (*S*)-**29** and (*R*)-**29** respectively, were analyzed by Circular Dichroism (Figure 12).

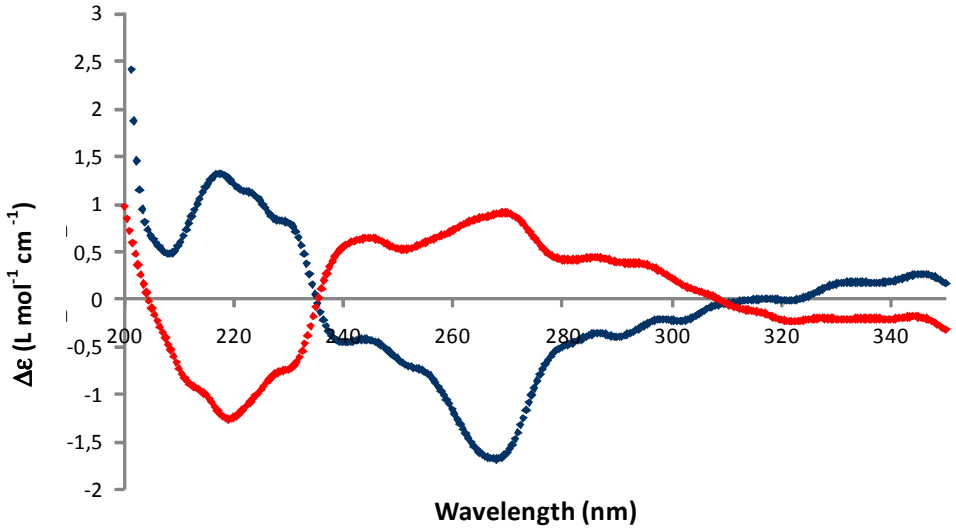

FIGURE 12. Circular dichroism spectra of oligoketones obtained by (*R*)-**29b +** (*R*)-**29** (blue curve) and (*S*)-**29b +** (*S*)-**29** (red curve).

The oligomers were optically active, but the CD curves were not symmetric. The low molar ellipticity values observed indicated a low stereoregular structure. As expected, the oligomers obtained with *rac*-**29b** + *rac*-**29** did not show any optical activity.

The CD curve analysis combined with the ^{1}H-NMR data (Table 5) indicated that a high enantioface discrimination took place for the insertion of the first two styrene units but, afterwards, a loss of enantioface discrimination occurred, thus suggesting that the chirality of (*S*)-**29b** or (*R*)-**29b** catalyst site was not sufficient to overcome the effect of the chirality of the growing chain. Furthermore, the opposite sign of the ellipticity of the CD band for the oligoketones indicated that, for the first two repetitive units, the opposite enantioface of styrene was inserted into the oligoketone chain when ligand (*S*)-**29** or (*R*)-**29** was used.

These results suggested that when an excess of ligand was present, a different catalytic species might be formed, with respect to that generated by the complex only. It is reasonable to assume that two molecules of N-N' ligand were bound to the same Pd-centre. Actually when the oligomerization reactions were carried out by adding different amounts of the free ligand with respect to palladium, no effect on the productivity and on the product features was observed (Table 6): in all the catalytic runs a value of 150 g PK/g Pd was obtained. Thus suggesting that only a small

percentage of the pre-catalyst was transformed into the active species, that should have two molecules of N-N' bound to palladium.

TABLE 6. CO/styrene oligomerization: effect of [Pd]/[ligand] ratio.

[free lig]/[Pd]	Yield (mg)	Productivity (g PK/g Pd)	A/B (%)	A (%)	
				l	*u*
0.1/1	207	151	63/37	> 99	–
0.5/1	203	150	64/36	> 99	–
0.25/1	202	149	62/38	> 99	–

Pre-cat.: [Pd(CH_3)(*rac*-**29**)(CH_3CN)][PF_6], reaction conditions: see Figure 8.

Complex *rac*-**29b** was also proved to be catalyst for the oligomerization of CO with 4-methylstyrene. The reaction was carried out under the same conditions used for styrene (Table 7).

TABLE 7. CO/alkene oligomerization: effect of the alkene nature.

Olefin	Yield (mg)	Productivity (g PK/g Pd)	A/B (%)	A(%)	
				l	*u*
styrene	254	185	63/37	40	60
4-CH_3-styrene	405	295	67/33	42	58

Pre-cat: [Pd(*rac*-**29**)(CH_3)($NCCH_3$)][PF_6], reaction conditions: see Figure 8.

As for styrene, also for 4-methylstyrene the product isolated at the end of catalytic run was the corresponding oligoketone as characterized by ESI-MS and NMR spectroscopy. In addition, the concomitant formation of poly-(4-methylstyrene) was observed.

The productivity in CO/4-methylstyrene oligomers was higher than that obtained with styrene, in analogy with the results reported in the literature for the CO/vinyl arene copolymerization.[5,24]

No effect of the nature of the vinyl arene on the regioisomeric and diasteroisomeric ratio of the oligomers end groups was found.

3.5. MECHANISTIC INVESTIGATIONS

With the aim to understand the role played by the second molecule of the N-N' ligand, the complexes $[Pd(N\text{-}N')_2(CH_3)][PF_6]$ (N-N'= *rac*-**29**, (*R*)-**29**, **31**, *rac*-**32**) containing two molecules of the N-N' ligand were synthesized from the corresponding monocationic derivatives, through an exchange reaction of the coordinated acetonitrile with a second molecule of the nitrogen-donor ligand (Scheme 8).[31,32]

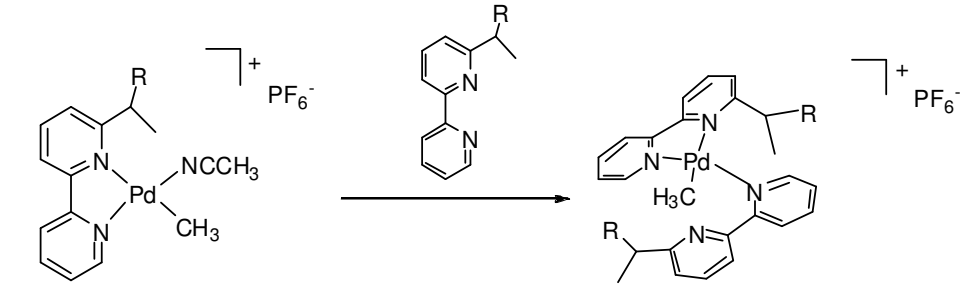

R = -OCH3 **29b**, -CH3 **31b**, -CH2CH3 **32b**

R = -OCH3 **29c**, -CH3 **31c**, -CH2CH3 **32c**

SCHEME 8. Synthesis of the $[Pd(N\text{-}N')_2(CH_3)][PF_6]$ complexes **29c**, **31c**, **32c**. Reaction conditions: CH_2Cl_2, r. t.

Single crystals, suitable for X-ray analysis, of *rac*-**29c** derivative were obtained upon addition of diethyl ether to a CD_2Cl_2 solution of the complex, kept overnight at 4 °C (Figure 13). The palladium ion has the typical square planar coordination geometry. One molecule of the N-N' ligand acts as a bidentate ligand, while the second molecule shows a monodentate coordination being bound to the metal centre with the nitrogen atom of the unsubstituted pyridine ring. This bond is *trans* to the Pd-N bond of the unsubstituted pyridine ring of the chelating N-N' molecule, while the Pd-N bond of the substituted pyridine ring is *trans* to the Pd-CH_3 fragment. The second nitrogen atom of the monocoordinated N-N' ligand occupies a pseudo-apical position at 2.656(4) Å from Pd, indicating a weak interaction between these two atoms. In the literature there are few other examples of palladium-organometallic complexes of general formula $[Pd(N\text{-}N)_2(L)][X]$ (in which N-N = Ar-BIAN, phen and its derivatives; L = CH_3, CH_2NO_2; X = triflate, PF_6^-) with two molecules of bidentate nitrogen ligands, one of which acting

as a monodentate ligand. They involve bis(aryl)acenaphthenequinonediimine ligands (Ar-BIAN)[31], or 1,10-phenanthroline and their derivatives.[32]

In the reported crystal structures the Pd---N interaction, where the nitrogen atom belongs to the uncoordinated ring of the N-N molecule, has a distance varying between 2.562(6) Å and 2.73(8) Å. The Pd---N4 distance found in the crystal structure of *rac*-**29c** falls in this range.

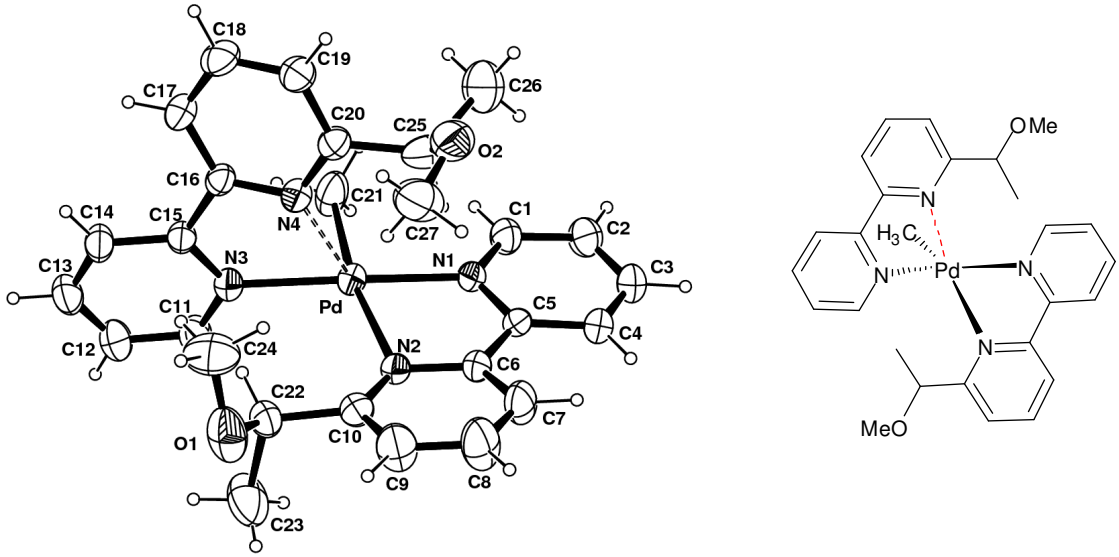

FIGURE 13. ORTEP drawing of the cation [Pd(*rac*-**29**)$_2$(CH$_3$)]$^+$ (**29c**). Only a stereoisomer is reported for clarity. Coordination bond lengths [Å] and angles [°]: Pd-CH$_3$ 2.026(4), Pd-N(1) 2.055(3) Pd-N(3) 2.087(4), Pd-N(2) 2.247(3), Pd---N(4) 2.656(4), N(1)-Pd-N(2) 78.10(15)°, N(1)-Pd-N(3) 172.31(16)°, C(21)-Pd-N(1) 92.91(18)°, N(3)-Pd-N(2) 106.58(14)°, C(21)-Pd-N(2) 170.39(18)°, C(21)-Pd-N(3) 82.74(18)°.

A shared feature of the [Pd(N-N)$_2$(L)][X] complexes reported in literature was the equivalence in solution of the two N-N molecules, as shown by NMR studies, that appeared to be in contrast with the structure in the solid state. Low temperature NMR experiments evidenced the presence of a fluxional process, which rendered both of the two molecules of N-N ligand as well as both halves of each of them equivalent.[31,32b,c]

Complexes *rac*-**29c**, (*R*)-**29c**, **31c**, **32c** were also characterized in solution by recording ^{1}H NMR spectra in CD$_2$Cl$_2$, at room temperature.

In the ^{1}H NMR spectrum of (*R*)-**29c** two signals for the Pd-CH$_3$ fragment were present, together with two sets of resonances for all the protons of the N-N' ligand (Figure 14a). The number of signals and their integration indicated the presence in solution of two species. In each species the two molecules of N-N' ligand are equivalent and NOE

experiments, performed both upon irradiation of the $H^{6'}$ signal or the Pd-CH_3 singlet, evidence the relative *cis* position of these two groups. A ROESY experiment indicate that these two species are in exchange with a rate that, at room temperature, is slow on the NMR time scale.

The ^{1}H NMR spectrum of (*rac*)-**29c** showed the same signals observed in the spectrum of (*R*)-**29c** plus an additional set of resonances with chemical shift values similar to those found for (*R*)-**29c**, indicating that other two species were present in solution (Figure 14b).

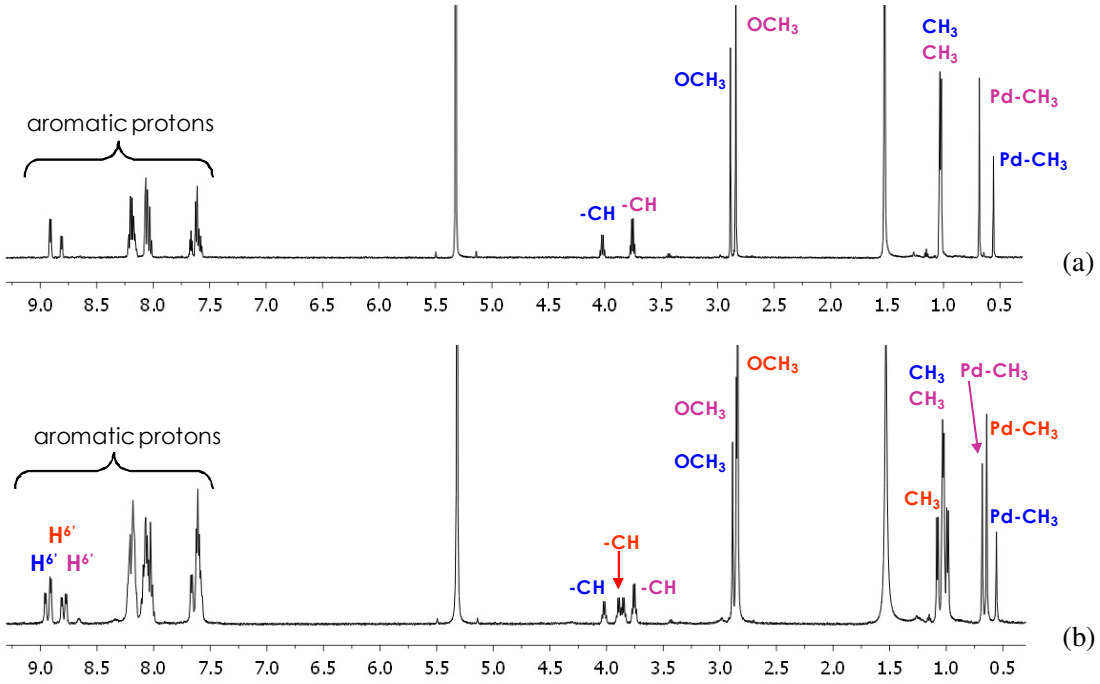

FIGURE 14. ^{1}H NMR spectra in CD_2Cl_2, at room temperature, of: (a) (*R*)-**29c**; (b) (*rac*)-**29c**.

With the aim to explain these static proton NMR spectra, a frozen trigonal bipyramid coordination geometry of palladium was assumed (Figure 15). The coordination positions in the equatorial plane are occupied by the methyl group and the nitrogen atoms of the two substituted pyridine rings, while the two nitrogen donors of the unsubstituted rings are in the axial positions. In this geometry the palladium is a stereogenic centre and the species present in the solution of (*R*)-**29c** are the two diastereoisomers differing for the palladium absolute configuration, R,R,Δ_{Pd} and R,R,Λ_{Pd}. For the complex (*rac*)-**29c** the signals of the two diasteroisomers R,S,Δ_{Pd} and R,S,Λ_{Pd} were also evident.

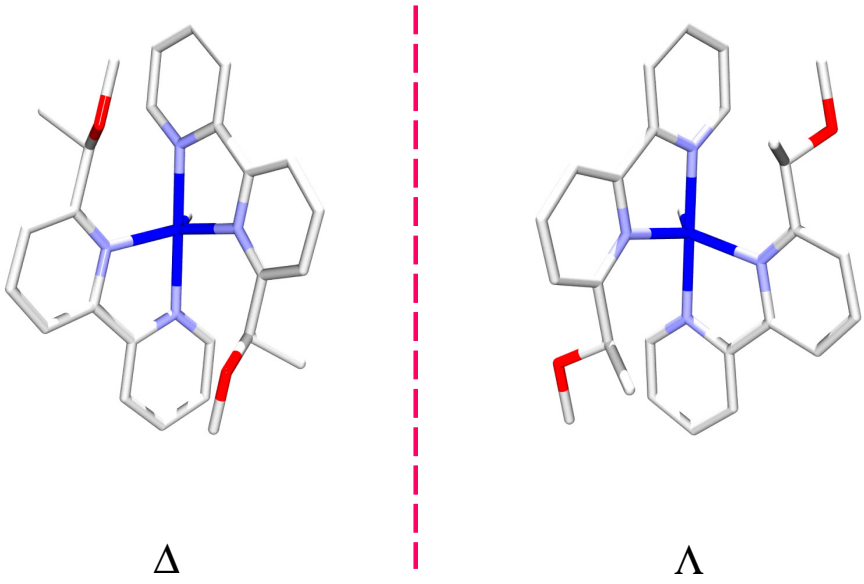

FIGURE 15. Computer modelling of the two diastereoisomeric palladium complexes.

This hypothesis was also confirmed by the ^{1}H NMR spectra of complexes **31c** and **32c**. In particular, in the region of the aliphatic protons signals of **32c**, having the racemic *rac*-6-*sec*-butyl-2,2'-bipyridine coordinated to palladium, the resonances of four species were evident, that were assigned to the racemic and the *meso* forms of the Pd-complex (Figure 16).

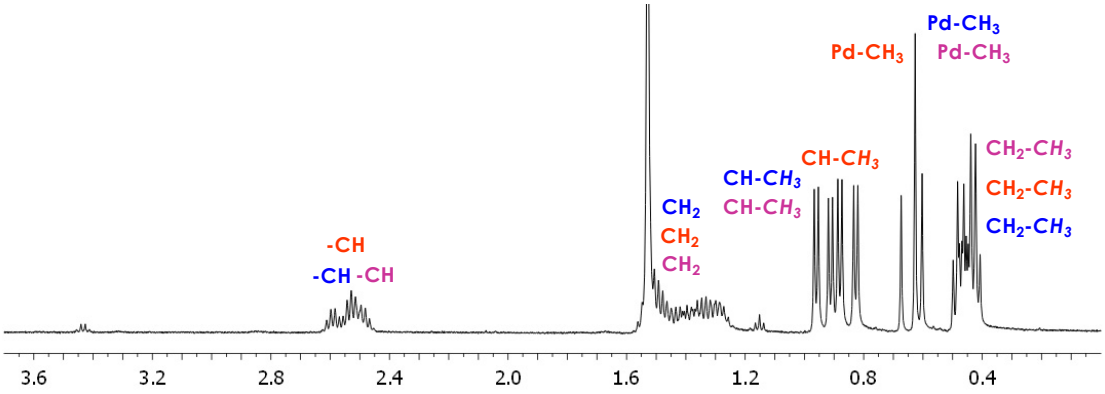

FIGURE 16. ^{1}H NMR spectrum in CD_2Cl_2, at room temperature, of **32c**. Region of aliphatic protons.

Finally, in the spectrum of complex **31c**, having the 6-*iso*-propyl-2,2'-bipyridine, two doublets were observed for the methyl groups of the *iso*-propyl substituent indicating that they are diastereotopic (Figure 17). Since the ligand is achiral, the unique source of chirality is the stereogenic palladium.

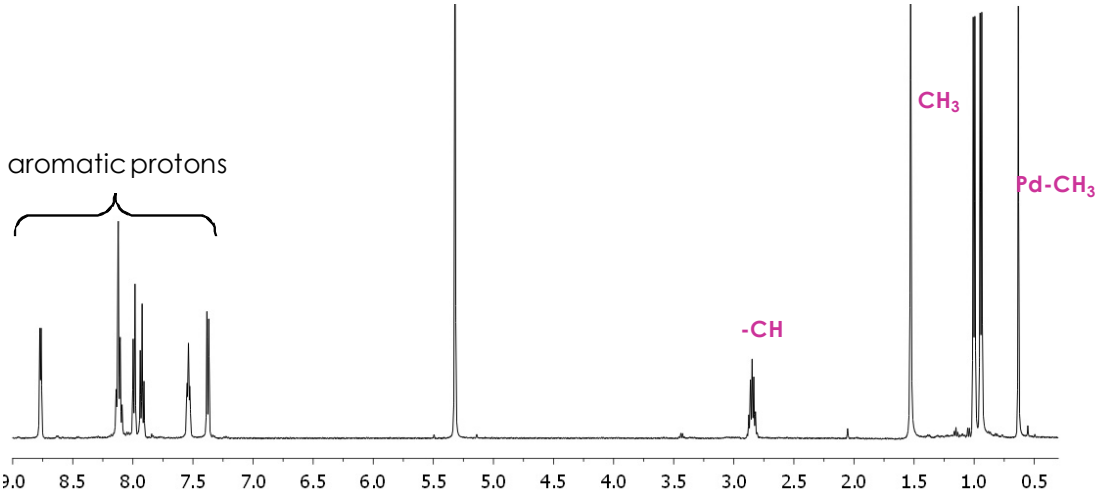

FIGURE 17. ^{1}H NMR spectrum in CD_2Cl_2, at room temperature, of **31c**.

Palladium(II) has a strong preference, in the absence of a particularly bulky environment, for the square planar coordination geometry and this is confirmed by the crystal structure of (*rac*)-**29c**. Thus, even for complexes *rac*-**29c,** (*R*)-**29c**, **31c**, **32c**, as reported in the literature for the [Pd(N-N')$_2$(L)][X] derivatives, a fluxional process that renders equivalent the two molecules of N-N' should be present in solution and the two modelled pentacoordinated molecules represent two limiting structures. At room temperature, the rate of this process is slow on the NMR time scale.

To gain some insights into the mechanism of the co-oligomerization reaction, the reactivity of complexes *rac*-**29b**, *rac*-**29c** and (*R*)-**29c** with labelled carbon monoxide was studied by *in situ* NMR spectroscopy.

When ^{13}CO was bubbled for 5 min into a 10 mM solution of complex *rac*-**29b**, in CD_2Cl_2, at 25 °C, in the ^{1}H NMR spectrum of the resulting solution the signal of the Pd-CH_3 disappeared, replaced by a doublet at 2.92 ppm. The signal of free acetonitrile was present, while no signal due to free *rac*-**29**, was observed. In the carbonyl region of the ^{13}C NMR spectrum the two signals at 214.0 and 173.6 ppm were assigned to the carbonyl group of the Pd-acetyl fragment and to the CO bonded to Pd, respectively (Figure 18a). On the basis of these data and on the literature, [30,32c,33] it was reasonable to assume that the species resulting from the carbonylation reaction was the Pd-acetyl-carbonyl derivative [Pd($COCH_3$)(CO)(*rac*-**29**)][PF_6]. No information was obtained about the geometry of this species (Scheme 9a).

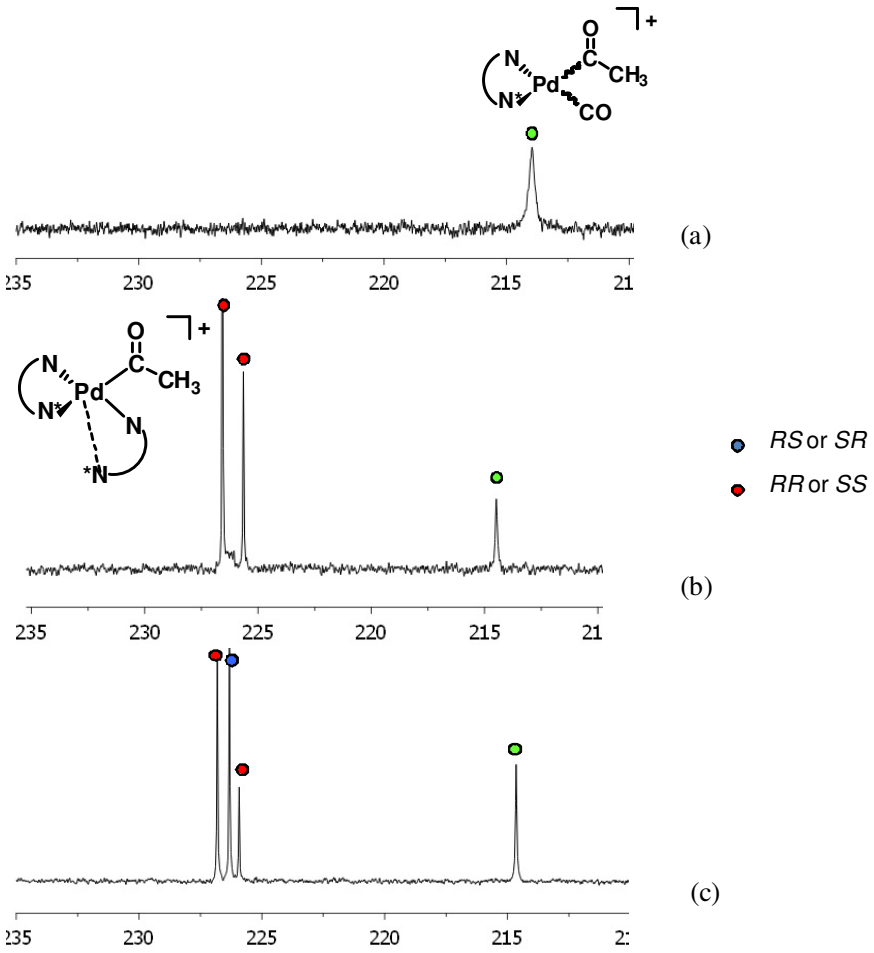

FIGURE 18. ^{13}C NMR spectra in CD_2Cl_2, at r. t. of: (a) *rac*-**29b** + ^{13}CO; (b) (*R*)-**29c** + ^{13}CO; (c) *rac*-**29c** + ^{13}CO. Carbonyl region.

The same experiment, under the same conditions, was carried out on complexes *rac*-**29c** and (*R*)-**29c**. In the ^{1}H NMR spectrum of the solution obtained from the reaction of (*R*)-**29c** with ^{13}CO, no signal due to the Pd-CH_3 complex was present anymore, and two new doublets at 1.94 and 1.99 ppm appeared. No signal due to the free ligand was evident and all the signals of the ligand were shifted with respect to the same resonances in the precursor (Figure 19). Analogous variations were observed in the spectrum of the solution resulting from the reaction of *rac*-**29c** with labelled carbon monoxide. The carbonyl region of the corresponding ^{13}C NMR spectra showed, in addition to the signals at 214.7 and 172.9 ppm, two or three new resonances at 225.9 (*RR* or *SS*), 226.3 (*RS* or *SR*), and 226.8 (*RR* or *SS*) ppm, depending if the complex with the *R* enantiomer or the racemic form of the ligand was studied (Figure 18 band c). These NMR data indicated that even the complexes *rac*-**29c** and (*R*)-**29c** easily

reacted with CO at room temperature leading to the palladium-acetyl species containing both N-N' ligands coordinated to the metal ion, $[Pd(N\text{-}N')_2(COCH_3][PF_6]$. This species was in equilibrium with the corresponding Pd-acetyl-carbonyl derivative $[Pd(COCH_3)(CO)(N\text{-}N')][PF_6]$ (Scheme 9b).

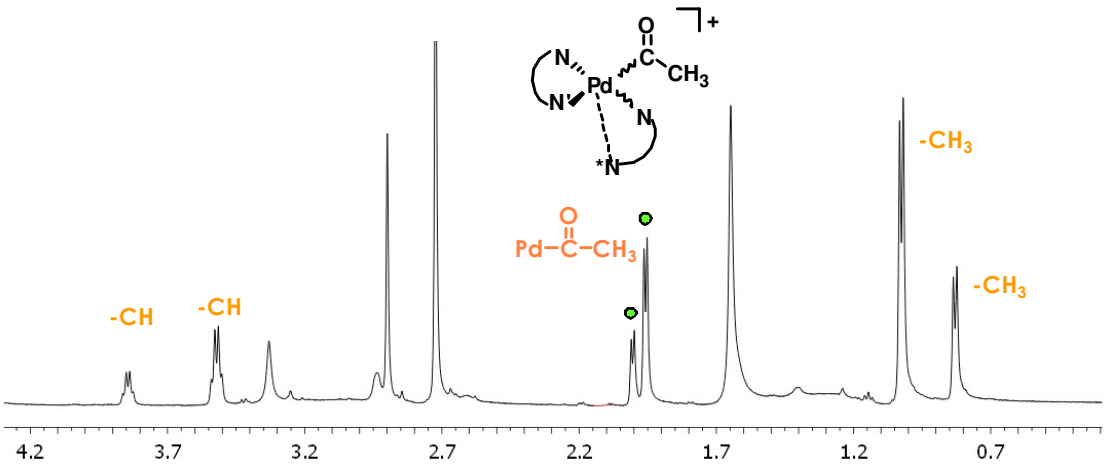

FIGURE 19. ^{1}H NMR spectra in CD_2Cl_2 of (*R*)-**29c** + ^{13}CO; region of aliphatic protons.

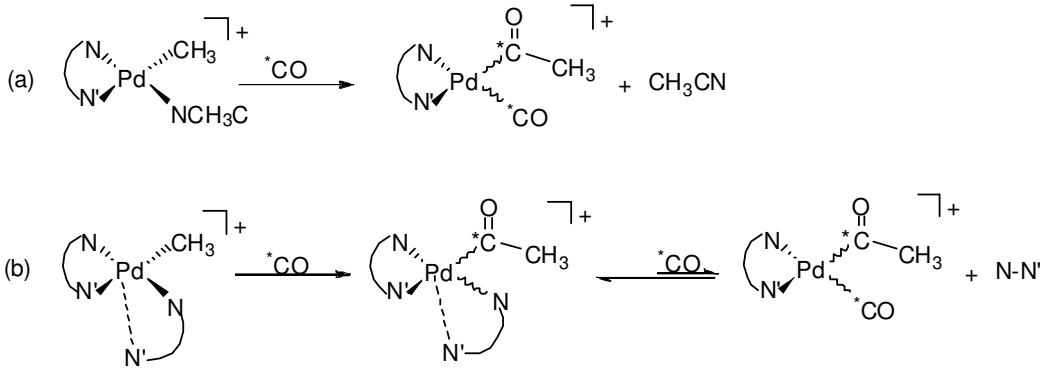

SCHEME 9. Reactivity with ^{13}CO of complexes **29b** (a), *rac*-**29c** and (*R*)-**29c** (b).

An analogous reactivity with carbon monoxide was reported in the literature for complexes $[Pd(N\text{-}N)_2(CH_3)][PF_6]$ (N-N = phen and its substituted derivatives).[32c]

On the basis of these NMR studies and of the co-oligomers end-groups it has been possible to depict an hypothesis for the mechanism of the oligomerization reaction (Scheme 10).

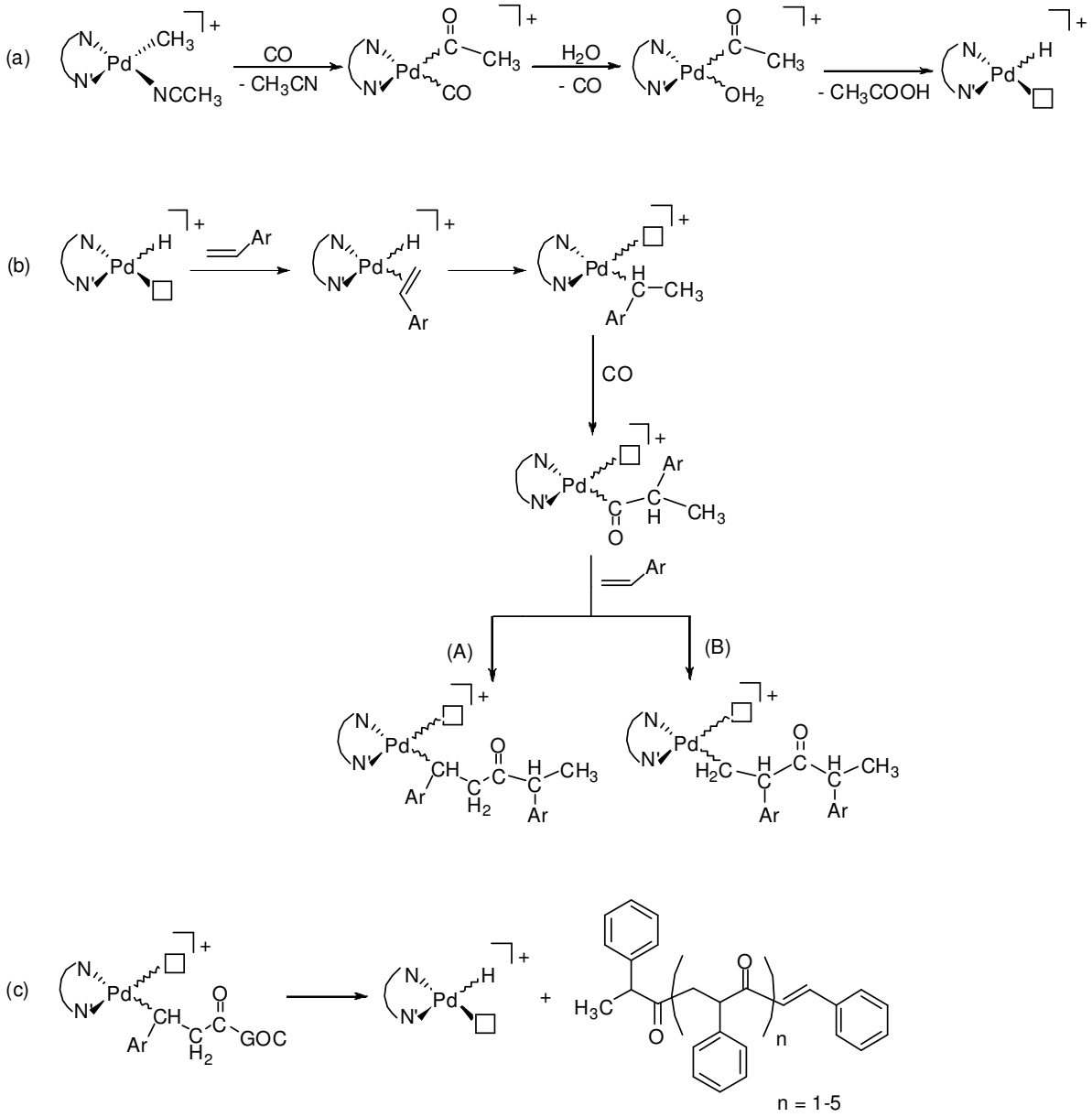

SCHEME 10. The proposed mechanism: (a) activation step; (b) insertion of the first two repetitive units; (c) termination step (GOC = growing oligomer chain).

The catalitycally active species is the Pd-H intermediate that might be formed from the pre-catalyst via insertion of carbon monoxide into the Pd-CH_3 bond, followed by the nucleophilic attack of water (present in traces in TFE) on the Pd-acetyl intermediate, leading to acetic acid and the Pd-H (Scheme 10a). On the latter the coordination/insertion of styrene occurs with a secondary regiochemistry, followed by the insertion of CO into the Pd-alkyl bond. Afterwards, the second molecule of styrene inserts into the Pd-acetyl bond, but the insertion reaction is not regiospecific anymore, since the insertion with a primary regiochemistry also takes place (Scheme 10b). The

growing of the oligomeric chain proceeds up to a maximum of five repetitive units, then a β-hydrogen elimination occurs with the formation of the co-oligomer having a vinylic termination and of the Pd-hydride that can start a new catalytic cycle.

An analogous mechanism might be proposed for the oligomerization reaction carried out in the presence of an excess of the N-N' ligand with the only difference that it was reasonable to assume that both molecules of nitrogen-donor ligand were bonded to palladium during the oligomerization process, maybe both of them in a unidentate fashion (Scheme 11). Their presence in the palladium coordination sphere is of importance to determine the enantioface selection for at least the first two inserted molecules of styrene.

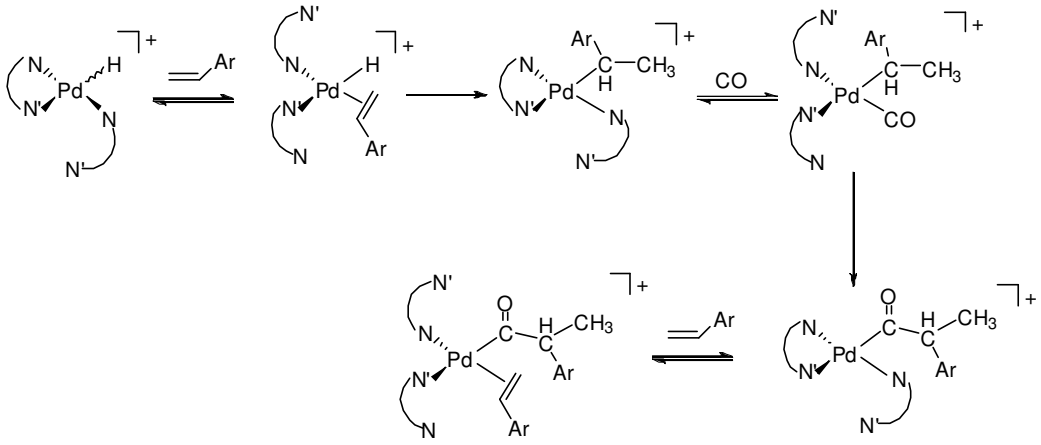

SCHEME 11. The proposed mechanism for complexes $[Pd(N\text{-}N')_2(CH_3)][PF_6]$.

3.6. CONCLUSIONS

The effect of the substituent in *ortho* position with respect to a N-donor atom of bipyridine and pyridine-triazole ligands was investigated. In particular, chiral 6-(1-methoxyethyl)-2,2'-bipyridine ligand both as racemate and in the enantiopure forms were synthestized from the respective alcohols. The optically pure alcohols intermediates (*R*)-**37** and (*S*)-**37** were obtained by chemoenzimatic synthesis, such as baker's yeast bioreduction and lipase catalyzed dynamic kinetic resolution, that had demonstrated to be superior methods for the synthesis of nonracemic bypiridine ethanol systems in good yield and optical purity (e.e. 99%).

The monocationic Pd(II) complexes of general formula $[Pd(CH_3)(CH_3CN)(N\text{-}N')][PF_6]$ **29b-30b** containing the new N-N' ligands were prepared from the neutral derivatives $[Pd(CH_3)(Cl)(N\text{-}N')]$ **29a-30a** (N-N' = **29-30**) and their activity was compared to that of complexes with the already known ligands **31** and *rac*-**32**.

All of the Pd-complexes **29-32a-b** have shown to be pre-catalysts for the styrene carbonylation reaction leading to oligoketones with up to 5 insered repetitive units. The nature of the N-N' ligand remarkably influenced the productivity of the catalytic system, in particular the steric hindrance of the alkyl substituents played a relevant role: the higher productivity was achieved with the complex (*S*)-**29b** (194 g PK/g Pd), while the triazole ligand (**30**) gave the least productive catalyst.

In order to evaluate if the ligand chirality effects were present, the activity of complexes *rac*-**29b** and (*R*)- and (*S*)-**29b** in the oligomerization reactions was investigated. The ligand chirality affected the region- and diasterochemistry of the oligomer end-groups. indeed in each case the oligomers were obtained in the two regioisomeric forms A and B, being A the major species formed. The formation of the species B, indicated that a styrene insertion with primary regiochemistry also accurred, that was observed for the first time in a catalytic system based on N-N' ligands.[34] As for the diasteroisomeric ratio (A_l/A_u), it was low using *rac*-**29b**, whereas it increased, in a opposite way, using (*R*)- and (*S*)-**29b**. Moreover the addition of 0.5 eq of free ligand with respect to palladium, in the catalytic mixture, resulted in a decrease in the productivity, and in a complete stereoselectivity in the A_l diastereoisomer formation. In order to understand the role of the second molecule of the ligand the corresponding bisbipyridine complexes of general formula $[Pd(N\text{-}N')_2(CH_3)][PF_6]$ (N-N' = *rac*-, (*R*)-, and (*S*)-**29**) were synthesized. The NMR studies confirmed that the second molecule of ligand plays a crucial role in determining the styrene enantioface discrimination at least for the insertion of the first two styrene molecules.

Finally the study of the reactivity of $[Pd(N\text{-}N')_2(CH_3)][PF_6]$ complewes with labelled carbon monoxide evidenced the preferential formation of the Pd-acetylspecies with two N-N' molecules bonded to the same Pd-centre over that of the Pd-acetyl-carbonyl derivative with only one molecules of N-N' in the Pd-coordination sphere. By considering the high affinity of palladium for carbon monoxide, this result is of remarkable importance.

REFERENCES

1. (a) Drent, E.; Budzelaar, P. H. M. *Chem. Rev.* **1996,** *96*, 663-681. (b) Bianchini, C.; Meli, A. *Coord. Chem. Rev.* **2002,** *225*, 35-66. (c) Durand, J.; Milani, B. *Coord. Chem. Rev.* **2006,** *250*, 542-560. (d) Lai, T.-W.; Sen, A. *Organometallics* **1984,** *3*, 866-870. (e) Nakano, K.; Kosaka, N.; Hiyama, T.; Nozaki, K. *Dalton Trans.* **2003**, 4039-4050. (f) García Suárez, E. J.; Godard, C.; Ruiz, A.; Claver, C. *Eur. J. Inorg. Chem.* **2007,** 2582-2593.
2. Bastero, A.; Ruiz, A.; Claver, C.; Castillón, S. *Eur. J. Inorg. Chem.* **2001**, 3009-3011.
3. Bastero, A.; Claver, C.; Ruiz, A.; Castillon, S.; Daura, E.; Bo, C.; Zangrando, E. *Chem. Europ. J.* **2004,** *10*, 3747-3760.
4. Milani, B.; Scarel, A.; Mestroni, G.; Gladiali, S.; Taras, R.; Carfagna, C.; Mosca, L. *Organometallics* **2002,** *21*, 1323-1325.
5. Scarel, A.; Milani, B.; Zangrando, E.; Stener, M.; Furlan, S.; Fronzoni, G.; Mestroni, G.; Gladiali, S.; Carfagna, C.; Mosca, L. *Organometallics* **2004,** *23*, 5593-5605.
6. Durand, J.; Zangrando, E.; Stener, M.; Fronzoni, G.; Carfagna, C.; Binotti, B.; Kamer, P. C. J.; Muller, C.; Caporali, M.; van Leeuwen, P. W. N. M.; Vogt, D.; Milani, B. *Chem. Eur. J.* **2006**, *12*, 7639–7651.
7. (a) Stoccoro, S.; Alesso, G.; Cinellu, M. A.; Minghetti, G.; Zucca, A.; Bastero, A.; Claver, C.; Manassero, M. *J. Organometal Chem.* **2002,** *664*, 77-84. (b) Milani, B.; Alessio, E.; Mestroni, G.; Sommazzi, A.; Garbassi, F.; Zangrando, E.; Bresciani-Pahor, N.; Randaccio, L. *J. Chem. Soc., Dalton Trans.* **1994**, 1903-1911.
8. Barsacchi, M.; Consiglio, G.; Medici, L.; Petrucci, G.; Suter, U. W. *Angew. Chem. Int. Ed. Eng.* **1991,** *30*, 989-991.
9. Consiglio, G.; Nefkens, S. C. A.; Pisano, C. *Inorg. Chim. Acta* **1994,** *220*, 273-281.
10. Sperrle, M.; Consiglio, G. *J. Organometal. Chem.* **1996**, *506*, 177-180.
11. (a) Drent, E.; Keijsper, J. J., US patent 5225523, **1993**. (b) Mul, W. P.; Dirkzwager, H.; Broekhuis, A. A.; Heeres, H. J.; Van der Linden, A. J.; Orpen, A. G. *Inorg. Chim. Acta* **2002**, *327*, 147. (c) SRI international, Carilite® thermoset resins, Information sheet, www.sri.com.
12. (a) Van Der Heide, E.; Vietje, G.; Wang, P. C., US patent 56840,80, **1997**. (b) Wong, P. K.; Pace, A. R.; Weber, R. C., US patent 5955563, **1999**. (c) Broekhuis, A.A.; Freriks, J. US Patent 5,952,459 **1999**;
13. Constable, E. C.; Heirtzler, F.; Neuburger, M.; Zehnder, M. *J. Am. Chem. Soc.* **1997**, *119*, 5606-5617.
14. (a) Santaniello, E.; Ferraboschi, P.; Grisenti, P.; Manzocchi, A. *Chem. Rev*. **1992**, *92*, 1071–1140. (b) Czuck, S.; Blanzer, B. I. *Chem Rev*. **1991***, 91*, 49–97. (c) Servi, S. *Synthesis* **1990**, 1–25.
15. *Hydrolases in Organic Synthesis: Regio- and Stereoselective Biotransformations* (Eds.: U. T. Bornscheuer, R. J. Kazlauskas), Wiley-VCH, Weinheim, **2005**, 2nd Edition. (b) Schmid, R. D.; Verger, R. *Angew. Chem., Int. Ed.* **1998**, *37*, 1608–1633.
16. Felluga, F.; Baratta, W.; Fanfoni, L.; Pitacco, G.;; Rigo, P.; Benedetti, F. *J. Org. Chem.* **2009**, *74*, 3547-3550.
17. Uenishi, J.; Hiraoka, T.; Hata, S.; Nishiwaki, K.; Yonemitsu O. *J. Org. Chem.* **1998**, *63*, 2481-2487.

18. Rotticci, D.; Hæffner, F.; Orrenius, C.; Norin, T.; Hult, K. *J. Mol. Catal.B: Enzym.* **1998**, *5*, 267–272. (b) Chen, C.-S.; Fujimoto, Y.; Girdaukas, G.; Sih, C. J. *J. Am. Chem. Soc.* **1982**, *104*, 7294–7299.
19. Prelog, V. *Pure Appl.Chem.* **1964**, *9*, 119–122.
20. Landa, A.; Minkkila, A.¸ Blay, G.¸ Joergensen, K. A. *Chem. Eur. J.* **2006**,*12*, 3472-3483.
21. Bolm, C.; Ewald, M.; Felden, M.; Schlingloff, G. *Chem. Ber.* **1992**, 125, 1169-1190.
22. Appukkuttan, P.; Dehaen, W.; Fokin, V. V., Van der Eycken, E. *Org. Lett*. **2004**, *6*, 4223-4225.
23. (a) Kaussmann, T.; Konig, J.; Woltermann, A. *Chem. Ber.* **1976**, *109*, 3864. (b) Botteghi, C.; Chelucci, G.; Marchetti, M. *Synth. Commun.* **1982**, *12*, 25-33. (c) Azzena, U.; Chelucci, G.; Delogu, G.; Gladiali, S.; Marchetti, M.; Soccolini, F.; Botteghi, C. *Gazz. Chim. Ital.* **1986**, *116*, 307. (d) Botteghi, C.; Chelucci, G.; Chessa, G.; Delogu, G.; Gladiali, S.; Soccolini F. *J. Organomet. Chem.* **1986**, *304*, 217-225.
24. (a) Scarel, A.; Durand, J.; Franchi, D.; Zangrando, E.; Mestroni, G.; Milani, B.; Gladiali, S.; Carfagna, C.; Binotti, B.; Bronco, S.; Gragnoli, T. *J. Org. Chem.* **2005**, *690*, 2106–2120. (b) Brookhart, M.; Wagner, M. I.; Balavoine, G. G. A.; Haddou, H. A. *J. Am. Chem. Soc.* **1994**, *116*, 3641–3642. (c) Carfagna, C.; Gatti, G.; Martini, D.; Pettinari, C. *Organometallics* **2001**, *20*, 2175–2182.
25. Rülke, R. E.; Ernesting, J. M.; Spek, A. L.; Elsevier, C. J.; van Leeuwen, P. W. N. M.; Vrieze, K. *Inorg. Chem.* **1993**, *32*, 5769-5778.
26. Aeby A.; Gsponer A.; Sperrle M.; Consiglio G.; *J. Orgamet. Chem.* **2000**, *603*, 122-127.
27. Milani, B.; Anzilutti, A.; Vicentini, L.; Sessanta o Santi, A.; Zangrando, E.; Geremia, S.; Mestroni, G., *Organometallics* **1997**, *16*, 5064-5075.
28. Sperrle, M.; Aeby, A.; Consiglio, G.; Pfaltz, A. *Helv. Chim. Acta* **1996**, *79*, 1387-1392.
29. Nozaki, K.; Sato, N.; Tonomura, Y.; Yasutomi, M.; Takaya, H.; Hijama, T.; Matsubara, T.; Koga, N. *J. Am. Chem. Soc.* **1997**, *119*, 12779-12795.
30. Axet, M. R.; Amoroso, F.; Bottari, G; D'Amora, A.; Zangrando, E.; Faraone, F.; Drammi, D.; Saporita, M.; Carfagna, C.; Natanti, P.; Seraglia, R.; Milani, B. *Organometallics* **2009**, *28*, 4464-4474.
31. Groen, J. H.; de Jong, B. J.; Ernsting, J. M.; van Leeuwen, P. W. N. M.; Vrieze, K.; Smeets, W. J. J.; Spek, A. L. *J. Organomet. Chem.* **1999**, 573, 3-13.
32. (a) Garrone, R.; Romano, A. M.; Santi, R.; Millini, R. *Organometallics* **1998**, *17*, 4519-4522. (b) Milani, B.; Corso, G.; Zangrando, E.; Randaccio, L.; Mestroni, G. *Eur. J. Inorg. Chem.* **1999**, 2085-2093. (c) Milani B.; Marson A.; Zangrando E.; Mestroni G.; Ernsting J. M.; Elsevier C. J.; *Inorg. Chim. Acta* **2002**, *327*, 188-201.
33. Bastero, A.; Ruiz, A.; Claver, C.; Milani, B. *Oranometallics* **2002**, *21*, 5820-5829.
34. Brookhart, M.; Rix, F. C.; De Simone, J. M.; Barborak, J. C. *J. Am. Chem. Soc.* **1992**, *114*, 5894-5895.

Chapter 4:
Synthesis and application of P-N ligands

4.1. HYBRID PHOSPHOROUS-NITROGEN DONOR LIGANDS

The concept of *hemilability* has been coined for ligands possessing a combination of soft and hard donor atoms. A distinguished family of *hemilable* ligands is that combining phosphorous and nitrogen atoms. One important property of these potentially multidentate ligands is that they can stabilize metal ions in a variety of oxidation states and geometries. These ligands can display quite different coordination modes, in fact the π-acceptor character of phosphorous atom can stabilize a metal center in a low oxidation state, while the nitrogen σ-donor ability makes the metal more susceptible to oxidative addition reactions. These properties can help to stabilize intermediate oxidative states or geometries during a catalytic cycle.[1] The possibility of varying the electronic and steric properties of this kind of ligands allows to obtain potentially multidentate ligands that are able to bind or bridge one or more metallic ions affording homo- or hetero-, bi- or polymetallic complexes. [1,2]

Unsymmetrical P-N ligands play an important role in catalysis thanks to their bonding versatility. Despite their wide applications in asymmetric synthesis,[3] only few papers reported the use of P-N ligands in transition metal catalyzed oligomerization, polymerization and copolymerization reactions of aromatic olefins. In the field of ethylene homo- and co-, oligo- and polymerization, in fact, a lot of coordination and reaction studies were reviewed, in particular Ni(II) complexes with very different kinds of P-N ligands were used (Figure 1).[4]

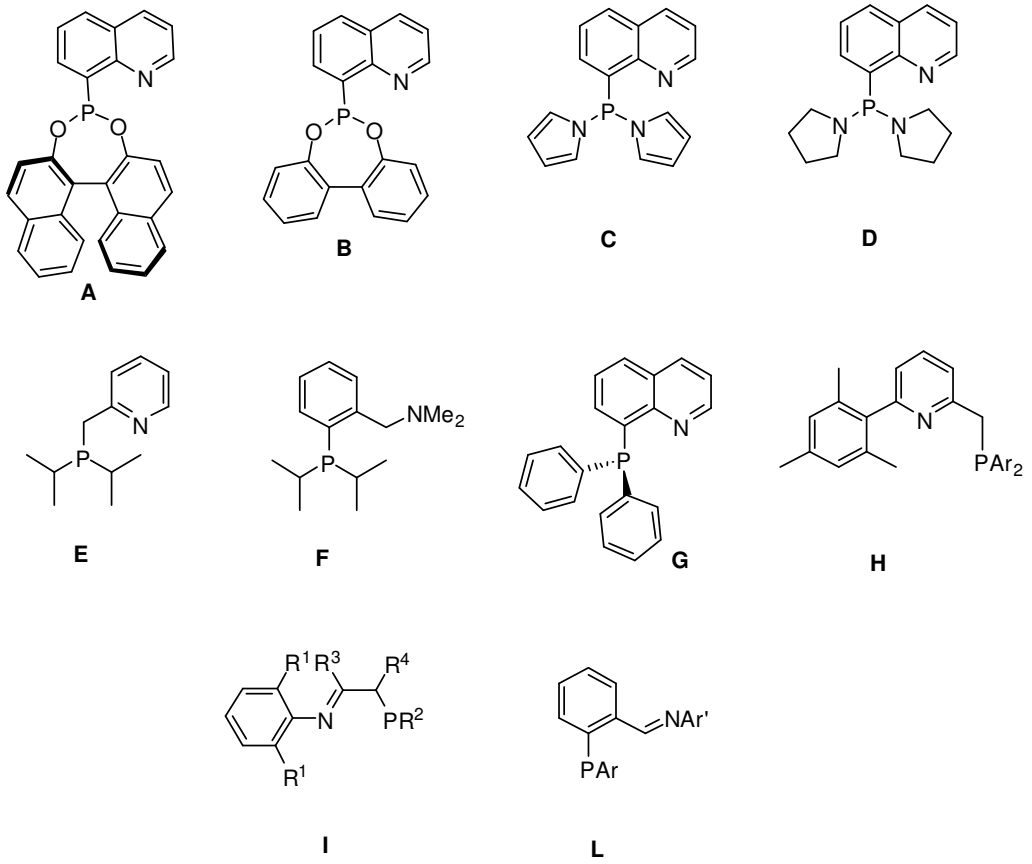

FIGURE 1. Examples of P-N ligands applied in ethylene oligo- and polymerization reactions.

The reported structures are only few examples of the very large family of P-N ligands used to perform oligo-[4b,c] and polyethylene[4d,e] synthesis or CO/ethylene copolymerizations.[4a] They give an idea about the versatility of the possible ligands available, with different steric and electronic properties. Differently, papers that describe P-N ligands application in CO/alkene copolymerization are rare. Pd(II) complexes with ligands **A-D** were investigated as pre-catalysts in CO/styrene copolymerization by Consiglio,[4a] but the results were unsuccessful. The most promising P-N ligands studied in the CO/styrene copolymerization were oxazoline-phosphine type ligands (Figure 2).[5]

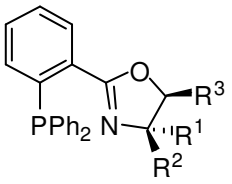

R^1=H, CH_3, CH_2Ph, CH_2OCH_3, *t*-Bu
R^2=H, CH_3, CH_2Ph
R^3=H,Ph

FIGURE 2.

Their cationic diaquo Pd(II) complexes showed good activity and selectivity in producing isotactic copolymers, but only at very high CO pressure (320 bar),[6] in fact the productivity increased, on increasing P_{CO}.

With the aim of looking for a new Pd(P-N) system which might catalyze CO/styrene copolymerization under mild conditions, new chiral P-N ligands have been developed from an original idea of Prof. Sergio Castillón (University Rovira i Virgili, Tarragona, Spain). The new ligands, unlike the previous discussed structures, consist on a proline-pyridine skeleton bound to a phosphine group through two N-P bonds (Figure 3).

44 (PNCO) **45** (PN)

FIGURE 3. The new optically pure P-N ligands.

Ligands **44** (PNCO) and **45** (PN) were synthesized starting from the enantiomerically pure L-proline following a procedure reported for the synthesis of similar ligands in Figure 4.[3]

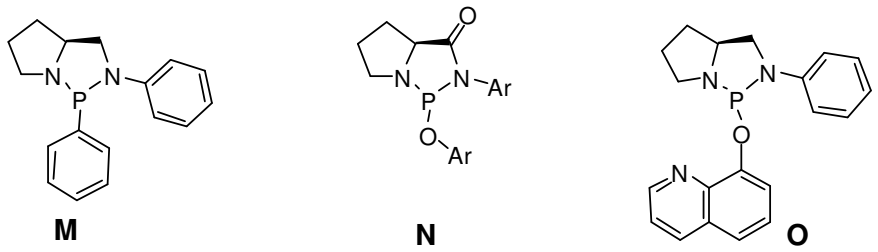

M **N** **O**

FIGURE 4.

Ligands **M-O** were used in different systems and for different synthesis. For instance ligand **M** was applied in asymmetric copper-catalyzed cyclopropanation;[3b] iridium complexes containing **N** were good pre-catalysts for enantio- and regioselective allylic etherification,[3f] and **O** was used in the enantioselective allylic amination studies.[1] No evidences about the application of these chiral ligands in CO/styrene copolymerization were reported.

4.2. SYNTHESIS OF PNCO AND PN LIGANDS

The optically pure PNCO and PN ligands were synthesized from amide (*S*)-**46** and amine (*S*)-**47**, respectively. These parental compounds were prepared following a literature procedure (Scheme 1).[8-12]

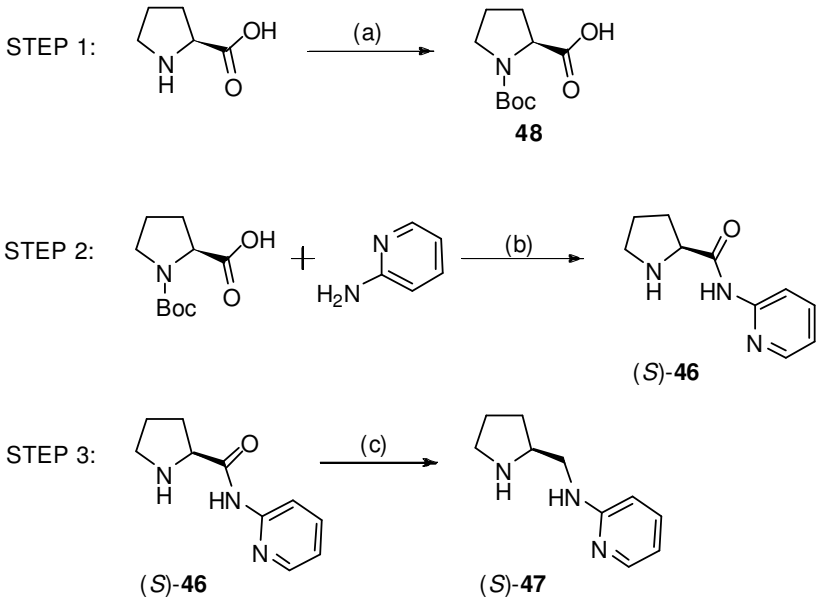

SCHEME 1. Synthesis of chiral precursors of **46** and **47**. Reaction conditions: (a) NEt_3, DCM, Boc_2O. (b) i. EDC, DCM ii. TFA, DCM. (c) $LiAlH_4$, THF.

The first step consists on the proline's amine group protection (**48**) with a standard procedure using di-*tert*-butyl-dicarbonate,[7] followed by the coupling that was carried out with a revisited procedure involving only EDC as a condensation reagent instead of DCC[8] or DCC/HOBt.[9]

The reaction between the Boc-proline and the commercially available 2-aminopyridine afforded a protected amide which was treated in acid medium[10] to obtain the amide (*S*)-**46**. By reduction of the carbonyl group with $LiAlH_4$ (STEP 3) the pure amine (*S*)-**47** was achieved after column chromatography.[11]

The last step was the most sensitive of the whole synthesis, in fact phosphine derivatives could be quickly converted into the relative phosphine-oxide by the air oxygen or by oxygen traces present in solvents. To avoid oxidation only distilled and degassed solvents were used, and all reactions involved phosphines were performed with Schlenk technique under inert atmosphere. Thus, amide (*S*)-**46** and amine (*S*)-**47** were reacted with bis(diethylamino)-phenylphosphine in toluene at 90 °C over night (Scheme 2).[12]

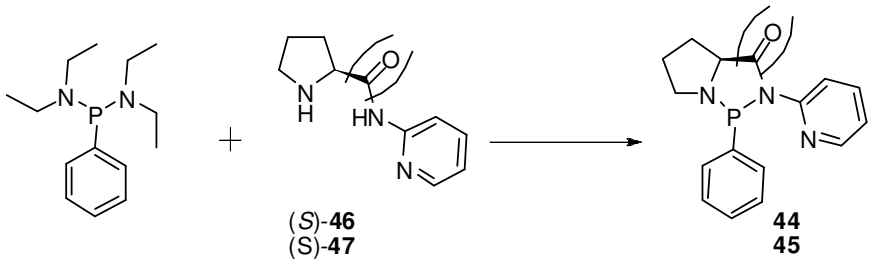

SCHEME 2. The last step of chiral ligands **44** and **45** synthesis. Reaction conditions: toluene, 90 °C.

This reaction was completely stereoselective affording only one of the two possible diasteroisomers α- and β- (Figure 5).[3f-13]

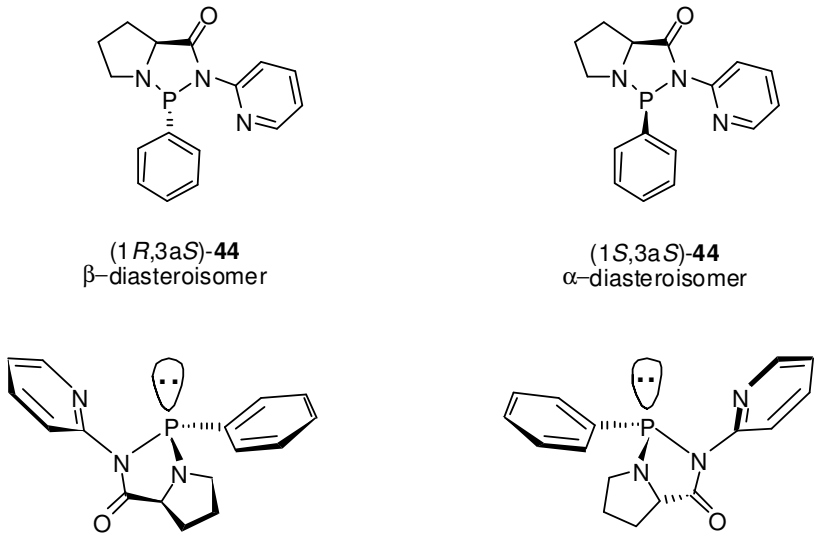

FIGURE 5. α- and β-diasteroisomers of compound **44.**

In agreement with the literature data,[3f] for ligand **44** only the signal of the β-diasteroisomer, in which the stereogenic phosphorous has the *R* configuration, has been recognized by ^{31}P-NMR analysis. The same considerations could be applied to compound **45**.

Ligands **44** and **45** differ for the presence of the carbonyl group on the bridge connecting the nitrogen atom bound to the pyridine ring and the stereogenic carbon of the pyrrolidine ring. Both new optically active phosphine-nitrogen ligands have been fully characterized by NMR and chirooptical analysis.

4.3. SYNTHESIS OF Pd(II) COMPLEXES CONTAINING PNCO AND PN LIGANDS

4.3.1. Neutral Complexes

The Pd(II) system chosen to study the coordination capability of the new ligands was [Pd(COD)(CH_3)(Cl)] (COD = 1,5-cyclooctadiene). This complex is the usual parental compound for the synthesis of neutral complexes stabilized by N-N ligands and then used in CO/styrene copolymerization in their cationic forms (see Chapter 3 and references therein). [Pd(COD)(CH_3)(Cl)] was synthesized following the two step procedure reported in the literature (Scheme 3).[14]

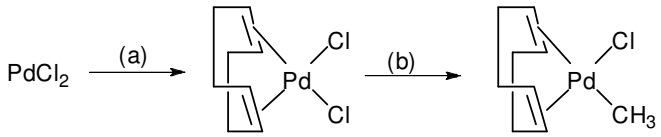

SCHEME 3. Synthesis of the [Pd(COD)(CH_3)(Cl)]. Reaction conditions: (a) i. H_2O/HCl (37%) 1:1, r.t., 30 min; ii. EtOH, 1,5-cyclooctadiene. (b) DCM, $(CH_3)_4Sn$, r.t.

Starting from $PdCl_2$ and using an excess of 1,5-cyclooctadiene, the derivative [Pd(COD)Cl_2] was obtained in 92% yield. The dichloride derivative was reacted with tetra-methyl-tin to provide the transmethylation reaction and the product [Pd(COD)(CH_3)(Cl)] in high yield.

Initially the coordination behavior of PNCO and PN to palladium was studied by in situ NMR spectroscopy of the CD_2Cl_2 solution containing [Pd(COD)(CH_3)(Cl)] and 1 equivalent of the proper ligand. For both ligands the reaction progress, monitored by ^{1}H- and ^{31}P-NMR spectroscopy, showed that the ligand coordinated almost instantaneously to the metal centre: no signals of the free ligand were present after 5 min from the mixing of the two species (Scheme 4).

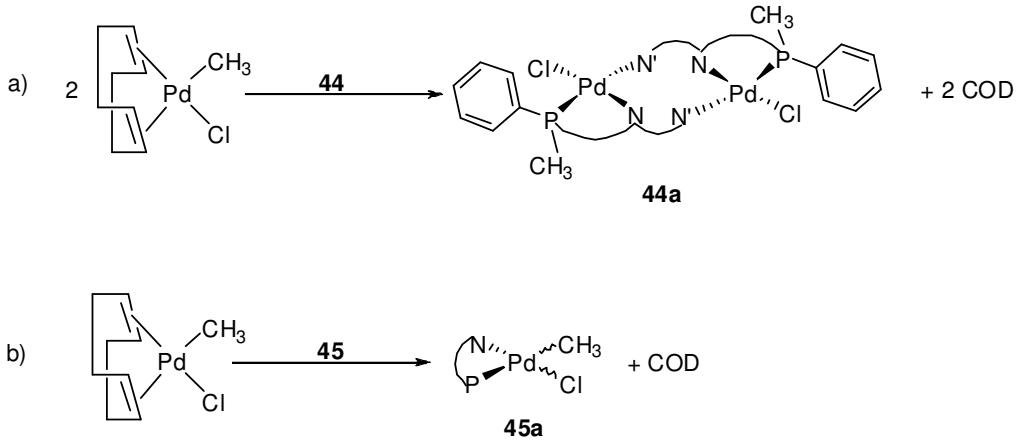

SCHEME 4. Schematic representation of the neutral complexes formation: a) with PNCO, b) with PN.

The neutral complexes were fully characterized in CD_2Cl_2 solution by multinuclear NMR spectroscopy (Figure 6, Table 1).

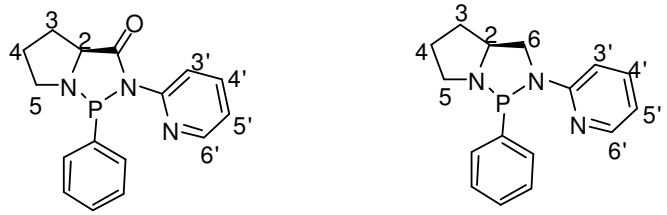

FIGURE 6. Protons numbering scheme.

TABLE 1. Selected chemical shift values for the free ligands and the neutral complexes.[a]

P-N/complex	^{31}P	CIS[b] (δ_l-δ_c)	CH_3	$J_{P\text{-}CH3}$ (Hz)
44	106.3			
44a	67.0 (M) 75.6 (m)	39.3 (M) 30.7 (m)	2.12 (M) 2.45 (m)	13 (M) 11.5 (m)
45	99.7			
45a	119.9 (M) 133.8 (m)	- 20.2 (M), - 34.0 (m)	0.69 (M) 1.65 (m)	2 (M) 8.5 (m)

[a] Spectra recorded in CD_2Cl_2 at r. t., values in ppm. M = major species, m = minor species. [b] CIS = Coordination Induced Shift for -CH in the complexes (δ_c) and in the free ligand (δ_l).

In the ^1H NMR spectra of both neutral species the $-CH_3$ group, that was bound to Pd in the metal precursor, generated two doublets at very different chemical shift: 0.69 and 1.64 ppm for **45a** and 2.12 e 2.45 ppm for **44a**. These signals indicated for both

complexes the presence, in solution, of two different species, that were in ratio of 9:1 and 2:1 for **44a** and **45a**, respectively. The ^{31}P NMR spectra confirmed these results showing two singlets for each complex. Interestingly, the ^{31}P NMR signals of the two complexes showed opposite variation of the chemical shift with respect to the free ligands, depending on the nature of the P-N ligand: an upfield shift in the case of **44a** (CIS -34.0 and -20.2 ppm), and a downfield shift for **45a** (CIS 39.3 and 30.7 ppm) (Table 1).

The NMR analysis showed also the characteristic signals of the ligand protons shifted with respect to those of the free ligands, that was diagnostic of the coordination to the palladium centre.

The comparison of ^{1}H and ^{31}P NMR spectra of **44a** and **45a** suggests that from the reactivity of **44** and **45** with [Pd(COD)(CH_3)(Cl)] two different complexes were obtained depending on the nature of the ligand. In particular, for ligand **45** the data indicated that the isolated species was the expected mononuclear complexes [Pd(**45**)(CH_3)(Cl)] (**45a**) (Figure 7).[4a-15] It is reasonable to assume that the two species observed in solution for **45a** were the *cis* and *trans* isomers differing for the relative position of the Pd-CH_3 fragment with respect to the two halves of the ligand. Conventionally we called *trans* the isomer having the Pd-CH_3 in *trans* to the Pd-P bond (Figure 7).

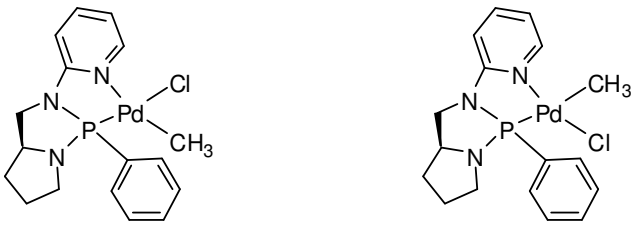

cis-**45a**
major isomer

trans-**45a**
minor isomer

FIGURE 7. *cis* and *trans* isomers of complex **45a**.

The downfield shifted ^{31}P signals for complex **45a**, and the $J_{Pd\text{-}CH3}$ values suggested that the major isomer was the *cis* isomer. This is in agreement with the complex electronic pattern: chloride is *trans* to the better donor atom (phosphorous), while methyl is in *trans* to the poor donor (nitrogen) (Figure 7)[4a] and with the fact that the ligands having the highest *trans* influence are *cis* to each other.

The nature of the neutral complex **44a** with ligand **44** was elucidated after the characterization of the corresponding cationic derivative.

4.3.2. Cationic Complexes

The reaction between the neutral complexes **44a-45a** and CH_3CN, at room temperature, with $AgPF_6$ was unsuccessful. When the same reaction was carried out with pyridine or its derivatives, 4-methyl-pyridine and 4-trifluoromethyl-pyridine, instead of CH_3CN, the corresponding cationic complexes were isolated (Scheme 5).

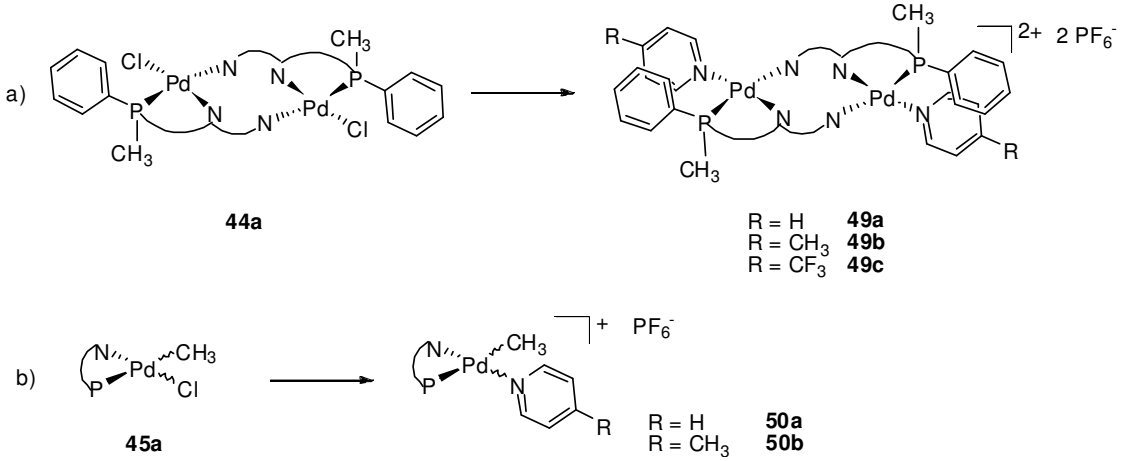

SCHEME 5. Synthesis of the cationic complexes a) with PNCO, b) with PN. Reaction conditions: CH_2Cl_2, $AgPF_6$, pyridine-type ligands.

Complexes **49a-c** and **50a-b** were fully characterized by ^{1}H and ^{31}P NMR spectroscopy (Table 2).

TABLE 2. Selected chemical shift values for the neutral and the cationic complexes.[a]

Complex	^{31}P	CIS[b] (δ_l-δ_c)	CH_3	$J_{P\text{-}CH3}$ (Hz)
44a	67.0 (M) 75.6 (m)	39.3 (M) 30.7 (m)	2.12 (M) 2.45 (m)	13 (M) 11.5 (m)
49a	50.7	55.6	2.38	11.5
49b	50.7	55.6	2.36	11.5
49c	50.7	55.6	2.38	11.5
45a	119.9 (M) 133.8 (m)	- 20.2 (M) - 34.0 (m)	0.69 (M) 1.65 (m)	2 (M), 8.5 (m)
50a	122.9[c]	- 23.2	1.71	8.5
50b	122.9 (M) 134.2 (m)	- 23.2 (M) - 34.5 (m)	0.50 (M) 1.72 (m)	1.5 (M) 8.5 (m)

[a] Spectra recorded in CD_2Cl_2 at r. t., values in ppm. M = major species, m = minor species. [b] CIS = Coordination Induced Shift for -CH in the complexes (δ_c) and in the free ligand (δ_l). [c]The NMR spectrum indicate the presence of unreacted **45a** and of a new species in low amount, that should reasonably be major isomer of the target product **50a**.

For complex **49b** single crystals suitable for X-ray analysis were obtained. Even though the quality of the crystals was not excellent, it was possible to characterize the palladium coordination sphere and the ligand molecule (Figure 8).

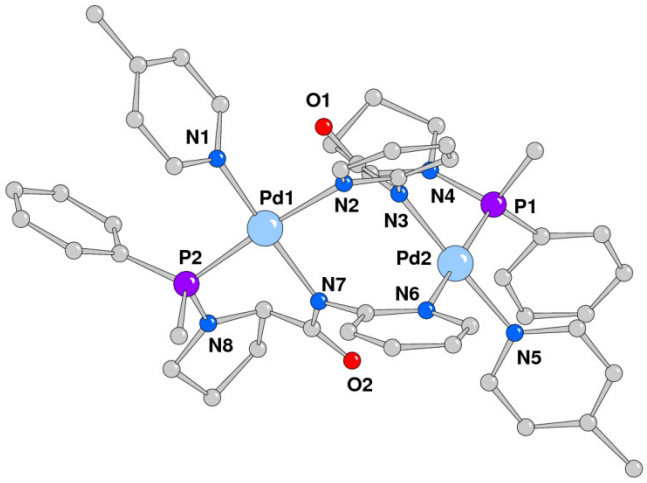

FIGURE 8. Crystal structure of the cation of complex **49b**. selected bond lengths [Å] and angles [°]: Pd1-N1 2.037(17), Pd1-N7 2.10(3), Pd1-N2 2.145(15), Pd1-P2 2.204(11), Pd2-N3 2.06(3), Pd2-N5 2.104(19), Pd2-N6 2.095(14), Pd2-P1 2.207(14), N1-Pd1-N7 173.7(10), N1-Pd1-N2 86.7(8), N7-Pd1-N2 89.3(9), N1-Pd1-P2 97.4(7), N7-Pd1-P2 86.3(8), N2-Pd1-P2 174.2(6), N3-Pd2-N5 177.1(10), N3-Pd2-N6 88.5(9), N5-Pd2-N6 89.9(8), N3-Pd2-P1 88.8(9), N5-Pd2-P1 92.4(8), N6-Pd2-P1 170.2(7).

The X-ray structure evidenced the dinuclear nature of the complex, in which two ligand molecules bridged two Pd ions. A peculiarity of this system was the transmethylation reaction occurred between the metal centers and the phosphorous atoms; to the best of our knowledge no evidence of this phenomena has been previously reported in the literature.

It is worth noting that **44** acted as a tridentate ligand being coordinated to one Pd ion with the phosphorous atom and the amidic nitrogen, that is prone to the coordination due to the cleavage of the P-N_{amidic} bond, and to the other Pd ion with the pyridine nitrogen. In the same way a second ligand molecule bound the two palladium ions leading to an head-to-tail dinuclear complex. The palladium complex geometry was, as usual, square planar with no particular distortion. The coordination sphere of each palladium was completed by the monodentate 4-methyl-pyridine, that showed a π-stacking interaction with the phenyl ring bonded to phosphorous.

As regard complexes **49a-c** with PNCO ligand, both the ^{31}P and the ^{1}H signals were shifted compared to the same signals in the neutral compound **44a**. The signals of the protons of the pyridine-type ligand coordinated to palladium were also present. It is worth noting that the ^{31}P and the CH_3 group signals were not affected by the fourth ligand nature, as well as the value of the P- CH_3 coupling constant, the latter being

very similar to the value found for the complex **44a** (Table 2). On the basis of these NMR data it is reasonable to assume that all the synthesized complexes containing ligand **44** are dinuclear species with a geometry analogous to that observed in the solid state for **49b**.

The ^{1}H NMR spectrum of **49b** at room temperature showed a single signal at low field for protons in *ortho* position of the 4-picoline. In the homonuclear COSY spectrum this signal was not associated with any cross peak; moreover this signal was broad, thus indicating the presence of a dynamic phenomenon in solution. In order to understand the nature of this phenomenon we studied spectral variations upon decreasing temperature in the range + 25 °C ÷ - 35 °C.

Upon decreasing temperature the signal at low fields attributed to the *o*-protons of 4-picoline became broader, until when at T = - 20 °C, it disappeared indicating that the coalescence temperature has been reached. A further decrease of temperature (up to - 35 °C) resulted in its splitting into two signals at 8.44 and 8.63 ppm, which were correlated with the signals at 6.87 and 7.33 ppm in the homonuclear COSY spectrum recorded at - 35 °C (Figure 9). These signals were assigned to the *ortho* and *meta* protons of the 4-picoline ligand bound to palladium. In addition to these signals, even the peaks of the phenyl ring bound to phosphorus varied with temperature. These NMR data indicated the presence of a dynamic process in solution, which mainly involved the 4-picoline, that, due to coordination to palladium, had lost the C_2 symmetry axis passing through the nitrogen atom and the *p*-CH_3 group. Thus, the two halves of 4-picoline were no longer equivalent. This suggested that the fluxional process was an hindered rotation around the Pd-N bond, due to the π-stacking interaction between the 4-picoline and the phenyl ring bound to the phosphorus atom. Indeed, both for *ortho* and *meta* picoline's protons, the signal at higher fields could be attributed to the half of the 4-picoline falling into the shielding cone of the phenyl ring.

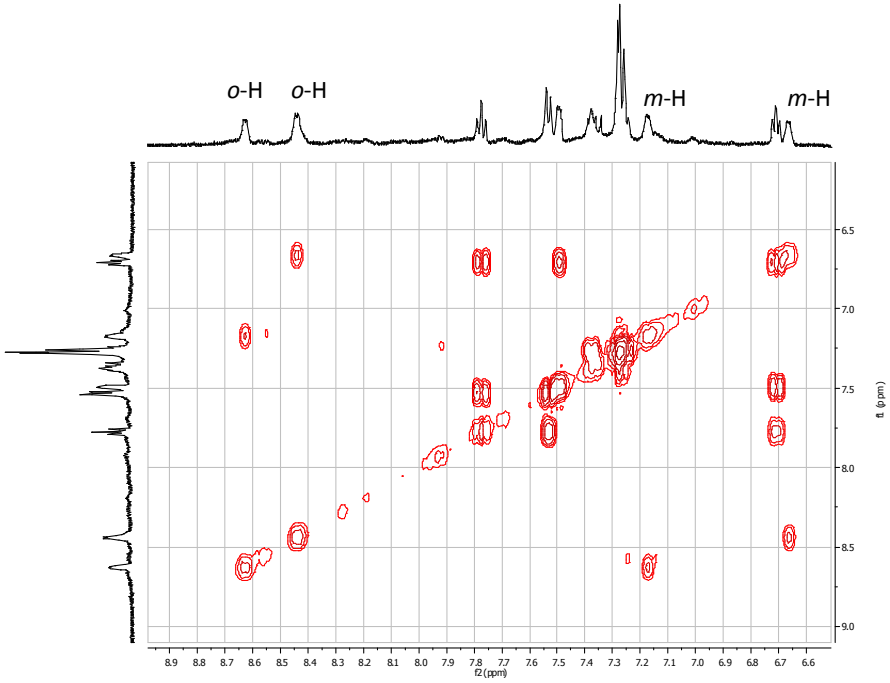

FIGURE 9. Homonuclear COSY spectrum of **49b**, in CD_2Cl_2 at -35 °C: the *ortho* and *meta* protons of 4-picoline are evidenced.

As expected complexes **49a-c** were optically active and the chirooptical analysis (CD and α, Figure 10) showed the same Cotton effect for all of them, that confirmed the same configuration for each system.

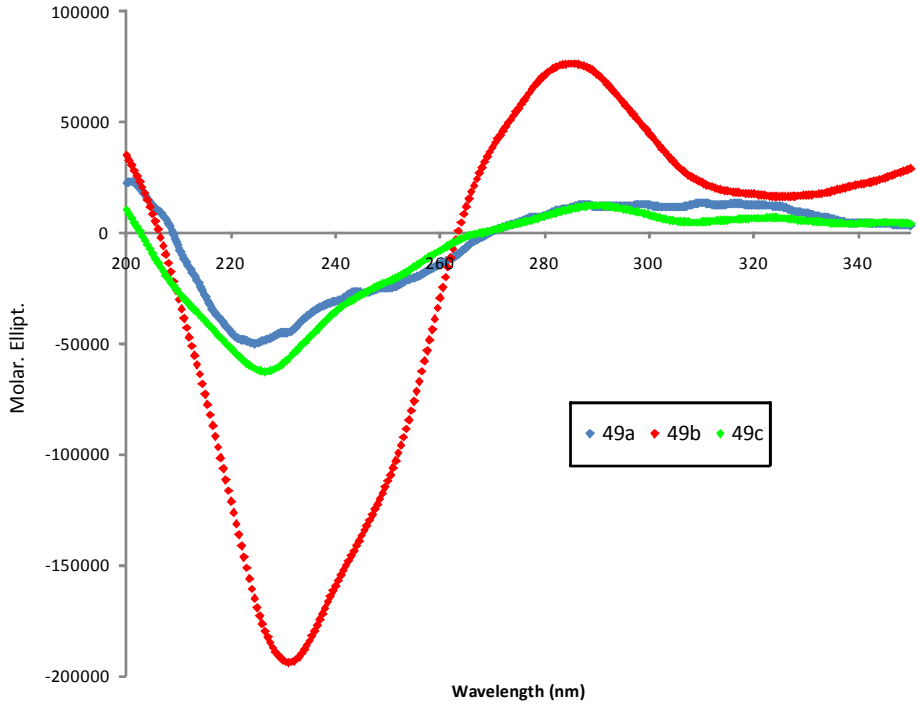

FIGURE 10. CD spectra of complexes **49a-c** (1 x 10^{-4} M in CH_3OH).

Complexes **50a-b** were also characterized in CD_2Cl_2 solution by multinuclear NMR spectroscopy. As in the case of the corresponding neutral derivative **45a**, even for **50b** two species were present in solution (Table 2), showing chemical shift values very similar to those of the parent compound for the Pd-CH_3 fragment (^{1}H NMR spectrum) and for the phosphorus atom (^{31}P NMR spectrum). Both the presence of the signals of 4-picoline in the ^{1}H NMR spectrum and the strong IR bands typical of the hexafluorophosphate anion indicate the formation of the desired product [Pd(CH_3)(**45**)(4-CH_3Py)][PF_6].

As far as the solid isolated from the reactivity of **45a** with pyridine is concerned, the NMR characterization indicate the presence of unreacted palladium precursor and of a new species, that should reasonably be the target product [Pd(CH_3)(**45**)(Py)][PF_6]. Further investigations are required.

4.4. CATALYTIC ACTIVITY OF THE CATIONIC COMPLEXES

Initially the cationic complexes **49a-c** were tested as pre-catalysts for the CO/styrene copolymerization under standard conditions: T = 30 °C, 1 atm of CO, [styrene]/[Pd] = 6800, an excess of benzoquinone with respect to palladium ([BQ]/[Pd] = 40), 24 hours, in 2,2,2-trifluoroethanol (TFE). No polymer was isolated at the end of the catalytic runs. After drying the reaction mixture an oil was obtained that was characterized as *trans*-1,3-diphenyl-1-butene. Despite the optical activity of the complexes, the product was always obtained as racemic mixture.

Reference experiments were carried out converting *in situ* the neutral complex **44a** in the cationic form by $AgPF_6$ addition, and varying some reaction parameters.

TABLE 3. Styrene dimerization: *in situ* experiments.

Entry	Cat Pd (mol)	$AgPF_6$ (mol)	P_{CO} (atm)	Product	Conversion[a] (%)
1	1.27×10^{-5}	1.27×10^{-5}	1	1,3-diPh-1-butene	low
2	/	1.27×10^{-5}	1	No reaction	/
3	1.27×10^{-5}	/	1	Mixture of products	/
4	1.27×10^{-5}	1.27×10^{-5}	/	1,3-diPh-1-butene	11

Pre-cat: [Pd(CH_3PNCO)(Cl)]$_2$ (**44a**); reaction conditions: [BQ]/[Pd] = 40, T = 30 °C, [styrene]/[Pd] = 6800, styrene V = 10 mL, TFE V = 20 mL. [a] Conversion determined by weight after 24h.

The results, summarized in Table 3, indicated that the Pd-complex acted as catalyst for the styrene dimerization reaction (Scheme 7) and showed the inhibiting effect of CO in this reaction (entry 1 vs 4).

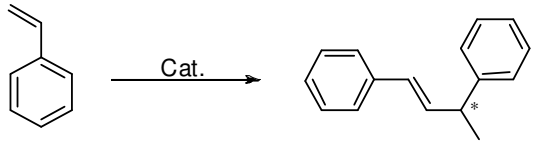

trans-1,3-diphenyl-1-butene

SCHEME 7. Styrene dimerization reaction.

In the literature some examples of co-dimerization of styrene with α-olefins catalyzed by Pd[16] , Co[17] and Ni[18] complexes have been reported. Only few articles discussed the styrene dimerization, in particular the most recent work[19] reported the non selective styrene dimerization catalyzed by $[Pd(acac)_2]/[BF_3]$ system that yielded also to styrene trimers and polymers. In the present case only the *trans*-1,3-diphenyl-1-butene was obtained, the characteristic value of the $J_{HHtrans}$ = 15 Hz and the IR band at 965 cm^{-1}attributable to the $\delta_{C\text{-}H}$ vibration of *trans* structure confirm the product geometry.[19]

The styrene dimerization was followed by HRGC analysis By using the cationic complex **49b**, the effect of temperature was investigated evidencing a remarkable influence of this parameter on the catalytic activity. In particular, at T = 30 °C or 50 °C an induction time was observed, that it is not evident at 70 °C any more (Figure 11).

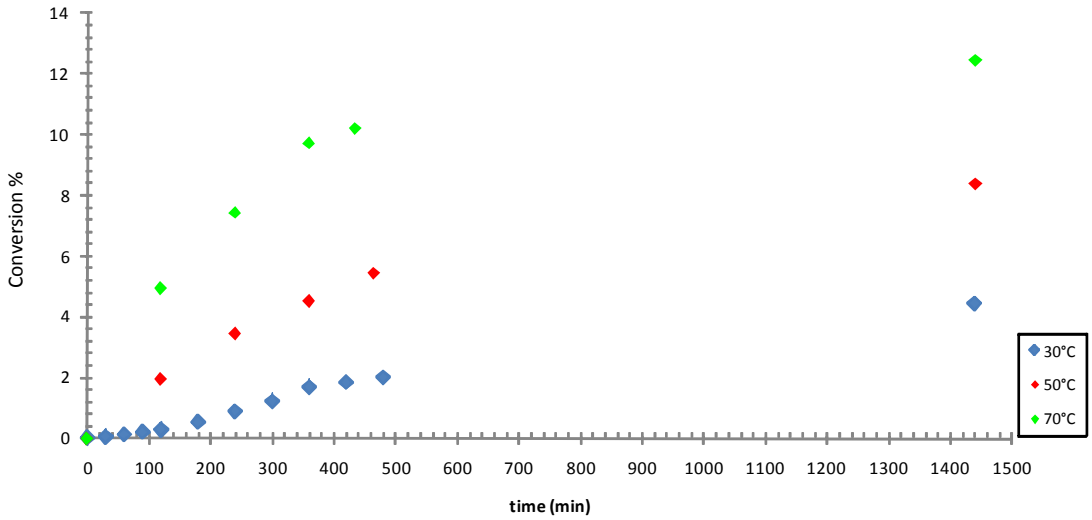

FIGURE 11. Styrene dimerization: effect of the temperature. Pre-cat $[Pd(CH_3PNCO)(4\text{-}CH_3Py)]_2[PF_6]_2$ (**49b**); reaction conditions: $n_{Pd} = 1.27 \times 10^{-5}$mol, [BQ]/[Pd] = 40, styrene/Pd = 6800, styrene V = 10 mL, TFE V = 20 mL.

Working at 70 °C the catalyst activity was remarkably improved with respect to that obtained at 30 °C (entries 1 and 3, Table 4).

TABLE 4. Styrene dimerization: effect of temperature.

Entry	T (°C)	TON[a]	Conversion[b] (%)
1	30	301	4.41
2	50	571	8.35
3	70	850	12.41

Pre-cat: $[Pd(CH_3PNCO)(4\text{-}CH_3Py)]_2[PF_6]_2$; reaction conditions: see Figure 11. [a] Turnover number (moles of substrate converted per mole of catalyst after 24 hours). [b] Conversion determined by HRGC analysis after 24 h.

A 50% decrease of [styrene]/[Pd] ratio, realized by increasing the amount of the palladium pre-catalyst, led to an additional improvement of the conversion up to 16 %. (Figure 12).

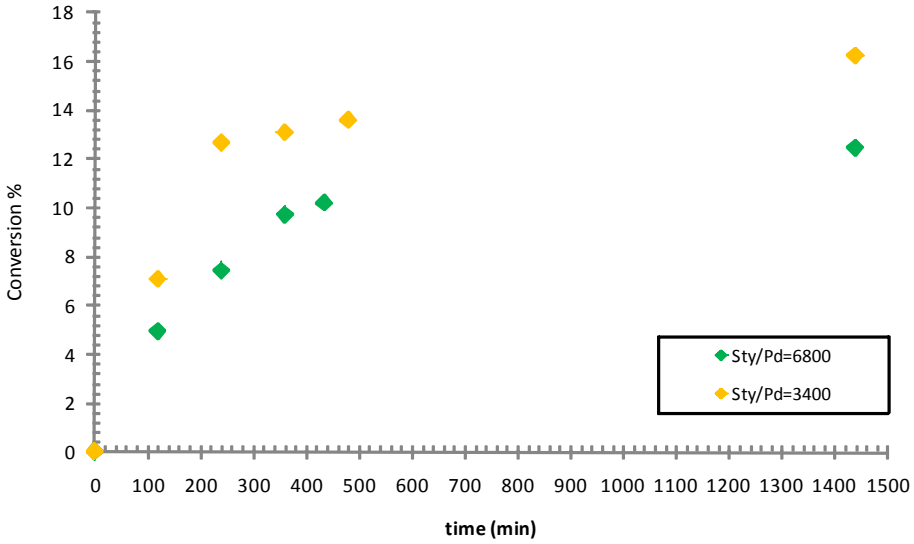

FIGURE 12. Styrene dimerization: effect of the [styrene]/[Pd] ratio. Pre-cat $[Pd(CH_3PNCO)(4\text{-}CH_3Py)]_2[PF_6]_2$; reaction conditions: $n_{Pd} = 2.54 \times 10^{-5}$mol, [BQ]/[Pd] = 40, T = 70°C, styrene V = 10 mL, TFE V = 20 mL.

Thus, the temperature of 70 °C and a styrene to Pd ratio of 3400 were considered now standard conditions, and working with these values, the effect of the different pyridine-type ligand in fourth position was investigated (Figure 13).

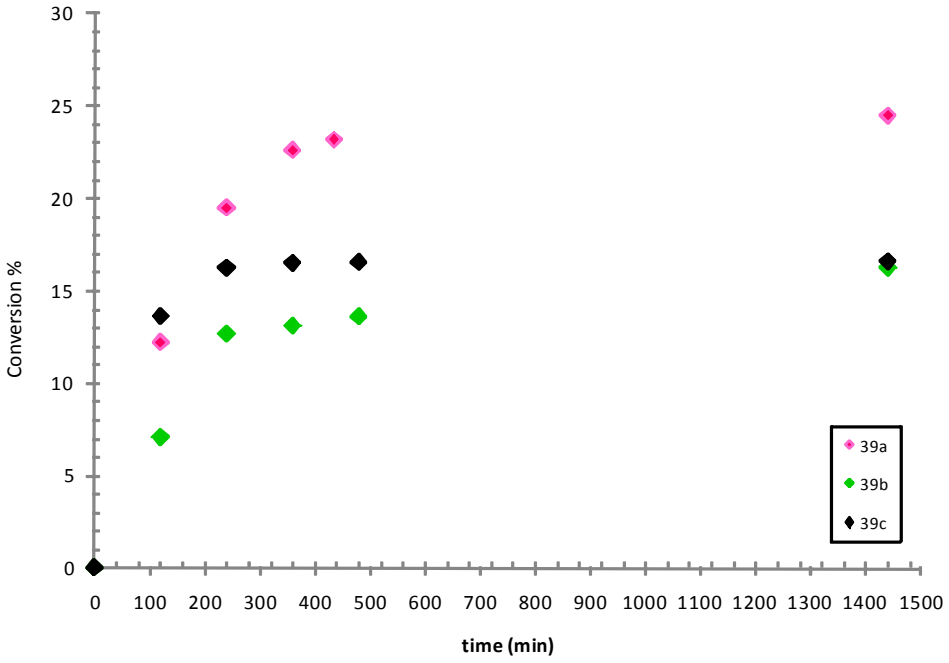

FIGURE 13. Styrene dimerization: effect of the fourth ligand nature. Reaction conditions: $n_{Pd} = 2.54 \times 10^{-5}$mol, [BQ]/[Pd] = 40, T = 70°C, [styrene]/[Pd] = 3400, styrene V = 10 mL, TFE V = 20 mL.

Each complex tested generated an active species for the styrene dimerization, but showing modest catalytic activity and leading to a maximum conversion of 25%, after 24 h, reached with complex **49a** (Table 5, entry 1).

This catalytic trend evidences that the nature of the fourth ligand affects both the activity and the stability of the catalyst, which appear to be related to the Lewis basicity of this ligand. Indeed, within the first two hours of reaction, the catatytic activity increases on decreasing the Lewis basicity of the pyridine-type ligand, being the complex **49c** with the 4-CF_3Py the most active and complex **49b** with 4-CH_3Py the least active among those tested (Figure 13 and Table 5).

TABLE 5. Styrene dimerization: effect of the fourth ligand nature.

Entry	Complex	Conversion[b] (%) (2h)	TON[a] (2h)	Conversion[b] (%) (24 h)	TON[a] (24h)
1	**49a**	12.19	374	24.43	750
2	**49b**	7.08	217	16.26	499
3	**49c**	13.6	417	16.56	567

Reaction conditions: see Figure 13. [a] Turnover number (moles of substrate converted per mole of catalyst). [b] Conversion determined by HRGC analysis after 24 h.

On the other hand for longer reaction times both catalysts generated by **49b** and **49c** deactivated, while the catalyst obtained from complex **49a** was active for at least 8 h.

To gain some information on the catalyst stability, the effect of [1,4-benzoquinone]/[palladium] ratio was studied by varying the amount of BQ present in the reaction mixture and using complex **49a** as pre-catalyst (Figure 14).

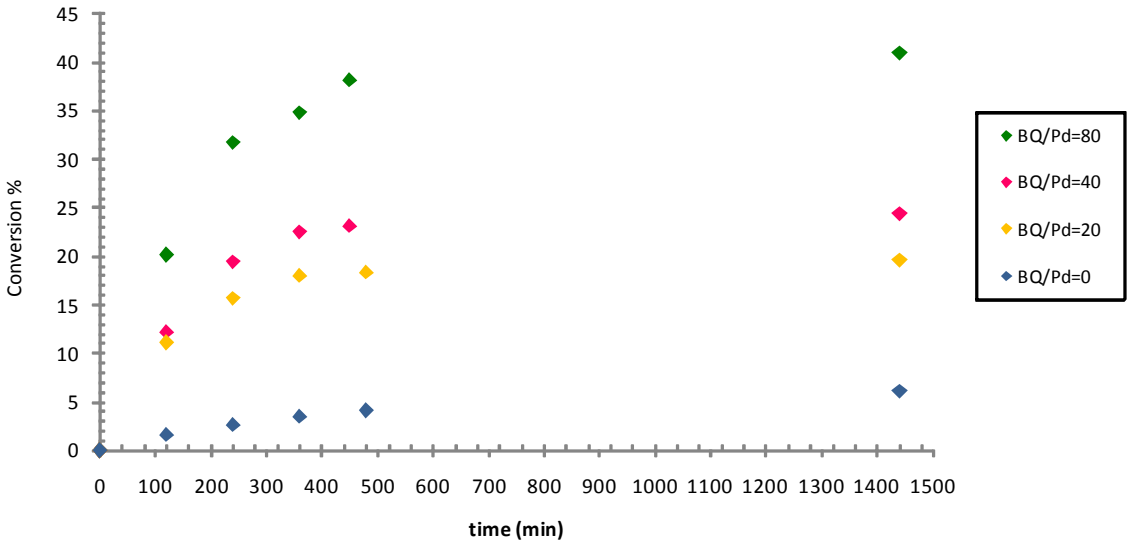

FIGURE 14. Styrene dimerization: effect of the [BQ]/[Pd] ratio. Pre-cat: $[Pd(CH_3PNCO)(Py)]_2[PF_6]_2$ (**49a**), reaction conditions: see Figure 13.

The variation of [BQ]/[Pd] ratio (Figure 14) evidences that the productivity increases on increasing the [BQ]/[Pd]. Noteworthy, when the oxidant was not added to the reaction mixture the formation of product was very low, and after 24 h only 6% of the dimer was isolated. The addition of a remarkable excess of 1,4-benzoquinone with respect to the palladium ([BQ]/[Pd] = 80) resulted in prolonging the catalyst lifetime and increasing its activity, reaching a conversion into the product of 40% after 24 h. The addition of benzoquinone did not show any particular effect on the product nature. The catalytic activity of complexes **50a-b** is currently under study.

4.5. MECHANISTIC INSIGHTS

From these catalytic data no information on the nature of the catalytic species can be derived, *i. g.* if a mononuclear or a dinuclear species is the active catalyst. Nevertheless, the trend reported in Figure 13 and Table 5 suggests that the activation step requires the dissociation of the monodentate pyridine-type ligand.

From the nature of the product obtained from this catalytic reaction some mechanistic speculations can be drawn. The following discussion is based on considering the catalyst as a mononuclear species with the ligand chelating the palladium centre with the phosphorous and the amidic nitrogen.

The active species is a Pd-hydride intermediate, that might be formed from the reaction of the pre-catalyst with the TFE and traces of water present in the solvent. An analogous activation step has been proposed for the Pd-complexes with N-N' ligands (see Chapter 3).

On the Pd-H, styrene coordination occurs, followed by styrene insertion with a secondary regiochemistry leading to the Pd-alkyl intermediate **51a** (Scheme 8a). On this species the second molecule of styrene coordinates and inserts, always with a secondary regiochemistry leading to the Pd-alkyl intermediate **51b** (Scheme 8b), on which a β-hydrogen elimination takes place yielding the 1,3-diphenyl-1-butene as the product and the Pd-H which can start a new catalytic cycle (Scheme 8c).

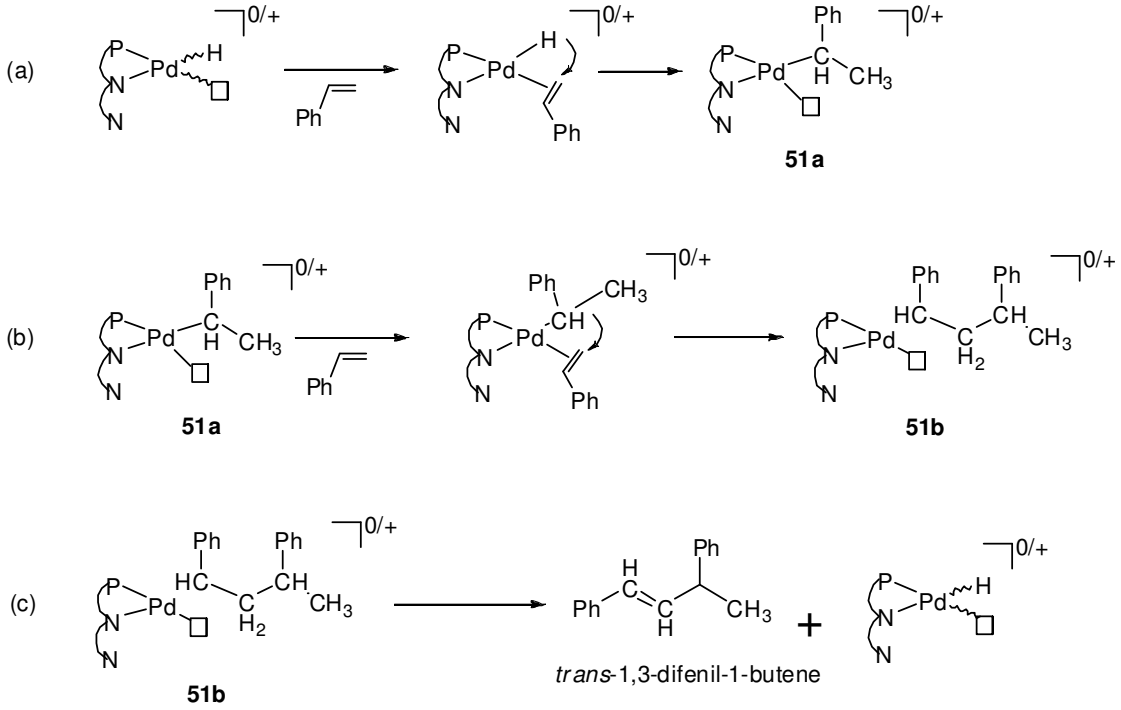

SCHEME 8. The proposed main steps of the catalytic cycle.

Thus, on the studied complexes the styrene insertion is a regiospecific reaction.

4.6. CONCLUSIONS

Optically pure hybrid P-N ligands **44** and **45** were synthesized starting from L-proline and their coordination chemistry to palladium was studied. Both neutral and cationic complexes were prepared and fully characterized, finding that the two ligands coordinated differently the palladium centre depending on their nature. In particular, the derivative **44** led to a dinuclear complex, while **45** to a mononuclear species. The cationic complexes **49a-c**, with different pyridine-type ligands in fourth position, have

been deeply investigated and all of them generated catalytic species for the styrene dimerization reaction yielding in all cases the *trans*-1,3-diphenyl-1-butene selectively as product. The reaction conditions were optimized investigating the effects of temperature, [styrene]/[Pd] ratio and [BQ]/[Pd] ratio, and the role played by the fourth pyridine-type ligand.

Actually, the complex **49a**, that was the most active among those tested, is under investigation in the styrene/ethylene co-dimerization reaction, that is of considerable importance from an industrial point of view. In fact, the selective co-dimerization between styrene and ethylene to give 3-phenyl-1-butene is investigated as a model reaction for the synthesis of drugs as Ibuprofene and Naproxen.[20]

REFERENCES

1. Espinet, P.; Soulantica, K., *Coord. Chem. Rev.* **1999**, *193-195*, 499-556.
2. Maggini, S., *Coord. Chem. Rev.* **2009**, *253*, 1793-1832.
3. (a) Giuri, P.J.; Saunders, C.P. *Adv. Synth. Catal.* **2004**, *346*, 497-537. (b) Mothes, E.; Sentets, S.; Luquin, M. A.; Lugan, N.; Lavigne, G., *Organometallics* **2008**, *27*, 1197-1206. (c) Arrayas, R.G.; Adrio, J.; Carrettero, J. C. *Agew. Chem. Int. Ed.* **2006**, *45*, 7674-7715. (d) Cipot, J.; McDonald, R.; Ferguson, M. J.; Schatte, G.; Stradiotto, G. *Organometallics* **2007**, *26*, 594-608. (e) Brumel, J. M.; Legand, O.; Reymond, S.; Buono, G. *J. Am. Chem. Soc.* **1999**, *121*, 5807-5808. (f) Kimura, M.; Uozomi, Y. *J. Org. Chem* **2007**, *72*, 707-714. (g) Franciò, G.; Drommi, D.; Graiff, C.; Faraone, F.; Tiripicchio, A. *Inorg. Chimica Acta* **2002**, *338*, 59-69.
4. (a) Sirbu, D.; Consiglio, G.; Gischig, S., *J. Org. Chem.* **2006**, *691*, 1143-1150. (b) Bluhm, M. E.; Folli, C.; Walter, O.; Döring, M., *J. Mol. Catal. A: Chemical* **2005**, *229*, 177-181. (c) Sun, W.-H.; Li, Z.; Hu, H.; Wu, B.; Yang, H.; Zhu, N.; Leng, X.; Wang, H. *New J. Chem.* **2002**, *26*, 1474-1478. (d) Chen, H.-P.; Liu, Y.-H.; Peng, S.-M.; Liu, S.-T. *Organometallics* **2003**, *22*, 4893-4899. (e) Daugulis, O.; Brookhart, M. *Organometallics* **2002**, *21*, 5926-5934.
5. Aeby, A.; Consiglio, G. *Inorg. Chimica Acta* **1999**, *296*, 45-51.
6. Gsponer, A.; Schmid, T.M.; Consiglio, G. *Helv. Chim. Acta* **2001**, *84*, 2986-2995.
7. Pettit, G. R.; Singh, S. B.; Herald, D.L.; Lloyd-Williams, P.; Kantoci, D.; Burkett, D. D.; Barkoczy, J.; Hogan, F.; Wardlaw, T. R. *J. Org. Chem.* **1994**, *59*, 6287-6295.
8. Xu, X.-Y.; Tang, Z.; Wang, Y.-Z.; Luo, S.-W.; Cun, L.-F.; Gong, L.-Z. *J. Org. Chem.* **2007**, *72*, 9905-9913.
9. Luo, S.; Xu, H.; Li, J.; Mi, L. Z. X.; Zheng, X.; Cheng, J-P. *Tetrahedron* **2007**, *63*, 11307-11314.
10. Bartoli, G.; Bosco, M.; Dalpozzo, R.; Giuliani, A.; Marcantoni, E.; Mercozzi, T.; Sambri, L.; Torregiani, E., *J. Org. Chem.* **2002**, *67*, 9111-9114.
11. Torisawa, Y.; Hashimoto, A.; Okouchi, M.; Iimori, T.; Nagasawa, M.; Hino, T.; Nakagawa, M. *Bioorg. Med. Chem. Lett.* **1996**, *6*, 2565-2570.
12. Brumel, J.M.; Legrand, O.; Reymond, S.; Buono, G. *J. Am. Chem. Soc.* **1999**, 121, 24, 5807-5808.

13. Legrand, O.; Brumel, J.M.; Constantieux, T.; Buono, G. *Chem. Eur. J.* **1998**, *4*, 1061-1067.
14. Rülke, R.E.; Ernsting, J.M.; Spek, A.L.; Elsevier, C.J., van Leeuwen, P.W.N.M.; Vrieze, K. *Inorg. Chem.* **1993**, *32*, 5769-5778.
15. Del Campo, O.; Carbayo, A.; Cuevas, J.V.; García-Herbosa, G.; Muñoz, A. *Eur. J. Inorg. Chem.* **2009**, 2254-2260.
16. (a) Britovsek, G. J. P.; Cavell, K. J.; Keim, W. *J. Mol. Cat. A: Chem.* **1996**, *110*, 77-87. (b) Bayersdorfer, R.; Ganter, B.; Englert, U.; Keim, W.; Vogt, D. *J. Organomet. Chem.* **1998**, *552*, 187-194. (c) Eggeling, E. B.; Hovestad, N. J.; Jastrzebsji, J. T. B. H.; Vogt, D.; van Koten, G. *J. Org. Chem.* **2000**, *65*, 8857-8865.
17. Muthukumaru Pillai, S.; Tembe, G. L.; Ravindranathan, M. *J. Mol. Cat.* **1993**, *84*, 77-86.
18. (a) Wilke, G. *Angew. Chem. Int. Ed. Engl*. **1988**, *27*, 185-206. (b) Park, H.; RajanBabu, T. V. *J. Am. Chem. Soc.* **2002**, *124*, 734-735. (c) Faissner, R.; Huttner, G. *Chem. Eur. J.* **2003**, 2239-2244.
19. Mayagmarsuren, G.; Tkach, V. S.; Shmidt, F. K.; Mohamad, M.; Suslov, D. S. *J. Mol. Cat. A: Chem.* **2005**, *235*, 154-160.
20. Sonowane, H. R.; Bellur, N. S.; Ahuja, J.; Kulkarni, D. G. *Tetrahedron: Asymmetry* **1992**, *3*, 163-192.

Experimental

Chapter 5

General

^{1}H NMR and ^{13}C NMR spectra were run at 400 and 500 MHz for proton and 100.1 MHz for carbon using deuterochloroform and methylene chloride as solvents and tetramethylsilane as internal standard, the spectra were recorded at 25°C where not differently indicated. Optical rotations and CD spectra were determined at 25 °C. HRGC analyses were run on a OV 1701 capillary column (25 m x 0.32 mm), carrier gas He, 40 KPa, split 1:50 and in a SE 30 capillary column (30m x 0.32 mm) carrier gas He 50 KPa, split 1:60. Chiral High Resolution GC analyses were run on a Shimadzu GC-14B instrument, the capillary columns being Chiraldex™ type G-TA, γ-cyclodextrin (40m X 0.25mm) (carrier gas Helium, 180 KPa, split 1:100), or DiMePe β-cyclodextrin (25m X 0.25mm) (carrier gas He, 110 KPa, split 1:50); TLC were performed on silica gel, using light petroleum-ethyl acetate or methylenechloride-methanol mixtures as the eluent. Flash chromatography was run on silica gel, 230 – 400 mesh using mixtures of light petroleum 40-70°C or chloroform and ethyl acetate as the eluent. CAL-B (Novozyme® 435) was purchased from Novo Nordisk A/S, 7000 u/g. Dry Yeast from *Saccaromyces Cerevisiae* Type II was purchased from Sigma-Aldrich. All complexes synthesis were carried out under argon atmosphere with Schlenk technique and at room temperature. The synthesis of chiral PN ligands were carried out with Schlenk technique and using freshly distilled and degassed solvents.

SYNTHESIS OF LIGANDS

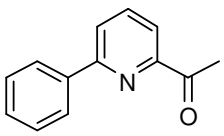

2-Acetyl-6-phenylpyridine (6). Ketone **6** was prepared by means of a Suzuki–Miyaura cross-coupling reaction. Palladium (II) acetate (5 mg, Mw 224, 0.025 mmol,), triphenylphosphine (0.02 g, Mw 262.28, 0.076 mmol), 2.0 M aqueous K_2CO_3 (5.0 mL, 10 mmol,) and distilled water (10 ml) were added to a degassed solution of 2-acetyl-6-bromopyridine (1.3 g, Mw 200, 6.50 mmol) and phenylboronic acid (1.0 g, Mw 121.93, 8.2 mmol) in 1-propanol (16.0 mL), and the mixture was refluxed overnight. After cooling at room temperature, distilled water (5.0 mL) was added and the mixture was extracted with ethyl acetate, (2 x 25 mL). The organic layer was dried over anhydrous Na_2SO_4 and the solvent was evaporated to give the crude ketone, which was purified on a SiO_2 column (petroleum ether 100%, then gradient to 2% ethyl acetate).

Yield 92%. **^{1}H NMR (400 MHz, $CDCl_3$)** δ 2.83 (s, 3H, COC*H*$_3$), 7.46-7.54 (m, 3H), 7.89-7.91 (m, 3H), 8.11 (m, 2H). **^{13}C NMR 100.1 MHz, $CDCl_3$)** δ 25.4, 119.4, 123.0, 126.5, 128.5, 129.1, 137.3, 138.0, 153.0, 155.9, 200.0. **ESI-MS** 198 ($M+H^+$), 220 ($M+Na^+$).

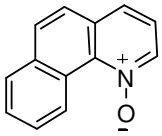

Benzo[*h*]quinoline-1-oxide (10). To a solution of benzo[*h*]quinoline (5 g, Mw 179.22, 28 mmol) in 112 mL $CHCl_3$ cooled to 0°C, was added a solution of MCPBA (12 g, Mw 172.17, 42 mmol, 60% purity) in 280 mL of $CHCl_3$. The resulting mixture was stirred at room temperature for 5 days, then washed with 5% solution of K_2CO_3 (4 x 125 mL), dried on sodium sulfate and concentrated under reduced pressure. Purification with column chromatography ($CHCl_3$, then $CHCl_3$/CH_3OH 8:2 as eluent) gave pure **10** in 83% yield as a crystalline solid (m.p. 122 °C). **^{1}H NMR (400 MHz, $CDCl_3$)** δ 7.43 (dd, *J* = 1.6, 6.4 Hz, 1H), 7.68 (d, *J* = 8.8 Hz, 1H), 7.77-7.82 (m, 3H), 7.88 (d, *J* = 8.8 Hz, 1H), 7.95 (m, 1H), 8.69 (dd, *J* = 1.2, 6.4 Hz, 1H), 10.86 (m, 1H). **^{13}C NMR (100.1 MHz, $CDCl_3$)** δ 121.2, 125.0, 125.8, 127.8, 128.0, 128.3, 129.1, 130.6, 131.3, 134.1, 139.3. **ESI-MS** 196 ($M+H^+$), 218 ($M+Na^+$).

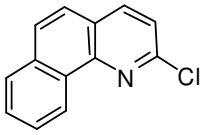

2-Chlorobenzo[*h*]quinoline (11a-b). A mixture of **10** (4.533 g, Mw 195.22, 23 mmol) in 28 mL (Mw 153.33, δ 1,675 g/mL, 312 mmol) of $POCl_3$ was refluxed for 30 min. The cooled reaction mixture was poured into crusher ice, neutralized with NH_3 32% solution and extracted with CH_2Cl_2 (3 x 100 mL). the combined extracts were washed with water, dried on Na_2SO_4 and evaporated under reduce pressure. The residue was flash-chromatographed with CH_2Cl_2 as the eluent to give **(11a)** as the less-polar fraction (white solid m.p. 111 °C) . **^{1}H NMR (400 MHz $CDCl_3$)** δ 7.52 (d, *J* = 8.4 Hz, 1H), 7.67-7.76 (m, 3H), 7.85 (d, *J* = 9.2, 1H), 7.92 (m, 1H), 8.14 (d, *J* = 8.4, 1H), 9.23 (m, 1H). **^{13}C NMR (100.1 MHz, $CDCl_3$)** δ 122.6, 124.5, 124.7, 124.9, 127.3, 127.7, 128.1, 128.7, 130.5, 133.8, 138.5, 146.6, 149.8. **ESI-MS** 214 ($M+H^+$), 236 ($M+Na^+$).

4-Chlorobenzo[*h*]quinoline (11b) was isolated from the above flash-chromatography as the more polar fraction (10% yield). **^{1}H NMR (400 MHz $CDCl_3$)** δ 7.661 (d, *J* = 4.8

Hz, 1H), 7.72-7.79 (m, 2H), 7.93 (m, 2H), 8.14 (d, *J* = 9.2 Hz, 1H), 8.87 (d, *J* = 4.8 Hz, 1H), 9.29 (m, 1H).

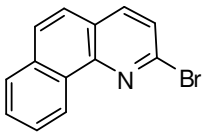

2-Bromobenzo[*h*]quinoline (12). A solution of 2-chlorobenzo[*h*]quinoline **(11a)** (4.225 g, Mw 213.66, 20 mmol), and bromotrimethylsilane (5.28 mL, Mw 153.10, δ 1.160 g/mL, 40 mmol) in propionitrile (20 mL) was heated under reflux 4 days. The mixture was poured into a 2M NaOH solution/ice mixture, and the aqueous solution extracted with diethyl ether (3 x 50mL). The combined organic phase was dried and evaporated to dryness obtaining **12** without further purifications. Yellow solid (96 % yield) m.p. 113-114 °C. **IR (nüjol)** 1621, 1577, 1561, 1463, 1020, 838, 798, 750, 741, 714 cm^{-1}. **^{1}H NMR (400 MHz $CDCl_3$)** δ 7.66 (dd, *J* = 8, 2 Hz, 2H), 7.73 (m, 2H), 7.85 (d, *J* = 8.8 Hz, 1H), 7.91 (m, 1H), 8.02 (d, *J* = 8.0, 1H), 9.22 (m, 1H). **^{13}C NMR (100.1 MHz, $CDCl_3$)** δ 124.6, 124.8, 125.2, 126.2, 127.4, 127.8, 128.3, 129.0, 130.5, 133.9, 138.2, 141.0, 144.0, 147.3. **ESI-MS** 258, 260 ($M+H^+$).

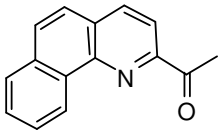

2-Acetylbenzo[*h*]quinoline (7). To a stirred solution of **12** (1.520 g, Mw 258.11, 5.98 mmol) in dry THF (36 mL), *n*-BuLi (4 mL, 6.18 mmol, 1.6 M in hexane solution) was added dropwise at -78 °C during 5-10 min under inert atmosphere (Ar). The resulting dark red solution was stirred for 1h, then anhydrous DMA (0.6 mL, Mw 87.12, δ 0.942 g/mL, 6.45 mmol) was added at the same temperature. The reaction mixture was stirred for further 60 min and then the temperature was left to rise spontaneously ovenight. The solution was then quenched with HCl 1M (7.5 mL) and the two phases was separated. The organic layer was concentrated under reduce pressure, the residue was washed with water and extracted with Et_2O. The organic phase was dried over $MgSO_4$, evaporation of the solvent gave the crude ketone **7** which was chromatographed on SiO_2 column (eluent: EP/EtOAc). 61% yield. **^{1}H NMR (400 MHz, $CDCl_3$)** δ 3.00 (s, 3H, $COCH_3$), 7.68 – 7.83 (m, 3H); 7.91 (d, *J* = 9.1 Hz, 1H), 7.95 (d, *J* = 8.4 Hz, 1H); 8.27 (AB quartet, *J* = 8.4 Hz, 2H), 9.37 (dm, 1H). **^{13}C NMR (100.1 MHz, $CDCl_3$)** δ 25.8, 118.9, 124.5, 124.9, 127.5, 128.1, 128.3, 128.6, 130.0, 131.6, 133.7, 136.5, 145.4, 151.6, 200.7. **ESI-MS** 222.1 ($M+H^+$), 244.1 ($M+Na^+$).

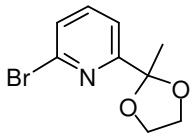

6-Bromo-2-(2'-methyl-1',3'-dioxolan-2'-yl)pyridine (Br-36). A solution of 1.0 g (Mw 200, 5 mmol) of 2-Acetyl-6-bromo pyridine, 0.34 mL (Mw 62.07, δ 1.113 g/mL, 6 mmol) of 1,2-ethandiol and 0.1 g (Mw 200, 0.5 mmol) of 4-toluensulfonic acid in 15 mL of benzene was heated for 24 h under reflux in a Dean-Stark apparatus. The mixture was cooled to room temperature, and washed twice with satured Na_2CO_3 (15 mL). The aqueous phase was washed with benzene and the combined organic extracts dried on dry Na_2SO_4. After solvent removal at low pressure the crude was purified *via* column chromatography (PE/EtOAc as eluant). 93% yield. **^{1}H NMR (400 MHz, $CDCl_3$)** δ 1.72 (s, 1H), 3.84-3.95 (m, 2H), 4.04-4.15 (m, 2H), 7.41 (dd, J = 2.0, 6.8 Hz, 1H), 7.49-7.58 (m, 2H). **^{13}C NMR (75 MHz, $CDCl_3$)** δ 25.1, 65.1, 108.0, 118.2, 127.5, 138.7, 142.0, 162.5.

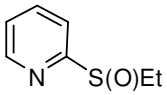

Ethyl 2-pyridyl sulfoxide (35). To a solution of 2-mercaptopyridine (8.040 g, Mw 111.17, 72 mmol) in 72 mL of aqueous 1 N NaOH were added 5.8 mL (Mw 155.97, δ 1.95 g/mL, 73 mmol). The mixture was stirred vigorously over night and then extracted with Et_2O (3 x 30 mL). The combined ethereal extract were washed with 2 N NaOH (2 x 20 mL), once with brine and dried on Na_2SO_4. Evaporation of the solvent *in vacuo* gave 2-(2-mercaptoethyl)pyridine as a pale orange oil in 95% yield. This product was used in the next step without further purification. The 2-(2-mercaptoethyl)pyridine (9.526 g, Mw 139.22, 68 mmol) was dissolved in 144 mL of CH_3OH and 21 g (Mw 494.65, 34 mmol, 80% purity) of magnesium monoperoxyphthalate was added in several portions while the temperature was maintained at 0°C. The mixture was stirred overnight and carefully concentrated by rotary evaporation keeping the bath temperature bellow 50°C. To the viscous slurry obtained H_2O was added and the resulting mixture was extracted with $CHCl_3$. The organic extracts were washed with brine (2 x 20 mL) and dried (Na_2SO_4). Solvent removal under reduce pressure gave a crude which was cromatographed on SiO_2 (Et_2O/EtOAc as eluant), 80% yield. **^{1}H NMR (400 MHz, $CDCl_3$)** δ 1.20 (t, J = 7.4 Hz, 3H), 2.90-2.97 (m, 1H), 3.15-3.22 (m, 1H), 7.37 (ddd, J = 1.5, 4.7, 7.3 Hz, 1H),

7.93 (dt, *J* = 1.7, 7.6 Hz, 1H), 8.00 (dt, *J* = 1.1, 7.5 Hz, 1H), 8.62 (dd, *J* = 1.6, 4.7 Hz, 1H).

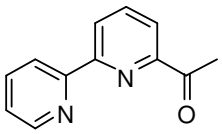

6-Acetyl-2,2'-bipiridine (33). A slurry of 4.412 g (Mw 244.08, 18 mmol) of **Br-36** in 100 mL of freshly distilled THF, was cooled in a acetone/liquid nitrogen bath (- 80 °C) under argon atmosphere and 13.5 mL (1.6 M in *n*-hexane, 22 mmol) of *n*-Butyllithium was added dropwise. After being stirred for 45', a solution of **35** (5 g, Mw 152.17, 32 mmol) in THF (50 mL) was dropped in the mixture at -70°C. the intensely red mixture was stirred overnight at room temperature and then quenched wit satured NH_4Cl solution (40 mL). the organic phase was separated, the aqueous phase was washed twice with ethyl acetate (40 mL) and the combined organic extracts were dried (Na_2SO_4) and evapored at low pressure. The remaining red oil was stirred for 3 h at 60°C in 2 M HCl (85 mL) and cooled to room temperature, EtOAc (30 mL) was added and the mixture was carefully neutralized by addition of solid $NaHCO_3$. The resulting mixture was extracted with EtOAc (4 x 30 mL) and the combined organic phases were washed repeatedly with water and once with brine, then dried on Na_2SO_4 and evapored. The residual solid was purified by column chromatography (CH_2Cl_2/EtOAc as eluant) obtaining the ketone **33** in 60% yield. **^{1}H NMR (400 MHz, $CDCl_3$)** δ 2.81 (s, 3H, C*H*$_3$CO), 7.31 (ddd, *J* = 1.2, 4.7, 7.5 Hz, 1H), 7.82 (dt, *J* = 1.7, 7.7 Hz, 1H), 7.90 (t, *J* = 7.8 Hz, 1H), 8.02 (dd, *J* = 1.2, 7.7 Hz, 1H), 8.49 (d, *J* = 8.0 Hz, 1H), 8.59 (dd, *J* = 1.2, 7.8 Hz, 1H), 8.67 (dm, *J* = 4.8 Hz, 1H). **^{13}C NMR (100.1 MHz, $CDCl_3$)** δ 25.8,121.0, 121.4, 124.1, 124.2, 136.9, 137.7, 149.2, 152.9, 155.3, 155.3, 200.0. **ESI-MS** 199 ($M+H^+$), 221 ($M+Na^+$).

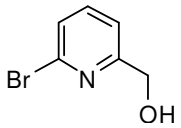

(6-bromopyridin-2-yl)methanol (40). Was prepared in quantitative yield by $NaBH_4$ reduction of 6-bromo-2-pyridinecarboxaldehyde (see the general procedure for the synthesis of racemic alcohol reported below). **^{1}H NMR (400 MHz, $CDCl_3$)** δ 3.20 (s, 1H, O*H*), 4.63 (s, 2H, C*H*$_2$), 7.15-7.46 (m, 3H). **^{13}C NMR (100.1 MHz, $CDCl_3$)** δ 64.1, 119.3, 126.5, 139.1, 141.2, 161.4.

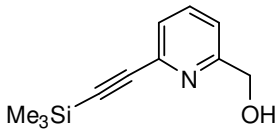

(6-((Trimethylsilyl)ethynyl)pyridin-2-yl)methanol (41). Trimethylsilylacetylene (1.11 mL, Mw 98.22, δ 0.695 g/mL, 8.0 mmol) was added to a stirred solution of **40** (376 mg, Mw 188.02, 2.0 mmol), $Pd(PPh_3)_4$ (48 mg, Mw 1155.58, 0.04 mmol) and CuI (11 mg, Mw 190.45, 0.08 mmol) in 8 mL of triethylamine. The mixture, from which a white precipitate formed, was heated at 50°C then cooled at room temperature. The conversion of into the product was complete in a few minutes (TLC with ethyl acetate). After addition of ether, the solution was washed with aq. NH_4Cl (sat.), dried over Na_2SO_4, and evaporated to give a crude product which was used in the further step without purification. For analytical pourposes, a pure sample of **41** was obtained by flash chromatrography (eleuent petroleum ether/ethyl acetate 3:2) **^{1}H NMR (400 MHz, $CDCl_3$)** δ 0.36 (s, 9H, Me_3Si), 4.57 (s, 2H, CH_2OH), 7.21 (d, J = 7.7 Hz, 1H, H^5), 7.35 (d, J = 7.7 Hz, 1H, H^3), 7.62 (t, J = 7.7 Hz, 1H ,H^4). **^{13}C NMR (100.1 MHz, $CDCl_3$)** δ –0.4 ($SiMe_3$), 64.3 (CH_2OH), 95.1, 103.4, 120.0, 126.0, 136.7, 141.8, 159.9. **ESI-MS** 206.1 ($M+H^+$).

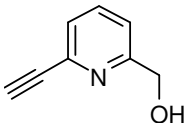

(6-Ethynylpyridin-2-yl)methanol (42). The crude **41** (410 mg, Mw 205.33, 2 mmol assuming a 100% yield in the previous step) was dissolved in THF, then Bu_4NF (1M solution in THF, 3 mL, 3 mmol) was added at room temperature. After 10 min stirring, ether was added and the solution washed with water first, then with sat. NH_4Cl, finally dried over Na_2SO_4 and evaporated to give an oily residue which was purified on column chromatography (petroleum ether/ethyl acetate 8:2); yield 78%. Crystalline product, mp 108 °C. **^{1}H NMR (400 MHz, $CDCl_3$)** δ 3.15 (s, 1H, CCH), 3.90 (bs, OH), 4.73 (s, 2H. CH_2OH), 7.29 (d, J = 7.9 Hz, 1H), 7.36 (d, J = 7.7 Hz, 1H), 7.64 (dd, J = 7.7, 7.9 Hz, 1H). **^{13}C NMR (100.1 MHz, $CDCl_3$)** δ 64.2 (t, CH_2OH), 77.4, 82.4, 120.4, 126.0, 136.9, 141.0, 160.2. **ESI-MS** 156.1 ($M+Na^+$).

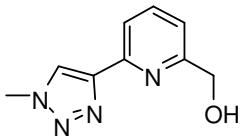

(6-(1-methyl-1*H*-1,2,3-triazol-4-yl)pyridin-2-yl)methanol (43). Acetylene **42** (0.146 g, Mw 133.15, 1.1 mmol), CH_3I (0.142 g, Mw 141.94, 1.0 mmol), and sodium azide

(0.071 g, Mw 65.01, 1.1 mmol) were suspended in a 1:1 mixture of water and *tert*-BuOH (1 mL each) in a 10 mL glass vial equipped with a small magnetic stirring bar. CuI (0.1 g, Mw 190.45, 0.52 mmol) was added and the mixture was irradiated under MW for 10 min at 100 °C, using an irradiation power of 100 W. A yellow precipitate was filtered off, and the solution concentrated to dryness *in vacuo*, giving a residue from which compound **43** was obtained in a 74% yield after flash chromatography. White solid, mp > 200°C; **IR (Nujol)** 3445, 3310, 3063, 1599, 1580 cm^{-1}. **^{1}H NMR (400 MHz, $CDCl_3$)** δ 4.14 (s, 3H, CH_3N), 4.76 (s, 2H, CH_2OH), 4.82 (s, 1H, O*H*), 7.16 (d, *J* = 7.9 Hz, 1H, H^3), 7.74 (t, *J* = 7.9 Hz, 1H, H^4), 8.01 (d, *J* = 7.9 Hz , 1H, H^5), 8.12 (s, 1H, triazole**^{13}C NMR (from CH COSY, 100.1 MHz, $CDCl_3$)** δ 36.8 (*C*H_3N), 63.9 (*C*H_2OH), 118.7 (C^5 Py), 119.6 (C^3 Py), 123.1 (C^5 triazole), 137.6 (d, C-4 py), 148.1, 148.9, 158.7. **ESI-MS** 191.1 (M+H^+), 214.1 (M + Na^+).

Racemic alcohol synthesis: general procedure

$NaBH_4$ (190 mg, Mw 37.82, 5 mmol) was added portionwise, at room temperature, to an ethanol solution of prochiral ketone (5 mmol). The mixture was stirred for 2 h (TLC); the solvent was evaporated under reduced pressure and the residue was washed with saturated solution of NH_4Cl and extracted with CH_2Cl_2. The organic phase was dried on anhydrous Na_2SO_4 and evaporated to give the racemic alcohol in 99% yield, which was used without further purification.

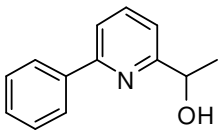

(±)-2-(1-Hydroxyethyl)-6-phenylpyridine (*rac*-13). ^{1}H NMR (400 MHz, $CDCl_3$) δ 1.55 (d, *J* = 6.4 Hz, 3H, CHCH_3), 4.75 (d, *J* = 4.4 Hz, 1H, O*H*), 4.95 (m, *J* = 2.0, 4.4, 6.4 Hz, 1H, C*H*CH_3), 7.20 (ddd, *J* = 0.7, 1.5, 7.6 Hz, 1H), 7.41-7.51 (m, 3H), 7.65 (d, *J* = 7.2 Hz, 1H), 7.76 (dd, *J* = 7.6, 8.0 Hz, 1H), 8.03 (m, 2H). **^{13}C NMR (100.1 MHz, $CDCl_3$)** δ 24.2, 68.5, 118.2, 118.8, 126.8, 128.7, 129.1, 137.6, 138.7, 155.6, 162.5. **ESI-MS** 200 (M+H^+), 222 (M+Na^+).

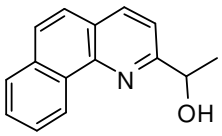

(±)-2-(1-Hydroxyethyl)benzo[*h*]quinoline (*rac*-14). IR (neat) 3403, 3050, 1623, 1596, 1566, 1504 cm^{-1}; **^{1}H NMR (400 MHz, $CDCl_3$)** δ 1.64 (d, *J* = 6.6, 3H, CH_3CH),

5.12 (dq, *J* = 4.4, 6.6 Hz, 1H, C*H*OH), 5.26 (d, *J* = 4.4 Hz, 1H, O*H*), 7.47 (d, *J* = 8.0 Hz, 1H), 7.70 (d, *J* = 9.0 Hz, 1H), 7.73 (m, 3H), 7.93 (dd, *J* = 1.8, 8.8 Hz, 1H), 9.29 (dm, 1H). **^{13}C NMR (100.1 MHz, $CDCl_3$)** δ 24.7, 68.8, 118.4, 124.2, 124.9, 125.4 , 127.0, 127.4, 127.8, 128.3 , 131.4, 133.7, 136.8, 145.9, 158.9. **ESI-MS** 224.1 ($M+H^+$), 246.1 ($M+Na^+$).

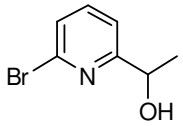

(±)-1-(6-bromopyridin-2-yl)ethanol (*rac*-22). From 2-acetyl-6-bromopyridine: **^{1}H NMR (400 MHz, $CDCl_3$)** δ 1.48 (d, *J* = 6.4 Hz, 3H, CH*CH_3*), 3.40 (d, *J* = 4.9 Hz, 1H, O*H*), 4.86 (m, 1H, *C*HCH_3), 7.28 (d, *J* = 7.7 Hz, 1H), 7.38 (d, *J* = 8.0 Hz, 1H), 7.55 (dd, *J* = 7.6, 8.0 Hz, 1H). **^{13}C NMR (100.1 MHz, $CDCl_3$)** δ 24.5, 69.6, 118.9, 127.0, 139.6, 141.6, 165.6. **ESI-MS** 202, 204 ($M+H^+$).

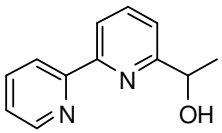

(±)-1-(2,2'-bipyridin-6-yl)ethanol (*rac*-37). ^{1}H NMR (400 MHz, $CDCl_3$) δ 1.56 (d, *J* = 6.4 Hz, 3H, CH_3), 4.59 (d, *J* = 4.8 Hz, 1H, OH), 4.97 (m, 1H, C*H*CH_3), 7.29 (d, *J* = 7.6 Hz, 1H), 7.33 (ddd, *J* = 1.2, 4.8, 7.6 Hz, 1H), 7.84 (m, 2H), 8.33 (d, *J* = 7.6 Hz, 1H), 8.43 (dm , *J* = 8.0 Hz, 1H), 8.68 (dm, *J* = 4.8 Hz, 1H). **^{13}C NMR (100.1 MHz, $CDCl_3$)** δ 24.1, 68.7, 119.3, 119.7, 120.9, 123.6, 136.7, 137.6, 148.9, 154.2, 155.4, 162.4. **ESI-MS** 202 ($M+H^+$), 223 ($M+Na^+$).

Enantiopure *sec*-alcohols synthesis

1. **Baker'yeast reduction**

To a stirred suspension of dry baker's yeast (15.5 g/mmol substrate) in phosphate buffer (Na_2HPO_4/KH_2PO_4 0.1 M, pH 7.4, 1000 mL) was added glucose (112 g) or sucrose (56 g). The mixture was pre-incubated for 30 min at 37 °C and the prochiral ketone (3.6 mmol) was added at room temperature. The reaction was monitored by HRGC. At the end of the reaction, (reaction time depending on the substrate) the broth was extracted with ether. The organic phase was dried and evaporated to give a residue which was chromatographed on SiO_2 (PE/EtOAc as eluent).

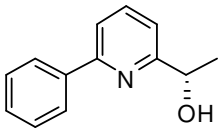

(*S*)-(+)-2-(1-Hydroxyethyl)-6-phenylpyridine ((*S*)-13). 6 days**,** 76% yield at 98%conv., e.e.>99.9% (by HRGC), $[\alpha]_D$ +22.0 (c 0.55, $CHCl_3$) [lit.: $[\alpha]_D$ +28.0 (*c* 1.00, $CHCl_3$)].

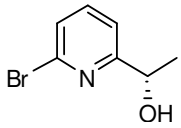

(*S*)-(–)-1-(6-bromopyridin-2-yl)ethanol ((*S*)-22). 24 h**,** 87% yield at 97% conv., e.e. = 96% (by HRGC), $[\alpha]_D$ – 7.2 (*c* 0.25, $CHCl_3$) [lit.: $[\alpha]_D$ – 11 (*c* 2.15, $CHCl_3$)].

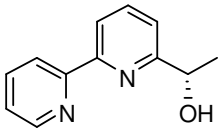

(*S*)-(+)-1-(2,2'-bipyridin-6-yl)ethanol ((*S*)-37). 48 h, 75% yield at 93% conv., e.e. = 99% (by HRGC), $[\alpha]_D$ + 21.7 (*c* 0.35, $CHCl_3$) [lit.: $[\alpha]_D$ + 26 (*c* 1.62, $CHCl_3$)].

2. Enzymatic acetylation of racemic secondary alcohols

A mixture of the racemic secondary alcohol (0.5 mmol), CAL-B (Novozyme® 435, 50 mg), anhydrous *tert*-butyl methyl ether (8.4 mL) and vinyl acetate (140 µL, Mw 86.09, δ 0.934 g/mL, 1.55 mmol) was vigorously stirred at 28 °C under an argon athmosphere. At approximately 50% conversion (determined by HRGC) the mixture was filtered through celite, the pad was washed with dichloromethane and the combined organic phases were evaporated under reduced pressure. The crude reaction mixture was purified by flash column chromatography (petroleum ether/ethyl acetate as eluent) to obtain the (*R*)- acetates and the unreacted (*S*)-alcohols.

(*R*)-(+)-2-(1-Acetoxyethyl)-6-phenylpyridine 45% yield, e.e. > 99.9%

(*S*)-(+)-2-(1-Hydroxyethyl)-6-phenylpyridine 50% yield, e.e. = 79%

(*R*)-(+)-2-(1-Acetoxyethyl)benzo[*h*]quinoline 40% yield, e.e. > 99%

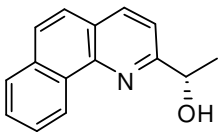

(*S*)-(+)-2-(1-Hydroxyethyl)benzo[*h*]quinoline ((*S*)-14) obtained by this route (47% at 44% conversion) had e.e. = 86% (from the ^{1}H-NMR analysis of the corresponding Mosher's ester), $[\alpha]_D$ +58.0 (c 0.4, $CHCl_3$).

3. Dynamic kinetic resolution of racemic secondary alcohols

Catalyst $[Ru_2(CO)_4(\mu\text{-}H)(C_4Ph_4\text{-}COHOCC_4Ph_4)]$ (21 mg, Mw 1085.15, 0.04 mmol) and Novozyme® 435 (60 mg) were suspended in toluene, under argon. A degassed solution of the racemic alcohol (2 mmol) and 4-chlorophenyl acetate (1.02 g, Mw 170.59, 6 mmol) in toluene (5 mL) was transferred to this suspension, and the mixture was stirred under argon, at 70 °C, until complete conversion (HRGC). The enzyme was filtered off, and the reaction mixture was separated on silica (petroleum ether/ethyl acetate as eluent) to yield optically pure (*R*)-acetate.

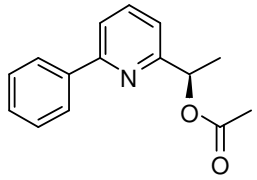

(*R*)-(+)-2-(1-Acetoxyethyl)-6-phenylpyridine ((*R*)-15) was obtained in 71% yield, after chromatography, from the DKR of alcohol **13** (93% conversion), e.e. > 99.9% (by chiral HRGC), $[\alpha]_D$ + 87.0 (c 0.25, $CHCl_3$); [lit.: $[\alpha]_D$ +86.0 (*c* 1.00, $CHCl_3$) e.e. = 98%]. **^{1}H NMR (400 MHz, $CDCl_3$)** δ 1.66 (d, J = 6.4 Hz, 3H, CH_3CH), 2.15 (s, 3H, CH_3CO), 6.01 (q, J = 6.4 Hz, 1H, C*H*OAc), 7.27 (d, J = 8 Hz, 2H), 7.45 (m, 3H), 7.64 (dd, J = 0.8, 7.6 Hz, 1H), 7.74 (dd, J = 7.6, 8.0 Hz, 1H), 8.03 (m, 2H). **^{13}C NMR (100.1 MHz, $CDCl_3$)** δ 20.6, 21.3, 73.3, 118.4, 119.2, 126.9, 128.7, 128.9, 137.3, 139.2, 156.6, 160.2, 170.3. **ESI MS** 242 ($M+H^+$), 264 ($M+Na^+$).

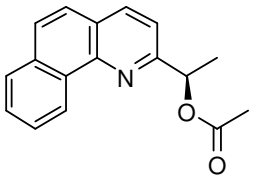

(*R*)-(+)-1-(benzo[*h*]quinolin-2-yl)ethyl acetate ((*R*)-16). e.e. > 99.9 % at 90 % conv., yield 75%, $[\alpha]_D$ + 119.0 (c 0.5, $CHCl_3$). **IR (neat)** 3050, 1738, 1623, 1596, 1566, 1504 cm^{-1}. **^{1}H NMR (400 MHz, $CDCl_3$)** δ 1.64 (d, J = 6.6, 3H, CH_3CH), 2.19 (s, 3H, CH_3CO), 6.22 (q, J = 6.6 Hz, 1H, CH_3C*H*), 7.58 (d, J = 8.0 Hz, 1H), 7.65 (d, J = 9.2 Hz, 1H), 7.70 (m, 2H), 7.89 (dd, J = 1.5, 8.8 Hz, 3H), 8.17 (d, J = 8.0 Hz, 1H), 9.34 (d, J = 7.3 Hz, 1H). **^{13}C NMR (100.1 MHz, $CDCl_3$)** δ 20.7, 21.4, 73.7, 118.7, 124.6, 125.0, 125.4, 126.9, 127.6, 127.65, 128.1, 131.4, 133.7, 136.5, 145.6, 158.9, 170.5. **ESI MS** 266.1 ($M+H^+$), 288.2 ($M+Na^+$).

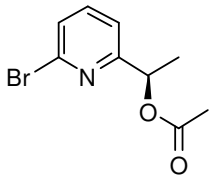

(*R*)-(+)-1-(6-bromopiridyn-2-yl)ethyl acetate ((*R*)-23). e.e. = 98.6% (by chiral HRGC) at 88 % conv., yield 78%. $[\alpha]_D$ + 70 (c 0.5, $CHCl_3$) [lit.: $[\alpha]_D$ + 72 (c 2.09, $CHCl_3$)]. **^{1}H NMR (400 MHz, $CDCl_3$)** δ 1.51 (d, J = 6.7 Hz, 3H, CH_3CH), 2.13 (s, 1H, CH_3CO), 5.86 (q, J = 6.7 Hz, 1H, CH_3CH), 7.29 (d, J = 7.7 Hz, 1H), 7.43 (d, J = 7.7 Hz, 1H), 7.55 (dd, J = 7.7, 8.0 Hz, 1H). **^{13}C NMR (100.1 MHz, $CDCl_3$)** δ 20.6, 21.1, 72.3, 118.9, 127.0, 139.0, 141.5, 161.8, 170.0. **ESI MS** 245, 247 ($M+H^+$).

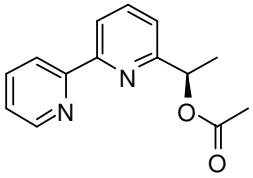

(*R*)-(+)-1-(2,2'-bipyridin-6-yl)ethyl acetate ((*R*)-38). e.e. > 99.9 % (by chiral HRGC) at 78 % conv., yield 60%. $[\alpha]_D$ + 89 (c 0.5, $CHCl_3$) [lit.: $[\alpha]_D$ + 85 (c 1.87, $CHCl_3$)]. **IR (neat)** 1735 cm^{-1}. **^{1}H NMR (400 MHz, $CDCl_3$)** δ 1.66 (d, J = 6.8 Hz, 3H, CH_3CH), 2.15 (s, 3H, CH_3CO), 6.02 (q, J = 6.8 Hz, 1H, CH_3CH), 7.30 (m, 1H), 7.35 (d, J = 7.6 Hz, 1H), 7.81 (t, J = 8.0 Hz, 2H), 8.31 (d, J = 8.0 Hz, 1H), 8.46 (dm, J = 8.0 Hz, 1H), 8.66 (dm, J = 4.8 Hz, 1H). **^{13}C NMR (100.1 MHz, $CDCl_3$)** δ 20.5, 21.2, 73.1, 119.7, 120.1, 121.3, 123.7, 136.8, 137.5, 148.9, 155.3, 156.0, 159.6, 170.2. **ESI-MS** 243 ($M+H^+$).

Acetate hydrolysis: general procedure.

The acetate (1.4 mmol) was hydrolyzed by K_2CO_3 (193 mg, Mw 138.21, 1.4 mmol) in methanol/water (1:1) mixture at room temperature following the reaction with TLC. Methanol was evaporated under reduced pressure, and the aqueous phase was extracted with CH_2Cl_2 (3 × 20 mL). The combined organic phases were washed with brine, dried over Na_2SO_4, and concentrated in *vacuum*. Flash chromatography on silica (eluent depending on the substrate: CH_2Cl_2/Ethyl Acetate for **37**, EP/EtOAc other alcohols) gave the pure alcohol quantitatively.

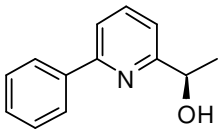

(*R*)-(–)-2-(1-Hydroxyethyl)-6-phenylpyridine ((*R*)-13). e.e. > 99.9% (by chiral HRGC) $[\alpha]_D$ –24.0 (c 0.30, $CHCl_3$).

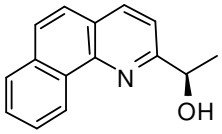

(*R*)-(–)-2-(1-Hydroxyethyl)benzo[*h*]quinoline ((*R*)-14). e.e. > 99.9% (from the ^1H NMR analysis of the corresponding Mosher's ester), $[\alpha]_D$ – 85.3 (c 0.3, $CHCl_3$).

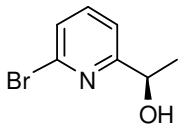

(*R*)-(+)-1-(6-bromopyridin-2-yl)ethanol ((*R*)-22). e.e. = 98.6% (by chiral HRGC), $[\alpha]_D$ + 12 (*c* 0.5, $CHCl_3$).

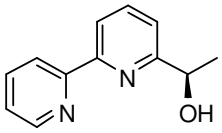

(*R*)-(–)-1-(2,2'-bipyridin-6-yl)ethanol ((*R*)-37). e.e.>99.9% (by chiral HRGC), $[\alpha]_D$ – 21.3 (c 0.6, $CHCl_3$).

Mosher's ester synthesis: general procedure

To a solution of 0.01 mmol of alcohol Et_3N (4μL, Mw 101.19, δ 0.726 g/mL, 0.03 mmol) and DMAP (a small crystal, ca. 1 mg) were added at room temperature, then a solution of (*R*)-(–)-Mosher's chloride (0.012 mmol) in DCM was added dropwise and the total mixture refluxed, the reaction was followed with TLC. The crude mixture was the evaporated and the residue recovered with a 5% solution of citric acid and extracted with DCM. The organic phases were dried on Na_2SO_4 and evapored. The ^1H-NMR analysis to get e.e.% value of alcohols were done on the crude diasteromeric Mosher's esters.

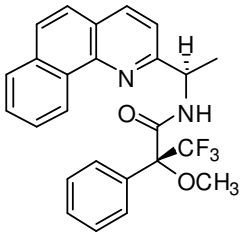

(*R,R*)

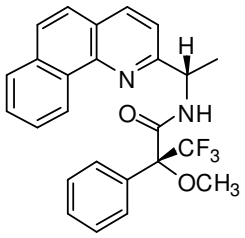

(*R,S*)

N-(1-(benzo[*h*]quinolin-2-yl)ethyl)-3,3,3-trifluoro-2-methoxy-2-phenylpropanamide.^{1}H NMR (400 MHz, $CDCl_3$) δ 1.83 (d, 3H, CH_3CH *RR* diast.), 1.89 (d, 3H, CH_3CH *RS* diast.), 8.11 (d, 1H, aromatic proton *RS* diast.), 8.18 (d, 1H, aromatic proton *RR* diast.),9.27 (d, 1H, H^{10} *RS* diast.), 9.35 (d, 1H, H^{10} *RR* diast.).

Transformation of the alcohols into amines with inversion of configuration (S_N2): general procedure

Diphenylphoshoroazidate (2.2 mL, Mw 275.20, δ = 1.717 g/mL, 10 mmol) was added dropwise, at 0 °C, under argon atmosphere, to a solution of alcohol (7.0 mmol) and DBU (1.5 mL, Mw 152.24, δ = 1.019 g/mL, 10 mmol) in dry toluene and the reaction mixture was stirred for 2 h at 0 °C, then at 50 °C overnight (room temperature overnight to obtain **(*S*)-(–)-24** and **(*R*)-(+)-24**). The resulting two-phase mixture was extracted with brine, and 5% HCl. The organic phase was dried over Na_2SO_4 and the solvent was evaporated *in vacuo.* The crude reaction mixture was purified by flash chromatography (eluent: petroleum ether/ethyl acetate 8:2) giving the pure azide (75%).

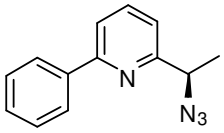

(*R*)-(+)-2-(1-Azidoethyl)-6-phenylpyridine ((*R*)-17) e.e. > 99.9% (by chiral HRGC), $[\alpha]_D$ +9.4 (c 0.85, $CHCl_3$), [lit.: + 7.4 (c 2.4 $CHCl_3$). **IR (neat)** 3063, 2099, 1590, 1574, 1516 cm^{-1}. **^{1}H NMR (400 MHz, $CDCl_3$)** δ 1.67 (d, J = 6.9 Hz, 3H, CH_3CH); 4.66 (q, J = 6.9 Hz, 1H, CH_3C*H*), 7.26 (dd, J = 0.7, 5.8 Hz, 1H), 7.42 (m, 1H), 7.47 (m, 2H), 7.68 (dd, J = 1.1, 8.0 Hz, 1H), 7.77 (dd, J = 7.7, 8.0 Hz, 1H), 8.05 (dm, 2H). **^{13}C NMR (100.1 MHz, $CDCl_3$)** δ 20.0, 61.4, 118.8, 119.4, 127.0, 128.7, 129.1, 137.7, 139.0, 156.9, 160.0. **ESI-MS** 225.1 ($M+H^+$), 247.0 ($M+Na^+$).

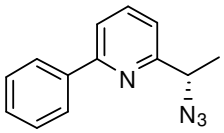

(*S*)-(–)-2-(1-Azidoethyl)-6-phenylpyridine ((*S*)-17). e.e. = 97% (by chiral HRGC), 75% yield (from **(*R*)-13** having > 99.9% e.e.), [α]D –9.2 (c 0.7, CHCl3).

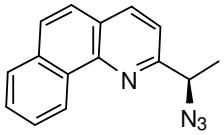

(*R*)-(+)-2-(1-Azidoethyl)benzo[*h*]quinoline ((*R*)-18). e.e. = 80% , [α]D = + 11.6 (c 0.8, CHCl3) 75% yield from **(*S*)-14**. **IR (neat)** 3051, 2105, 1623, 1594, 1566, 1504 cm^{-1}. **^{1}H NMR (400 MHz, $CDCl_3$)** δ 1.78 (d, J = 7.0 Hz, 3H, CH_3CH), 4.83 (q, J = 6.6 Hz, 1H, CH_3CH), 7.53 (d, J = 8.0 Hz), 7.67 (d, J = 8.8 Hz, 1H), 7.71 (m, 3H), 7.80 (d, J = 8.8 Hz, 1H), 7.89 (dd, J = 1.5, 9.0 Hz, 1H), 8.18 (d, J = 8.0 Hz, 1H), 9.33 (dd, J = 1.1, 8.0 Hz, 1H). **^{13}C NMR (100.1 MHz, $CDCl_3$)** δ 20.1, 61.7, 118.9, 124.7, 124.9, 125.5, 127.0, 127.7, 127.8, 128.2, 131.4, 133.8, 135.8, 144.3, 162.0. **ESI-MS** 271.1 ($M+Na^+$).

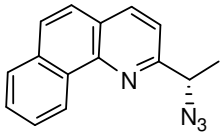

(*S*)-(–)-2-(1-Azidoethyl)benzo[*h*]quinoline ((*S*)-18). e.e.= 95%, [α]D –15.3 (c 0.8, CHCl3), 75% yield from **(*R*)-14**.

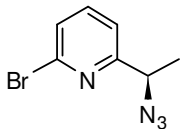

(*R*)-(+)-2-(1-azidoethyl)-6-bromopyridine ((*R*)-24). e.e. = 95%, [α]D + 15 (c 0.25, $CHCl_3$), 70% yield from **((*S*)-22)** (e.e. = 96%).**IR (neat)** 3357, 2981, 2932, 2106, 1581, 1557, 1432, 1406 cm^{-1}**. ^{1}H NMR (400 MHz, $CDCl_3$)** δ 1.59 (d, J = 6.8 Hz, 3H, CH_3CH), 4.66 (q, J = 6.8 Hz, 1H, CH_3CH), 7.33 (d, J = 7.6 Hz, 1H), 7.41 (d, J = 8.0 Hz, 1H), 7.57 (dd, J = 7.6, 8.0 Hz, 1H). **^{13}C NMR (100.1 MHz, $CDCl_3$)** δ 20.3, 61.1, 119.3, 127.3, 139.4, 141.7, 161.7. **ESI-MS** 250 ($M+Na^+$).

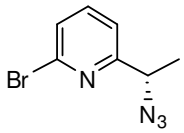

(*S*)-(–)-2-(1-azidoethyl)-6-bromopyridine ((*S*)-24). e.e. = 97%, $[\alpha]_D$ **–** 15.5 (c0.25, $CHCl_3$), 70% yield from **((*R*)-22)** (e.e. = 98%).

Azide reduction: general procedure

H_2O (0.16 g, 9 mmol) and PPh_3 (1.4 g, Mw 262.28, 5.4 mmol) were added to a solution of the azide (4.5 mmol) in THF (10 mL). The mixture was refluxed until the starting material had disappeared (TLC) and then concentrated *in vacuo*. The residue was partitioned between water and dichloromethane and the organic phase was dried over anhydrous Na_2SO_4. The solvent was evaporated under reduced pressure to give the crude amine which was purified by flash chromatography (eluent: $CHCl_3$, then EtOAc/CH_3OH 8:2).

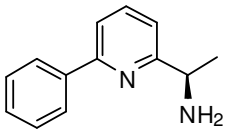

(*R*)-(+)-2-(1-Aminoethyl)-6-phenylpyridine ((*R*)-4) e.e. > 99.9%, 97% yield, $[\alpha]_D$ = +10.5 (c 0.4, EtOH) [lit.: + 2.0, c 2.0, EtOH). **IR (neat)** 3363, 3049, 2967, 2925, 1595, 1564, 846, 736 cm^{-1}. **^{1}H NMR (400 MHz, $CDCl_3$)** δ 1.48 (d, J = 7.0 Hz, 3H, CH_3CH), 1.87 (bs, 2H, NH_2), 4.19 (q, J = 7.7 Hz, 1H, CH_3CH), 7.21 (d, J = 7.7 Hz, 1H) 7.41 (m, 1H) 7.47 (m, 2H), 7.59 (dd, J = 0.8, 8.0 Hz, 1H), 7.70 (dd, J = 7.6, 8.0 Hz, 1H), 8.04 (dm, 2H); **^{13}C NMR (100.1 MHz, $CDCl_3$)** δ 24.5, 52.5, 118.4, 126.9, 128.6, 128.8, 137.2, 137.5, 156.4, 165.3; **ESI-MS** 199.1 ($M+H^+$).

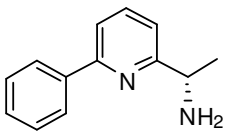

(*S*)-(–)-2-(1-Aminoethyl)-6-phenylpyridine ((*S*)-4). e.e. = 97%, 95% yield, $[\alpha]_D$ – 8.6 (c 0.35, EtOH).

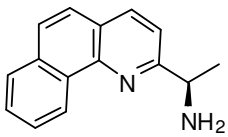

(*R*)-(–)-2-(1-Aminoethyl)benzo[*h*]quinoline ((*R*)-5). e.e. = 80% (by ^{1}H NMR analysis of the corresponding mandelic acid amide), 95% yield from **(*R*)-14**; $[\alpha]_D$ – 17.8 (c 0.45, $CHCl_3$). **IR (neat)** 3363, 3359, 3049, 1623, 1595, 1564, 1502 cm^{-1}. **^{1}H**

NMR (400 MHz, $CDCl_3$) δ 1.57 (d, J = 6.6, 3H, CH_3CH), 2.10 (bs, 2H, NH_2), 4.40 (q, J = 6.6 Hz, 1H, CH_3CH), 7.51 (d, J = 8.2 Hz, 1H), 7.65 – 7.78 (m and d, 3H), 7.90 (dd, J = 1.9, 8.0 Hz, 1H), 8.12 (d, J = 8.2 Hz, 1H), 9.36 (dd, J = 1.9, 7.4 Hz, 1H). **^{13}C NMR (100.1 MHz, $CDCl_3$)** δ 24.7, 52.9, 118.7, 124.4, 124.9, 125.1, 126.7, 127.0, 127.7, 128.0, 131.4, 133.7, 136.3, 145.6, 164.4. **ESI-MS** 223.1 ($M+H^+$).

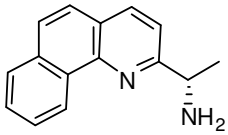

(*S*)-(+)-2-(1-Aminoethyl)benzo[*h*]quinoline ((*S*)-5). e.e. **=** 95% (by ^{1}H NMR analysis of the corresponding mandelic acid amide), 94% yield from **(*S*)-14**, $[\alpha]_D$ + 21.0 (c 0.45, $CHCl_3$).

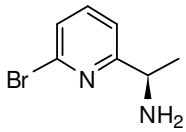

(*R*)-(+)-1-(6-bromopyridin-2-yl)ethanamine ((*R*)-21). e.e. = 95%, 90% yield, $[\alpha]_D$ + 15 (c 0.25, CH_3OH). **^{1}H NMR (400 MHz, $CDCl_3$)** δ 1.42 (d, J = 6.8 Hz, 3H CHCH_3), 1.79 (bs, 2H, NH_2), 4.13 (q, J = 6.8 Hz, 1H, CHCH$_3$), 7.28 (d, J = 7.2 Hz, 1H), 7.34 (d, J = 8.0 Hz, 1H), 7.50 (t, J = 7.6 Hz, 1H). **^{13}C NMR (100.1 MHz, $CDCl_3$)** δ 24.2, 52.2, 118.8, 126.2, 139.0, 141.7, 179.6; **ESI-MS** 184, 186 (M–NH_2), 201, 203 ($M+H^+$), 223, 225 ($M+Na^+$).

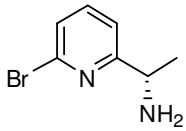

(*S*)-(–)-1-(6-bromopyridin-2-yl)ethanamine ((*S*)-21). e.e. = 97%, 96 % yield, $[\alpha]_D$ **–** 15.5 (c 0.25, CH_3OH).

Mandelic's amide synthesis: general procedure

A solution of (*R*)-(–)-mandelic acid (31 mg, Mw 152.15, 0.202 mmol) in dry DMF was stirred at room temperature and HOBt (27 mg, Mw 135.13, 0.202 mmol), Et_3N (37 µL, Mw 101.19, δ 0.726 g/mL, 0.270 mmol) and the amine (0.135 mmol) were added, the solution's pH has to be close to 8. The mixture was cooled to 0°C and EDC (38 mg, Mw 191.70, 0.20 mmol) was added portion wise. The reaction was run at 0°C for 1h then refluxed until the disappearance of the reactants (TLC). The solvent was evapored and the crude recovered with brine and extracted with EtOAc, the combined organic extracts were washed with a solution of 5% citric acid and then with a solution of

satured $NaHCO_3$, the organic phase was dried on Na_2SO_4 and evapored. The ^1H NMR analysis to get e.e.% value of the amines were done on the crude diasteromeric mixture of mandelic's amides.

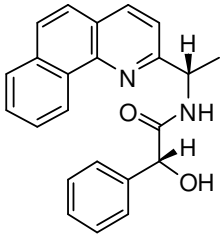

(*R,R*)

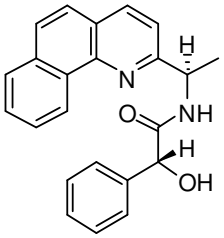

(*R,S*)

N-(1-(benzo[*h*]quinolin-2-yl)ethyl)-2-hydroxy-2-phenylacetamide. ^{1}H NMR (400 MHz, $CDCl_3$) δ 1.55 (d, 3H, C*H*$_3$CH *RS* diast.), 1,62 (d, 3H, C*H*$_3$CH *RR* diast.), 8.9 (m, 1H, H^{10} *RR* diast.), 9.00 (m, 1H, H^{10} *RS* diast.).

Synthesis of CNN pincer ligands 4a-h: general procedure

CNN pincer ligands characterized by different Ar groups were synthesized by means of a Suzuki–Miyaura cross-coupling reaction. Palladium (II) acetate (2.2 mg, Mw 224, 0.01 mmol,), triphenylphosphine (8 mg, Mw 262.28, 0.03 mmol), 2.0 M aqueous K_2CO_3 (5 mL, 9.78 mmol,) and distilled water (4 ml) were added to a degassed solution of **(*S*)** or ***(R)*-21** (0.520 g, Mw 201.06, 2.58 mmol) and phenylboronic acid (3.26 mmol) in 1-propanol (16.5 mL), and the mixture was refluxed overnight.

After cooling at room temperature and solvent evaporation, satured $NaHCO_3$ solution (10.0 mL) was added and the mixture was extracted with ethyl acetate, (4 x 15 mL). The organic layer was dried over anhydrous Na_2SO_4 and the solvent was evaporated to give the crude amine which was purified on a SiO_2 column (150 mL PE/EtOAc 8:2, 150 mL PE/EtOAc 1:1 then EtOAc/MeOH/NH_3 90:10:0.1).

With this procedure were synthesized:

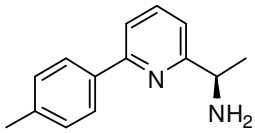

(*R*)-(+)-1-(6-*p*-tolylpyridin-2-yl)ethanamine ((*R*)-4d). e.e. = 80%, 78 % yield, $[\alpha]_D$ **+** 2 (c 0.75, CH_3OH). **IR (neat)** 3355, 2966, 2922, 1589, 1586, 1446, 800 cm^{-1}. **^{1}H NMR (400 MHz, $CDCl_3$)** δ 1.48 (d, *J* = 6.8 Hz, 3H, CHC*H*$_3$), 2.21 (bs, 2H, N*H*$_2$), 2.40 (s, 3H, *p*-Tol C*H*$_3$), 4.19 (q, *J* = 6.8 Hz, 1H, C*H*CH$_3$), 7.17 (d, *J* = 7.6 Hz, 1H), 7.27 (d, *J* = 8.4 Hz, 2H), 7.56 (d, *J* = 8.8 Hz, 1H), 7.68 (dd, *J* = 7.6, 8.0 Hz, 1H), 7.93 (d, *J* = 8.4

Hz, 2H). **^{13}C NMR (100.1 MHz, $CDCl_3$)** δ 21.2, 24.4, 52.4, 118.1, 126.8, 129.4, 136.7, 137.2, 138.8, 156.5, 165.0. **ESI-MS** 213 ($M+H^+$), 196 ($M–NH_2$).

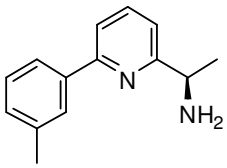

(*R*)-(–)-1-(6-*m*-tolylpyridin-2-yl)ethanamine ((*R*)-4c). e.e. = 80%, 80 % yield, $[\alpha]_D$ – 6.4 (c 0.9, CH_3OH). **IR (neat)** 3359, 3051, 2966, 2923, 1572, 1447, 782 cm^{-1}. **^{1}H NMR (400 MHz, $CDCl_3$)** δ 1.49 (d, *J* = 6.8 Hz, 3H, CHC*H*$_3$), 2.11 (bs, 2H, N*H*$_2$), 2.44 (s, 3H, *m*-Tol C*H*$_3$), 4.21 (q, *J* = 6.8 Hz, 1H), 7.20 (d, *J* = 7.6 Hz, 1H), 7.23 (m, 1H), 7.35 (dd, *J* = 7.6, 8.0 Hz, 1H), 7.57 (d, *J* = 7.6 Hz, 1H), 7.69 (dt, *J* = 0.4, 0,8, 7.6, 1H), 7.81 (dm, *J* = 8 Hz, 1H), 7.85 (m, 1H). **^{13}C NMR (100.1 MHz, $CDCl_3$)** δ 21.7, 24.6, 52.6, 118.4, 118.7, 124.1, 127.7, 128.6, 129.7, 137.3, 138.3, 139.6, 156.8, 165.2. **ESI-MS** 213 ($M+H^+$), 235 ($M+Na^+$), 196 ($M–NH_2$).

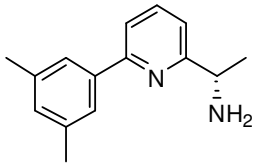

(*S*)-(–)-1-(3,5-dimethylphenyl)pyridine-2-yl)ethanamine ((*S*)-4g). e.e. = 95%, 70 % yield, $[\alpha]_D$ – 1.1 (c 0.45, $CHCl_3$). **^{1}H NMR (400 MHz, $CDCl_3$)** δ 1.50 (d, *J* = 6.4 Hz, 3H, CHC*H*$_3$), 2.40 (s, 6H, 3,5-C*H*$_3$-Ar), 2.56 (bs, 2H, N*H*$_2$), 4.23 (q, *J* = 6.4 Hz, 1H, C*H*CH$_3$), 7.05 (s, 1H), 7.19 (d, *J* = 7.6 Hz, 1H), 7.56 (d, *J* = 7.6 Hz, 1H), 7.62 (s, 2H), 7.68 (dd, *J* = 7.6, 8 Hz, 1H). **^{13}C NMR (100.1 MHz, $CDCl_3$)** δ 21.4, 24.2, 52.4, 118.3, 118.8, 124.8, 130.6, 137.2, 138.2, 139.4, 156.9, 164.6. **ESI-MS** 227 ($M+H^+$), 210 ($M–NH_2$).

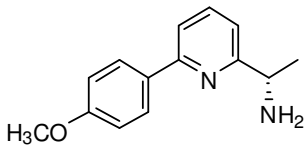

(*S*)-(–)-1-(6-(4-methoxyphenyl)pyridin-2-yl)ethanamine ((*S*)-4e). e.e. = 95%, 70 % yield, $[\alpha]_D$ – 3.3 (c 0.35, $CHCl_3$). **^{1}H NMR (400 MHz, $CDCl_3$)** δ 1.48 (d, *J* = 6.8 Hz, 3H, CHC*H*$_3$), 2.47 (bs, 2H, N*H*$_2$), 3.86 (s, 3H, OC*H*$_3$), 4.19 (q, *J* = 6.8 Hz, 1H, C*H*CH$_3$), 6.99 (dm, *J* = 8.8 Hz, 2H), 7.14 (d, *J* = 7.6 Hz, 1H), 7.52 (d, *J* = 7.6 Hz, 1H), 7.66 (dd, *J* = 7.6, 8 Hz, 1H), 7.99 (dm, *J* = 8.8 Hz, 2H). **^{13}C NMR (100.1 MHz, $CDCl_3$)** δ 24.3, 52.4, 55.3, 114.0, 117.7, 117.8, 128.1, 132.1, 137.2, 156.1, 160.4, 164.7. **ESI-MS** 229 ($M+H^+$), 212 ($M–NH_2$).

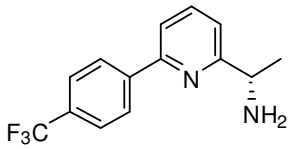

(*S*)-(+)-1-(6-(4-(trifluoromethyl)phenyl)pyridin-2-yl)ethanamine ((*S*)-4f). e.e. = 95%, 75 % yield, $[\alpha]_D$ + 3.6 (c 0.6, $CHCl_3$). **^{1}H NMR (400 MHz, $CDCl_3$)** δ 1.50 (d, *J* = 6.4 Hz, 3H, CHC*H*$_3$), 1.99 (bs, 2H, N*H*$_2$), 4.24 (q, *J* = 6.4 Hz, 1H, C*H*CH_3), 7.29 (d, *J* = 7.6 Hz, 1H), 7.63 (d, *J* = 7.2, 1H), 7.72 (d, *J* = 8 Hz, 2H), 7.75 (dd, *J* = 7.6, 8 Hz, 1H), 8.16 (dm, *J* = 8.4 Hz, 2H). **^{13}C NMR (100.1 MHz, $CDCl_3$)** δ 24.5, 52.5, 119.0, 119.6, 125.6, 125.7, 127.3, 130.9 (q, CF_3) 137.6, 142.7, 155.0, 165.3. **ESI-MS** 267 ($M+H^+$), 250 ($M-NH_2$).

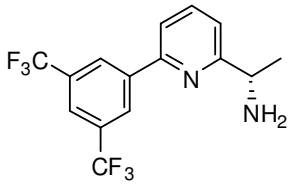

(*S*)-(–)-1-(6-(3,5-bis(trifluoromethyl)phenyl)pyridin-2-yl)ethanamine ((*S*)-4h). e.e. = 95%, 90 % yield, $[\alpha]_D$ – 1.2 (c 0.9, $CHCl_3$). **^{1}H NMR (400 MHz, $CDCl_3$)** δ 1.51 (d, *J* = 6.8 Hz, 3H, CHC*H*$_3$), 1.91 (bs, 2H, N*H*$_2$), 4.27 (q, *J* = 6.8 Hz, 1H, C*H*CH_3), 7.36 (d, *J* = 8 Hz, 1H), 7.68 (dd, *J* = 0.8, 7.6 Hz, 1H), 7.80 (dd, *J* = 7.6, 8 Hz, 1H), 7.91 (s, 1H), 8.49 (s, 2H). **^{13}C NMR (100.1 MHz, $CDCl_3$)** δ 24.6, 52.5, 118.8, 120.3, 122.3, 122.4, 124.8, 127.0, 132.0 (q, CF_3), 138.0, 141.4, 153.3, 165.9. **ESI-MS** 335 ($M+H^+$), 318 ($M-NH_2$).

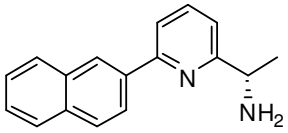

(*S*)-(+)-1-(6-(naphthalen-2-yl)pyridin-2-yl)ethanamine ((*S*)-4a). e.e. = 98%, 95 % yield, $[\alpha]_D$ + 1.4 (c 0.6, $CHCl_3$). **IR (neat)** 3355, 3056, 2967, 2925, 1573, 1475, 1445, 807, 742 cm^{-1}. **^{1}H NMR (400 MHz, $CDCl_3$)** δ 1.53 (d, *J* = 6.4 Hz, 3H, CHC*H*$_3$), 1.94 (bs, 2H, N*H*$_2$), 4.25 (q, *J* = 6.4, 1H, C*H*CH_3), 7.25 (d, *J* = 4.4 Hz, 1H), 7.51 (m, *J* = 0.8, 4.0, 4.4 Hz, 2H), 7.75 (m, *J* = 4.4 Hz, 2H), 7.87 (m, 1H), 7.95 (m, *J* = 6.8, 8.8 Hz, 2H), 8.21 (dd, *J* = 1.6, 8.4 Hz, 1H), 8.50 (s, 1H). **^{13}C NMR (100.1 MHz, $CDCl_3$)** δ 24.6, 52.6, 118.5, 118.7, 124.7, 126.2, 126.4, 127.6, 128.3, 128.7, 133.5, 133.6, 136.8, 137.3, 156.3, 165.4. **ESI-MS** 249 ($M+H^+$), 271 ($M+Na^+$) 232 ($M-NH_2$).

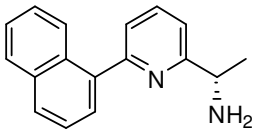

(*S*)-(+)-1-(6-(naphthalen-1-yl)pyridin-2-yl)ethanamine ((*S*)-4b). e.e. = 98%, 73 % yield, $[\alpha]_D$ **+** 1.5 (c 0.65, $CHCl_3$). **^{1}H NMR (400 MHz, $CDCl_3$)** δ 1.52 (d, J = 6.8 Hz, 3H, CHCH_3), 2.37 (bs, 2H, NH_2), 4.28 (q, J = 6.8 Hz, 1H, CHCH$_3$), 7.33 (d, J = 8 Hz, 1H), 7.42-7,61 (m, 4H), 7.78 (dt, J = 0.8, 8 Hz, 1H), 7.90 (d, J = 8 Hz, 2H). **^{13}C NMR (100.1 MHz, $CDCl_3$)** δ 24.4, 52.5, 128.3, 123.2, 125.3, 125.7, 125.8, 126.3, 127.5, 128.3, 128.8, 131.2, 134.0, 137.0, 158.5, 165.0. **ESI-MS** 249 (M+H$^+$), 232 (M–NH$_2$).

Alcohol methylation: general procedure

NaH (0.127 g, Mw 24, 5 mmol, 60% purity) was put in a three necks flask under Ar atmosphere and washed 2 times with freshly distilled THF. At 0°C the alcohol (2.5 mmol) dissolved in THF and CH_3I (0.203 mL, Mw 141.94, δ 2.23 g/mL, 5 mmol) were added and the mixture stirred at 0°C for 5 hours (TLC CH_2Cl_2/CH_3OH 9:1). The reaction was quenched with sat. NH_4Cl and the product extracted three times with CH_2Cl_2. The organic phases collected were dried on Na_2SO_4 and evapored getting pure methyl ether in 80-90% yield.

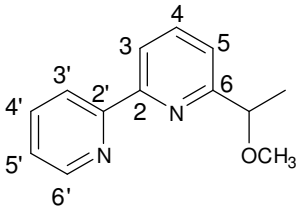

(±)-6-(1-methoxyethyl)-2,2'-bipyridine (*rac*-29). **^{1}H NMR (400 MHz, $CDCl_3$)** δ 1.53 (d, J = 6.8 Hz, 3H, CHCH_3), 3.36 (s, 3H, OCH_3), 4.53 (q, J = 6.8 Hz, 1H, CHCH$_3$), 7.29 (m, 1H, H$^{5'}$), 7.44 (d, J = 7.6 Hz, 1H, H^5), 7.8 (td, J = 2, 7.6 Hz, 1H, H$^{4'}$), 7.83 (t, J = 8 Hz, 1H, H^4), 8.28 (dd, J = 0.8, 7.6 Hz, 1H, H$^{3'}$), 8.44 (d, J = 8 Hz, 1H, H^3), 8.63 (dm, J = 4.8 Hz, 1H, H$^{6'}$). **^{13}C NMR (100.1 MHz, $CDCl_3$)** δ 22.2 (CHCH$_3$), 56.9 (OCH$_3$), 80.9 (CHCH$_3$), 119.6 (C^3), 119.8(C^5), 121.3 (C$^{3'}$), 123.7 (C$^{5'}$), 136.9 (C$^{4'}$), 137.7 (C^4), 149.2 (C$^{6'}$), 155.4 (C$^{2'}$), 156.3 (C^2), 162.7 (C^6). **ESI-MS** 215 (M+H$^+$), 237 (M+Na$^+$).

(*R*)-(+)-(6-(1-methoxyethyl)-2,2'-bipyridine ((*R*)-29): e.e. > 99.9% (by HRGC). $[\alpha]_D$ + 106.5 (*c* 0.6, $CHCl_3$).

(*S*)-(–)-(6-(1-methoxyethyl)-2,2'-bipyridine ((*S*)-29): e.e. = 99% (by HRGC). $[\alpha]_D$ – 83.5 (*c* 0.4, $CHCl_3$).

An alternative synthesis of both racemic and optically pure 6-(1-methoxyethyl)-2,2'-bipyridine (29) has been developed starting from either racemic or optically pure 1-(6-bromopyridin-2-yl)ethanol (22):

The alcohols were methylated using NaH and CH_3I in dry THF (see the general procedure for alcohol methylation), **(*rac*)-2-bromo-6-(methoxyethil)pyridine (Br-39)** and **(*S*)-2-bromo-6-(methoxyethil)pyridine ((*S*)-39)** were obtained in 98% yield and used in the next step without further purification. **^{1}H NMR (400 MHz, $CDCl_3$)** δ 1.43 (d, J = 6.6 Hz, CHCH_3, 3H), 3.31 (s, OCH_3, 3H), 4.39 (q, J = 6.6 Hz, CHCH$_3$, 1H), 7.37 (t, J = 7.7 Hz, 2H), 7.56 (t, J = 7.7 Hz, 1H).**^{13}C NMR (100.1 MHz, $CDCl_3$)** δ 22.32, 57.06, 80.20, 118.43, 126.58, 139.18, 141.27, 165.18. **ESI-MS** 215, 217 (M+H$^+$), 237, 239 (M+Na$^+$), 183, 185 (M–OCH$_3$).

A solution of the methoxy derivative (0.5 g, Mw 216.8, 2.3 mmol) in freshly distilled THF (19 mL) was cooled with a acetone/liquid nitrogen bath (-90°C) under argon atmosphere and treated with 1.76 mL of n-butyllithium (1.6 M in n-hexane, 2.7 mmol), the reaction temperature was maintained bellow -70°C and the mixture stirred for 45'. **35** dissolved in dry THF was then added dropwise. The intensely red solution was stirred overnight at room temperature. After removal of the solvent under reduce pressure the crude was purified by column chromatography (CH_2Cl_2/EtOAc as eluent). This protocol gave **29** in 60% yield.

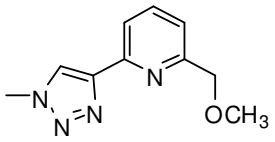

2-(Methoxymethyl)-6-(1-methyl-1H-1,2,3-triazol-4-yl)pyridine 30. white solid, mp 78-9 °C. **IR (Nujol)** 3147, 1604, 1578, 1116 cm^{-1}. **^{1}H NMR (400 MHz, $CDCl_3$)** δ 3.42 (s, 3H, CH_3O), 4.11 (s, 3H, CH_3N), 4.58 (s, 2H, CH_2OCH$_3$), 7.32 (d, J = 7.7, 1H, H^3), 7.72 (t, J = 7.7, 1H, H^4), 7.98 (d, J = 7.7, 1H, H^5), 8.10 (s, 1H, triazolo). **^{13}C NMR (fom CH COSY, 100.1 MHz, $CDCl_3$)** δ 36.7 (*C*H$_3$N), 58.7 (*C*H$_3$O), 75.5 (*C*H$_2$OMe), 118.7 (C^5 py), 120.3 (d, C^3 py), 123.1 (d, C^5 triazole), 137.3 (d, C^4 py), 148.6, 149.6, 158.1. **ESI-MS** 227.0 (M+Na$^+$).

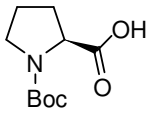

N-(*tert*-butoxycarbony1)-(*S*)-proline (48). Triethylamine (16.5 mL, Mw 101.19, δ 0.726 g/mL, 0.12 mmol) was added to an ice-cold suspension of (*S*)-proline (10.0 g, Mw 115.13, 0.09 mol) in dichloromethane (200 mL). Next, di-*tert*-butyl dicarbonate

(27.2 g, Mw 218.25, 0.13 mol) in dichloromethane (10 mL) was added over 10 min, and the mixture was stirred at 0°C for 2.5 h. The reaction was discontinued by addition of saturated aqueous citric acid (50 mL), and the organic phase was washed with brine (2 x 50 mL) and water (50 mL). Removal in *vacuum* of solvent yielded a crude product which was dissolved in hot acetyl acetate. Following addition of hexane (500 mL) Boc-(*S*)-Pro **(48)** crystallized from the cooled solution to yield 17.8 g, 95%. mp 135-137°C. **IR (nujol)** 3430, 1671 cm^{-1}. **^{1}H NMR (400 MHz, $CDCl_3$)** δ 1.47 (bs, 9 H, *t*-Bu) 2.0-1.8 (m, 4 H), 3.5-3.3 (m, 2 H), 4.4-4.1 (m, 1 H, C*H*CO), 7.5 (bs, 1 H).

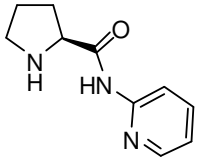

(*S*)-(–)-N-(pyridine-2-yl)pyrrolidine-2-carboxamide ((*S*)-46). Compounds **48** (1.000 g, Mw 215.12, 4.65 mmol) was dissolved in dichloromethane (20 mL). The solution was cooled to 0 °C, and EDC (0.908 g, Mw 191.71, 4.74 mmol) was added. The solution was stirred at 0 °C for 1/2 h and then 2-aminopyridine (0.439 g, Mw 94.12, 4.65 mmol) was added in one portion. The mixture was left at room temperature and followed with TLC (EtOAc/CH_3OH/NH_3 8:2:0.1). After removal of the solvent under reduced pressure, the residue was purified by column chromatography on silica gel (petroleum ether/ethyl acetate 3:7, petroleum ether/ethyl acetate 4:6, then petroleum ether/ethyl acetate/ammonia 4:6:0.2) to give Boc-protected-**(*S*)-46** as white solid. $[\alpha]_D$ – 71 (*c* 0.25, CH_3OH). **^{1}H NMR (400 MHz, $CDCl_3$)** δ 1.26-1.42 (bs, 9H, *t*-Bu), 1.69 (bs, 1H), 1.91 (m, 2H), 2.24 (bs, 1H), 3.53 (bs, 2H), 4.32 (bs, 1H, C*H*CO), 7.01 (bs, 1H), 7.68 (bs, 1H), 8.21 (d, J = 8 Hz, 1H), 8.28 (dm, 1H), 9.22 (bs, 1H, N*H*). **^{13}C NMR (100.1 MHz, $CDCl_3$)** δ 21.4, 24.8, 28.3, 47.2, 62.3, 80.96, 113.8, 119.78, 138.22, 148.0, 151.8, 155.2, 172.0. **ESI-MS** 292 ($M+H^+$), 314 ($M+Na^+$).

Boc-protected-**(*S*)-46** (1.508 g, Mw 291.35, 5.17 mmol) was dissolved in 15 mL of trifluoroacetic acid solution (40% in CH_2Cl_2) at 0°C and the solution was stirred for 2 h at room temperature. Then trifluoroacetic acid was neutralized by addition of Et_3N (15 mL, Mw 101.19, δ 0.726 g/mL, 0.10 mmol) at 0°C. The solution was washed with H_2O, dried over anhydrous Na_2SO_4, and concentrated under reduce pressure obtaining **(*S*)-46** as a yellow oil in 90% yield. $[\alpha]_D$ – 56.4 (*c* 0.5, CH_3OH). **IR (neat)** 3276, 2969, 2870, 1692, 1589, 1574, 1510, 1434, 1299, 1148, 1095, 779. **^{1}H NMR (400 MHz, $CDCl_3$)** δ 1.69 (m, 2H), 1.97 (m, 1H), 2.16 (m, 1H), 2.54 (bs, 1H, N*H*-amine), 3.00 (m,

2H), 3.84 (dd, *J* = 4, 5.2 Hz, 1H, C*H*CO), 6.97 (ddd, *J* = 0.8, 2.4, 4.8 Hz, 1H), 7.64 (td, *J* =2, 8 Hz, 1H), 8.20 (d, *J* = 8.4 Hz, 1H), 8.24 (dm, *J* = 4.8 Hz, 1H), 10.17 (bs, 1H, N*H*-amide). **^{13}C NMR (100.1 MHz, $CDCl_3$)** δ 26.3, 30.9, 47.4, 61.0, 113.6, 119.7, 138.3, 148.0, 151.2, 174.4. **ESI-MS** 192 ($M+H^+$), 214 ($M+Na^+$).

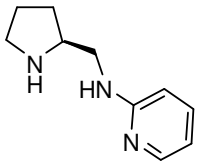

(*S*)-(+)-N-(pyrrolidin-2-ylmethyl)pyridin-2-amine ((*S*)-47). To a cooled (-10°C) and stirred solution of the amide **(*S*)-46** (0.304 g, Mw 191.11, 1.05 mmol) in dry THF (42 mL) was added $LiAlH_4$ (0.470 g, Mw 37.95, 12.4 mmol) portionwise, and the mixture was stirred at r.t. until almost all of the starting material was consumed. The mixture was concentrated and the residue diluted with CH_2C1_2, in a ice-bath the reaction was quenched by the careful addition of NaOH 2 M. Stirring was continued to obtain a clear organic layer and the white residue was filtered off. The two-phases mixture was separated and the aquous layer was extracted with CH_2C1_2. The combined organic phases were dried over anhydrous Na_2SO_4, and evapored. The product **(*S*)-47** was obtained as a yellow oil in 90% yield without further purifications. $[\alpha]_D$ + 28.86 (*c* 0.35, CH_3OH). **IR (neat)** 3287, 2961, 2870, 1606, 1518, 1488, 1291, 771, 736. **^{1}H NMR (400 MHz, $CDCl_3$)** δ 1.47 (m, 1H), 1.75 (m, 2H), 1.89 (m, 1H), 2.52 (bs, 1H, N*H*-prolinic amine), 2.93 (td, *J* = 0.8, 6.4 Hz, 1H), 3.14 (m, 1H), 3.39 (m, 2H), 4.94 (bs, 1H, N*H*-amine), 6.4 (dt, *J* = 0.8, 8.4 Hz, 1H), 6.53 (ddd, *J* = 0.8, 2, 5.2 Hz, 1H), 7.36 (ddd, *J* = 0.4, 1.6, 6.8 Hz, 1H), 8.04 (dm, *J* = 5.6 Hz, 1H). **^{13}C NMR (100.1 MHz, $CDCl_3$)** δ 25.5, 29.0, 46.2, 58.3, 107.9, 112.8, 137.3, 147.7, 158.8. **ESI-MS** 178 ($M+H^+$).

P-N ligands synthesis: general procedure

Amide **(*S*)-46** or amine **(*S*)-47** (1.05 mmol) was put in a Schlenk and azeotropically dried three times with distilled and degassed toluene. 5 mL of toluene were then added and under Ar atmosphere and 0°C bis(diethylamino)-phenylphosphine (244 μL, Mw 252.34, δ 0.971 g/mL, 0.94 mmol) was added dropwise. The reaction mixture was heated to 90°C and stirred overnight. The cooled solution was evapored in *vacuo*. Compound **44** was washed 7 times with distilled and degassed *n*-pentane obtaining a

white solid. Compound **45** was used as crude reaction product (viscous orange oil) without further purifications.

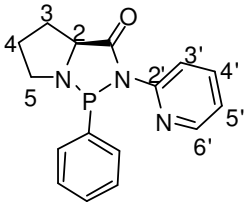

(1*R*,3a*S*)-(–)-1-phenyl-2-(pyridin-2-yl)tetrahydro-1*H*-pyrrolo[1,2-c][1,3,2]diazaphosphol-3(2*H*)-one (44). $[\alpha]_D$ –128.9 (*c* 0.35, CH_3OH). **^{1}H NMR (500 MHz, CD_2Cl_2)** δ 1.72 (m, 1H, CH_2, H^4), 1.87 (m, 1H, CH_2, H^4), 2.18 (m, 1H, CH_2, H^3), 2.24 (m, 1H, CH_2, H^3), 3.39 (m, 1H, CH_2, H^5), 3.46 (m, 1H, CH_2, H^5), 4.16 (dd, *J* = 3, 9 Hz, 1H, C*H*, H^2), 7.04 (dd, *J* = 2, 5.5 Hz, 1H, $H^{4'}$), 7.35 (m, 3H, Ph), 7.57 (m, 2H, Ph), 7.73 (td, *J* = 1.5, 8 Hz, 1H, $H^{5'}$), 8.25 (dm, *J* = 4 Hz, 1H, C*H*, $H^{3'}$), 8.33 (dm, *J* = 8.5 Hz, 1H, C*H*, $H^{6'}$). **^{13}C NMR (100.1 MHz, $CDCl_3$)** δ 26.5 (C^4), 30.9 (C^3), 55.4 (C^5), 68.3 (C^2), 114.4 ($C^{6'}$), 120.1 ($C^{4'}$), 128.6 (C_{Ph}-P), 129.8 (Ph), 130.0 (Ph), 138.3 ($C^{5'}$), 147.7 ($C^{3'}$), 152.4 ($C^{2'}$), 178.1 (*C*O). **^{31}P NMR (500 MHz, CD_2Cl_2)** δ 106.29. **ESI-MS** 298.1 ($M+H^+$), 320.1 ($M+Na^+$).

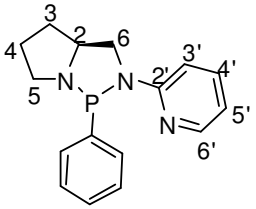

(1*R*,3a*S*)-(–)-1-phenyl-2-(pyridin-2-yl)hexahydro-1*H*-pyrrolo[1,2-c][1,3,2]-diazaphosphole (45). $[\alpha]_D$ –170.6 (*c* 0.485, CH_3OH). **^{1}H NMR (500 MHz, CD_2Cl_2)** δ 1.78 (m, 2H, CH_2, H^4 and 1H, CH_2, H^3), 2.07 (m, 1H, CH_2, H^3), 3.08 (m, 1H, CH_2, H^6), 3.31 (m, 1H, CH_2, H^5), 3.37 (m, 1H, CH_2, H^5), 3.55 (m, 1H, CH_2, H^6), 4.00 (q, *J* = 2, 18.5 Hz, 1H, C*H*, H^2), 6.61 (d, *J* = 8 Hz, 1H, $H^{5'}$), 6.64 (ddd, *J* = 1, 2, 5 Hz, 1H, $H^{3'}$), 7.30 (m, 3H, Ph), 7.47 (m, 2H, Ph and 1H, $H^{4'}$), 8.10 (dm, *J* = 4.5 Hz, 1H, $H^{6'}$). **^{13}C NMR (100.1 MHz, CD_2Cl_2)** δ 26.1 (C^4), 31.3 (C^3), 52.2 (C^6), 52.6 (C^5), 64.8 (C^2), 108.5 ($C^{5'}$), 113.7 ($C^{3'}$), 128.5 (Ph), 129.2 (Ph), 129.9 (C_{Ph}-P), 137.9 ($C^{4'}$), 148.7 ($C^{6'}$). **^{31}P NMR (500 MHz, CD_2Cl_2)** δ 99.71. **ESI-MS** 284.1 ($M+H^+$).

SYNTHESIS OF THE COMPLEXES

Neutral complexes: general procedure to obtain [Pd(N-N')(CH_3)Cl], [Pd(PNCO)(CH_3)Cl]$_2$, and [Pd(PN)(CH_3)Cl].

1.50 mmol of ligand was added to a solution of [Pd(COD)(CH_3)Cl] (332 mg, Mw 265.96, 1.25 mmol) in freshly distilled dicholoromethane and stirred at room temperature.

Pd-(N-N') complexes: after 3 h, diethyl ether was added and the product precipitated as a yellow solid. Average yield: 90%.

Pd-(P-N) complexes: after 1.5 h, the reaction mixture was concentrated and *n*-hexane was added to precipitate the products as a yellow-orange solid. Average yield: 80-90%.

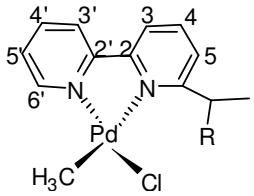

R = -OCH_3 (**29a**)
= -CH_3 (**31a**)
= -CH_2CH_3 (**32a**)

[Pd(29)(CH_3)Cl] (29a). ^{1}H NMR (500 MHz, $CDCl_3$) δ 1.32 (s, 3H, C*H*$_3$-Pd), 1.49 (d, 3H, C*H*$_3$CH), 3.43 (s, 3H, OC*H*$_3$), 6.20 (m, 1H, CH_3C*H*), 7.49 (t, 1H, $H^{5'}$), 7.80 (dd, 1H, H^5), 7.96-8.05 (m, 4H, $H^{3',4'}$ and $H^{3,4}$), 8.63 (d, 1H, $H^{6'}$).

[Pd(31)(CH_3)Cl] (31a). Elementar Anal. Calc. for $C_{14}H_{17}ClN_2Pd$: C 47.34; H 4.79; N 7.89. Found: C 47.38; H 4.45; N 7.30. **^{1}H NMR (500 MHz, $CDCl_3$)** δ 1.32 (s, 3H, C*H*$_3$-Pd), 1.33 (d, 6H, CH(C*H*$_3$)$_2$), 4.74 (m, 1H, C*H*(CH$_3$)$_2$), 7.48 (d, 2H, $H^{5,5'}$), 7.89 (m, 2H, $H^{3,4}$), 8.01 (m, 2H, $H^{3',4'}$), 8.63 (d, 1H, $H^{6'}$).

[Pd(32)(CH_3)Cl] (32a). ^{1}H NMR (500 MHz, CD_2Cl_2) δ 0.88 (t, 3H, CH_2C*H*$_3$), 1.18 (s, 3H, C*H*$_3$-Pd), 1,27 (d, 3H, CHC*H*$_3$), 1.60-1.74 (m, 2H, CHC*H*$_2$CH$_3$), 4,57 (m, 1H, C*H*CH$_3$), 7.48 (m, 2H, $H^{5,5'}$), 7.91 (m, 2H, $H^{3,4}$), 8.01-8.04 (m, 2H, $H^{3',4'}$), 8.61 (d, 1H, $H^{6'}$).

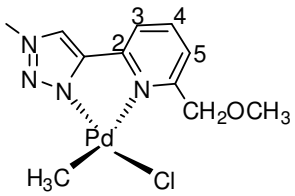

[Pd(30)(CH_3)Cl] (30a). ^{1}H NMR (500 MHz, DMSO-d^6, 60 °C) δ 1.01 (s, 3H, C*H*$_3$-Pd), 3.40 (s, 3H, CH_2OC*H*$_3$), 4.09 (s, 3H, N-C*H*$_3$), 4.58 (s, 2H, C*H*$_2$OCH$_3$), 7.38 (s, 1H, H^3), 7.91 (s, 2H, $H^{4,5}$), 8.52 (s, 1H, $H^{5'}$).

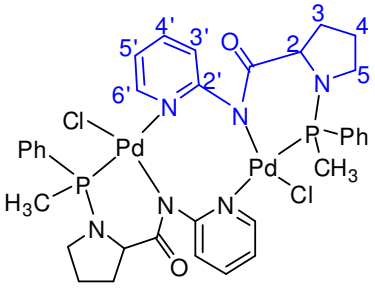

[Pd(PNCO)(CH$_3$)Cl]$_2$ (44a). [α]$_D$ –7.6 (*c* 0.29, CH$_3$OH). **IR (nujol)** 1693 cm^{-1}. **^{1}H NMR (500 MHz, CD$_2$Cl$_2$)** δ 1.94-2.11 (m, 2H, C*H*$_2$, H^4 and 1H, C*H*$_2$, H^3), 2.12 (d, *J* = 13 Hz, 3H, C*H*$_3$-P), 2.45 (d, *J* = 11.5 Hz, 3H, C*H*$_3$-P minority isomer), 2.61 (m, 1H, C*H*$_2$, H^3), 3.29 (m, *J* = 7.5 Hz, 1H, C*H*$_2$, H^5), 3.39 (m, 1H, C*H*$_2$, H^5), 3.81 (m, 1H, C*H*, H^2), 6.91 (t, *J* = 6 Hz, 1H, C$^{5'}$), 7.55 (tm, *J* = 2.5, 7 Hz, 2H, *m*-H-Ph), 7.59 (m, 1H, *p*-H-Ph), 7.68 (td, *J* = 1.5, 8 Hz, 1H, H$^{4'}$), 7.79 (d, *J* = 8,5 Hz, 1H, H$^{3'}$), 7.96 (m, *J* = 2.5 Hz, 1H, H$^{6'}$), 8.06 (dd, *J* = 5.5, 7.5 Hz, 2H, *o*-H-Ph). **^{13}C NMR (100.1 MHz, CD$_2$Cl$_2$)** δ 15.3 (*C*H$_3$-P), 25.4 (C^4), 29.7 (C^3), 49.6 (C^5), 65.0 (C^2), 115.2 (C$^{3'}$), 117.9 (C$^{5'}$), 128.8 (*p*-Ph), 129.6 (*o*-Ph), 132.3 (*m*-Ph), 133.0 (Ph-P), 140.5 (C$^{4'}$), 144.7 (C$^{6'}$), 170.3 (*C*O). **^{31}P NMR (500 MHz, CD$_2$Cl$_2$)** δ 67.05 (minority isomer), 75.57 (major isomer). Isomers ratio 9:1.

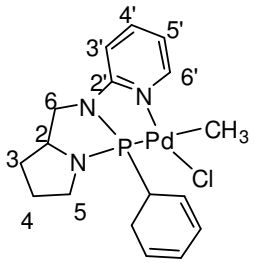

[Pd(PN)(CH$_3$)Cl] (45a). [α]$_D$ – 20.4 (*c* 0.12, CH$_3$OH). **^{1}H NMR (500 MHz, CD$_2$Cl$_2$)** δ 0.69 (d, *J* = 2 Hz, 3H, C*H*$_3$-Pd, *cis* isomer), 1.57 (m, 1H, H^3, *cis* isomer), 1.65 (d, *J* = 8.8 Hz, 3H, C*H*$_3$-Pd, *trans* isomer), 1.94 (m, 2H, H^4, *cis* isomer), 2.18 (m, 1H, H^3, *cis* isomer), 2.64-3.00 (m, aliphatic proton of the *trans* isomer), 3.29 (m, 1H, H^6 *cis* isomer), 3.49 (m, 1H, H^5, *cis* isomer), 3.70 (m, 1H, H^6 and 1H, H^5, *cis* isomer), 3.86 (m, aliphatic protons, *trans* isomer), 4.06 (m, 1H, H^2 *cis* and aliphatic protons of the *trans* isomer), 6.67 (d, *J* = 8.5 Hz, 1H, H$^{3'}$), 6.85 (d, *J* = 8 Hz, 1H, H$^{3'}$, *trans* isomer), 6.95 (m, 1H, H$^{5'}$ of both *cis* and *trans* isomers) 7.07 (t, *J* = 7.5 Hz, Ph, *trans* isomer), 7.46 (m, 3H, Ph, *cis* isomer and Ph protons of the *trans* isomer), 7.73 (m, 2H, Ph and 1H, H$^{4'}$, *cis* isomer and Ph H$^{4'}$, *trans* isomer), 8.98 (m, 1H, H$^{6'}$). **^{13}C NMR (100.1 MHz, CD$_2$Cl$_2$)** 18.5 (*C*H$_3$-Pd, *trans* isomer), 26.2 (C^4, *cis* isomer), 32.8 (C^3, *cis*

isomer), 51.6 (C^6, *cis* isomer), 52,2 (C^5, *cis* isomer), 65.9 (C^2, *cis* isomer), 109.6 ($C^{3'}$, *cis* isomer), 110.4 ($C^{3'}$, *trans* isomer), 116.5 ($C^{5'}$, *cis* isomer), 123.4 ($C^{5'}$, *trans* isomer), 127.0 (Ph, *trans* isomer), 128.6 (Ph, *cis* isomer), 130.2 (Ph, *cis* isomer), 131.5 (Ph, *trans* isomer), 137.7 (Ph, *cis* isomer), 139.9 ($C^{4'}$, *cis* isomer and $C^{4'}$, *trans* isomer), 148.7 ($C^{6'}$, *cis* isomer). **^{31}P NMR (500 MHz, CD_2Cl_2)** δ 119.9 (*cis* isomer), 133.7 (*trans* isomer). Ratio *cis*/*trans* 2:1.

Cationic complexes: general procedure to obtain: [Pd(N-N')(CH_3)($NCCH_3$)][PF_6]

All complexes were obtained starting from the corresponding neutral derivatives upon addition of $AgPF_6$ in a mixture of CH_2Cl_2 and CH_3CN. [Pd(N-N')(CH_3)Cl](**1a-4a**) (0.40 mmol) was dissolved in the minimal amount of CH_2Cl_2 under Ar. To the mixture obtained a solution of $AgPF_6$ (121 mg, Mw 252.83, 0.48 mmol) in CH_3CN (6 mL) was added, leading to the precipitation of AgCl. After 3 h, the solution was filtered over Celite and concentrated to minimal volume under *vacuum*. Upon addition of diethyl ether the product precipitate as a white solid. Average yield: 80%.

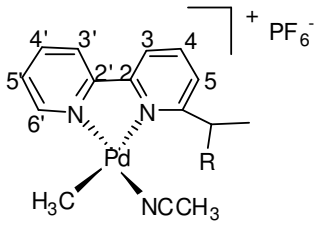

R = -OCH_3 (**29b**)
= -CH_3 (**31b**)
= -CH_2CH_3 (**32b**)

[Pd(29)(CH_3)($NCCH_3$)][PF_6] (29b). ^{1}H NMR (500 MHz, CD_2Cl_2) δ 1.35 (s, 3H, C*H*$_3$-Pd), 1.53 (d, 3H, C*H*$_3$CH), 2.49 (s, 3H, CNC*H*$_3$), 3.32 (s, 3H, OC*H*$_3$), 4.68 (m, 1H, CH_3C*H*), 7.64 (t, 1H, $H^{5'}$), 7.86 (d, 1H, H^5), 8.16-8.24 (m, 4H, $H^{3',4'}$ and $H^{3,4}$), 8.56 (d, 1H, $H^{6'}$).

^{13}C NMR (500 MHz, CD_2Cl_2) δ -4.44 (*C*H_3-Pd), 22.69 (*C*H_3CH), 56.97 (O*C*H_3), 79.39 (CH_3*C*H), 121.77-124.03 ($C^{4,4'}$), 123.94 ($C^{5'}$), 126.51 (C^5), 140.70 ($C^{4,4'}$), 148.62 ($C^{6'}$).

[Pd(31)(CH_3)($NCCH_3$)][PF_6] (31b). Elementar Anal. Calc. for $C_{16}H_{20}F_6N_3Pd$: C 37.99; H 3.96; N 8.31. Found: C 37.52; H 3.26; N 7.55. **^{1}H NMR (500 MHz, $CDCl_3$)** δ 1.30 (s, 3H, C*H*$_3$-Pd), 1.38 (d, 6H, CH(C*H*$_3$)$_2$), 2.46 (s, 3H, NCC*H*$_3$), 3.42 (m, 1H, C*H*(CH_3)$_2$), 7.61 (d, 2H, $H^{5,5'}$), 8.07-8.17 (m, 4H, $H^{3',4'}$ and $H^{3,4}$), 8.53 (d, 1H, $H^{6'}$). **^{13}C NMR (500 MHz, CD_2Cl_2)** δ 6.67 (*C*H_3-Pd), 22.76 (CH(*C*H_3)$_2$), 36.58 (*C*H(CH_3)$_2$), 120.47-123.29 ($C^{3,3'}$), 123.83-126.45 ($C^{5,5'}$), 140.39 ($C^{4,4'}$), 148.75 ($C^{6'}$).

[Pd(32)(CH$_3$)(NCCH$_3$)][PF$_6$] (32b). ^{1}H NMR (500 MHz, CD$_2$Cl$_2$) δ 0.89 (t, 3H, CHCH$_2$C*H$_3$*), 1.32 (s, 3H, C*H$_3$*-Pd), 1.38 (d, 3H, C*H$_3$*CH), 1.77 (m, 2H, CHC*H$_2$*CH$_3$), 2.46 (s, 3H, NCC*H$_3$*), 3.22 (m, 1H, CH$_3$C*H*), 7.56 (dd, 1H, H^5), 7.63 (dt, 1H, H$^{5'}$), 8.05-8.21 (m, 4H, H$^{3,3',4,4'}$), 8.56 (d, 1H, H$^{6'}$). **^{13}C NMR (125.68 MHz, CD$_2$Cl$_2$)** δ 3.3 (NC*C*H$_3$), 6.44 (*C*H$_3$-Pd), 11.3 (CHCH$_2$*C*H$_3$), 20.0 (*C*H$_3$CH), 29.4 (CH*C*H$_2$CH$_3$), 43.5 (CH$_3$*C*H), 120.8-122.3 (C$^{3,3'}$), 126.2-126.9 (C$^{5,5'}$), 140.3 (C$^{4,4'}$), 148.5 (C$^{6'}$).

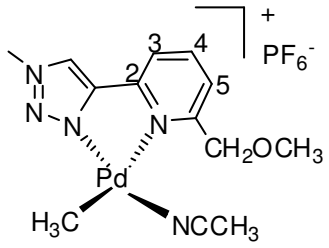

[Pd(30)(CH$_3$)(NCCH$_3$)][PF$_6$] (30b). ^{1}H NMR (500 MHz, DMSO-d^6, 60°C) δ 0.98 (s, 3H, C*H$_3$*-Pd), 2.04 (s, 3H, free NCC*H$_3$*), 3.38 (s, 3H, OC*H$_3$*), 4.13 (s, 3H, N-C*H$_3$*), 4.53 (s, 2H, C*H$_2$*OCH$_3$), 7.39 (s, 1H, H^3), 7.94 (s, 2H, H^{4,5}),8.59 (s, 1H, H$^{5'}$).

General procedure to obtain [Pd(CH$_3$)(N-N')$_2$][PF$_6$]

To a suspension of 0.20 mmol of [Pd(N-N')(CH$_3$)(NCCH$_3$)][PF$_6$] (**29b**-**32b**) in 20 mL of CH$_2$Cl$_2$, 0.26 mmol of the free N-N' ligand was added (Pd/free ligand=1/1.3), yielding an orange/yellow solution. After 10 min the solution was filtered and concentrated in *vacuo* to induce precipitation of the product as a yellow/orange solid. The solid was removed by filtration, washed with diethyl ether and dried. Average yield: 90%

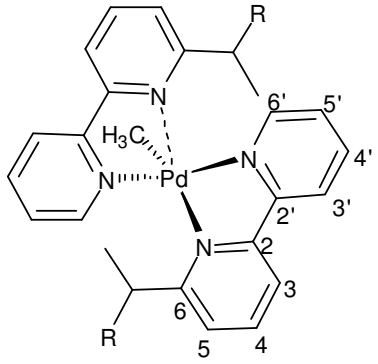

R = -OCH$_3$ (**29c**)
= -CH$_3$ (**31c**)
= -CH$_2$CH$_3$ (**32c**)

[Pd(29)$_2$(CH$_3$)][PF$_6$] (29c). ^{1}H NMR (500 MHz, CD$_2$Cl$_2$) δ 0.56 (*RR* or *SS*, s, 3H, C*H$_3$*-Pd), 0.64 (*RS*/*SR*, s, 3H, C*H$_3$*-Pd), 0.68 (*RR* or *SS*, s, 3H, C*H$_3$*-Pd), 0.99 (*RR* or *SS*, 3H, C*H$_3$*CH), 1.03 (dd, *RS*/*SR*, 3H, C*H$_3$*CH), 1.08 (*RR* or *SS*, 3H, C*H$_3$*CH), 2.84 (*RR* or *SS*, 3H, OC*H$_3$*), 2.85 (*RR* or *SS*, 3H, OC*H$_3$*), 2.89 (s, *RS* or *SR*, 3H, OC*H$_3$*), 3.76 (*RR* or *SS*, m, 1H, CH$_3$C*H*), 3.85 (*RS* or *SR*, m, 1H, CH$_3$C*H*), 3.89 (*RS* or *SR*, m, 1H, CH$_3$C*H*),

4.02 (*RR* or *SS*, m, 1H, CH_3CH), 7.57-7.67 (*RR*/*SS* and *RS*/*SR*, m, aromatic protons), 7.99-8.21 (*RR*/*SS* and *RS*/*SR*, m, aromatic protons), 8.77 (*RR* or *SS*, d, 1H, $H^{6'}$), 8.81 (*RS* or *SR*, d, 1H, $H^{6'}$), 8.91 (*RS* or *SR*, d, 1H, $H^{6'}$), 8.96 (*RR* or *SS*, d, 1H, $H^{6'}$).

[Pd(31)$_2$(CH$_3$)][PF$_6$] (31c). ^{1}H NMR (500 MHz, CD$_2$Cl$_2$) δ 0.63 (s, 6H, CH_3-Pd), 0.94 (d, 3H, $CH(CH_3)_2$), 0.99 (d, 3H, $CH(CH_3)_2$), 2.85 (m, 2H, $CH(CH_3)_2$), 7.38 (d, 2H, H^5), 7.53 (t, 2H, $H^{5'}$), 7.91 (d, 2H, H^3), 8.00 (d, 2H, H^4), 8.12 (m, 4H, $H^{3',4'}$), 8.76 (d, 2H, $H^{6'}$).

[Pd(32)$_2$(CH$_3$)][PF$_6$] (32c). ^{1}H NMR (500 MHz, CD$_2$Cl$_2$) δ 0.50-0.41 (m, 4H, CH-CH_3), 0.60 (s, 3H, CH_3-Pd), 0.63 (s, 3H, CH_3-Pd), 0.67 (s, 3H, CH_3-Pd), 0.83 (d, 3H, CH_3CH), 0.89 (d, 3H, CH_3CH), 0.92 (d, 3H, CH_3CH), 0.97 (d, 3H, CH_3CH), 1.27-1.53 (m, 4H, CH-CH_3), 2.45-2.63 (m, 4H, $CHCH_3$), 7.31-7.36 (m, aromatic protons), 7.53-7.57 (m, aromatic protons), 8.11-8.18 (m, aromatic protons), 8.78 (d, 1H, $H^{6'}$), 8.83 (d, 2H, $H^{6'}$), 8.86 (d, 1H, $H^{6'}$).

General procedure to obtain: [Pd(CH$_3$PNCO)(Py)]$_2$[PF$_6$]$_2$, [Pd(CH$_3$PNCO)(4-CH$_3$Py)]$_2$[PF$_6$]$_2$, [Pd(CH$_3$PNCO)(4-CF$_3$Py)]$_2$[PF$_6$]$_2$, [Pd(PN)(CH$_3$)(Py)][PF$_6$], [Pd(PN)(CH$_3$)(4-CH$_3$-Py)][PF$_6$].

All complexes were obtained starting from the corresponding neutral derivatives upon addition of $AgPF_6$ in a mixture of CH_2Cl_2 and pyridine or pyridine derivatives. Neutral catalyst **44a** or **45a** (0.22 mmol) was dissolved in the minimal amount of CH_2Cl_2 under Argon and kept in the dark. To the obtained solution was added a solution of $AgPF_6$ in CH_2Cl_2 (0.0615 g, Mw 252.83, 0.24 mmol), and then dropwise the pyridine derivatives leading to the precipitation of AgCl. After 1.5 h, the solution was filtered over Celite and concentrated to minimal volume under vacuum. Upon addition of diethyl ether the product precipitate as a white solid. Average yield: 50-70% depending on the pyridine derivatives added.

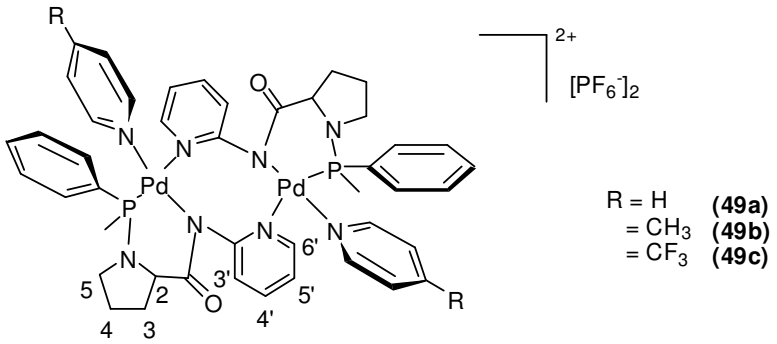

[Pd(CH$_3$PNCO)(Py)]$_2$[PF$_6$]$_2$ (49a). [α] = + 90.9 (c = 0.11 in CH$_3$OH). **IR (nujol)** 1706, 842, 557 cm^{-1}.**^{1}H NMR (500 MHz, CD$_2$Cl$_2$, - 40°C)** δ 2.09 (m, 2H, CH_2, H^5), 2.32 (m, 1H, CH_2, H^3), 2.38 (d, J = 11.5 Hz, 3H, CH_3-P), 2.92 (m, 1H, CH_2, H^3 and 1H, CH_2, H^4), 3.21 (m, 1H, CH_2, H^4), 5.03 (m, J = 4.5, 11 Hz, 1H, CH, H^2), 6.72 (t, J = 6 Hz, 1H, H$^{5'}$), 6.87 (t, J = 6.5 Hz, 1H, *m*-Py), 7.33 (m, 5H, Ph and 1H, *m*-Py), 7.56 (m, 1H, H$^{6'}$ and 1H, *p*-Py), 7.62 (d, J = 8 Hz, 1H, H$^{3'}$), 7.81 (t, J = 7.5 Hz, 1H, H$^{4'}$), 8.66 (d, J = 5.5 Hz, 1H, *o*-Py), 8.85 (d, J = 5.5 Hz, 1H, *o*-Py) **^{31}P NMR (500 MHz, CD$_2$Cl$_2$)** δ 50.73.

[Pd(CH$_3$PNCO)(4-CH$_3$Py)]$_2$[PF$_6$]$_2$ (49b).IR (nujol) 1711, 842, 557 cm^{-1}. **^{1}H NMR (500 MHz, CD$_2$Cl$_2$, - 35°C)** δ 2.09 (m, 2H, CH_2, H^5), 2.20 (s, 3H, CH_3-Py), 2.29 (m, 1H, CH_2, H^3), 2.35 (d, J = 11.5 Hz, 3H, CH_3-P), 2.89 (m, 1H, CH_2, H^4), 2.93 (m, 1H, CH_2, H^3), 3.20 (m, 1H, CH_2, H^4), 5.00 (m, 1H, CH, H^2), 6,67 (bs, 1H, *m*-4-CH$_3$Py), 6.71 (t, J = 5.5 Hz, 1H, H$^{5'}$), 7.17 (bs, 1H, *m*-4-CH$_3$Py), 7.34 (m, 5H, Ph), 7.53 (m, 1H, H$^{6'}$), 7.60 (d, J = 8 Hz, 1H, H$^{3'}$), 7.80 (dt, J =1.5, 7.5 Hz, 1H, H$^{4'}$), 8.44 (bs, 1H, *o*-4-CH$_3$Py), 8.63 (bs, 1H, *o*-4-CH$_3$Py). **^{31}P NMR (500 MHz, CD$_2$Cl$_2$)** δ 50.73.

[Pd(CH$_3$PNCO)(4-CF$_3$Py)]$_2$[PF$_6$]$_2$ (49c).[α] = + 120.5 (c = 0.22 in CH$_3$OH). **^{1}H NMR (500 MHz, CD$_2$Cl$_2$, - 40°C)** δ 2.13 (m, 2H, CH_2, H^5), 2.36 (m, 1H, CH_2, H^3), 2.40 (d, J = 11.5 Hz, 3H, CH_3-P), 2.95 (m, 1H, CH_2, H^4 and 1H, CH_2, H^3), 3.22 (m, 1H, CH_2, H^4), 5.06 (m, 1H, CH, H^2), 6.77 (t, J = 6 Hz, 1H, H$^{5'}$), 7.08 (bs, 1H, *m*-4-CF$_3$Py), 7.22 (bs, 1H, *m*-4-CF$_3$Py), 7.31 (m, 3H, Ph), 7.40 (m, 2H, Ph) 7.66 (m, 1H, H$^{6'}$ and 1H, H$^{3'}$), 7.85 (t, J =6.5 Hz, 1H, H$^{4'}$), 8.97 (d, J = 6 Hz, 1H, *o*-4-CF$_3$Py), 9.18 (d, J = 6 Hz, 1H, *o*-4-CF$_3$Py). **^{31}P NMR (500 MHz, CD$_2$Cl$_2$)** δ 50.73.

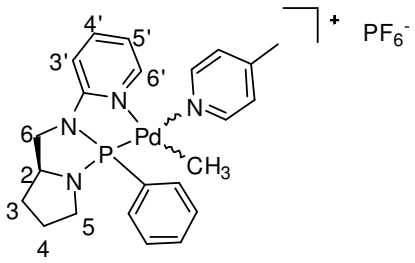

[Pd(PN)(CH$_3$)(4-CH$_3$Py)] (50b). $[\alpha]_D$ – 12.3 (*c* 0.105, CH_3OH). **^{1}H NMR (500 MHz, CD_2Cl_2)** δ 0.50 (d, *J* = 1.5 Hz, 3H, C*H$_3$*-Pd, *cis* isomer), 1.00 (m, aliphatic protons *trans* isomer), 1.65 (m, 1H, H^3, *cis* isomer), 1.72 (d, *J* = 8.5 Hz, 3H, C*H$_3$*-Pd, *trans* isomer), 1.98 (m, 2H, H^4, *cis* isomer), 2.24 (m, 1H, H^3, *cis* isomer), 2.30 (s, 3H, CH_3-Py, *trans* isomer), 2.39 (s, 3H, CH_3-Py, *cis* isomer), 2.73 (m, aliphatic proton of the *trans* isomer), 3.05 (m, 1H, H^4 *cis* isomer), 3.31 (m, 1H, H^6, *cis* isomer), 3.54 (m, 1H, H^5, *cis* isomer), 3.65 (m, 1H, H^6, *cis* isomer) 3.74 (m, 1H, H^5, *cis* isomer), 4.12 (m, 1H, H^2, *cis* isomer), 6.82 (m, 1H, Py), 7.24 (m, Py), 7.46-7.57 (m, Ph and Py), 7.78-7.86 (m, Ph and Py), 7.83 (d, 1H, Py), 8.49 (m, 1H,Py). **^{31}P NMR (500 MHz, CD_2Cl_2)** δ 122.9 (*cis* isomer), 136.2 (*trans* isomer). Ratio *cis*/*trans* 2:1.

CATALYSIS

General procedure for oligomerization reactions

All experiments were carried out in a three-necked, 75 mL glass reactor equipped with a magnetic stirrer and connected to a temperature controller. After establishment of the reaction temperature (30 °C), the pre-catalyst (1.27 x 10^{-2} mmol), 1,4-benzoquinone (54.9 mg, Mw 108.09, 0.508 mmol), styrene (10 mL, Mw 104.15, δ 0.909 g/mL, 87 mmol), and TFE (20 mL) were placed inside. CO was bubbled through the solution for 10 min; afterward a 4 L balloon filled with CO was connected to the reactor. The system was stirred at the same temperature for 24 h to give a yellow solution. The reaction mixture was then poured into methanol (100 mL) and stirred for 1 h at room temperature, and the solvent was evaporated until to obtain a yellow/orange oil. The product was dried under *vacuum*. **^{1}H NMR (500 MHz, $CDCl_3$)** CO/styrene oligomers: δ 1.40 (d, B$_l$ 3H, -(Ph)CH-C*H$_3$*), 1.48 (d, A$_u$ 3H, -(Ph)CH-C*H$_3$*), 2.57-3.53 (broad, -(Ph)CH-C*H$_2$*-CO-), 3.65 (m, A$_u$ 1H, CH_3-C*H*(Ph)-), 3.91 (m, B$_l$ 1H, CH_3-C*H*(Ph)-), 4.03 (m, A$_l$ 1H, CH_3-C*H*(Ph)-), 3.81-4.55 (broad, CO-C*H*(Ph)-), 6.41 (pst, A$_u$ 1H, (Ph-C*H*=CH-), 6.73 (pst, A$_l$ 1H, (Ph-C*H*=CH-), 6.97 (m, B$_l$ 1H, Ph-C*H*=CH-), 7.10-8.21 (aromatic protons). **^{13}C NMR (100 MHz, $CDCl_3$)** δ 17.18 (B$_l$ -(Ph)CH-*C*H$_3$), 17.63

(A_l -(Ph)CH-*C*H_3), 21.29 (A_u -(Ph)CH-*C*H_3), 29.47 (-(Ph)CH-*C*H_2-CO-), 30.02, 42.32-44.26, 42.43 (A_u CH_3-*C*H(Ph)-), 52.42 (A_l CH_3-*C*H(Ph)-), 53.23 (B_l CH_3-*C*H(Ph)-), 52.02-53.28 (CO-*C*H(Ph)-), 116.37 (A_l Ph-*C*H=CH-), 128.47 (C_{arom}), 135.38 (A_u Ph-*C*H=CH-), 136.19 (B_l Ph-*C*H=CH-), 208.17-209.10 (broad, CO).

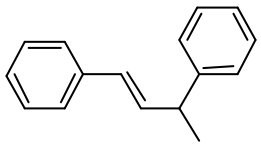

Styrene dimerization reaction

All experiments were carried out in a three-necked, 75 mL glass reactor equipped with a magnetic stirrer and connected to a temperature controller. After establishment of the reaction temperature (70 °C), the pre-catalyst (0.0254 mmol), 1,4-benzoquinone (54.9 mg, Mw 108.09, 0.508 mmol), styrene (10 mL, Mw 104.15, δ 0.909 g/mL, 87 mmol), and TFE (20 mL) were placed inside. The system was stirred at the same temperature for 24 h. At the end of the reaction time the two layers formed was separed (dimer was the least dense phase), the residue of Pd(0) was filtered on a short pad of Celite then washed with methylene chloride. The product was dried under *vacuum*. **IR (neat)** 3081, 3059, 3025, 2964, 2928, 2870, 1945, 1873, 1806, 1599, 1492, 1450, 965 cm^{-1}. **^{1}H NMR (400 MHz, $CDCl_3$)** δ 1.47 (d, 3H, *J* = 7 Hz, C*H*$_3$CH), 3.65 (m, 1H, CH_3C*H*), 6.42 (m, 2H, *J* = 5.16, 16.2 Hz, *H*C=C*H trans*), 7.19-7.48 (m, 10H, Ph). **^{13}C NMR (100 MHz, $CDCl_3$)** δ 21.2, 42.5, 126.1, 126.2, 127.0, 127.3, 128.5, 135.1, 137.5, 145.6.